

**MODULATING LIPSOMAL STEALTH PROPERTIES TO EVADE
RES AND TARGET TUMORS**

A Dissertation
Presented to
The Academic Faculty

by

Kathleen Margaret McNeeley

In Partial Fulfillment
of the Requirements for the Degree
Doctor of Philosophy in the
School of Biomedical Engineering

Georgia Institute of Technology
December, 2008

**MODULATING LIPOSOMAL STEALTH PROPERTIES TO EVADE
RES AND TARGET TUMORS**

Approved by:

Dr. Ravi V. Bellamkonda, Advisor
School of Biomedical Engineering
Georgia Institute of Technology

Dr. Gang Bao
School of Biomedical Engineering
Georgia Institute of Technology

Dr. Andrew Lyon
School of Chemistry & Biochemistry
Georgia Institute of Technology

Dr. Niren Murthy
School of Biomedical Engineering
Georgia Institute of Technology

Dr. Ananth Annapragada
School of Health Information Sciences
*University of Texas-Houston Health
Science Center*

Date Approved: 08/22/2008

ACKNOWLEDGEMENTS

The work presented here could not have been completed without the help, guidance, and support from a number of people. I would like to take this opportunity to express my sincere gratitude for the encouragement I received while completing this dissertation work.

First, I would like to thank my advisor, Dr. Ravi Bellamkonda, for his continual support and advice over the course of this project. I am grateful for the opportunities provided to me as a member of the lab and for the ability to develop as a scientist under his guidance. I have enjoyed working on this challenging project and have learned many lessons along the way. I would also like to express my appreciation to the members of my Ph.D. thesis committee, Dr. Ananth Annapragada, Dr. Gang Bao, Dr. Andrew Lyon, and Dr. Niren Murthy, who provided me with insightful advice over the duration of this research.

I certainly would not have made it through this work without the support and encouragement from friends and family. I would like to thank Vince Potts for enduring my unconventional working hours over the course of this project and particularly for tolerating my irritable temperament while finishing up. My parents have been invaluable. I sincerely appreciate the free automobile services, home repairs, and catering, however, most importantly, I could not have completed this work without the long-distance moral support you have continually provided. No one else deals with my supreme ability to vent better than you, and your responses have always helped me to cope with any situation that presented itself. In addition, I have been incredibly blessed to have a large family, and I would like to take this opportunity to acknowledge the help and support of

my siblings, Heather, Patrick, Megan, Erin, and Ryan. Whether it was just cheering me up or attempting to discuss my work, you have always been there for me and I am forever grateful.

Finally, I would like to thank my friends and previous and present members of the Neurological Biomaterials and Therapeutics Laboratory. You have been a tremendous help during this process and created a fun and enjoyable working environment. I would like to thank current lab members and staff, Efstathios Karathanasis, Lohitash Karumbaiah, George McConnell, Abhiruchi Agarwal, Hyun-Jung Lee, Isaac Clements, Vivek Mukhatyar, Jennifer Munson, Ben Roller, and Michael Tanenbaum for all of your help and support which always made it easier to overcome difficulties and challenges. In addition, I would particularly like to mention my appreciation for Dr. Rupal Thazhath and Dr. Ryan Gilbert. Your support, mentoring, and advice have been an immense help. I have greatly appreciated the ability to discuss my research with you over the years, especially at times when no one else understood my studies.

TABLE OF CONTENTS

	Page
ACKNOWLEDGEMENTS	iii
LIST OF TABLES	x
LIST OF FIGURES	xi
SUMMARY	xiv
CHAPTER 1. INTRODUCTION	1
1.1. STATEMENT OF PROBLEM	1
1.2. HYPOTHESIS	3
1.3. OBJECTIVES	4
1.4. REFERENCES	6
CHAPTER 2. CURRENT STATE OF GLIOMA THERAPIES	8
2.1. CURRENT TREATMENTS FOR BRAIN TUMORS ARE INSUFFICIENT	8
2.2. CURRENT TREATMENT MODALITIES	8
2.2.1. SURGICAL RESECTION	9
2.2.2. RADIOSURGERY	10
2.2.3. WHOLE-BRAIN RADIATION THERAPY	11
2.2.4. TRADITIONAL CHEMOTHERAPY	11
2.3. NOVEL TREATMENT APPROACHES	13
2.3.1. NOVEL RADIOTHERAPY TECHNIQUES	13
2.3.2. LOCALIZED CHEMOTHERAPY	14
2.3.2.1. Intra-Arterial Delivery	14
2.3.2.2. Convection Enhanced Delivery	15
2.3.2.3. Implantable Drug Depots	15
2.3.3. TARGETED SYSTEMIC DELIVERY OF CHEMOTHERAPEUTICS	16
2.3.3.1. Direct Drug Modification	17
2.3.3.2. Targeted Nanocarriers	18
2.4. CONCLUSIONS	18
2.5. REFERENCES	20
CHAPTER 3. THERAPEUTIC NANOCARRIERS FOR DRUG DELIVERY TO TUMORS	24
3.1. INTRODUCTION	24
3.2. TYPES OF NANOCARRIERS USED FOR TARGETED DELIVERY TO TUMORS	24
3.2.1. POLYMERIC NANOPARTICLES	26
3.2.2. POLYMERIC MICELLES	27
3.2.3. DENDRIMERS	30
3.2.4. CARBON NANOTUBES	32
3.2.5. LIPOSOMES	34

3.2.5.1. Formulation Components	35
3.2.5.2. Preparation Techniques	39
3.2.5.3. Drug Loading	40
3.2.5.3.1. Passive Loading	40
3.2.5.3.2. Remote Loading	41
3.2.5.4. Passive Targeting with Liposomes	44
3.2.5.5. Active Targeting with Liposomes	46
3.2.5.5.1. Targeting Agent Selection	48
3.2.5.5.2. Targeting Agent Incorporation Decreases Circulation Times and Passive Targeting to Tumor	51
3.2.5.6. Use of Cleavable Phospholipid-PEG Chains in Liposomes	52
3.3. CONCLUSIONS	54
3.4. REFERENCES	57
CHAPTER 4. EVALUATION OF ALTERNATIVE TARGETING AGENTS TO IMPROVE TREATMENT EFFICACY	73
4.1. INTRODUCTION	73
4.2. MATERIALS AND METHODS	75
4.2.1. SYNTHESIS AND MICELLE FORMATION OF DSPE-PEG ₃₃₅₀ -NGR	75
4.2.2. PREPARATION OF APN-TARGETED LIPOSOMAL NANOCARRIERS	76
4.2.3. PREPARATION OF OX26 LIPOSOMAL NANOCARRIERS	77
4.2.4. ACTIVE LOADING OF DOXORUBICIN INTO LIPOSOMES	77
4.2.5. TUMOR CELL CULTURE	77
4.2.6. TUMOR INOCULATION	78
4.2.7. IMMUNOHISTOCHEMISTRY FOR CHARACTERIZATION OF APN EXPRESSION	78
4.2.8. SURVIVAL STUDIES EVALUATING TREATMENT EFFICACY	79
4.2.9. <i>IN VIVO</i> CIRCULATION STUDIES	80
4.2.10. BIODISTRIBUTION IN TUMOR INOCULATED ANIMALS	80
4.3. RESULTS	81
4.3.1. IMMUNOHISTOCHEMISTRY FOR CHARACTERIZATION OF APN EXPRESSION	81
4.3.2. SURVIVAL STUDIES EVALUATING TREATMENT EFFICACY	82
4.3.3. <i>IN VIVO</i> CIRCULATION STUDIES	85
4.3.4. BIODISTRIBUTION IN TUMOR INOCULATED ANIMALS	87
4.4. DISCUSSION	91
4.5. CONCLUSIONS	97
4.6. REFERENCES	99
CHAPTER 5. DECREASED CIRCULATION TIME OFFSETS INCREASED EFFICACY OF PEGYLATED NANOCARRIERS TARGETING FOLATE RECEPTORS OF GLIOMA	102
5.1. ABSTRACT	102
5.2. INTRODUCTION	103
5.3. MATERIALS AND METHODS	107
5.3.1. MATERIALS	107
5.3.2. LIPOSOME FORMULATION	108
5.3.3. DSPE-PEG ₃₃₅₀ -FOLATE CONJUGATE SYNTHESIS	109

5.3.4. DSPE-PEG ₃₃₅₀ -FOLATE INSERTION INTO PREFORMED LIPOSOMAL NANOCARRIERS	110
5.3.5. REMOTE LOADING OF DOXORUBICIN	111
5.3.6. PLASMA CLEARANCE	112
5.3.7. 9L GLIOMA CELL CULTURE	112
5.3.8. TUMOR INOCULATION	113
5.3.9. IMMUNOHISTOCHEMISTRY FOR CHARACTERIZATION OF ANGIOGENESIS	114
5.3.10. BIODISTRIBUTION IN TUMOUR INOCULATED ANIMALS	115
5.3.11. SURVIVAL STUDIES	116
5.4. RESULTS	117
5.4.1. PLASMA CLEARANCE STUDIES	117
5.4.2. TUMOR GROWTH CURVE	118
5.4.3. NESTIN EXPRESSION	119
5.4.4. ORGAN DISTRIBUTION STUDIES	119
5.4.5. SURVIVAL STUDIES	123
5.5. DISCUSSION	123
5.6. CONCLUSIONS	127
5.7. ACKNOWLEDGEMENTS	128
5.8. REFERENCES	129
CHAPTER 6. MASKING AND TRIGGERED UNMASKING OF TARGETING LIGANDS ON NANOCARRIERS IMPROVES DRUG DELIVERY TO BRAIN TUMORS	137
6.1. ABSTRACT	137
6.2. INTRODUCTION	138
6.3. RESULTS AND DISCUSSION	141
6.4. METHODS	153
6.4.1. SYNTHESIS OF DSPE-S-S-PEG ₅₀₀₀	153
6.4.2. THIOLYTIC CLEAVABILITY OF DSPE-S-S-PEG	154
6.4.3. <i>IN VIVO</i> CIRCULATION STUDIES	154
6.4.4. <i>IN VITRO</i> STUDIES	156
6.4.5. TUMOR INOCULATION	157
6.4.6. FLOW CYTOMETRIC STUDIES	157
6.4.7. STATISTICAL ANALYSIS	159
6.5. COMPETING FINANCIAL INTERESTS	159
6.6. ACKNOWLEDGEMENTS	159
6.7. SUPPLEMENTARY INFORMATION	160
6.8. REFERENCES	164
CHAPTER 7. SUMMARY OF FINDINGS	169
7.1. INTRODUCTION	169
7.2. EVALUATION OF ALTERNATIVE TARGETING AGENTS TO IMPROVE TREATMENT EFFICACY	170
7.3. DECREASED CIRCULATION TIME OFFSETS INCREASED EFFICACY OF PEGYLATED NANOCARRIERS TARGETING FOLATE RECEPTORS OF GLIOMA	172

7.4. MASKING AND TRIGGERED UNMASKING OF TARGETING LIGANDS ON NANOCARRIERS IMPROVES DRUG DELIVERY TO BRAIN TUMORS	176
7.5. CONCLUSIONS	181
7.6. REFERENCES	183
CHAPTER 8. FUTURE PERSPECTIVES	186
8.1. BIODISTRIBUTION STUDIES	186
8.2. SPATIAL DISTRIBUTION WITHIN TUMOR	187
8.3. <i>IN VIVO</i> CYTOTOXICITY	189
8.4. TUMOR MODEL SELECTION	189
8.4.1. TUMOR TYPE	189
8.4.2. SITE OF IMPLANTATION	190
8.5. <i>IN VIVO</i> THERAPEUTIC EFFICACY	191
8.5.1. TREATMENT REGIMEN	191
8.5.2. OUTCOME MEASURES	192
8.6. ADDRESSING EXTRAVASATION AND DIFFUSION LIMITATIONS	193
8.6.1. METHODS TO INCREASE EXTRAVASATION TO TUMOR	193
8.6.2. INCREASING DIFFUSION OF TARGETED AGENTS AFTER EXTRAVASATION	194
8.7. ALTERNATIVE TARGETING AGENTS	195
8.8. CONTRAST AGENT DELIVERY	195
8.9. CONCLUSIONS	196
8.10. REFERENCES	197
APPENDIX A. IMAGING NANOPROBE FOR PREDICTION OF NANOPARTICLE CHEMOTHERAPY USING MAMMOGRAPHY	200
A.1. ABSTRACT	201
A.2. INTRODUCTION	202
A.3. MATERIALS AND METHODS	203
A.3.1. FABRICATION OF THE NANOSCALE X-RAY PROBE	203
A.3.2. ANIMAL MODEL	204
A.3.3. X-RAY IMAGING	204
A.3.4. PRELIMINARY DOSE STUDY	205
A.3.5. EFFICACY PREDICTION STUDY	205
A.3.6. IMAGE ANALYSIS	206
A.3.7. IMMUNOHISTOCHEMISTRY AND HISTOLOGICAL EVALUATION OF EXPLANTED TUMORS	207
A.3.8. DATA AND STATISTICAL ANALYSIS	208
A.4. RESULTS	208
A.4.1. IMAGING USING A CLINICAL MAMMOGRAPHY SYSTEM	208
A.4.2. HISTOLOGICAL EVALUATION OF EXTRAVASATED PROBE TUMOR DISTRIBUTION	211
A.4.3. TUMOR IMAGING	211
A.4.4. QUANTIFYING TREATMENT EFFICACY AS A FUNCTION OF PROBE EXTRAVASATION	212
A.5. DISCUSSION	215
A.6. PRACTICAL APPLICATIONS	218

A.7. REFERENCES
BIBLIOGRAPHY

219
223

LIST OF TABLES

Table 3.1: Various nanocarrier-based drug delivery platforms	25
Table 6.1: Phospholipid-PEG components (mol %) for each nanocarrier formulation	142
Table 6.2: Flow cytometric analysis of uptake of liposomal formulations by tumor cells recovered from 9L/LacZ tumors in rats	150

LIST OF FIGURES

	Page
Figure 3.1: Chemical structures of DSPC, DSPE, and cholesterol	38
Figure 3.2: Ammonium sulfate driven remote loading of doxorubicin	43
Figure 3.3: Passive accumulation of long-circulating liposomal nanocarriers into tumors via the EPR effect	45
Figure 3.4: Active targeting of liposomal nanocarriers to tumors using ligands targeted to over-expressed receptors on tumor cells and uptake via receptor-mediated endocytosis	47
Figure 4.1: Aminopeptidase N is selectively over-expressed by 9L glioma tumors <i>in vivo</i>	82
Figure 4.2: Use of NGR peptide to target liposomal DXR to APN does not prolong survival of tumor-bearing rats	83
Figure 4.3: Use of OX26 antibody to target liposomal DXR to TfR does not prolong survival of tumor-bearing rats	84
Figure 4.4: APN-targeted liposomes retain the ability to evade the RES	86
Figure 4.5: Inclusion of OX26 antibody to facilitate active targeting of sterically stabilized liposomes to TfR significantly decreases circulation times	87
Figure 4.6: Targeting to TfR with OX26 alters the biodistribution of liposomal DXR 20 hours after treatment administration	88
Figure 4.7: Targeting to TfR with OX26 alters the biodistribution of liposomal DXR 50 hours after treatment administration	90
Figure 4.8: Targeting to TfR with lower levels of OX26 exposes the minimum number of antibodies necessary to achieve selective delivery to the brain 50 hours after treatment administration	91
Figure 5.1: Plasma clearance of liposomal doxorubicin formulations	117
Figure 5.2: 9L glioma growth curve in Fisher 344 rats	118
Figure 5.3: Nestin expression in normal brain and 9L glioma tumor	120
Figure 5.4: Biodistribution of liposomal doxorubicin formulations in Fisher 344 rats with 9L glioma tumor	121

Figure 5.5: Survival of Fisher 344 rats with 9L glioma tumor in response to treatment	122
Figure 6.1: Schematic depicting FR-targeted nanocarrier options	139
Figure 6.2: Inclusion of 8% DSPE-S-S-PEG ₅₀₀₀ prolongs circulation of FR-targeted nanocarriers	143
Figure 6.3: DSPE-S-S-PEG ₅₀₀₀ enables triggered uptake of DXR encapsulated within liposomal nanocarriers by glioma cells	144
Figure 6.4: Cytotoxicity of liposomal DXR is controllably altered through the inclusion of DSPE-S-S-PEG ₅₀₀₀	146
Figure 6.5: <i>In vivo</i> cellular uptake of liposomes is enhanced when folate on FR-targeted nanocarriers is masked during circulation and ultimately exposed after extravasation into tumor	148
Figure 6.6: Cysteine cleavage of PEG and exposure of folate on FRT liposomal nanocarriers at the target site significantly increases frequency of drug uptake by tumor cells	149
Figure 6.7: Matrix assisted laser desorption ionization time-of-flight mass spectrum (MALDI-TOFMS) of DSPE-S-S-PEG ₅₀₀₀	160
Figure 6.8: Supplement to Figure 6.2: Inclusion of 8% DSPE-S-S-PEG ₅₀₀₀ prolongs circulation of FR-targeted nanocarriers	161
Figure 6.9: Supplement to Figure 6.4: Cytotoxicity of liposomal DXR is controllably altered through the inclusion of DSPE-S-S-PEG ₅₀₀₀	162
Figure 6.10: Cytotoxicity of liposomal DXR as a function of applied DXR concentration	163
Figure A.1: Estimation of the 49 kVp rhodium/rhodium x-ray spectrum with the added 0.254 mm copper filter, according to the XSPECT simulation program	209
Figure A.2: Whole body images of a rat with a breast tumor in its right flank obtained using a clinical digital mammography system	210
Figure A.3: X-ray images display the 5-day intratumoral fate of the probe in a rat breast tumor model	210
Figure A.4: X-ray images of two tumors before and after injection of the probe at a dose of 455 mg I/kg	211

Figure A.5: Microdistribution of the probe in a breast tumor lesion 48 h after IV injection of rhodamine-tagged iodinated liposomes	212
Figure A.6: The 3-day pattern of the enhancement following injection of the probe to a group of rats indicates a high variability of the tumors leakiness	213
Figure A.7: Correlation of the tumor growth ($K^{\text{tumor growth}}$) and the prognostic assessment ($K^{\text{enhancement}}$)	214

SUMMARY

Existing therapies for the treatment of glioma remain problematic while the incidence of malignant gliomas is growing, leading to an increasing demand for more effective treatment options. Currently, patients diagnosed with malignant brain tumors have a very poor prognosis with a median survival rate of less than one year and an overall 5-year survival rate as low as 34.1%. Brain tumors continue to be a challenge to treat because they are inherently diffuse, highly invasive, and non-localized. For these reasons, it is imperative that treatments for brain and nervous system cancers are improved.

Liposomal nanocarriers offer much promise in the delivery of chemotherapeutic drugs to solid tumors because they may be specifically targeted to tumors thereby shielding healthy organs from the toxic side effects of incorporated chemotherapeutics. Passive targeting of liposomes is achieved through the inclusion of PEG to evade the RES and prolong circulation in the bloodstream. Since tumor vasculature exhibits increased permeability, prolonged circulation results in passive accumulation of liposomes to tumor. Active targeting to tumor is accomplished through the inclusion of agents targeted to over-expressed receptors on tumor cells. *In vitro* studies with a wide variety of targeting agents have demonstrated the potential for increased cytotoxicity of actively targeted liposomes due to specific uptake by tumor cells. *In vivo*, however, actively targeted liposomal nanocarriers have failed to meet the expectations established by the promising outcomes of *in vitro* studies. This is attributed to the fact that the

inclusion of targeting agents results in accelerated clearance from the bloodstream and reductions in passive targeting to tumor thereby offsetting the benefits of active targeting.

The central focus of this thesis was to engineer a multi-functional nanoscale drug delivery system which would enable active targeting without compromising RES evasion and passive accumulation to tumor. It was shown that the use of folate targeting ligands in sterically stabilized liposomal formulations significantly reduced blood circulation times. To address this issue and prevent RES recognition of folate on targeted liposomal formulations, a cysteine cleavable phospholipid-PEG conjugate was utilized to “mask” adjacent targeting ligands while liposomes were in circulation. This system enabled controlled ligand presentation using an exogenous trigger. Once passive accumulation at the tumor was achieved, cysteine was administered to detach PEG chains, expose folate, and promote uptake by tumor cells. *In vivo* studies demonstrated that cleavable DSPE-PEG₅₀₀₀ was capable of concealing folate on liposomes to maintain prolonged circulation times. *In vitro* uptake and cytotoxicity studies verified the ability to conceal and expose folate on demand, permitting receptor mediated targeting and delivery of large drug payloads into the nucleus of target cells. Finally, studies conducted to analyze drug uptake by tumor cells *in vivo* confirmed that delivery was enhanced when tumor-inoculated animals received targeted liposomes containing cleavable PEG chains followed by a cysteine infusion to expose folate. These results indicate that detachable PEG chains can be used in targeted liposomal formulations to enhance efficacy of chemotherapy in the treatment of glioma.

CHAPTER 1. INTRODUCTION

1.1. STATEMENT OF PROBLEM

Current approaches for the treatment of glioma are limited in their effectiveness because malignant brain tumors are characteristically diffuse, highly invasive, and non-localized [1]. Upon diagnosis of malignant gliomas, surgical removal of the accessible tumor follows; however, due to the invasive nature of malignant gliomas, complete surgical resection is a rarity. Therefore, conventional therapies include radiation therapy and chemotherapy after surgical resection. Treatment regimens including radiation and systemic chemotherapy have been minimally effective [2, 3]. The success of systemic chemotherapy for intracranial tumors is critically dependent on the access that these agents have to tumors which is limited even with the so-called leaky vasculature across the blood-brain barrier (BBB). Indeed BBB associated limitations restrict therapies to low molecular weight, uncharged, and lipophilic agents. Use of implantable biodegradable drug depots is one strategy to localize delivery of chemotherapeutics and is currently used in clinical practice [4]. Gliadel[®], an FDA approved BCNU-loaded polyanhydride polymer wafer, has resulted in improved survival rates [5]. However, the drug diffused from a central core usually cannot reach the tumor periphery where the most aggressive cancer cells persist, and median survival has only shown to be extended about 2.2-3.4 months for patients with newly-diagnosed high grade glioma [5, 6] and a mere 2 months for patients with recurrent disease [5, 7]. Conversely, drug delivery via systemic intravascular administration utilizes the tumor's own blood supply for transport allowing for drug delivery throughout the tumor. Systemic delivery of long circulating liposomal nanocarriers has exhibited increased chemotherapeutic drug delivery to solid

tumors [8] due to the combination of prolonged circulation in blood and preferential accumulation in solid tumors by passive convective transport through leaky endothelium because of the discontinuity in the abnormal tumor vascular—the so called enhanced permeability and retention (EPR) phenomenon [9].

Nanocarrier mediated therapy of gliomas shows promise because multi-functional nanocarriers can theoretically be designed not only to carry a range of chemotherapeutic or anti-invasive agents, but also to both passively and actively target intracranial tumors such as gliomas. ‘Passive’ targeting results from prolonged circulation of nanocarriers allowing for accumulation at sites with abnormal, leaky vasculature. In recent studies on a rat brain glioma, effective ‘passive’ tumor dosing was achieved by i.v. injections of drug-loaded liposomal nanocarriers [10]. It has been demonstrated in patients with glioblastomas and metastatic brain tumors that long circulating liposomal nanocarriers selectively overcome the BBB in the tumor lesions resulting in 13-19 times higher accumulation in the glioblastoma as compared to the normal brain [11]. However, passive targeting does not address uptake by tumor cells after extravasation.

Therefore, for further increase in efficacy and specificity, liposomal nanocarriers can potentially be tagged with targeting molecules that bind to receptors over-expressed on tumor cells for ‘active’ targeting. The initial enthusiasm of the active targeting strategies has however been limited due to disappointing *in vivo* performance of the targeted nanocarriers compared to non-targeted nanocarriers. It has been shown that the presence of targeting ligands compromises blood circulation time of nanocarriers [8, 12-15] and decreases passive accumulation of carriers to tumors [16] as extravasation is directly proportional to circulation time and concentration in blood [17]. This is not

unexpected as long circulation time of liposomal nanocarriers is due to a polyethylene glycol (PEG) shielding (3-10% of the lipid is typically PEGylated), and when targeting ligands are employed, they are usually conjugated on the free end of the PEG chain resulting in recognition by the reticulo-endothelial system (RES) and accelerated clearance by the liver. As a result, fewer ‘targeted’ nanocarriers are able to reach the tumor site and consequently the gains from active targeting after extravasation into the tumor are compromised [16].

1.2. HYPOTHESIS

The ability to actively target systemically delivered drugs to tumors while retaining the full capability of passive accumulation remains an unresolved problem. Overcoming this challenge requires that circulation times be unaffected by the incorporation of targeting agents while the ability to actively target tumor cells at the target site is retained. We believe that targeting ligands may be ‘masked’ by ‘burying’ them within adjacent longer PEG chains on the nanocarrier surface so that circulation times are not compromised as seen with non-masked ligand presenting nanocarriers. To enable ligand binding to tumor cells *after* extravasation to tumor site, ligand-masking PEG chains may be fabricated to be susceptible to cleavage by a safe ‘cleaving agent’ (cysteine) that is administered intravenously after the nanocarriers have extravasated to the tumors. The central hypothesis of this thesis is that the use of targeting ligands that are masked while in circulation, but unmasked after extravasation will significantly enhance targeted nanocarrier delivery to tumor compared to non targeted nanocarriers or targeted, unmasked nanocarriers.

1.3. OBJECTIVES

The overall purpose of the work described in this thesis is to successfully optimize targeted drug delivery to tumors *in vivo* with an emphasis on achieving maximized drug accumulation at the target site with limited uptake by healthy organs. To do so, both passive and active targeting of chemotherapeutic agent to tumor should be employed where each method of targeting, while used concurrently, retains optimal performance.

To meet this goal, the following objectives were set:

1. To design and fabricate an actively targeted liposomal doxorubicin formulation and characterize *in vivo* performance.
2. To reduce RES clearance of actively targeted liposomal formulations by masking targeting ligands with cleavable PEG chains.
3. To demonstrate ligand activity masking and unmasking on targeted nanocarriers using cleavable PEG chains.
 - a. Determine ability to modulate uptake and cytotoxicity of targeted formulations with cleavable PEG chains *in vitro*.
 - b. Evaluate passive accumulation and active targeting of liposomal nanocarrier chemotherapeutics *in vivo* using a rat intracranial tumor model.

Fulfillment of these objectives would also address some of the engineering challenges of nanoscale drug delivery to tumors. In general, there are currently no means to control the introduction of ligands on targeted nanocarrier drug delivery systems after *in vivo* administration. The scheme presented here would allow for precise control over

an engineered nanoscale system for drug delivery. Cleavable phospholipid-PEG conjugates would confer the ability to control the time and location of ligand presentation *in vivo*. Masking and triggered unmasking of biological entities on targeted nanocarriers would serve to 1) prevent degradation of targeting agents to ensure that they are intact at the site of action, and 2) reduce the immunogenicity of incorporated agents to inhibit RES recognition and clearance. Control over ligand presentation would ensure that targeted nanocarriers only act when necessary at the tumor site since activation would be initiated through an external trigger.

1.4. REFERENCES

- [1] Black, K. L. and Pikul, B. K., Gliomas--past, present, and future. *Clin Neurosurg* 45, 160-163 (1999).
- [2] Barker, F. G., 2nd, Chang, S. M., Gutin, P. H., et al., Survival and functional status after resection of recurrent glioblastoma multiforme. *Neurosurgery* 42, 709-720; discussion 720-703 (1998).
- [3] Fine, H. A., Dear, K. B., Loeffler, J. S., et al., Meta-analysis of radiation therapy with and without adjuvant chemotherapy for malignant gliomas in adults. *Cancer* 71, 2585-2597 (1993).
- [4] Wang, P. P., Frazier, J. and Brem, H., Local drug delivery to the brain. *Adv Drug Deliv Rev* 54, 987-1013 (2002).
- [5] GLIADEL Wafer [package insert]. Bloomington, MN: MGI PHARMA, INC.; 2006.
- [6] Valtonen, S., Timonen, U., Toivanen, P., et al., Interstitial chemotherapy with carmustine-loaded polymers for high-grade gliomas: a randomized double-blind study. *Neurosurgery* 41, 44-48; discussion 48-49 (1997).
- [7] Brem, H., Piantadosi, S., Burger, P. C., et al., Placebo-controlled trial of safety and efficacy of intraoperative controlled delivery by biodegradable polymers of chemotherapy for recurrent gliomas. The Polymer-brain Tumor Treatment Group. *Lancet* 345, 1008-1012 (1995).
- [8] Gabizon, A., Horowitz, A. T., Goren, D., et al., *In vivo* fate of folate-targeted polyethylene-glycol liposomes in tumor-bearing mice. *Clinical Cancer Research* 9, 6551-6559 (2003).
- [9] Jain, R. K., Normalizing tumor vasculature with anti-angiogenic therapy: a new paradigm for combination therapy. *Nat Med* 7, 987-989 (2001).
- [10] Arnold, R. D., Mager, D. E., Slack, J. E. and Straubinger, R. M., Effect of repetitive administration of Doxorubicin-containing liposomes on plasma pharmacokinetics and drug biodistribution in a rat brain tumor model. *Clin Cancer Res* 11, 8856-8865 (2005).

- [11] Koukourakis, M. I., Koukouraki, S., Fezoulidis, I., et al., High intratumoural accumulation of stealth liposomal doxorubicin (Caelyx) in glioblastomas and in metastatic brain tumours. *Br J Cancer* 83, 1281-1286. (2000).
- [12] Pastorino, F., Brignole, C., Marimpietri, D., et al., Vascular damage and anti-angiogenic effects of tumor vessel-targeted liposomal chemotherapy. *Cancer Res.* 63, 7400-7409 (2003).
- [13] Pan, X. Q., Hang, H. and Lee, R. J., Antitumor activity of folate receptor-targeted liposomal doxorubicin in a KB oral carcinoma murine xenograft model. *Pharmaceutical research* 20, 417-422 (2003).
- [14] Wu, J., Liu, Q. and Lee, R. J., A folate receptor-targeted liposomal formulation for paclitaxel. *Int J Pharm* 316, 148-153 (2006).
- [15] Huwylar, J., Wu, D. and Pardridge, W. M., Brain drug delivery of small molecules using immunoliposomes. *Proc Natl Acad Sci U S A* 93, 14164-14169 (1996).
- [16] McNeeley, K., Annapragada, A. and Bellamkonda, R., Decreased circulation time offsets increased efficacy of PEGylated nanocarriers targeting folate receptors of glioma. *Nanotechnology* 18, 1-11 (2007).
- [17] Gabizon, A. and Papahadjopoulos, D., Liposome formulations with prolonged circulation time in blood and enhanced uptake by tumors. *Proc Natl Acad Sci U S A* 85, 6949-6953 (1988).

CHAPTER 2. CURRENT STATE OF GLIOMA THERAPIES

2.1. CURRENT TREATMENTS FOR BRAIN TUMORS ARE INSUFFICIENT

Current therapies for the treatment of gliomas remain problematic while the incidence of malignant gliomas is growing, leading to an increasing demand for more effective treatment options [1]. It is estimated that there will be 21,810 new cases and 13,070 deaths from cancers of the brain or nervous system in the United States in 2008, and 1 in 165 people will be diagnosed with cancer of the brain or nervous system in their lifetime [2]. Evidence suggests that the incidence of malignant brain tumors may be increasing particularly in the elderly [3], and gliomas are the second leading cause of death amongst children. Patients diagnosed with malignant brain tumors have a very poor prognosis with a current overall 5-year survival rate of merely 34.1% [2].

Brain tumors continue to be a challenge to treat because they are inherently diffuse, highly invasive, and non-localized. These tumors exhibit aberrant proliferation, reduced apoptosis, evasion of external growth control and immunoregulation, and resistance to therapeutics [4]. Instead of completely and permanently eliminating a malignant brain tumor, current treatments have typically been shown to merely prolong patient survival [5, 6, 1]. For these reasons, it is imperative that treatments for brain and nervous system cancers are improved.

2.2. CURRENT TREATMENT MODALITIES

Historically, the standard treatment of malignant gliomas has typically consisted of surgical resection followed by radiotherapy. Chemotherapy has also been utilized in combination under certain circumstances. Patient care is individualized on the basis of

prognostic factors including patient age, Karnofsky Performance Status (KPS) score, and tumor size, location, and histology [7, 8]. Other treatment options currently in use or under investigation include localized radiotherapy, localized chemotherapy, and targeted systemic chemotherapy. Novel treatment techniques continue to increase, and the National Cancer Institute reports over 400 clinical trials currently recruiting patients with brain tumors for the investigation of new treatment options [9]. In addition, the abundance of ongoing pre-clinical studies adds to the development of more effective treatments. Current research studies, however, must ensure that newly developed treatments not only improve long term survival rates, but also address patient quality of life, specifically considering the drastic side-effects often associated with current treatments which serve to reduce patient compliance. Here, the traditional treatment strategies as well as those recently developed or in development for the treatment of brain tumors are discussed.

2.2.1. SURGICAL RESECTION

Surgical resection is often the first line of defense in the treatment of brain tumors. It is performed to confirm tumor histology and to achieve maximal resection. Numerous studies have validated the benefit of surgery by comparing survival times between patients treated with radiation versus those undergoing craniotomy in addition to whole-brain radiotherapy [10, 11]. Patients who underwent surgery demonstrated a significant increase in median survival and experienced longer functional independence. Radical resection often leads to a better prognosis for patients [12, 13]. Surgical resection, however, is often incapable of completely removing deeply penetrating and diffuse brain tumors and typically results in tumor recurrence immediately adjacent to the

site of removal. It has been shown that greater than 95% of the brain tumor must be surgically excised to prevent progression of the disease [14]. Recurrence of tumors is common following surgical resection since it is often difficult to completely eradicate both the tumor and the invading tumor front without harming the adjacent healthy brain tissue, and recurrence of tumor invariably results in neurological deterioration and death. In addition, there are many risks associated with surgical resection since it is a highly invasive procedure. Some reported risks include operative death, infection, seizures, brain fluid flow blockage, peritumoral edema, and impaired neurological functions [15]. To reduce these risks, more effective and safer therapeutic procedures or adjuvant therapies must be developed for the treatment of malignant brain tumors.

2.2.2. RADIOSURGERY

Surgical resection may not be an option for patients if the brain tumor is located in an unresectable location or if the glioma is recurrent. In these cases, radiosurgery provides an acceptable treatment alternative [16]. Radiosurgery uses stereotaxy to precisely localize focal radiation typically delivered at doses between 54-60 Gy. Prescribed dose varies based on tumor size, location, and previous radiation treatments [16]. The target volume includes the tumor bed as well as an additional margin accounting for tumor infiltration into the surrounding healthy tissue [12]. Computed tomography (CT) or magnetic resonance imaging (MRI) is used to locate the tumor prior to radiosurgery. The most commonly used radiosurgery system is the Gamma Knife, which centers converging gamma radiation beams at the desired target [16]. Radiosurgery has proven effective at local tumor control and prolonging patient survival [17]. In addition, radiosurgery is less invasive than conventional surgical resection.

Despite these advantages, tumor recurrence and side effects similar to those reported for surgical resection are often associated with radiosurgery. In addition, stereotaxic radiosurgery often results in the development of late side effects due to the high radiation dose required per treatment [18].

2.2.3. WHOLE-BRAIN RADIATION THERAPY

Both surgical resection and radiosurgery typically require adjuvant postsurgical therapy due to the infiltrative nature of glioma. Whole-brain radiation therapy (WBRT) is often utilized for this purpose at a dosage ranging between 10-30 Gy [19]. WBRT has also traditionally been used to treat glioma due to concerns of multicentricity. While the use of WBRT has proven to provide swift attenuation of neurological symptoms, improve quality of life, enhance control of tumor progression, and decrease the likelihood of neurological death [19, 20], there still remain many complications associated with the procedure. The penetration of radiation therapy is limited by the energy of the incident photons, and increasing the energy to allow for deeper penetration invariably results in irradiation of healthy tissue. Resultant side effects may be either acute or late in occurrence and include fatigue, hair loss, scalp irritation, nausea, memory loss, mental deterioration, hormonal deficiencies, headaches, seizures, and possible death. In addition, prognosis after treatment tends to be poor with a median survival of merely 12 months following the combination of surgery and radiation therapy [1].

2.2.4. TRADITIONAL CHEMOTHERAPY

Currently, systemic chemotherapy is not the primary treatment choice for malignant brain tumors; however it may be utilized as an adjuvant therapy. Unfortunately, systemic delivery of chemotherapeutics exposes healthy organs to the

toxic side effects of the drug due to non-specific uptake. As a result, a lower dosage of the drug must be administered, causing the overall efficacy of the treatment to be decreased offering only a marginal impact on patient survival. In addition, brain tumors are unique from other types of cancer due to the presence of the blood brain barrier. Even though the BBB within the tumor environment is compromised exhibiting large inter-endothelial junctions (100-780 nm), delivery of traditional chemotherapeutics utilized as treatments for other types of cancer is limited. Patients with recurrent or high grade glioma will typically be administered small, lipophilic chemotherapeutics capable of crossing the BBB as an adjuvant treatment.

Temozolomide, as part of an adjuvant therapy, is the most commonly utilized chemotherapeutic drug for clinical treatment of glioma. Temozolomide has recently gained popularity over the traditionally used BCNU because it can be administered in oral form. Use of temozolomide (and other similar drugs) is primarily due to its physical properties (hydrophobicity and small size), which allow it to cross the BBB to reach tumor cells. However, if other drugs could reach the tumor (i.e. cross the BBB), temozolomide would have no advantage over these drugs. Primary toxicities associated with temozolomide include nausea and myelosuppression which result from non-specific drug uptake by healthy cells. These side effects lower the drug therapeutic index which makes dosing more difficult and thereby reduces treatment efficacy.

Theoretically, the BBB permeability of existing anticancer drugs utilized to treat other types of tumors could be increased by modifying them to be more lipophilic. However, clinical trials have demonstrated no significant increase in therapeutic efficacy using chemotherapeutics modified to increase lipophilicity [21]. Instead of altering the

drug itself, other efforts have focused on altering the BBB by infusing hyperosmolar mannitol causing dehydration of the endothelial cells followed by their shrinkage [22]. While hydrophilic drugs could penetrate better the disrupted BBB, the invasiveness of this method restricts its chronic use. Encapsulation of traditional chemotherapeutics within long-circulating nanocarriers has been shown to circumvent the issues of transport across the BBB by increasing the number of passages through the microvascular bed thereby escalating the probability of extravasation into tumor [23-25]. In addition, entrapment of drug reduces associated side-effects by shielding non-target organs from exposure. These nanocarriers may also be targeted to brain tumors to further increase treatment efficacy (See Section 2.2.3.2).

2.3. NOVEL TREATMENT APPROACHES

2.3.1. NOVEL RADIOTHERAPY TECHNIQUES

Localized radiotherapy techniques have recently been developed in an attempt to avoid the typical side effects associated with WBRT resulting from healthy tissue exposure. Brachytherapy involves interstitial delivery of radiotherapy. In this process, radiotherapy is directed to tumor in order to spare nearby normal brain tissue. This form of radiotherapy differs from radiosurgery because it involves the use of isotopes rather than gamma rays to treat the tumor. Iodine-125 (I^{125}) seeds have been studied most frequently and can be implanted permanently or temporarily at the tumor site. Unfortunately, studies have failed to demonstrate a significant advantage of this technique compared to WBRT, and reported complications such as isotope shift, neurologic decline, exacerbation of seizures, infection, and arterial occlusion, have made it so that this technique is rarely used today [26, 27].

A more promising development has been the GliSite Radiation Therapy System. This temporary brachytherapy technique utilizes an expandable balloon filled with I¹²⁵ solution implanted at the tumor resection site. The balloon adheres to the walls of the resection cavity and ensures a more homogeneous dose distribution of radiation [28]. Preliminary studies show potential, demonstrating a median survival time of 12.7 months for patients with recurrent glioma [29].

Another approach to improve local dose intensification of radiation is to use systemically delivered radiosensitizers. Many different agents have been reported including hypoxic sensitizers, s-phase sensitizers, and cytotoxic agents, however, with the exception of the cytotoxic agent, temozolamide, none of these treatments has demonstrated a distinct enhancement in therapeutic efficacy compared to radiotherapy alone [30]. In addition, systemic delivery of these radiosensitizers subjects non-target organs to the toxic effects of these drugs and delivery to tumor may be limited by the BBB. For the radiosensitizers to be effective, large numbers of molecules per cell may be required, and this may not be feasible for gliomas without use of delivery vehicles.

2.3.2. LOCALIZED CHEMOTHERAPY

Localized chemotherapeutic approaches are currently in use and under investigation in an attempt to circumvent the side effects associated with traditional systemic chemotherapy. These techniques are used to deliver drug directly to the tumor site.

2.3.2.1. Intra-Arterial Delivery

This technique was developed to deliver chemotherapeutics through the carotid artery to increase the amount of drug in contact with the BBB in an effort to enhance

transport into the brain while reducing systemic toxicity. The feasibility of drug transport across the BBB using this technique has been demonstrated with nitrosoureas; however, clinical studies have not yet demonstrated a clear advantage to this technique compared to traditional intravenous delivery. Significant risks are associated with intra-arterial delivery including local infarctions, leukoencephalopathy, and heightened neurotoxic effects [31]. In addition, technical difficulty and inadequate drug distribution within the tumor have limited the success of this treatment method [32].

2.3.2.2. Convection Enhanced Delivery

In an attempt to localize chemotherapeutics to the delivery site, a method has been developed using catheter systems to deliver chemotherapeutics directly to the tumor site [33, 34]. The advantage of this method is that chemotherapeutics may be able to reach a large brain volume and delivered in a sustained fashion. In addition, the BBB is bypassed and drug half-lives are prolonged. This treatment must be reserved for patients with non-resected tumors because it relies on directional flow from the bulk tumor mass to the periphery. This flow is reversed upon surgical removal of tumor due to the creation of an empty resection cavity. Limitations of convection enhanced delivery include drug uptake by healthy cells, high invasiveness, and a limited delivery area without the placement of multiple catheters. Despite successful results, associated risks such as infection, catheter blockage, inadequate drug distribution, elevated neurotoxic effects, and patient discomfort have limited clinical use of this technique.

2.3.2.3. Implantable Drug Depots

Implantable biodegradable drug depots positioned within brain tumors are currently being used in clinical practice in an effort to prevent exposure of healthy organs

to the toxic side effects of chemotherapeutics and to localize a chemotherapeutic and allow for prolonged and controlled drug delivery [35]. Gliadel[®] is an intracranial implantable polyanhydride polymer loaded with BCNU. BCNU (carmustine) has been widely used as a systemic agent due to its lipophilicity but efficacy is restricted by the dose-limited side effects [21, 36]. On the other hand, Gliadel[®] has produced better results for patients with grade IV glioma extending the median survival by 13.4 weeks compared to placebo [37, 38]. This method, however, relies on drug diffusion from a central core and short diffusion distances from the wafer limit the drug's accessibility to the entire tumor. As a result, drug usually cannot reach the tumor periphery where the most aggressive cells persist. In addition, BCNU released from the degradable wafer is non-specific and therefore cytotoxic to adjacent populations of healthy cells. Possible risks of this system include infection and uncontrolled drug release after implantation leading to local neurotoxicity. In addition, Gliadel wafers are unable to precisely conform to the resection cavity which could lead to incomplete exposure of the remaining tumor cells.

2.3.3. TARGETED SYSTEMIC DELIVERY OF CHEMOTHERAPEUTICS

Local treatment strategies discussed thus far have been developed in an attempt to alleviate some of the side effects associated with traditional treatment of glioma. While treatments are geographically localized to tumor, they remain non-specific and normal cells located within and/or near the tumor site will inevitably be affected by these treatment strategies. In addition, these local treatment options do not address the invasiveness of gliomas. Many of the treatments presents thus far suffer from diffusion limitations or simple inability to access the distant spread of tumor and the invasive cells

located at the edge of the tumor lesion. Chemotherapy via systemic intravascular administration utilizes the tumor's own blood supply for transport allowing for drug delivery throughout the entire tumor and is minimally non-invasive. The addition of targeting agents increases treatment specificity and reduces toxic side effects of the chemotherapeutic drugs. As with traditional chemotherapy, the BBB may be a formidable obstacle; however, transport into the tumor may be facilitated by transient disruption of the BBB, through drug modifications to increase lipophilicity, or by prolonging drug circulation times to increase transport based on the enhanced permeability and retention effect. The latter method is referred to as "passive targeting" and will be described in greater detail in Chapter 3.

2.3.3.1. Direct Drug Modification

Chemotherapeutic drugs may be chemically modified to enable specific targeting to tumor. Possible targeting agents include tumor-specific antibodies, antibody fragments, ligands, and peptides. BBB transport may also be facilitated by creating lipophilic drug analogs. The limitations of these approaches, however, include low drug payloads delivered to tumor, accelerated clearance due to binding of plasma proteins, reduced solubility in the brain interstitial fluid, and renal clearance due to small size of drug conjugates. In addition, monoclonal antibody-drug conjugates utilized to target tumors have been shown to exhibit decreased potency compared to the parent drug [39]. This may be attributed to heterogeneity of antigen expression within tumor, inefficient internalization of conjugated drug, inability to cleave the conjugate and release active free drug, or the development of drug resistance by cancer cells.

2.3.3.2. Targeted Nanocarriers

The use of targeted nanocarriers to deliver chemotherapeutics allows for higher drug payloads, drug protection from degradation, increased drug solubility, ability to evade the immune system and prolong drug half-lives, multi-valent binding, and/or facilitated delivery across the BBB. In particular, the delivery of increased drug payloads enables successful treatment of drug resistant cells due to saturation of drug efflux pumps. These characteristics make targeted nanocarriers ideal candidates for specific delivery of chemotherapeutics to tumors. Targeted nanocarrier drug delivery systems will be discussed in more detail in Chapter 3.

2.4. CONCLUSIONS

Traditional treatments for brain cancer have failed to significantly alter the reported median survival rate over the past three decades. The current median survival rate is less than one year with a reported 5-year survival rate of merely 34.1%. Adjuvant treatments to surgical resection are mandatory; however, the main disadvantage of these therapies is that they are non-selective and subsequently toxic to healthy tissues. Localization of radiation or chemotherapeutics has been investigated, however, these approaches remain non-specific with the ability to injure normal cells, and these approaches limit treatment of the tumor periphery where the most aggressive cancer cells persist. Tumor recurrence due to incomplete removal ultimately results in neurological deterioration and death. For these reasons, it is imperative that current therapeutic efficacy is improved through the development of innovative, specifically-targeted systemic treatment strategies utilizing the tumor's own blood supply given that the tumor is highly invasive and local therapies have demonstrated only limited enhancement in

survival. The use of targeted nanocarriers will allow for the protection of healthy tissues from the toxic effects of chemotherapeutics while enabling the delivery of large drug payloads to tumor.

2.5. REFERENCES

- [1] Mohan, D. S., Suh, J. H., Phan, J. L., et al., Outcome in elderly patients undergoing definitive surgery and radiation therapy for supratentorial glioblastoma multiforme at a tertiary care institution. *Int J Radiat Oncol Biol Phys* **42**, 981-987 (1998).
- [2] Ries, L., Melbert, D., Krapcho, M., et al. (eds.) *SEER Cancer Statistics Review, 1975-2005*, National Cancer Institute. Bethesda, MD, http://seer.cancer.gov/csr/1975_2005/, based on November 2007 SEER data submission, posted to the SEER web site, 2008. Accessed June 1, 2008.
- [3] Hess, K. R., Broglio, K. R. and Bondy, M. L., Adult glioma incidence trends in the United States, 1977-2000. *Cancer* **101**, 2293-2299 (2004).
- [4] Burger, P. C., Vogel, F. S., Green, S. B. and Strike, T. A., Glioblastoma multiforme and anaplastic astrocytoma. Pathologic criteria and prognostic implications. *Cancer* **56**, 1106-1111 (1985).
- [5] Barker, F. G., 2nd, Chang, S. M., Gutin, P. H., et al., Survival and functional status after resection of recurrent glioblastoma multiforme. *Neurosurgery* **42**, 709-720; discussion 720-703 (1998).
- [6] Black, K. L. and Pikul, B. K., Gliomas--past, present, and future. *Clin Neurosurg* **45**, 160-163 (1999).
- [7] National Comprehensive Cancer Network: Central Nervous System Cancers Version 1.2008. Available at: http://www.nccn.org/professionals/physician_gls/pdf/cns.pdf. Accessed June 19, 2008.
- [8] Ewend, M. G., Elbabaa, S. and Carey, L. A., Current treatment paradigms for the management of patients with brain metastases. *Neurosurgery* **57**, S66-77; discussion S61-64 (2005).
- [9] www.cancer.gov/clinicaltrials, Vol. 2008: National Cancer Institute, 2008. Accessed June 19, 2008.
- [10] Patchell, R. A., Tibbs, P. A., Walsh, J. W., et al., A randomized trial of surgery in the treatment of single metastases to the brain. *N Engl J Med* **322**, 494-500 (1990).

- [11] Vecht, C. J., Haaxma-Reiche, H., Noordijk, E. M., et al., Treatment of single brain metastasis: radiotherapy alone or combined with neurosurgery? *Ann Neurol* **33**, 583-590 (1993).
- [12] Broniscer, A., Past, present, and future strategies in the treatment of high-grade glioma in children. *Cancer Invest* **24**, 77-81 (2006).
- [13] Hess, K. R., Extent of resection as a prognostic variable in the treatment of gliomas. *J Neurooncol* **42**, 227-231 (1999).
- [14] Keles, G. E., Anderson, B. and Berger, M. S., The effect of extent of resection on time to tumor progression and survival in patients with glioblastoma multiforme of the cerebral hemisphere. *Surg Neurol* **52**, 371-379 (1999).
- [15] Sills, A. K., Current treatment approaches to surgery for brain metastases. *Neurosurgery* **57**, S24-32; discussion S21-24 (2005).
- [16] McDermott, M. W. and Sneed, P. K., Radiosurgery in metastatic brain cancer. *Neurosurgery* **57**, S45-53; discussion S41-44 (2005).
- [17] Nwokedi, E. C., DiBiase, S. J., Jabbour, S., et al., Gamma knife stereotactic radiosurgery for patients with glioblastoma multiforme. *Neurosurgery* **50**, 41-46; discussion 46-47 (2002).
- [18] Mehta, M. P., The physical, biologic, and clinical basis of radiosurgery. *Curr Probl Cancer* **19**, 265-329 (1995).
- [19] Mehta, M. P. and Khuntia, D., Current strategies in whole-brain radiation therapy for brain metastases. *Neurosurgery* **57**, S33-44; discussion S31-34 (2005).
- [20] Order, S. E., Hellman, S., Von Essen, C. F. and Kligerman, M. M., Improvement in quality of survival following whole-brain irradiation for brain metastasis. *Radiology* **91**, 149-153 (1968).
- [21] Kornblith, P. L. and Walker, M. D., *In "Advances in Neuro-oncology"*. (Future Publishing Co., Mount Kisco, NY, 1988).

- [22] Rapoport, S. I., Osmotic opening of the blood-brain barrier: principles, mechanism, and therapeutic applications. *Cell Mol Neurobiol* **20**, 217-230 (2000).
- [23] Koukourakis, M. I., Koukouraki, S., Fezoulidis, I., et al., High intratumoural accumulation of stealth liposomal doxorubicin (Caelyx) in glioblastomas and in metastatic brain tumours. *Br J Cancer* **83**, 1281-1286. (2000).
- [24] Sharma, U. S., Sharma, A., Chau, R. I. and Straubinger, R. M., Liposome-mediated therapy of intracranial brain tumors in a rat model. *Pharm Res* **14**, 992-998. (1997).
- [25] Siegal, T., Horowitz, A. and Gabizon, A., Doxorubicin encapsulated in sterically stabilized liposomes for the treatment of a brain tumor model: biodistribution and therapeutic efficacy. *J Neurosurg* **83**, 1029-1037 (1995).
- [26] Laperriere, N. J., Leung, P. M., McKenzie, S., et al., Randomized study of brachytherapy in the initial management of patients with malignant astrocytoma. *Int J Radiat Oncol Biol Phys* **41**, 1005-1011 (1998).
- [27] Selker, R. G., Shapiro, W. R., Burger, P., et al., The Brain Tumor Cooperative Group NIH Trial 87-01: a randomized comparison of surgery, external radiotherapy, and carmustine versus surgery, interstitial radiotherapy boost, external radiation therapy, and carmustine. *Neurosurgery* **51**, 343-355; discussion 355-347 (2002).
- [28] Stubbs, J. B., Frankel, R. H., Schultz, K., et al., Preclinical evaluation of a novel device for delivering brachytherapy to the margins of resected brain tumor cavities. *J Neurosurg* **96**, 335-343 (2002).
- [29] Tatter, S. B., Shaw, E. G., Rosenblum, M. L., et al., An inflatable balloon catheter and liquid ¹²⁵I radiation source (GliaSite Radiation Therapy System) for treatment of recurrent malignant glioma: multicenter safety and feasibility trial. *J Neurosurg* **99**, 297-303 (2003).
- [30] Chang, J. E., Khuntia, D., Robins, H. I. and Mehta, M. P., Radiotherapy and radiosensitizers in the treatment of glioblastoma multiforme. *Clin Adv Hematol Oncol* **5**, 894-902, 907-815 (2007).
- [31] Giese, A. and Westphal, M., Treatment of malignant glioma: a problem beyond the margins of resection. *J Cancer Res Clin Oncol* **127**, 217-225 (2001).

- [32] Rautio, J. and Chikhale, P. J., Drug delivery systems for brain tumor therapy. *Current pharmaceutical design* **10**, 1341-1353 (2004).
- [33] Ratcheson, R. A. and Ommaya, A. K., Experience with the subcutaneous cerebrospinal-fluid reservoir. Preliminary report of 60 cases. *N Engl J Med* **279**, 1025-1031 (1968).
- [34] Saito, R., Krauze, M. T., Noble, C. O., et al., Convection-enhanced delivery of Ls-TPT enables an effective, continuous, low-dose chemotherapy against malignant glioma xenograft model. *Neuro Oncol* **8**, 205-214 (2006).
- [35] Wang, P. P., Frazier, J. and Brem, H., Local drug delivery to the brain. *Adv Drug Deliv Rev* **54**, 987-1013 (2002).
- [36] Walker, M. D., Green, S. B., Byar, D. P., et al., Randomized comparisons of radiotherapy and nitrosoureas for the treatment of malignant glioma after surgery. *N Engl J Med* **303**, 1323-1329 (1980).
- [37] Brem, H., Piantadosi, S., Burger, P. C., et al., Placebo-controlled trial of safety and efficacy of intraoperative controlled delivery by biodegradable polymers of chemotherapy for recurrent gliomas. The Polymer-brain Tumor Treatment Group. *Lancet* **345**, 1008-1012 (1995).
- [38] Valtonen, S., Timonen, U., Toivanen, P., et al., Interstitial chemotherapy with carmustine-loaded polymers for high-grade gliomas: a randomized double-blind study. *Neurosurgery* **41**, 44-48; discussion 48-49 (1997).
- [39] Kanellos, J., Pietersz, G. A. and McKenzie, I. F., Studies of methotrexate-mono-clonal antibody conjugates for immunotherapy. *J Natl Cancer Inst* **75**, 319-332 (1985).

CHAPTER 3. THERAPEUTIC NANOCARRIERS FOR DRUG DELIVERY TO TUMORS

3.1. INTRODUCTION

Nanocarriers have been studied extensively for the targeted delivery of therapeutic drugs, genes, or imaging agents to tumors in an attempt to increase selectivity of these agents and to enable delivery of large drug payloads to the target site. In contrast to large-scale drug delivery systems, nanocarriers enable easier penetration through biological and physiological barriers within the body due to their small size (at least one dimension between 1-100 nm) [1, 2]. Nanocarriers have been shown to improve drug stability *in vivo* and may serve to protect non-target organs from drug uptake. There are many different types of systemically delivered nanocarriers that are either currently being investigated or are clinically approved for drug delivery to tumors. Each class of nanoparticles encompasses different characteristics; however, the following essential conditions are universal [2]:

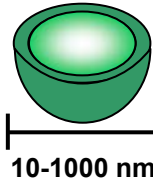
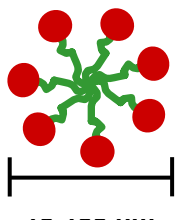
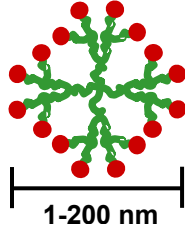
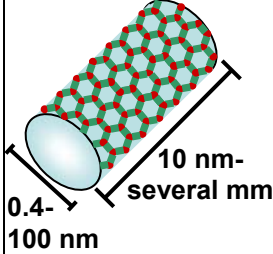
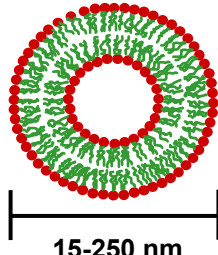
- 1) biodegradability
- 2) biocompatibility
- 3) non-immunogenicity
- 4) physical stability in the blood

3.2. TYPES OF NANOCARRIERS USED FOR TARGETED DELIVERY TO TUMORS

There exist numerous types of nanocarriers currently utilized for tumor targeted delivery applications. This chapter will focus on those designed with the capability to

transport chemotherapeutics to tumors. While this is not an exhaustive list, some of the most commonly used types of nanocarriers are reviewed here (Table 3.1).

Table 3.1. Various Nanocarrier-Based Drug Delivery Platforms

System	Material	Structure	Characteristics
Polymeric Nanoparticles	PLGA PLA PCL Chitosan HSA		--Sustained drug release --Limited control over degradation rates --Harsh formulation conditions
Polymeric Micelles	PLGA PLA PCL PPO poly(L-histidine) poly(L-aspartic acid) poly(L-glutamic acid)		--Prolonged circulation --Limited drug loading --Stability depends on CMC
Dendrimers	Polyamidoamine PEO Glycerol Succinic acid Phenylalanine Lactic acid		--Monodisperse --Multivalent --Limited drug loading
Carbon Nanotubes	Graphene		--Absorb heat for thermal ablation of tumors --High Stability --Non-biodegradable --Limited data on biocompatibility
Liposomes	Phospholipids Cholesterol Polyethylene glycol CHEMS Gangliosides		--Biocompatible --Passive accumulation to tumor --Efficient and stable drug loading --Heating required for entrapment of drug

3.2.1. POLYMERIC NANOPARTICLES

Polymeric nanoparticles are produced from natural or artificial polymers and range in size from 10 to 1000 nm. They can be formulated directly from polymers or from the polymerization of monomers. Nanospheres are spherical in shape and composed of a polymer matrix. Drugs are entrapped, encapsulated, or attached to the nanospheres for delivery to target sites. Nanocapsules are hollow spheres composed from natural or artificial polymers. The hollow central core may be utilized for drug encapsulation [4].

Many different polymers have been investigated for polymeric nanoparticles utilized for drug delivery due to intense research within the past decade. These biodegradable and biocompatible polymers are degraded either enzymatically or non-enzymatically within the body into inert compounds such as hydrogen, nitrogen, and water, removed by normal metabolic pathways, and then excreted. Polymers can be either natural or synthetic. Synthetic polymers typically degrade more slowly than natural polymers allowing for sustained drug delivery over a period of days to several weeks, however, harsher formulation conditions are often required involving organic solvents which must be thoroughly removed prior to patient administration [4]. Drug release rate is controlled through modulation of the polymers utilized in the nanoparticle formulation. The most commonly utilized polymers include poly(lactide-co-glycolide) (PLGA) [5, 6], polylactide acid (PLA) [7], poly ϵ -caprolactone (PCL) [8, 9], chitosan [10, 11], and human serum albumin [12].

The periphery of polymeric nanoparticles may be modified with targeting agents or additional polymers. Additional polymers may be used to further prolong circulation

of the nanoparticles and thereby improve drug pharmacokinetics. Specific targeting agents, such as those that bind to tumor receptors or tumor specific antigens, are often utilized to increase specificity of chemotherapeutics loaded in polymeric nanoparticles. For example, a recent study utilizing PLGA-PEG nanoparticles functionalized with an aptamer that binds to the prostate specific membrane antigen demonstrated a significant increase in delivery to prostate tumors in xenograft mouse models compared to non-targeted controls [13]. These findings confirm the applicability of polymeric nanoparticles as tumor targeted drug carriers.

3.2.2. POLYMERIC MICELLES

Micelles are structures formed by the spontaneous association of amphiphilic copolymers in an aqueous environment. The driving force for formation is primarily hydrophobic interactions causing the non-polar segments of the copolymer molecules to form the micellar core and the relatively polar segments to form the micellar corona positioned between the hydrophobic core and the aqueous bulk phase. The hydrophilic corona enables water solubility, prevents aggregation, and prevents protein absorption on micelles, while the hydrophobic core is used to encapsulate drugs and enables biodegradability [14]. Self-assembly is initiated when the block copolymers exceed a threshold concentration known as the critical micellization concentration (CMC). Below the CMC, the copolymers exist as single chains dispersed within the bulk phase. The CMC is an important factor in the design of micelles for drug delivery applications, because the stability of micelles, which are considerably diluted following i.v. administration to patients, is critically dependent on this number. CMCs of pharmaceutical micellar nanocarriers typically range between 10^{-6} to 10^{-4} μM [15].

Micelles with the lowest CMCs can withstand the greatest dilution which makes them better candidates for biomedical applications.

The CMC of micellar formulations can be altered by changing the properties of the block copolymers comprising the micelles. An increase in the hydrophobicity or size of the micelle core has been shown to result in a highly correlated decrease in the CMC [16]. In addition, an increase in the size of the hydrophilic segments serves to increase the CMC, albeit to a lesser extent. Hydrophobic additives incorporated into the micelle core have been shown to lower the CMC and increase the number of copolymers associating to form each micelle. The CMC is typically unaffected by temperature changes with the exception of micelles composed from poloxamers [17].

The micelle shape is typically spherical or globular and primarily depends on the length of the hydrophobic segments of the amphiphilic copolymers [18]. The size of micelles ranges between 10-100 nm, depending on copolymer length, molecular weight, and relative proportion of hydrophobic and hydrophilic segments, which all determine how well the copolymers pack within the micelle. The nanoscopic size of micelles facilitates sterile filtration prior to patient administration. In addition, the typical mass of an intact micelle varies between 100-1000 kDa which allows them to penetrate capillaries within the body and bypass glomerular filtration and excretion by the kidneys with a renal threshold of 42-50 kDa [19]. If diluted below the CMC, however, individual copolymers are rapidly removed by the kidneys [20].

The most commonly studied compounds used for the hydrophobic segment of copolymers comprising micelles can be classified into 3 groups: polyethers, polyesters, and polyamides. Hydrophobic polyesters, such as poly(L-lactide) (PLA), poly(lactide-

co-glycolide) (PLGA), and poly(ϵ -caprolactone) (PCL), are used most frequently. Polyesters are sensitive to hydrolytic degradation making them suitable biodegradable candidates for the micelle core. Poly(propylene oxide) (PPO) is an example of a commonly used polyether, and poly(L-histidine), poly(L-aspartic acid) derivatives, and poly(L-glutamic acid) derivatives are examples of polyamides utilized for the micelle core. Polyamides are often degraded by enzymes within the body; therefore, they are also considered to be biodegradable. The most commonly used polymer for the hydrophilic corona of micelles is polyethylene glycol (PEG) of molecular weight ranging from 1-15 kDa [21]. PEG is completely soluble in water, inexpensive, non-toxic, and uncharged. It also serves as an efficient steric barrier between micelles and plasma proteins responsible for removing foreign particles from the bloodstream promoting prolonged circulation times. Micelles using PEG in the corona have exhibited plasma half-lives of 18 hours after intravenous administration [22]. Alternatives to PEG for the hydrophilic portion of micelles include poly(N-vinyl pyrrolidone) (PVP) [23] and poly(vinyl alcohol) (PVA) [24]. Poloxamers are copolymers of PEG and PPO oriented in a PEG-PPO-PEG configuration. Also referred to as Pluronics, these polymers micellize with the PPO segments localizing in the hydrophobic core and the PEG segments forming the hydrophilic corona. Poloxamer micelles have been studied extensively and have been investigated for the delivery of doxorubicin [25-27], vinblastine [28], cisplatin [28], and nystatin [29].

The hydrophobic core of polymeric micelles makes them useful for the delivery of water insoluble drugs. Drugs may be encapsulated within the core [30] or covalently conjugated to the polymers comprising the micelles [31]. The corona serves to protect

the associated drugs from degradation prior to delivery. Sustained release of drug may be achieved if the drugs entrapped within the micelle possess extremely small (10^{-16} to 10^{-18} cm²/sec) diffusion coefficients [32]. Micellar drugs may be targeted to specific drug delivery sites by chemical conjugation of target-specific molecules to the micelle corona. In addition, micelles may be functionalized to allow triggered drug delivery. Various formulations have been studied including those sensitive to pH [33], temperature [34], and ultrasound [35].

3.2.3. DENDRIMERS

Dendrimers are nanocarriers composed of multiple highly-branched monomers forming a three dimensional treelike structure emerging from a central core. Dendrimers are typically globular or spherical in shape with diameters ranging from 1-200 nm although the most commonly utilized dendrimers composed from polyamidoamine typically do not exceed 15 nm in diameter [36]. Dendrimers tend to have high molecular weights despite their nanoscale size. Synthesis of dendrimers is stepwise producing highly regular branching patterns with repeated units and a distinct number of peripheral groups. Polymerization may proceed from the periphery and terminate at the central core or initiate from the core and terminate at the external surface. Branch lengths are limited by steric hindrance. The low polydispersity associated with these nanocarriers allows for reproducible pharmacokinetic behavior *in vivo*. The branching pattern of dendrimers enables the attachment of many drugs, targeting agents, and/or solubilizing groups to the periphery of a single carrier. As a result, dendrimers have been investigated for a variety of biological applications including gene delivery [37], magnetic resonance imaging [38], and anticancer therapeutics [39].

Dendrimers for the delivery of pharmaceuticals may be formulated from a variety of compounds. The most widely used dendrimer scaffolds in biology are those prepared from polyamidoamine. To avoid toxicity and liver accumulation, the surface amine groups of these dendrimers must be modified with neutral moieties. Other dendrimer formulations have been made from polyethylene oxide, glycerol, succinic acid, phenylalanine, or lactic acid [36].

The versatile nature of dendrimers allows them to deliver either hydrophobic or hydrophilic agents to a target site. Drugs may be covalently attached to functional groups on the dendrimer or simply associated with the internal core of the sphere by electrostatic interactions, hydrogen bonding, or hydrophobic interactions [40], however, studies investigating the noncovalent encapsulation of doxorubicin and methotrexate within polyamidoamine dendrimers showed that drugs were not readily retained in isotonic solutions and loading efficiencies were relatively low. A maximum of merely 6.5 DXR and 26 methotrexate molecules were loaded per dendrimer [41], therefore, this loading method has yet to be utilized as a common strategy. Covalent attachment of drugs is also limited since each drug molecule requires a functionalized branch of the dendrimer for attachment. Nonetheless, covalent attachment of chemotherapeutics such as DXR and cisplatin to dendrimers has been investigated and shown to be successful. Covalent association of DXR to PEO dendrimers resulted in a 9-fold increase in tumor delivery compared free DXR when administered to mice bearing subcutaneous C-26 tumors. In addition, survival was significantly enhanced for these animals compared to those receiving free DXR therapy. The reported antitumor effect was comparable to that achieved with Doxil[®], a clinically approved liposomal DXR treatment [39]. Tumor

targeting may be achieved with dendrimers through the covalent attachment of targeting agents. For example, it has been shown that the attachment of folic acid to polyamidoamine dendrimers carrying covalently attached methotrexate enhances uptake by human epithelial carcinoma (KB) cells *in vitro* [42]. Dendrimers serve as good candidates for anti-cancer therapy due to their monodispersity, multivalency, water solubility, and capability for surface modification.

3.2.4. CARBON NANOTUBES

Carbon nanotubes are cylinders formed from benzene rings and are single or multi-walled with a cage like structure. Single walled carbon nanotubes (SWNT) consist of a layer of graphene rolled into a cylinder while multi-walled carbon nanotubes (MWNT) are composed of multiple concentric layers of graphene rolled into cylinders spaced approximately 0.34 nm apart [43]. Diameters of SWNTs typically range from 0.4-3 nm, while MWNT diameters may reach up to 100 nm. Nanotube lengths vary from 10 nm up to several millimeters [44]. Without surface modification, carbon nanotubes are completely insoluble; however, the nanotubes may be covalently or non-covalently modified through the attachment of polymers, such as PEG, to increase solubility for biological applications. The external surface of carbon nanotubes may also be functionalized for the attachment of drugs or targeting agents to facilitate specific uptake by target cells [45]. Conversely, drugs, fullerenes, porphyrins, or metals may be trapped inside the nanotubes due to hydrophobic interactions for delivery to target sites. Due to the large available surface area of nanotubes, multiple types of targeting agents and/or drugs may be simultaneously attached providing a functional advantage in cancer therapy [46]. The tips at the ends of the nanotubes are best described as fullerene hemispheres

and are more reactive than the sidewalls of the nanotubes. As a result, most reactions typically occur at the tips of the nanotubes and at sidewall imperfections before occurring at the intact sidewalls [47].

Recent studies have demonstrated the ability to utilize carbon nanotubes in the treatment of cancer. Since carbon nanotubes intrinsically absorb near infrared (NIR) and radio waves resulting in the local generation of heat, they have been investigated in attempts to thermally ablate cancer cells. Experiments have been conducted using targeted [48, 49] or locally delivered non-targeted [50] nanotubes followed by the application of radiofrequency or NIR radiation to examine the effects on cancer cells. Kam, *et al.*, absorbed phospholipid-PEG-folate conjugates to carbon nanotubes and observed selective cancer cell death after exposing cultures to the targeted nanotubes and NIR light [48]. Another study demonstrated selective cancer cell death after targeting PEG coated carbon nanotubes to breast cancer cells using antibodies against insulin-like growth factor 1 receptor and human endothelial receptor 2 and applying NIR radiation [49]. Radio waves were utilized instead of NIR in another study since they can penetrate deeper through the body. Non-targeted carbon nanotubes were injected directly into a liver tumor before applying the radio waves. This resulted in cell death at the target site with slight damage to the neighboring healthy cells [50].

Carbon nanotubes have also been studied in the delivery of chemotherapeutics such as doxorubicin [51, 52] and methotrexate [53, 45] to directly kill cancer cells. Pastorin, *et al.* demonstrated efficient uptake of carbon nanotubes covalently loaded with methotrexate by Jurkat cells [53]. Another study investigated DXR loaded PEGylated carbon nanotubes and discovered that noncovalent association of DXR was highly

efficient due to Π -stacking and that binding efficiency and release rates were dependent on both pH and nanotube diameter. Nanotubes were targeted to tumor cells through covalent attachment of RGD peptide and after administering to U87MG cells, enhanced uptake and cytotoxicity was observed. In fact, IC_{50} values of the targeted nanotubes (3 μ M) approached values obtained with free DXR (2 μ M) [52].

The use of carbon nanotubes for the delivery of therapeutic molecules is a relatively new concept. Limited data exists regarding biocompatibility; however, the potential advantages of these nanocarriers compel further investigation of their use. Carbon nanotubes are highly stable due to their mechanical properties. In addition, they have been shown to effectively penetrate target cells, and their large surface area and internal volume allows for multiple functionalization and entrapment of therapeutic molecules [54, 55]. Disadvantages to their use include the fact that they are non-biodegradable, their large surface area may increase the probability of protein opsonization, chemical modification is required to ensure solubility in biological fluids, and they possess a strong tendency to aggregate. Despite these challenges, carbon nanotubes present a promising option for delivery of chemotherapeutics to tumors.

3.2.5. LIPOSOMES

Liposomes are closed spherical nanoscale vesicles composed of lipid bilayers. Multilamellar liposomes are composed from several lipid layers with alternating regions of hydrophobicity and hydrophilicity. Unilamellar liposomes consist of a single bilayer enclosing an aqueous core. Cholesterol is often incorporated into liposomes used for biological applications to enhance physical stability. Formed in a manner similar to

micellar formation, hydrophobic interactions play a central role in the self-assembly of liposomes from amphiphilic lipids.

3.2.5.1. Formulation Components

Liposomes may be composed from a variety of phospholipids, the most common being either natural (egg or soy) or synthetic phosphocholine. The phospholipid content typically varies anywhere from 55-100% (molar) of the liposome components. The chemical structure of a common formulation component, 1,2-distearoyl-sn-glycerophosphocholine (DSPC), is shown in Figure 3.1a. This molecule represents the typical structure of an amphipathic liposomal component and is composed of a polar phosphate head group bound to hydrocarbon chains. The hydrocarbon chains make up the hydrophobic portion of the molecule which forms the interior of the liposome bilayer. The polar head group forms the exterior of the bilayer and is in direct contact with the exterior and interior buffers. The level of fatty acid saturation on the selected lipids has an affect on the overall stability because it determines the susceptibility to oxidation. Typically, the more saturated a lipid the less vulnerable it is to oxidation. Phospholipids derived from biological sources, such as egg or soybean, tend to contain substantial levels of polyunsaturated fatty acids making them less stable than the synthetic equivalents. The phospholipid head group may be substituted by a functional group to allow attachment of other components such as polyethylene glycol and/or targeting moieties. 1,2-distearoyl-sn-glycero-3-phosphoethanolamine (DSPE) is an example of a functional phospholipid used to conjugate such agents (Figure 3.1b).

It is these phospholipids which primarily dictate the ultimate shape of the liposomes. Packing of the phospholipids to constitute the liposome bilayer is dependent

on the total length of the molecule and the respective sizes of the head groups and hydrocarbon chains. A so-called “packing factor” (P) may be determined from the lipid tail region volume (v) divided by the product of the cross-sectional area of the polar head group (a) and the total length of the phospholipid molecule (l) given by Equation 3.1 [56]:

$$P = \frac{v}{a \times l} \quad (\text{Equation 3.1})$$

Packing factors ranging between 0.5-1 typically lead to spherical bilayer vesicles.

Another characteristic to consider in the selection of phospholipids for liposome formulation is the phase transition temperature. The phase transition temperature is defined as the temperature at which the lipid physical state converts from an ordered gel phase to a disordered liquid crystalline phase and is depended on hydrocarbon chain length, degree of saturation, charge, and head group species. In the gel-like phase, hydrocarbon chains are fully extended and tightly packed while they are randomly oriented and fluid in the liquid phase [57]. Lengthened hydrocarbon chains and increased levels of saturation result in elevated phase transition temperatures due to stronger van der Waals interactions. The use of phospholipids with higher phase transition temperatures generates bilayers which are more stable [58]. This decreases the possibility for premature leakage of encapsulated components; however, considerations must be made to ensure that encapsulated drugs can still escape the liposomes once they reach the target site of action. In addition, the phase transition temperature of the liposome bilayer dictates the temperature above which sizing, drug loading, and insertion of additional components should occur since these processes are most efficient when the

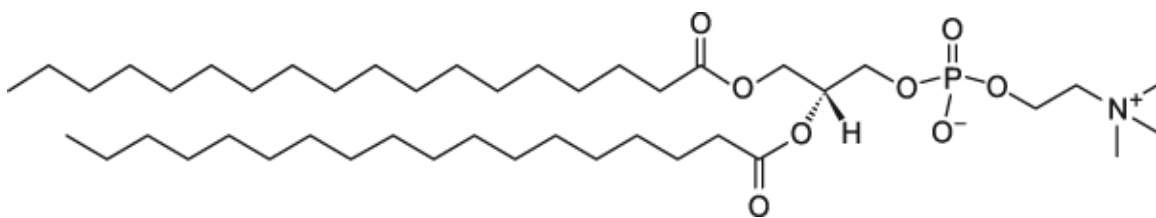
bilayer is in the crystalline fluid state. If the phase transition temperature of the selected phospholipids is too high, denaturation of proteins and/or drugs may occur during the sizing, loading, and/or insertion processes. Therefore, a careful balance must be met to ensure that the selected lipids have phase transition temperatures that prevent premature leakage of components but enable processing to occur at temperatures that are harmless to all liposomal components.

Cholesterol is often included into the liposomal formulation at a percentage of 30-45% (molar) to help modulate membrane fluidity, elasticity, and permeability and to instill stability (Figure 3.1c). Within the lipid bilayer, the polar head of cholesterol is aligned with the polar head of the phospholipids. As in biological cell membranes, the hydrophobic properties of cholesterol ensure that it resides in the interior portion of the bilayer where it serves to fill the gaps created by imperfect packing to inhibit flip-flop of membrane components and prevent movement of components within the bilayer. Cholesterol also adds rigidity to the liposomes by preventing phase transitions of the bilayer thereby decreasing leakage of components encapsulated within the liposomes or trapped within the bilayer [59]. In this manner, the amount of cholesterol utilized also has an effect on the ultimate phase transition temperature of the bilayer. Finally, some studies have shown that the inclusion of cholesterol may help to protect the bilayer from hydrolytic degradation by demonstrating that the water penetration depth into lipid bilayers is reduced when cholesterol is present [60].

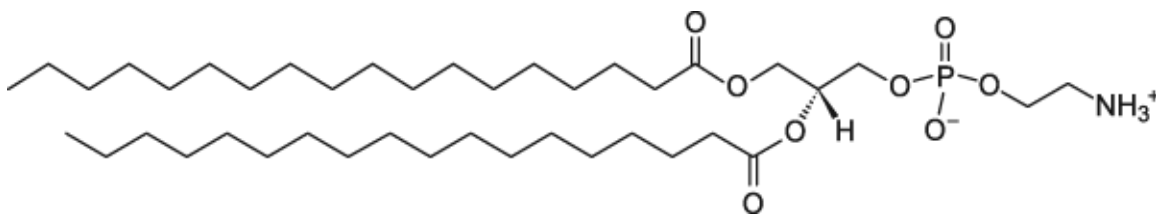
Other components are often included in liposomal formulations depending on the final application. If rapid release of internal components at altered pH is desired, pH sensitive lipids such as dioleoyl phosphatidyl ethanolamine (DOPE) and pH stabilizers

such as cholesteryl hemisuccinate (CHEMS) may be incorporated [61]. Cationic lipids are often used in liposomes intended for the delivery of DNA or gene products [62-64]. PEG is typically incorporated to enable RES evasion and prolonged circulation times while targeting agents may be inserted to facilitate specific targeting to tumor cells. Passive and active targeting of liposomes using these components will be discussed further in a later section of this chapter.

A



B



C

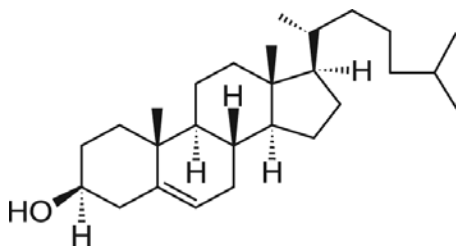


Figure 3.1. Chemical structures of DSPC (A), DSPE (B), and cholesterol (C).

3.2.5.2. Preparation Techniques

There exist numerous preparation techniques for liposomal formulations including detergent removal, emulsion removal, ethanol injection, and solvent removal. A more detailed discussion of these techniques may be found elsewhere [65]. Choice of preparation technique dictates final liposome size and number of bilayers. Solvent removal is one of the most commonly used techniques [66]. Lipids are dissolved in organic solvents such as chloroform or a mixture of chloroform and methanol to ensure a homogeneous mixture. Lipid solutions are typically prepared at a concentration ranging between 10-20 mg/ml depending on the lipid solubility. Solvent is subsequently removed by evaporation to produce a thin film of lipids. Hydration of the dry lipid film is accomplished through the addition of an aqueous medium (typically prepared at physiological osmolarity for *in vivo* applications) at a temperature above the highest phase transition temperature (T_c) of the lipids. Hydration produces large (200-1000 nm), multilamellar vesicles (LMV). Interlamellar spacing is dictated by the level of electrostatic repulsion between the polar head groups of the phospholipids.

Sizing of multilamellar liposomes is typically performed via sonication or extrusion. Sonication is performed at temperatures above the lipid T_c where sonic energy serves to disrupt the LMV and produce small unilamellar vesicles (SUV) ranging between 15-50 nm in diameter. Many factors help to determine final size including lipid composition, concentration and suspension volume, and sonication time and power. Unfortunately, sonication often results in size variations between batches. Extrusion involves forcing the LMV through etched polycarbonate filters with defined pore sizes. This process is typically performed under high pressure and at a temperature above the

lipid Tc. Diameters of the liposomes after extrusion tend to be close to the filter pore size. Extrusion through filters with 100 nm pores yields large, unilamellar vesicles (LUV) of reproducible size. Final diameter depends on lipid composition and the filter pore size.

3.2.5.3. Drug Loading

Drugs or other agents may be loaded within the liposomal bilayer or within the aqueous core. Drug loading within liposomes provides protection from degradation and elimination from the body while shielding non-target organs from the toxic effects of the drug. In particular, chemotherapeutic drugs, such as doxorubicin (DXR), are known to be myelosuppressive, GI toxic, and cardiotoxic. Encapsulation within liposomes alleviates some of these effects by primarily confining the drug to the vascular fluid thereby sparing healthy organs from exposure. Liposomal encapsulation of DXR has been shown to reduce the volume of distribution in humans from approximately 900 L/m² (for free DXR) to merely 2.75 L/m² (for liposomal DXR) verifying that liposomal DXR is primarily restricted to the vascular fluid volume [67].

Initially, the only option for liposomal encapsulation of therapeutic agents was through passive loading. A new advancement allowing for more efficient drug loading involves the use of transmembrane ion gradients and is termed ‘remote’ or ‘active’ loading. Both methods of liposomal drug encapsulation are discussed in the following sections.

3.2.5.3.1. *Passive Loading*

Passive drug entrapment is process where loading occurs during liposomal formulation. Aqueous drugs to be loaded within the internal core of the liposomes may

be mixed with the solution used to hydrate the lipid film prior to sizing. Lipophilic drugs, which will localize within the liposomal bilayer, are simply mixed with the lipids before solvent evaporation and subsequent hydration. Nonincorporated material is removed from loaded liposomes by dialysis or gel-filtration chromatography [68, 69].

Passive loading of aqueous compounds is an inefficient process. The amount of drug loaded is proportional to the initial drug concentration and the total inner volume of the liposomes. The available inner volume for loading is only a small fraction of the whole liposome suspension causing this loading method to be inefficient. The total inner volume of the liposomes available for passive encapsulation is a function of the initial lipid concentration and the liposome diameter [70]. Increasing the lipid concentration allows for an increase in the volume available for loading, however, this typically increases the viscosity of the liposomal formulation, and sizing is often more difficult when dealing with viscous solutions. An alternative approach is to preformulate and size the liposomes and subsequently concentrate the solution via diafiltration or rotary evaporation. The agent to be encapsulated is then introduced into the liposomes through several freeze-thaw cycles serving to transiently rupture the liposomes [71]. This method, however, may alter the liposome size distribution creating a heterogeneous solution with poor reproducibility [72]. In addition, highly viscous solutions which often result from passive encapsulation are not biocompatible for injection and passively loaded agents are more susceptible to leakage after dilution and/or liposome purification.

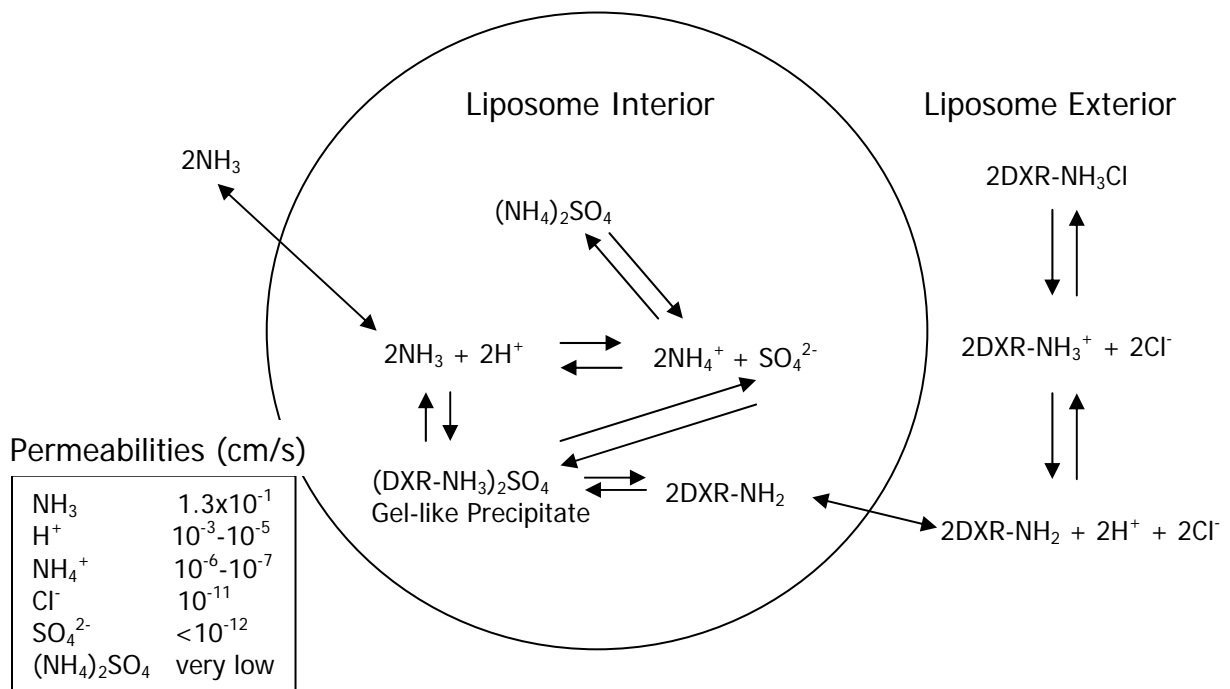
3.2.5.3.2. *Remote Loading*

The discovery of 'remote' loading techniques has provided a superior alternative to the inefficient process of passive drug loading. Remote loading allows for efficient

drug entrapment and stable retention of small molecules. This process is driven by an electrochemical potential created by pH or ion gradients established across the lipid bilayer of the liposomes. Gradients are established by preparing the liposomes in a buffer of specified pH and ion strength to be used as the internal volume buffer. The external phase is then exchanged for another buffer via dialysis, diafiltration, or size exclusion chromatography. Encapsulation is performed by mixing the liposomes with the compound of interest typically at a temperature above the phase transition temperature of the lipid bilayer to ensure fluidity and efficient transport across the bilayer. Interaction with ions within the liposomes effectively traps the drug within the core. This method enables encapsulation efficiencies approaching 100% and sustained entrapment of small molecules.

Remote loading has been reported most often with DXR, a small, weakly basic, amphiphilic drug ($pK_a \sim 8.3$). Liposomes are prepared in ammonium sulfate buffer and the external phase is exchanged for a non-acidic buffer. Uncharged DXR passively diffuses across the lipid bilayer to enter the liposome core where it interacts with dissociated ammonium sulfate forming a gel-like precipitate with the SO_4^{2-} anions (Figure 3.2). This precipitate is effectively trapped within the liposome creating a sink for accumulation of additional uncharged DXR [73]. To ensure that release of DXR upon entry into tumor cells can be achieved, a study designed to collapse the ammonium sulfate gradient through the use of the ionophore nigericin was conducted to ensure that the loading process is reversible. Fortunately, it was shown that when the gradient is collapsed, DXR, with full biological activity, is rapidly released from the liposomes [74].

Using an ammonium sulfate gradient DXR can be actively loaded into liposomes yielding high drug:phospholipid ratios. Amounts as high as 15,000 DXR molecules per liposome can be stably encapsulated through this method [75]. When liposomes are targeted through the inclusion of a few targeting moieties, the efficient loading of DXR attained through remote loading techniques allows for the delivery of high amounts of DXR per targeting vector. This is in stark contrast to the 1:1 targeting molecule to drug ratio attained through direct drug conjugation to individual targeting vectors confirming that targeted liposomes are a superior alternative to targeted drug conjugates.



Adapted from Bolotin et. al., J Liposome Res. 4(1), 1994 [3].

Figure 3.2. Ammonium sulfate driven remote loading of doxorubicin.

3.2.5.4. Passive Targeting with Liposomes

A major advantage of using long circulating liposomes came from the observation that carriers of relatively small size (~100 nm) can preferentially accumulate in solid tumors by passive convective transport [76] through the “leaky” vascular endothelium of tumors. The abnormal tumor vascular has been shown to be discontinuous with pores varying from 100 to 780 nm in size [77, 78]. Because tumor blood vessels are inherently leaky marked by compromised endothelial junctions, and lymphatic vessels of tumors are scarce, prolonged circulation of liposomes in the bloodstream allows for sustained drug accumulation at the tumor site. Due to longer blood residence time, repeated passage through the microvascular bed results in high levels of nanocarriers within the tumor which is known as the enhanced permeation and retention (EPR) phenomenon (Figure 3.3). Gabizon *et al.* have shown that the longer the blood circulation of liposomes, the higher their accumulation in the tumor [79]. When drugs are encapsulated in liposomes that are modified with flexible, water soluble polymers such as polyethylene glycol (PEG) chains to increase their surface hydrophilicity and prevent the adsorption of blood proteins and phagocytic uptake, the circulation time in the bloodstream is significantly prolonged. Coating liposomes with such polymers to inhibit protein opsonization is termed “steric stabilization”, and the resulting “Stealth” liposomes have been shown to evade clearance by the RES. For example, free DXR is cleared 450 times faster than PEGylated liposomal DXR [80]. The increased concentrations at the tumor site achieved through this method of passive targeting can greatly improve treatment efficacy. A recent study explored the performance of DXR-loaded liposomes in an orthotopic 9L rat brain glioma model [81]. Increased drug concentrations were observed in the brain tumor

consistent with passive accumulation of liposomes via the EPR phenomenon. In another study on patients with brain glioblastoma treated with DXR-loaded liposomes, the intratumoral drug accumulation was 13-19 times that recorded in normal brain [82]. Compared to long-circulating micelles, PEG coated liposomes have been shown to exhibit longer half-lives giving them a distinct advantage with regard to passive accumulation in tumors [83]. In studies, Doxil[®], the clinically approved PEGylated liposomal form of DXR, has exhibited prolonged circulation, sustained drug release, a higher tendency for extravasation into tumors, enhanced therapeutic index, and increased antitumor activity over free DXR. The clearance of liposomal DXR in humans has been reported as 0.041 L/h/m² whereas free DXR has been shown to clear at a much faster rate ranging from 24 to 35 L/h/m². This reduction in clearance results in an AUC for liposomal DXR which is approximately 2-3 orders of magnitude larger than that of free DXR [67].

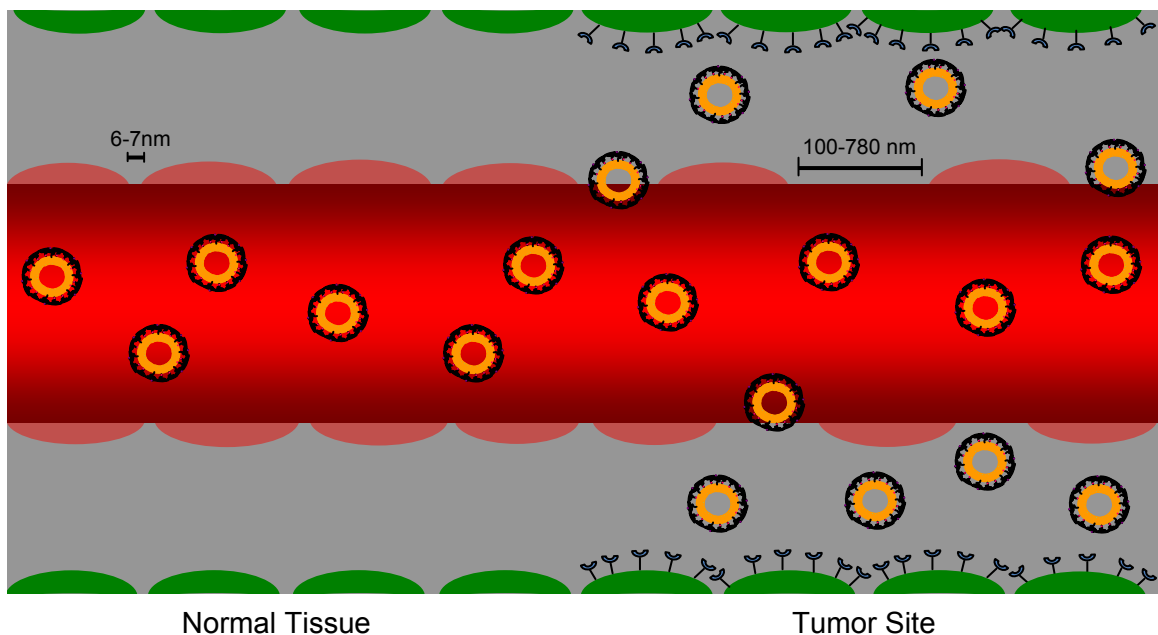


Figure 3.3. Passive accumulation of long-circulating liposomal nanocarriers into tumors via the EPR effect.

3.2.5.5. Active Targeting with Liposomes

To further increase uptake by tumor cells, targeting agents can be incorporated into liposomes to allow targeting to cells over-expressing tumor associated antigens or certain plasma membrane receptors (Figure 3.4). The incorporation of targeting ligands corresponding to specific cell markers, such as plasma membrane receptors, not only facilitates targeting to the cell but also drug retention at the target site by preventing retrograde movement of liposomes into the bloodstream. Targeting ligands can be chosen to bind receptors that undergo receptor-mediated endocytosis to facilitate drug uptake by cells [84, 85]. Targeting agents may be bound directly to lipid anchors on the liposomal bilayer or attached with a linker such as PEG. Attachment via PEG is preferable over direct attachment to lipid anchors because studies have shown that adjacent PEG chains, which must be incorporated for RES evasion for *in vivo* applications, inhibit binding to target cells when targeting ligands are grafted directly to the liposome surface [86-88]. Studies have even demonstrated interference in cell association when small targeting ligands, such as folate (441 Da), are attached to liposomes via PEG chains of the same length as adjacent PEG chains incorporated for steric stabilization. Therefore, most efficient active targeting to cells is attained when targeting agents are bound to liposomes by longer PEG chains [84].

Targeting agents may be incorporated into liposomal formulations by various methods. If the liposomes are formulated using functionalized lipids or PEG chains, targeting agents may be reacted with the end groups after the liposomes are formulated [89-91]. Another method involves the prefabrication of conjugates of the targeting agent either bound directly to a phospholipid (i.e. DSPE-ligand) or bound to a phospholipid via

PEG (i.e. DSPE-PEG-ligand). These conjugates may be included with the liposomal components during formulation [92, 93], or insertion of the conjugates may be conducted into preformed liposomes by mixing micelles of the conjugate with the liposomes at a temperature above the phase transition temperature of the liposome bilayer [94]. The latter method, termed “post-insertion”, is desirable because it provides increased flexibility regarding the choice of liposomal drug and ligand(s), it allows for greater control over the number of incorporated conjugates per liposome, and it provides the most economical use of the conjugates by preventing targeting ligands for being sequestered to the internal side of the bilayer [95].

Delivery of drug using actively targeted liposomes is preferable over direct conjugation to targeting moieties because (1) the drug-ligand conjugates have lower cytotoxic potencies [96] and (2) encapsulation yields a much higher drug cargo [73]. In addition, liposomes are typically larger than drug-ligand conjugates preventing

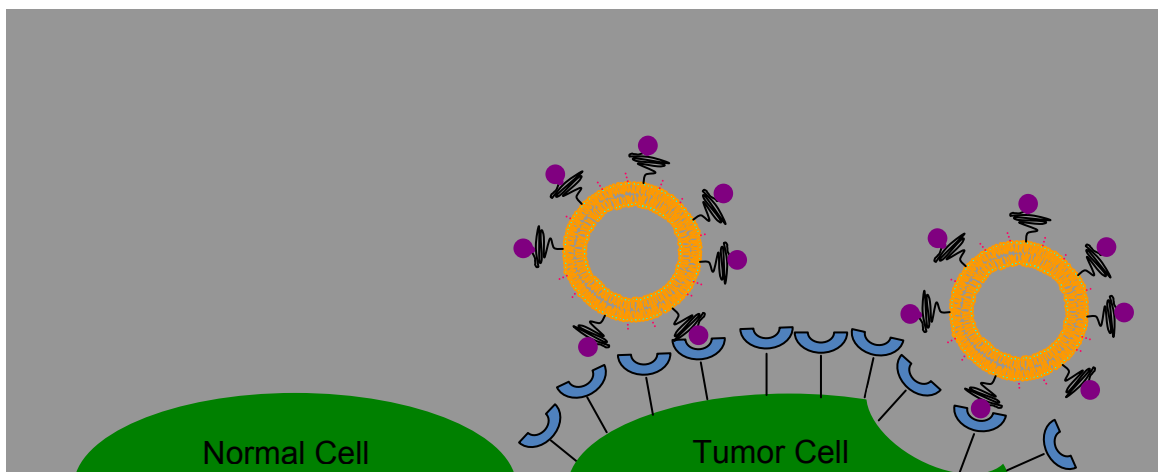


Figure 3.4. Active targeting of liposomal nanocarriers to tumors using ligands targeted to over-expressed receptors on tumor cells and uptake via receptor-mediated endocytosis.

glomerular filtration in the kidneys. This is advantageous because clearance is decreased, and the luminal side of the kidneys is spared exposure to drug. Finally, since single liposomes can be formulated to present multiple targeting ligands, multivalent binding results in increased avidity to tumor cells as shown by competitive binding assays [97].

3.2.5.5.1. Targeting Agent Selection

A number of agents have potential as liposomal targeting moieties for active targeting to tumors including antibodies or antibody fragments targeted to tumor antigens, ligands directed toward tumor cell plasma membrane receptors, or small peptides known to bind tumor cell surface determinants. Selection criteria may be based on a number of characteristics, however, foremost consideration should be given to immunogenicity of targeting agents, facilitation of entry into cells (i.e. via receptor-mediated endocytosis), and ability to enable nuclear localization of the entrapped drug cargo. In addition, targets should be easily accessible, have negligible expression in healthy tissues, and expression by tumor cells should be elevated, stable, and homogeneous [98].

Antibodies are highly specific and bind target antigens with high affinities, however, attachment of antibodies to liposomes has been shown to stimulate uptake by the RES, therefore, more recent studies have focused on the use of antibody fragments as an alternative to prevent premature clearance by Fc-receptor mediated uptake by the RES [77, 99]. Common tumor targets using liposomes functionalized with antibodies or antibody fragments include HER2 [86, 85, 100], disialoganglioside (GD2) [101], CD19 [102, 103], prostate-specific membrane antigen (PSMA) [104, 105], transferrin receptor [106-108], and epidermal growth factor receptor (EGFR) [109, 97]. Another drawback to

the use of antibodies or antibody fragments is that they are expensive to produce. The incorporation of small peptides into liposomes has been investigated to target aminopeptidase N [110, 111], matrix metalloproteinase (MMP) [112], and integrin [113, 114] on or around tumor cells. Liposomal incorporation of ligands associated with receptors over-expressed by tumor cells has also been studied extensively. Many different cell membrane receptors have been investigated as possible targets for liposomes using receptor associated ligands including transferrin receptors [115, 116], hyaluronan receptors [117], sigma receptors [118], and most commonly, folate receptors [84, 119, 75, 120-122, 93, 123-126, 97, 127, 128], which serve as the tumor associated target on which this thesis will focus.

The folate receptor (FR) is one of the numerous transmembrane receptors known to be over-expressed by tumors [129]. This 38,000 Da glycosylphosphatidylinositol-linked membrane protein exhibits restricted expression in normal adult epithelial tissues including the choroid plexus, bladder, testes, colorectum, and lung, however, expression is limited to the apical surface of cells placing FR out of direct contact with the bloodstream. The kidneys serve as an exception to this rule since FR is expressed by the proximal tubules, however, only those agents which are small enough to undergo glomerular filtration will come into contact with FR in the kidneys [130].

The primary biochemical role of folate in mammals is to mediate the transfer of one-carbon units in reactions that are important for DNA synthesis and replication, cell division, survival, and growth [130]. Methyl tetrahydrofolate derived from folate is essential for the regeneration of methionine from homocysteine. Methionine, in turn, is utilized for protein production or is converted to S-adenosylmethionine which serves as a

methyl donor in over 80 biological methylation reactions including the methylation of DNA, RNA, proteins, and phospholipids. Alternatively, folate may be used for de novo synthesis of deoxynucleoside triphosphates required for DNA synthesis [131]. As a result, FR is often over-expressed in rapidly dividing cells with increased demands for folate.

FR is an ideal tumor target because it is over-expressed by a wide variety of tumors including tumors of the ovary, lung, colon, endometrium, brain, breast, and kidney [132]. Upregulation is attributed to an increased cellular demand for folate due to elevated DNA synthesis and biological methylation reactions required for cellular division. The use of FR as a target for drug delivery systems is ideal since expression in normal tissues is restricted to the apical surface preventing exposure of non-target organs to intravenously delivered FR-targeted drugs. Folate has a high binding affinity for FR ($K_d < 1$ nM), and folate covalently bound to drugs has been shown to retain this high affinity as well as the ability to undergo receptor mediated endocytosis [133]. In addition, folic acid drug conjugates are delivered to the cytoplasm in a functionally active form. Unlike other receptor mediated drug delivery systems, since recovery of intact folate is essential to cells, the normal uptake mechanism bypasses lysosomes which would otherwise degrade folate prior to release into the cytoplasm [134, 135, 132].

FR-targeted formulations have been studied extensively and represent an ideal targeting system since FR is known to undergo receptor-mediated endocytosis facilitating drug delivery [119, 120, 122, 123, 136, 125, 63, 127, 137, 138, 128, 139]. Several *in vitro* liposomal studies utilizing FR as a target have demonstrated significantly higher cytotoxicities from FR-targeted formulations compared to non-targeted resulting from

increased uptake of drug by target cells [75, 123, 126]. Confocal microscopy has verified that drugs delivered via FR-targeted liposomes are rapidly transferred to the nuclei of target cells [75]. Others have shown that targeting to this receptor also confers the ability to overcome drug resistance, a common problem associated with chemotherapy [121].

3.2.5.5.2. Targeting Agent Incorporation Decreases Circulation Times and Passive Targeting to Tumor

Unfortunately, numerous studies have shown that targeting ligand attachment to PEG chains anchored in liposomal membranes results in accelerated plasma clearance even when additional PEG chains are included to prolong circulation [119, 75, 139]. The inability to extend circulation with traditional targeted formulations is due to the fact that PEG chains employed are either the same length or shorter than those used to tether targeting ligands to the nanocarriers, since longer adjacent PEG chains have been shown to inhibit binding to target cells. Decreased plasma concentrations of targeted formulations have been reported whether the targeting moiety is an antibody, receptor ligand, or small peptide. It is believed that targeting moieties anchored with similar length or longer PEG on the liposome surface retain the ability to interact with plasma proteins responsible for RES clearance. Specifically, folate receptor (FR)-targeted liposomes have been shown to suffer from rapid clearance due to the recognition of folate by the RES because folate was conjugated to a longer PEG₃₃₅₀ chain than the adjacent PEG₂₀₀₀ chains in an effort to overcome steric interference of PEG on binding of folate to target cells [84]. Studies investigating therapeutic efficacy of targeted nanocarriers often demonstrate no clear therapeutic advantage due to reduction in circulation times. In fact, when circulation is only slightly reduced, for example in immune-deficient animals, FR-

targeted liposomal treatments have demonstrated greater success on solid tumors [136]. In addition, a study utilizing an *in vivo* adoptive tumor growth assay, which is unaffected by pharmacokinetics, exhibited a distinct advantage of FR-targeted formulations over non-targeted in inhibiting tumor growth [121]. When administered to immunocompetent animals, studies have demonstrated no therapeutic advantage between non-targeted and FR-targeted formulations administered to mice bearing subcutaneous carcinomas [75]. Mice with FR-expressing ascites tumors, however, have been shown to survive longer on FR-targeted liposomal treatments [75, 125]. In another study, i.p. injections of FR-targeted liposomes into nude mice with a KB carcinoma prohibited tumor growth and increased survival greater than non-targeted formulations [136], whereas both the FR-targeted and non-targeted liposomes exhibited the same blood clearance profiles in the nude mice. These results make it clear that decreased circulation time of FR-targeted liposomal nanocarriers needs to be further investigated with an emphasis on discovering methods to address the negative consequences of folate inclusion within liposomal formulations before therapeutic advantages are realized.

3.2.5.6. Use of Cleavable Phospholipid-PEG Chains in Liposomes

In recent years, conjugates containing reversible disulphide linkages have been used by numerous investigators in drug delivery [140, 141]. Cleavable PEG conjugates have been utilized previously as mediators capable of destabilizing nanoparticles and promoting release of contents at the target site [142-144]. Some groups have investigated the use of cleavable PEG to stabilize pH sensitive liposomes to prolong circulation time in the bloodstream and demonstrated that these conjugates retain the ability to enable RES evasion *in vivo* [144]. Removal of the PEG coating was shown to destabilize the

liposomes promoting fusion and rapid release of liposomal contents in a pH dependent manner [142, 143, 145, 144]. In other studies, thiolytically cleavable PEG conjugates were used to trigger the release of drugs from inhalable agglomerated liposomes [146, 147].

Many different cleavable cross-linkers have been employed including those cleavable by matrix metalloproteinase [148, 149], acids [150], and most commonly, cysteine or other thiol reducing agents [142, 146, 147, 143, 151, 152, 145, 144]. Many conjugates containing reversible disulfide linkages have been studied to bind PEG to liposomal phospholipids including dithiobenzyl (DTB) [146, 145], dithiobis(succinimidyl propionate (DTSP) [142-144], and *N*-succinimidyl-3-(2-pyridyldithio) propionate (SPDP) [151, 152]. Thiol reducible cross-linkers offer the advantage of precise control over cleavage since they require an externally delivered reducing agent such as cysteine, which is only present in the unbound, reduced form at low concentrations in the body (~10 μ M in blood), to sever the linkage. In addition, cysteine is innocuous to the body at the doses administered for cleavage (~1 mmol/kg).

It has long been established that PEG chains are capable of creating a hydrophilic barrier around liposomes preventing binding of opsonins by steric hindrance and thereby preventing RES recognition. It is expected that binding to opsonins responsible for RES clearance will be prevented and protein deposition decreased in the same manner when targeting ligands are attached to PEG chains of shorter length than adjacent PEGs. By inhibiting the binding of plasma proteins to targeting ligands, longer PEG chains can effectively 'mask' targeting ligands and prevent clearance by the RES. In recent years, conjugates containing reversible disulphide linkages have been shown to enable

prolonged liposome circulation *in vivo* [144]. In addition, studies have demonstrated that cleavage of these conjugates *in vitro* completely restores binding to target cells due to exposure of targeting moieties promoting cell association [75, 151, 149]. This suggests that cleavable PEG conjugates could also be utilized to mask targeting ligands to prevent RES recognition and clearance while the liposomes are in circulation and then allow binding to cells after cleaving the PEG chains at the tumor site to expose the targeting ligands. By maximizing the passive accumulation of actively targeted liposomes to tumor while still retaining the ability to actively target tumor cells, the negative impact of targeting ligand insertion into liposomes can be addressed to realize the full potential of actively targeted formulations.

3.3. CONCLUSIONS

The inadequacy of current treatments for glioma needs to be addressed through the development of new alternatives providing improved treatment efficacy. Specifically, traditional systemically delivered chemotherapeutics are incapable of adequately accumulating in brain tumors and do not spare healthy tissues from the drug toxicity. Targeted chemotherapy using nanocarriers provides the opportunity for increased drug accumulation in tumor and minimized delivery to non-target organs.

Liposomal nanocarriers offer much promise in the delivery of chemotherapeutic drugs to solid tumors because they are biocompatible, they exhibit efficient and stable drug loading allowing for the delivery of large drug payloads to tumors and bypass of multidrug resistance efflux pumps [27], and they protect encapsulated drugs from premature degradation while shielding healthy organs from the toxic side effects of incorporated chemotherapeutics. Liposomes have been shown to favorably alter the

pharmacokinetics of encapsulated drug cargo. Most importantly, because hydrophilic barriers may be created through the inclusion of polymers such as PEG and targeting agents are easily incorporated, both passive and active targeting of chemotherapeutic drugs to tumors may be achieved using liposomal nanocarriers.

Since FR is known to be over-expressed by various tumors, numerous studies have investigated the use of incorporating folate as a targeting ligand into liposomal delivery vehicles loaded with DXR. There are problems, however, associated with this approach that have not yet been addressed. First, the incorporation of PEG is essential to allow prolonged circulation of FR-targeted liposomes, but the addition of this polymer hinders target cell association if it is longer than the PEG chains used to tether folate to the liposome, and drug uptake at the tumor site may be negatively affected as a result. Conversely, if shorter PEG chains are utilized, the attachment of folate to the exterior surface of liposomes has been shown to result in accelerated clearance of targeted formulations from plasma.

Cleavable PEG chains provide a potential solution to the issue of folate exposure on liposomes. They have been extensively studied for other liposomal applications and have demonstrated a proven ability to retain RES evasion capabilities of liposomes *in vivo*. In addition, *in vitro* studies have verified that removal of cleavable PEG chains restores the targeting capacity of liposomal nanocarriers. This suggests that the incorporation of a longer cysteine cleavable PEG conjugate into liposomal formulations should allow for enhanced control over folate exposure. When the liposomes are in circulation, the long cleavable PEG chains will inhibit binding of plasma proteins and effectively 'mask' the folate targeting ligands reducing RES clearance. After

extravasating into the target site, liposomes will be treated with systemic cysteine, which should localize to tumors due to its small size, to cleave the PEG chains and expose the targeting ligands, thereby promoting target cell uptake due to receptor binding. In this manner, folate is only exposed at the tumor site where it is needed and will not interfere with prolonged circulation of liposomes. Ultimately, tumor drug accumulation should improve since circulating drug levels will be maintained and subsequent receptor binding and uptake will prevent retrograde movement of drug from tumor. The following chapters further explore the consequences of folate inclusion within liposomal formulations and this novel approach to allow control at the nanoscale level by modulating the exposure of folate on liposomal nanocarriers.

3.4. REFERENCES

- [1] Jiang, W., Kim, B., Rutka, J. and Chan, W., Advances and challenges of nanotechnology-based drug delivery systems. *Expert Opin. Drug Deliv.* **4**, 621-633 (2007).
- [2] Lockman, P. R., Mumper, R. J., Khan, M. A. and Allen, D. D., Nanoparticle technology for drug delivery across the blood-brain barrier. *Drug Dev Ind Pharm* **28**, 1-13 (2002).
- [3] Bolotin, E. M., Cohen, R., Bar, L. K., et al., Ammonium sulfate gradients for efficient and stable remote loading of amphipathic weak bases into liposomes and ligandoliposomes. *Journal of Liposome Research* **4**, 455-479 (1994).
- [4] Parveen, S. and Sahoo, S. K., Polymeric nanoparticles for cancer therapy. *J Drug Target* **16**, 108-123 (2008).
- [5] Lin, R., Shi Ng, L. and Wang, C. H., In vitro study of anticancer drug doxorubicin in PLGA-based microparticles. *Biomaterials* **26**, 4476-4485 (2005).
- [6] Yemisci, M., Bozdag, S., Cetin, M., et al., Treatment of malignant gliomas with mitoxantrone-loaded poly (lactide-co-glycolide) microspheres. *Neurosurgery* **59**, 1296-1302; discussion 1302-1293 (2006).
- [7] Zhang, Z. and Feng, S. S., The drug encapsulation efficiency, in vitro drug release, cellular uptake and cytotoxicity of paclitaxel-loaded poly(lactide)-tocopheryl polyethylene glycol succinate nanoparticles. *Biomaterials* **27**, 4025-4033 (2006).
- [8] Devalapally, H., Duan, Z., Seiden, M. V. and Amiji, M. M., Paclitaxel and ceramide co-administration in biodegradable polymeric nanoparticulate delivery system to overcome drug resistance in ovarian cancer. *Int J Cancer* **121**, 1830-1838 (2007).
- [9] Shenoy, D. B. and Amiji, M. M., Poly(ethylene oxide)-modified poly(epsilon-caprolactone) nanoparticles for targeted delivery of tamoxifen in breast cancer. *Int J Pharm* **293**, 261-270 (2005).
- [10] Qi, L., Xu, Z. and Chen, M., In vitro and in vivo suppression of hepatocellular carcinoma growth by chitosan nanoparticles. *Eur J Cancer* **43**, 184-193 (2007).

- [11] Xu, Y. and Du, Y., Effect of molecular structure of chitosan on protein delivery properties of chitosan nanoparticles. *Int J Pharm* **250**, 215-226 (2003).
- [12] Dreis, S., Rothweiler, F., Michaelis, M., et al., Preparation, characterisation and maintenance of drug efficacy of doxorubicin-loaded human serum albumin (HSA) nanoparticles. *Int J Pharm* **341**, 207-214 (2007).
- [13] Cheng, J., Teply, B. A., Sherifi, I., et al., Formulation of functionalized PLGA-PEG nanoparticles for in vivo targeted drug delivery. *Biomaterials* **28**, 869-876 (2007).
- [14] Sutton, D., Nasongkla, N., Blanco, E. and Gao, J., Functionalized micellar systems for cancer targeted drug delivery. *Pharm Res* **24**, 1029-1046 (2007).
- [15] Torchilin, V. P., Micellar nanocarriers: pharmaceutical perspectives. *Pharm Res* **24**, 1-16 (2007).
- [16] Batrakova, E., Lee, S., Li, S., et al., Fundamental relationships between the composition of pluronic block copolymers and their hypersensitization effect in MDR cancer cells. *Pharm Res* **16**, 1373-1379 (1999).
- [17] Alexandridis, P., Athanassiou, V., Fukuda, S. and Hatton, T. A., Surface activity of poly(ethylene oxide)-block-poly(propylene oxide)-block-poly(ethylene oxide) copolymers. *Langmuir* **10**, 2604-2612 (1994).
- [18] Zhang, L., Yu, K. and Eisenberg, A., Ion-Induced Morphological Changes in "Crew-Cut" Aggregates of Amphiphilic Block Copolymers. *Science* **272**, 1777-1779 (1996).
- [19] Seymour, L. W., Duncan, R., Strohalm, J. and Kopecek, J., Effect of molecular weight (Mw) of N-(2-hydroxypropyl)methacrylamide copolymers on body distribution and rate of excretion after subcutaneous, intraperitoneal, and intravenous administration to rats. *J Biomed Mater Res* **21**, 1341-1358 (1987).
- [20] Torchilin, V. P., *Self-assembling complexes for gene delivery: from laboratory to clinical trial*. (Wiley, New York, 1998).
- [21] Kwon, G. S., Polymeric micelles for delivery of poorly water-soluble compounds. *Crit Rev Ther Drug Carrier Syst* **20**, 357-403 (2003).

- [22] Yamamoto, Y., Nagasaki, Y., Kato, Y., et al., Long-circulating poly(ethylene glycol)-poly(D,L-lactide) block copolymer micelles with modulated surface charge. *J Control Release* **77**, 27-38 (2001).
- [23] Benahmed, A., Ranger, M. and Leroux, J. C., Novel polymeric micelles based on the amphiphilic diblock copolymer poly(N-vinyl-2-pyrrolidone)-block-poly(D,L-lactide). *Pharm Res* **18**, 323-328 (2001).
- [24] Luppi, B., Orienti, I., Bigucci, F., et al., Poly(vinylalcohol-co-vinyloleate) for the preparation of micelles enhancing retinyl palmitate transcutaneous permeation. *Drug Deliv* **9**, 147-152 (2002).
- [25] Batrakova, E. V., Li, S., Vinogradov, S. V., et al., Mechanism of pluronic effect on P-glycoprotein efflux system in blood-brain barrier: contributions of energy depletion and membrane fluidization. *J Pharmacol Exp Ther* **299**, 483-493 (2001).
- [26] Danson, S., Ferry, D., Alakhov, V., et al., Phase I dose escalation and pharmacokinetic study of pluronic polymer-bound doxorubicin (SP1049C) in patients with advanced cancer. *Br J Cancer* **90**, 2085-2091 (2004).
- [27] Krishna, R. and Mayer, L. D., Multidrug resistance (MDR) in cancer. Mechanisms, reversal using modulators of MDR and the role of MDR modulators in influencing the pharmacokinetics of anticancer drugs. *Eur J Pharm Sci* **11**, 265-283 (2000).
- [28] Alakhov, V., Moskaleva, E., Batrakova, E. V. and Kabanov, A. V., Hypersensitization of multidrug resistant human ovarian carcinoma cells by pluronic P85 block copolymer. *Bioconjug Chem* **7**, 209-216 (1996).
- [29] Croy, S. R. and Kwon, G. S., The effects of Pluronic block copolymers on the aggregation state of nystatin. *J Control Release* **95**, 161-171 (2004).
- [30] Batrakova, E. V., Dorodnych, T. Y., Klinskii, E. Y., et al., Anthracycline antibiotics non-covalently incorporated into the block copolymer micelles: in vivo evaluation of anti-cancer activity. *Br J Cancer* **74**, 1545-1552 (1996).
- [31] Nakanishi, T., Fukushima, S., Okamoto, K., et al., Development of the polymer micelle carrier system for doxorubicin. *J Control Release* **74**, 295-302 (2001).

- [32] Teng, Y., Morrison, M. E., Munk, P., et al., Release Kinetics Studies of Aromatic Molecules into Water from Block Polymer Micelles *Macromolecules* **31**, 3578-3587 (1998).
- [33] Yoo, H. S., Lee, E. A. and Park, T. G., Doxorubicin-conjugated biodegradable polymeric micelles having acid-cleavable linkages. *J Control Release* **82**, 17-27 (2002).
- [34] Chung, J. E., Yokoyama, M. and Okano, T., Inner core segment design for drug delivery control of thermo-responsive polymeric micelles. *J Control Release* **65**, 93-103 (2000).
- [35] Pruitt, J. D. and Pitt, W. G., Sequestration and ultrasound-induced release of doxorubicin from stabilized Pluronic P105 micelles. *Drug Deliv* **9**, 253-258 (2002).
- [36] Cheng, Y., Wang, J., Rao, T., et al., Pharmaceutical applications of dendrimers: promising nanocarriers for drug delivery. *Frontiers in Bioscience* **13**, 1447-1471 (2008).
- [37] Dufes, C., Uchegbu, I. F. and Schatzlein, A. G., Dendrimers in gene delivery. *Adv Drug Deliv Rev* **57**, 2177-2202 (2005).
- [38] Konda, S. D., Aref, M., Wang, S., et al., Specific targeting of folate-dendrimer MRI contrast agents to the high affinity folate receptor expressed in ovarian tumor xenografts. *Magma* **12**, 104-113 (2001).
- [39] Lee, C. C., Gillies, E. R., Fox, M. E., et al., A single dose of doxorubicin-functionalized bow-tie dendrimer cures mice bearing C-26 colon carcinomas. *Proc Natl Acad Sci U S A* **103**, 16649-16654 (2006).
- [40] Gupta, U., Agashe, H. B., Asthana, A. and Jain, N. K., Dendrimers: novel polymeric nanoarchitectures for solubility enhancement. *Biomacromolecules* **7**, 649-658 (2006).
- [41] Kojima, C., Kono, K., Maruyama, K. and Takagishi, T., Synthesis of polyamidoamine dendrimers having poly(ethylene glycol) grafts and their ability to encapsulate anticancer drugs. *Bioconjug Chem* **11**, 910-917 (2000).

- [42] Quintana, A., Raczka, E., Piehler, L., et al., Design and function of a dendrimer-based therapeutic nanodevice targeted to tumor cells through the folate receptor. *Pharm Res* **19**, 1310-1316 (2002).
- [43] Iijima, S., Helical microtubules of graphitic carbon. *Nature (London)* **354**, 56-58 (1991).
- [44] Iijima, S. and Ichihashi, T., Single-shell carbon nanotubes of 1-nm diameter. *Nature (London)* **363**, 603-605 (1993).
- [45] Prato, M., Kostarelos, K. and Bianco, A., Functionalized carbon nanotubes in drug design and discovery. *Acc Chem Res* **41**, 60-68 (2008).
- [46] Khlobystov, A. N., Britz, D. A. and Briggs, G. A., Molecules in carbon nanotubes. *Acc Chem Res* **38**, 901-909 (2005).
- [47] Tasis, D., Tagmatarchis, N., Bianco, A. and Prato, M., Chemistry of carbon nanotubes. *Chem Rev* **106**, 1105-1136 (2006).
- [48] Kam, N. W., O'Connell, M., Wisdom, J. A. and Dai, H., Carbon nanotubes as multifunctional biological transporters and near-infrared agents for selective cancer cell destruction. *Proc Natl Acad Sci U S A* **102**, 11600-11605 (2005).
- [49] Shao, N., Lu, S., Wickstrom, E. and Panchapakesan, B., Integrated molecular targeting of IGF1R and HER2 surface receptors and destruction of breast cancer cells using single wall carbon nanotubes. *Nanotechnology* **18**, 315101 (2007).
- [50] Gannon, C. J., Cherukuri, P., Yakobson, B. I., et al., Carbon nanotube-enhanced thermal destruction of cancer cells in a noninvasive radiofrequency field. *Cancer* **110**, 2654-2665 (2007).
- [51] Ali-Boucetta, H., Al-Jamal, K. T., McCarthy, D., et al., Multiwalled carbon nanotube-doxorubicin supramolecular complexes for cancer therapeutics. *Chem Commun (Camb)* 459-461 (2008).
- [52] Liu, Z., Sun, X., Nakayama-Ratchford, N. and Dai, H., Supramolecular chemistry on water-soluble carbon nanotubes for drug loading and delivery. *ACS Nano* **1**, 50-56 (2007).

- [53] Pastorin, G., Wu, W., Wieckowski, S., et al., Double functionalization of carbon nanotubes for multimodal drug delivery. *Chem Commun (Camb)* 1182-1184 (2006).
- [54] Kostarelos, K., Lacerda, L., Pastorin, G., et al., Functionalized carbon nanotube cellular uptake and internalization mechanism is independent of functional group and cell type. *Nature Nanotechnology* **2**, 108-113 (2007).
- [55] Pantarotto, D., Singh, R., McCarthy, D., et al., Functionalized carbon nanotubes for plasmid DNA gene delivery. *Angew Chem Int Ed Engl* **43**, 5242-5246 (2004).
- [56] Israelachvili, J., in *Intermolecular and surface forces, Second edition* (Academic Press, San Diego, CA, 1992), pp. 366-394.
- [57] Small, D. M., *Handbook of lipid research: The physical chemistry of lipids, from alkanes to phospholipids*, Vol. 4. (Plenum Press, New York, NY, 1986).
- [58] Ellens, H., Bentz, J. and Szoka, F. C., Destabilization of phosphatidylethanolamine liposomes at the hexagonal phase transition temperature. *Biochemistry* **25**, 285-294 (1986).
- [59] Lasic, D., *Liposomes: From Physics to Applications*. (Elsevier, Amsterdam, 1993).
- [60] Simon, S. A. and McIntosh, T. J., Depth of water penetration into lipid bilayers. *Methods Enzymol* **127**, 511-521 (1986).
- [61] Ellens, H., Bentz, J. and Szoka, F. C., pH-induced destabilization of phosphatidylethanolamine-containing liposomes: role of bilayer contact. *Biochemistry* **23**, 1532-1538 (1984).
- [62] Campbell, R. B., Fukumura, D., Brown, E. B., et al., Cationic charge determines the distribution of liposomes between the vascular and extravascular compartments of tumors. *Cancer Res* **62**, 6831-6836 (2002).
- [63] Reddy, J. A., Abburi, C., Hofland, H., et al., Folate-targeted, cationic liposome-mediated gene transfer into disseminated peritoneal tumors. *Gene Ther* **9**, 1542-1550 (2002).

- [64] Zalipsky, S., Brandeis, E., Newman, M. S. and Woodle, M. C., Long circulating, cationic liposomes containing amino-PEG- phosphatidylethanolamine. *FEBS Lett* **353**, 71-74 (1994).
- [65] Lasic, D., in *Liposomes: from physics to applications*, edited by D. Lasic (Elsevier, New York, 1993), pp. 63-107.
- [66] Dass, C. R., Drug delivery in cancer using liposomes. *Methods Mol Biol* **437**, 177-182 (2008).
- [67] Doxil: Prescribing Information. Raritan, NJ: Ortho Biotech Products, LP; 2008.
- [68] Lasic, D. and Martin, F., *Stealth Liposomes*, 1st ed. (CRC Press, Boca Raton, Fla., 1995).
- [69] Torchilin, V. P. and Weissig, V., *Liposomes*. (Oxford University Press, New York, 2003).
- [70] New, R. R. C., *Liposomes: A Practical Approach*. (Oxford University Press, Oxford, UK, 1990).
- [71] Shi, N. and Pardridge, W. M., Noninvasive gene targeting to the brain. *Proc Natl Acad Sci U S A* **97**, 7567-7572. (2000).
- [72] Lasic, D. D., Ceh, B., Stuart, M. C., et al., Transmembrane gradient driven phase transitions within vesicles: lessons for drug delivery. *Biochim Biophys Acta* **1239**, 145-156 (1995).
- [73] Gabizon, A., Shmeeda, H. and Barenholz, Y., Pharmacokinetics of pegylated liposomal Doxorubicin: review of animal and human studies. *Clin Pharmacokinet* **42**, 419-436 (2003).
- [74] Horowitz, A. T., Barenholz, Y. and Gabizon, A. A., In vitro cytotoxicity of liposome-encapsulated doxorubicin: dependence on liposome composition and drug release. *Biochim Biophys Acta* **1109**, 203-209 (1992).

- [75] Gabizon, A., Shmeeda, H., Horowitz, A. T. and Zalipsky, S., Tumor cell targeting of liposome-entrapped drugs with phospholipid-anchored folic acid-PEG conjugates. *Adv Drug Deliv Rev* **56**, 1177-1192 (2004).
- [76] Maeda, H., The enhanced permeability and retention (EPR) effect in tumor vasculature: the key role of tumor-selective macromolecular drug targeting. *Adv Enzyme Regul* **41**, 189-207 (2001).
- [77] Maruyama, K., Takahashi, N., Tagawa, T., et al., Immunoliposomes bearing polyethyleneglycol-coupled Fab' fragment show prolonged circulation time and high extravasation into targeted solid tumors in vivo. *FEBS Lett* **413**, 177-180 (1997).
- [78] Siwak, D. R., Tari, A. M. and Lopez-Berestein, G., The potential of drug-carrying immunoliposomes as anticancer agents. Commentary re: J. W. Park et al., Anti-HER2 immunoliposomes: enhanced efficacy due to targeted delivery. *Clin. Cancer Res.*, 8: 1172-1181, 2002. *Clin Cancer Res* **8**, 955-956 (2002).
- [79] Gabizon, A. and Papahadjopoulos, D., Liposome formulations with prolonged circulation time in blood and enhanced uptake by tumors. *Proc Natl Acad Sci U S A* **85**, 6949-6953 (1988).
- [80] Gabizon, A., Catane, R., Uziely, B., et al., Prolonged circulation time and enhanced accumulation in malignant exudates of doxorubicin encapsulated in polyethylene-glycol coated liposomes. *Cancer Res* **54**, 987-992 (1994).
- [81] Arnold, R. D., Mager, D. E., Slack, J. E. and Straubinger, R. M., Effect of repetitive administration of Doxorubicin-containing liposomes on plasma pharmacokinetics and drug biodistribution in a rat brain tumor model. *Clin Cancer Res* **11**, 8856-8865 (2005).
- [82] Koukourakis, M. I., Koukouraki, S., Fezoulidis, I., et al., High intratumoural accumulation of stealth liposomal doxorubicin (Caelyx) in glioblastomas and in metastatic brain tumours. *Br J Cancer* **83**, 1281-1286. (2000).
- [83] Weissig, V., Whiteman, K. R. and Torchilin, V. P., Accumulation of protein-loaded long-circulating micelles and liposomes in subcutaneous Lewis lung carcinoma in mice. *Pharm Res* **15**, 1552-1556 (1998).

- [84] Gabizon, A., Horowitz, A. T., Goren, D., et al., Targeting folate receptor with folate linked to extremities of poly(ethylene glycol)-grafted liposomes: in vitro studies. *Bioconjug Chem* **10**, 289-298 (1999).
- [85] Kirpotin, D. B., Drummond, D. C., Shao, Y., et al., Antibody targeting of long-circulating lipidic nanoparticles does not increase tumor localization but does increase internalization in animal models. *Cancer Res* **66**, 6732-6740 (2006).
- [86] Kirpotin, D., Park, J. W., Hong, K., et al., Sterically stabilized anti-HER2 immunoliposomes: design and targeting to human breast cancer cells in vitro. *Biochemistry* **36**, 66-75 (1997).
- [87] Klibanov, A. L., Maruyama, K., Beckerleg, A. M., et al., Activity of amphipathic poly(ethylene glycol) 5000 to prolong the circulation time of liposomes depends on the liposome size and is unfavorable for immunoliposome binding to target. *Biochim Biophys Acta* **1062**, 142-148 (1991).
- [88] Mori, A., Klibanov, A. L., Torchilin, V. P. and Huang, L., Influence of the steric barrier activity of amphipathic poly(ethyleneglycol) and ganglioside GM1 on the circulation time of liposomes and on the target binding of immunoliposomes in vivo. *FEBS Lett* **284**, 263-266. (1991).
- [89] Allen, T. M., Brandeis, E., Hansen, C. B., et al., A new strategy for attachment of antibodies to sterically stabilized liposomes resulting in efficient targeting to cancer cells. *Biochim Biophys Acta* **1237**, 99-108 (1995).
- [90] Blume, G., Cevc, G., Crommelin, M. D., et al., Specific targeting with poly(ethylene glycol)-modified liposomes: coupling of homing devices to the ends of the polymeric chains combines effective target binding with long circulation times. *Biochim Biophys Acta* **1149**, 180-184 (1993).
- [91] Zalipsky, S., Puntambekar, B., Boulikas, P., et al., Peptide attachment to extremities of liposomal surface grafted PEG chains: preparation of the long-circulating form of laminin pentapeptide, YIGSR. *Bioconjug Chem* **6**, 705-708 (1995).
- [92] DeFrees, S., Phillips, L., Guo, L. and Zalipsky, S., Sialyl Lewis liposomes as a multivalent ligand and inhibitor of E-Selectin mediated cellular adhesion. *J Am Chem Soc* **118**, 6101-6104 (1996).

- [93] Lee, R. J. and Low, P. S., Delivery of liposomes into cultured KB cells via folate receptor- mediated endocytosis. *J Biol Chem* **269**, 3198-3204 (1994).
- [94] Zalipsky, S., Mullah, N., Harding, J. A., et al., Poly(ethylene glycol)-grafted liposomes with oligopeptide or oligosaccharide ligands appended to the termini of the polymer chains. *Bioconjug Chem* **8**, 111-118 (1997).
- [95] Zalipsky, S., Mullah, N. and Qazen, M., Preparation of poly(ethylene glycol)-grafted liposomes with ligands at the extremities of polymer chains. *Methods Enzymol* **387**, 50-69 (2004).
- [96] Ulbrich, K., Etrych, T., Chytil, P., et al., Antibody-targeted polymer-doxorubicin conjugates with pH-controlled activation. *J Drug Target* **12**, 477-489 (2004).
- [97] Saul, J. M., Annapragada, A. V. and Bellamkonda, R. V., A dual-ligand approach for enhancing targeting selectivity of therapeutic nanocarriers. *J Control Release* **114**, 277-287 (2006).
- [98] Sapra, P., Tyagi, P. and Allen, T., Ligand-targeted liposomes for cancer treatment. *Current Drug Delivery* **2**, 369-381 (2005).
- [99] Park, J. W., Hong, K., Kirpotin, D. B., et al., Anti-HER2 immunoliposomes: enhanced efficacy attributable to targeted delivery. *Clin Cancer Res* **8**, 1172-1181 (2002).
- [100] Park, J. W., Hong, K., Carter, P., et al., Development of anti-p185HER2 immunoliposomes for cancer therapy. *Proc Natl Acad Sci U S A* **92**, 1327-1331. (1995).
- [101] Brignole, C., Marimpietri, D., Pagnan, G., et al., Neuroblastoma targeting by c-myc-selective antisense oligonucleotides entrapped in anti-GD2 immunoliposome: immune cell-mediated anti-tumor activities. *Cancer Lett* **228**, 181-186 (2005).
- [102] Lopes de Menezes, D. E., Kirchmeier, M. J., Gange, J.-F., et al., Cellular trafficking and cytotoxicity of anti-cd19-targeted liposomal doxorubicin in B lymphoma cells. *Journal of Liposome Research* **9**, 199-228 (1999).

- [103] Sapra, P. and Allen, T. M., Improved outcome when B-cell lymphoma is treated with combinations of immunoliposomal anticancer drugs targeted to both the CD19 and CD20 epitopes. *Clin Cancer Res* **10**, 2530-2537 (2004).
- [104] Ikegami, S., Tadakuma, T., Yamakami, K., et al., Selective gene therapy for prostate cancer cells using liposomes conjugated with IgM type monoclonal antibody against prostate-specific membrane antigen. *Hum Cell* **18**, 17-23 (2005).
- [105] Ikegami, S., Yamakami, K., Ono, T., et al., Targeting gene therapy for prostate cancer cells by liposomes complexed with anti-prostate-specific membrane antigen monoclonal antibody. *Hum Gene Ther* **17**, 997-1005 (2006).
- [106] Cerletti, A., Drewe, J., Fricker, G., et al., Endocytosis and transcytosis of an immunoliposome-based brain drug delivery system. *J Drug Target* **8**, 435-446 (2000).
- [107] Gosk, S., Vermehren, C., Storm, G. and Moos, T., Targeting anti-transferrin receptor antibody (OX26) and OX26-conjugated liposomes to brain capillary endothelial cells using in situ perfusion. *J Cereb Blood Flow Metab* **24**, 1193-1204 (2004).
- [108] Huwyler, J., Wu, D. and Pardridge, W. M., Brain drug delivery of small molecules using immunoliposomes. *Proc Natl Acad Sci U S A* **93**, 14164-14169 (1996).
- [109] Mamot, C., Drummond, D. C., Greiser, U., et al., Epidermal growth factor receptor (EGFR)-targeted immunoliposomes mediate specific and efficient drug delivery to EGFR- and EGFRvIII-overexpressing tumor cells. *Cancer Res* **63**, 3154-3161 (2003).
- [110] Pastorino, F., Brignole, C., Di Paolo, D., et al., Targeting liposomal chemotherapy via both tumor cell-specific and tumor vasculature-specific ligands potentiates therapeutic efficacy. *Cancer Res* **66**, 10073-10082 (2006).
- [111] Pastorino, F., Brignole, C., Marimpietri, D., et al., Vascular damage and anti-angiogenic effects of tumor vessel-targeted liposomal chemotherapy. *Cancer Res.* **63**, 7400-7409 (2003).

- [112] Medina, O. P., Kairemo, K., Valtanen, H., et al., Radionuclide imaging of tumor xenografts in mice using a gelatinase-targeting peptide. *Anticancer Res* **25**, 33-42 (2005).
- [113] Lestini, B. J., Sagnella, S. M., Xu, Z., et al., Surface modification of liposomes for selective cell targeting in cardiovascular drug delivery. *J Control Release* **78**, 235-247. (2002).
- [114] Schiffelers, R. M., Koning, G. A., ten Hagen, T. L., et al., Anti-tumor efficacy of tumor vasculature-targeted liposomal doxorubicin. *J Control Release* **91**, 115-122 (2003).
- [115] Eavarone, D. A., Yu, X. and Bellamkonda, R. V., Targeted drug delivery to C6 glioma by transferrin-coupled liposomes. *J Biomed Mater Res* **51**, 10-14. (2000).
- [116] Hatakeyama, H., Akita, H., Maruyama, K., et al., Factors governing the in vivo tissue uptake of transferrin-coupled polyethylene glycol liposomes in vivo. *Int J Pharm* **281**, 25-33 (2004).
- [117] Peer, D. and Margalit, R., Tumor-targeted hyaluronan nanoliposomes increase the antitumor activity of liposomal Doxorubicin in syngeneic and human xenograft mouse tumor models. *Neoplasia* **6**, 343-353 (2004).
- [118] Banerjee, R., Tyagi, P., Li, S. and Huang, L., Anisamide-targeted stealth liposomes: a potent carrier for targeting doxorubicin to human prostate cancer cells. *Int J Cancer* **112**, 693-700 (2004).
- [119] Gabizon, A., Horowitz, A. T., Goren, D., et al., In vivo fate of folate-targeted polyethylene-glycol liposomes in tumor-bearing mice. *Clinical Cancer Research* **9**, 6551-6559 (2003).
- [120] Ghaghada, K. B., Saul, J., Natarajan, J. V., et al., Folate targeting of drug carriers: A mathematical model. *J Control Release* **104**, 113-128 (2005).
- [121] Goren, D., Horowitz, A. T., Tzemach, D., et al., Nuclear delivery of doxorubicin via folate-targeted liposomes with bypass of multidrug-resistance efflux pump. *Clin Cancer Res* **6**, 1949-1957 (2000).

- [122] Leamon, C. P., Cooper, S. R. and Hardee, G. E., Folate-liposome-mediated antisense oligodeoxynucleotide targeting to cancer cells: evaluation in vitro and in vivo. *Bioconjug Chem* **14**, 738-747 (2003).
- [123] Lee, R. J. and Low, P. S., Folate-mediated tumor cell targeting of liposome-entrapped doxorubicin in vitro. *Biochim Biophys Acta* **1233**, 134-144 (1995).
- [124] Ni, S., Stephenson, S. M. and Lee, R. J., Folate receptor targeted delivery of liposomal daunorubicin into tumor cells. *Anticancer Res* **22**, 2131-2135. (2002).
- [125] Pan, X. Q. and Lee, R. J., In vivo antitumor activity of folate receptor-targeted liposomal daunorubicin in a murine leukemia model. *Anticancer Res* **25**, 343-346 (2005).
- [126] Saul, J. M., Annapragada, A., Natarajan, J. V. and Bellamkonda, R. V., Controlled targeting of liposomal doxorubicin via the folate receptor in vitro. *J Control Release* **92**, 49-67 (2003).
- [127] Shmeeda, H., Mak, L., Tzemach, D., et al., Intracellular uptake and intracavitary targeting of folate-conjugated liposomes in a mouse lymphoma model with up-regulated folate receptors. *Mol Cancer Ther* **5**, 818-824 (2006).
- [128] Turk, M. J., Waters, D. J. and Low, P. S., Folate-conjugated liposomes preferentially target macrophages associated with ovarian carcinoma. *Cancer Lett* **213**, 165-172 (2004).
- [129] Weitman, S. D., Lark, R. H., Coney, L. R., et al., Distribution of the folate receptor GP38 in normal and malignant cell lines and tissues. *Cancer Res* **52**, 3396-3401 (1992).
- [130] Kelemen, L. E., The role of folate receptor alpha in cancer development, progression and treatment: cause, consequence or innocent bystander? *Int J Cancer* **119**, 243-250 (2006).
- [131] Choi, S. W. and Mason, J. B., Folate and carcinogenesis: an integrated scheme. *J Nutr* **130**, 129-132 (2000).
- [132] Low, P. S. and Antony, A. C., Folate receptor-targeted drugs for cancer and inflammatory diseases. *Adv Drug Deliv Rev* **56**, 1055-1058 (2004).

- [133] Leamon, C. P. and Low, P. S., Delivery of macromolecules into living cells: a method that exploits folate receptor endocytosis. *Proc Natl Acad Sci U S A* **88**, 5572-5576. (1991).
- [134] Leamon, C. P. and Low, P. S., Cytotoxicity of momordin-folate conjugates in cultured human cells. *J Biol Chem* **267**, 24966-24971 (1992).
- [135] Leamon, C. P., Pastan, I. and Low, P. S., Cytotoxicity of folate-Pseudomonas exotoxin conjugates toward tumor cells. Contribution of translocation domain. *J Biol Chem* **268**, 24847-24854 (1993).
- [136] Pan, X. Q., Hang, H. and Lee, R. J., Antitumor activity of folate receptor-targeted liposomal doxorubicin in a KB oral carcinoma murine xenograft model. *Pharmaceutical research* **20**, 417-422 (2003).
- [137] Sudimack, J. and Lee, R. J., Targeted drug delivery via the folate receptor. *Adv Drug Deliv Rev* **41**, 147-162 (2000).
- [138] Sudimack, J. J., Adams, D., Rotaru, J., et al., Folate receptor-mediated liposomal delivery of a lipophilic boron agent to tumor cells in vitro for neutron capture therapy. *Pharm Res* **19**, 1502-1508 (2002).
- [139] Wu, J., Liu, Q. and Lee, R. J., A folate receptor-targeted liposomal formulation for paclitaxel. *Int J Pharm* **316**, 148-153 (2006).
- [140] Saito, G., Swanson, J. A. and Lee, K. D., Drug delivery strategy utilizing conjugation via reversible disulfide linkages: role and site of cellular reducing activities. *Adv Drug Deliv Rev* **55**, 199-215 (2003).
- [141] West, K. R. and Otto, S., Reversible covalent chemistry in drug delivery. *Curr Drug Discov Technol* **2**, 123-160 (2005).
- [142] Ishida, T., Kirchmeier, M. J., Moase, E. H., et al., Targeted delivery and triggered release of liposomal doxorubicin enhances cytotoxicity against human B lymphoma cells. *Biochim Biophys Acta* **1515**, 144-158 (2001).
- [143] Kirpotin, D., Hong, K., Mullah, N., et al., Liposomes with detachable polymer coating: destabilization and fusion of dioleoylphosphatidylethanolamine vesicles

- triggered by cleavage of surface-grafted poly(ethylene glycol). *FEBS Lett* **388**, 115-118 (1996).
- [144] Zhang, J. X., Zalipsky, S., Mullah, N., et al., Pharmacological attributes of dioleoylphosphatidylethanolamine/cholesterylhemisuccinate liposomes containing different types of cleavable lipopolymers. *Pharmacol Res* **49**, 185-198 (2004).
- [145] Zalipsky, S., Qazen, M., Walker, J. A., 2nd, et al., New detachable poly(ethylene glycol) conjugates: cysteine-cleavable lipopolymers regenerating natural phospholipid, diacyl phosphatidylethanolamine. *Bioconjug Chem* **10**, 703-707 (1999).
- [146] Karathanasis, E., Ayyagari, A. L., Bhavane, R., et al., Preparation of in vivo cleavable agglomerated liposomes suitable for modulated pulmonary drug delivery. *J Control Release* **103**, 159-175 (2005).
- [147] Karathanasis, E., Bhavane, R. and Annapragada, A. V., Triggered release of inhaled insulin from the agglomerated vesicles: pharmacodynamic studies in rats. *J Control Release* **113**, 117-127 (2006).
- [148] Hatakeyama, H., Akita, H., Kogure, K., et al., Development of a novel systemic gene delivery system for cancer therapy with a tumor-specific cleavable PEG-lipid. *Gene Ther* **14**, 68-77 (2007).
- [149] Terada, T., Iwai, M., Kawakami, S., et al., Novel PEG-matrix metalloproteinase-2 cleavable peptide-lipid containing galactosylated liposomes for hepatocellular carcinoma-selective targeting. *J Control Release* **111**, 333-342 (2006).
- [150] Akiyama, Y., Nagasaki, Y. and Kataoka, K., Synthesis of heterotelechelic poly(ethylene glycol) derivatives having alpha-benzaldehyde and omega-pyridyl disulfide groups by ring opening polymerization of ethylene oxide using 4-(diethoxymethyl)benzyl alkoxide as a novel initiator. *Bioconjug Chem* **15**, 424-427 (2004).
- [151] Maeda, T. and Fujimoto, K., A reduction-triggered delivery by a liposomal carrier possessing membrane-permeable ligands and a detachable coating. *Colloids Surf B Biointerfaces* **49**, 15-21 (2006).
- [152] Mercadal, M., Domingo, J. C., Petriz, J., et al., Preparation of immunoliposomes bearing poly(ethylene glycol)-coupled monoclonal antibody linked via a cleavable

disulfide bond for ex vivo applications. *Biochim Biophys Acta* **1509**, 299-310 (2000).

CHAPTER 4. EVALUATION OF ALTERNATIVE TARGETING AGENTS TO IMPROVE TREATMENT EFFICACY

4.1. INTRODUCTION

Liposomal nanocarriers show vast potential in the field of chemotherapy particularly due to the demonstrated ability to passively accumulate to tumors increasing delivery to the target site while preventing uptake by non-target organs and reducing the side-effects commonly associated with traditional chemotherapeutics. Passive targeting to tumors is due to increased vascular permeability at the tumor site combined with the prolonged circulation of liposomes in the bloodstream. Elevated permeability results from the presence of enlarged interendothelial gaps along the emergent tumor vasculature, and an increased number of passages through the 'leaky' microvascular bed at the tumor site facilitates passive extravasation of liposomes. Prolonged circulation times are achieved through steric stabilization of liposomes upon the attachment of polyethylene glycol (PEG) to the external surface preventing RES recognition and clearance of the nanocarriers. While passive targeting of nanocarriers increases the delivery of chemotherapeutics to the tumor site, it does not facilitate uptake by the target cells after extravasation, therefore, active targeting agents are often incorporated to promote binding and uptake by tumor cells. Unfortunately, the exposure of targeting agents on the liposomal surface has been shown to increase RES recognition of nanocarriers thus reducing passive targeting to tumors. To address this issue, we have proposed controlling the exposure of targeting agents on the liposomal surface to enable both RES evasion and active tumor targeting. An alternative approach to maintain the RES evasion capability of targeted liposomes involves the use of small peptides as

targeting agents. Numerous studies have demonstrated that circulation times of PEGylated liposomes remain prolonged when small targeting agents such as peptides [1, 2] or antibody fragments [3, 4] are utilized in lieu of their larger counterparts. To further investigate the impact of targeting agent size on RES evasion and liposomal treatment efficacy, we have evaluated 2 targeted liposomal formulations. The targeting agents utilized were a small peptide (1984 Da) targeted to aminopeptidase N and a large antibody (~150 kDa) targeted to the transferrin receptor.

Aminopeptidase N (APN) is an ecto-enzyme involved in the activation of collagenase utilized for extracellular matrix degradation during tumor cell invasion [5]. APN has also been identified to play an essential role in capillary tube formation during angiogenesis [6]. APN is an ideal target for chemotherapeutics because it has been shown to be expressed by angiogenic vessels, whereas expression is absent or minimal in established blood vessels [7]. In addition, a peptide motif (NGR) has been identified which binds the APN isoform expressed by tumor vessels and not the isoforms present in normal epithelial or myeloid cells [8] and delivery of numerous agents to angiogenic vessels has already been proven to be successful with this targeting agent [7, 9]. Targeting to the tumor vasculature not only aids in the localization of drug at the tumor site but has also been shown to treat tumors indirectly through vascular damage and anti-angiogenic effects making vascular targets ideal for liposomal delivery of chemotherapeutics [9, 10]. For the studies reported here, we have utilized a 19 amino acid peptide containing a NGR residue sequence targeted to aminopeptidase N (APN) as the targeting agent for liposomal DXR. This longer sequence allowed for accessibility of the NGR motif for target cell binding while attached to the liposomal surface via

PEG₃₃₅₀. A terminal cysteine was selected to allow for conjugation to maleimide groups on PEG chains bound to DSPE. NGR was incorporated into the liposomal formulations so that it would be present on the external surface of the nanocarriers to enable active targeting to angiogenic vessels within tumor. Formulations containing this small targeting peptide were investigated *in vivo* to determine the effects on circulation times in the bloodstream and treatment efficacy.

In addition, we also investigated liposomal formulations targeted to the transferrin receptor (TfR), which is also known to be over-expressed by tumor vasculature [11-13]. TfR is involved in the endocytosis and transcytosis of transferrin, the blood plasma protein for iron ion delivery [14]. It serves as an ideal target for liposomal chemotherapeutics because it has been shown to be expressed on both the tumor vasculature and tumor cell membranes [15, 16]. In addition, TfR has been shown to be selectively expressed by the brain capillary endothelium [12] and has been demonstrated to facilitate transcytosis of TfR-targeted liposomal drugs across the BBB [17]. The agent utilized to target TfR in these studies was a large antibody, OX26, conjugated to the distal ends of PEG₂₀₀₀. Formulations targeted with this antibody to TfR were investigated *in vivo* to explore the effects on circulation times and biodistribution and the ability to prolong survival in tumor-inoculated animals.

4.2. MATERIALS AND METHODS

4.2.1. SYNTHESIS AND MICELLE FORMATION OF DSPE-PEG₃₃₅₀-NGR

1,2-Distearoyl-sn-glycerophosphoethanolamine (DSPE)-PEG₃₃₅₀-NGR peptide was synthesized by methods similar to those described previously. Briefly, 6.06 μmol DSPE-PEG₃₃₅₀-maleimide and 6.55 μmol NGR peptide (GNGRGGVRRSSSRTPSDKYC)

were dissolved in 600 μ L DMSO before adding 5.4 mL deionized water and reacting at room temperature for 5 hours. The micellar product was dialyzed to remove unreacted peptide and the final concentration was determined using a modified Lowry method (DC protein assay, Bio-Rad, Hercules, CA).

4.2.2. PREPARATION OF APN-TARGETED LIPOSOMAL NANOCARRIERS

A 62:35:3 molar ratio of 1,2-distearoyl-sn-glycero-phosphocholine (DSPC, Genzyme, Cambridge, MA)/cholesterol (Sigma, St. Louis, MO)/DSPE-PEG₂₀₀₀ (Avanti Polar Lipids, Birmingham, AL) was dissolved in 1 mL of ethanol at 60 °C. 0.005% (mol) of fluorescent phospholipid (β -DPH, Invitrogen, Carlsbad, CA) was used to track phospholipid content. The lipids were hydrated with 9 mL 400 mM ammonium sulfate and extruded five times through a 0.2 μ m and 10 times through a 0.1 μ m Nucleopore membrane. Liposome size was determined by dynamic light scattering (90 Plus Particle Size Analyzer, Brookhaven Instruments, Holtsville, NY). Liposomes were dialyzed against a phosphate-buffered saline solution to establish an ammonium sulfate gradient for doxorubicin loading. NGR liposomes were prepared by adding DSPE-PEG₃₃₅₀-NGR peptide micelles to liposomes and heating at 60 °C for 1 h. Unincorporated micelles were removed through dialysis. Liposomal NGR was determined using a DC protein assay (BioRad, Hercules, CA). The number of NGR peptides per liposome was determined by a ligand to phospholipid ratio, assuming 120,000 phospholipid molecules per liposome where phospholipid content was quantified by DPH fluorescence, yielding a bulk average for the number of peptides per liposome.

4.2.3. PREPARATION OF OX26 LIPOSOMAL NANOCARRIERS

To fabricate OX26 liposomes, OX26 was thiolated with a 4:1 molar excess of 2-iminothiolane (Sigma) by reacting at room temperature for 1 hour similar to methods described elsewhere [18]. OX26-thiol was added to liposomes formulated as described above from a 62:35:2:1 molar ratio of DSPC/cholesterol/DSPE-PEG₂₀₀₀/DSPE-PEG₂₀₀₀-maleimide and allowed to react overnight with terminal maleimide groups on PEG₂₀₀₀. Unreacted OX26 was removed by size exclusion chromatography. Amount of liposome-coupled OX26 was determined by a Bradford dye-binding procedure (protein assay, Bio-Rad, Hercules, CA) after lysis of liposomes with 20% SDS. The number of OX26 antibodies per liposome was determined by an antibody to phospholipid ratio as described above for APN peptide.

4.2.4. ACTIVE LOADING OF DOXORUBICIN INTO LIPOSOMES

Following ligand incorporation or coupling, liposomes were loaded with doxorubicin (DXR, Henry Schein Inc., Melville, NY) via the ammonium sulfate gradient [19]. In brief, liposomes were mixed with DXR reconstituted in phosphate buffered saline and heated for 1 hour at 60°C. Unencapsulated DXR was removed by dialysis. Loading efficiency was determined by a 480 nm absorbance reading after lysis with 5% TritonX100.

4.2.5. TUMOR CELL CULTURE

9L cells (a kind gift from the University of California at San Francisco/Neurosurgery Tissue Bank) were maintained in MEM/EBSS supplemented with 10% FBS and 0.05 mg/mL gentamicin under conditions of 5% CO₂ and 95% humidity. 9L cells were harvested with 0.05% trypsin/0.53 mM EDTA. Cells were

counted with Trypan blue and a hemacytometer. Prior to implantation, cells were resuspended in serum-free Leibovitz's L-15 medium to a concentration of 2×10^8 cells/ml.

4.2.6. TUMOR INOCULATION

All animal studies were conducted under a protocol approved by the Institutional Animal Care and Use Committee (IACUC) at Georgia Institute of Technology. A rat glioma model was established by surgically implanting 2×10^6 9L glioma cells into the frontal lobe of 11-12 week old male Fisher 344 rats. During surgery, anesthesia was maintained through the administration of 2-3% inhalant isoflurane. The incision site was shaved and the animal mounted in a stereotaxic frame. The scalp was opened to expose the skull, and a burr hole was drilled 2 mm anterior and 2 mm lateral to the bregma. 9L glioma cells in 10 μ l of Leibovitz's L-15 medium were slowly injected into the frontal lobe through a 21-gauge needle at a depth of 3 mm. The burr hole was then sealed with bone wax, and the scalp was sutured.

4.2.7. IMMUNOHISTOCHEMISTRY FOR CHARACTERIZATION OF APN EXPRESSION

To ensure that inoculated 9L glioma tumors upregulate APN, explanted brains were examined for APN expression. Twelve days after tumor inoculation, rats were anesthetized by an IP injection of 50, 10 and 1.67 mg/kg respectively of ketamine/xylazine/acetylpromazine and perfused with phosphate-buffered saline (PBS) containing heparin (1000 units/L) followed by 4% paraformaldehyde in PBS. Brains were explanted and stored in 4% paraformaldehyde for approximately 24 hours prior to being embedded in paraffin. Paraffin embedded tissues were sliced into 5 μ m sections using a rotary microtome. Representative sections containing tumor were immunostained for APN. In brief, sections were deparaffinized and rehydrated using xylene and a graded

series of alcohols and then washed in PBS. Antigen retrieval was performed by incubating the slides in a citrate buffer (19.7 mM citric acid, 8.2 mM sodium citrate, pH 6.0) at 80°C for 20 minutes and then treating with 0.1% trypsin in Tris buffered saline (136.9 mM NaCl, 20 mM Tris-HCl, pH 7.2) for 15 minutes at 37°C. Sections were then washed with 0.1% Tween 20 in Tris buffered saline (TBST). Endogenous peroxidase was blocked by treating with 1% H₂O₂ in PBS. After washing with TBST, sections were exposed to a mouse monoclonal antibody to APN (1 µg/ml) in TBST containing 4% normal goat serum overnight at 4°C. Sections were then washed with TBST before applying anti-mouse poly horseradish peroxidase (Chemicon, Temecula, CA) for 30 minutes at room temperature. After washing with TBST, sections were exposed to DAB chromogen-buffer (Chemicon, Temecula, CA) for 20 minutes, washed with TBST, and counterstained with Harris' hematoxylin.

4.2.8. SURVIVAL STUDIES EVALUATING TREATMENT EFFICACY

Four days or 12 days after tumor inoculation, animals were treated with either a saline sham, non-targeted 'Stealth', or targeted liposomal DXR i.v. injection (10 mg/kg doxorubicin; ~60 mg/kg lipid) via tail vein. Equivalent volumes of 0.9% sterile saline solution were administered to animals receiving sham injections. Animals selected to receive multiple treatments were administered either non-targeted or APN-targeted liposomal DXR (10 mg/kg) 7 days after receiving the initial treatment. Tumor growth was allowed to progress until the animal showed signs of morbidity, at which point, interventional euthanasia was administered. Time of death was determined to be the following day.

4.2.9. *IN VIVO* CIRCULATION STUDIES

Adult, male Fisher 344 rats were given an i.v. injection of liposomal DXR (10 mg/kg DXR; ~60 mg/kg lipid). Each group of animals received one of the following formulations: non-targeted with 3% DSPE-PEG₂₀₀₀, APN-targeted with DSPE-PEG₃₃₅₀-NGR and 3% DSPE-PEG₂₀₀₀, or TfR-targeted with DSPE-PEG₂₀₀₀-OX26 and 3% DSPE-PEG₂₀₀₀. Number of targeting agents incorporated within targeted liposomes was varied to determine the effect on circulation time. Blood was collected from the orbital sinus immediately before injection and at various time points after injection. Plasma was isolated from each blood sample by centrifuging at 2,200g for 15 minutes. Plasma was diluted 1:4 with deionized water before mixing 200µl with 100µl of 10% Triton X-100, 200µl of water, and 1500µl of acidified isopropanol (0.75N HCl). Mixtures were stored overnight at -20°C to extract the drug and then warmed to room temperature and vortexed for 5 minutes. The samples were then centrifuged at 15,000g for 20 minutes. Fluorescence of supernatants was analyzed to determine doxorubicin content ($\lambda_{\text{ex}}=485$, $\lambda_{\text{em}}=590$). Plasma samples obtained immediately prior to injection were used to correct for background fluorescence.

4.2.10. BIODISTRIBUTION IN TUMOR INOCULATED ANIMALS

Thirteen days after glioma inoculation, when tumor was deemed large enough for explantation, an orbital blood sample was collected from each animal prior to treating with either a saline sham, non-targeted 'Stealth', or TfR-targeted liposomal DXR i.v. injection (10 mg/kg doxorubicin; ~60 mg/kg lipid) via tail vein. At each of two designated time points following injection (20 or 50 hours), DXR biodistribution was assessed. Animals were anesthetized with an IP injection of 50, 10 and 1.67 mg/kg

respectively of ketamine/xylazine/acetylpromazine, and a cardiac blood sample was obtained. Animals were then perfused with heparinized PBS (1000 units/L) to remove the blood. The spleen, brain, heart, lungs, liver, and kidneys were explanted, washed with PBS, and blotted dry. Tumor, identified by discoloration and variation in tissue texture, was dissected from the brain using a dissecting microscope at 7x magnification. Organs were weighed and frozen at -20°C until ready to be processed.

Plasma was isolated from each cardiac blood sample obtained prior to perfusion by centrifuging at 2,200g for 15 minutes. Plasma samples were stored at -20°C until ready to be analyzed. Doxorubicin was extracted from plasma and tissue samples in a manner similar to that described elsewhere [20]. Plasma was diluted 1:4 with water. Organs were homogenized in distilled, deionized water (20% wt/vol) using a Polytron Homogenizer (Brinkmann Instruments, Westbury, NY). Homogenates and 25% plasma samples (200µl) were mixed with 100µl of 10% Triton X-100, 200µl of water, and 1500µl of acidified isopropanol (0.75N HCl). Mixtures were stored overnight at -20°C to extract the drug and then warmed to room temperature and vortexed for 5 minutes. The samples were then centrifuged at 15,000g for 20 minutes. Fluorescence of supernatants was analyzed to determine doxorubicin content ($\lambda_{ex}=485$, $\lambda_{em}=590$). Organ samples from an animal treated with a saline sham i.v. injection and plasma samples obtained prior to doxorubicin injection were used to correct for background fluorescence.

4.3. RESULTS

4.3.1. IMMUNOHISTOCHEMISTRY FOR CHARACTERIZATION OF APN EXPRESSION

While it has been previously established that APN is expressed by endothelial cells in angiogenic vessels [7, 8], there exists no information regarding expression by 9L

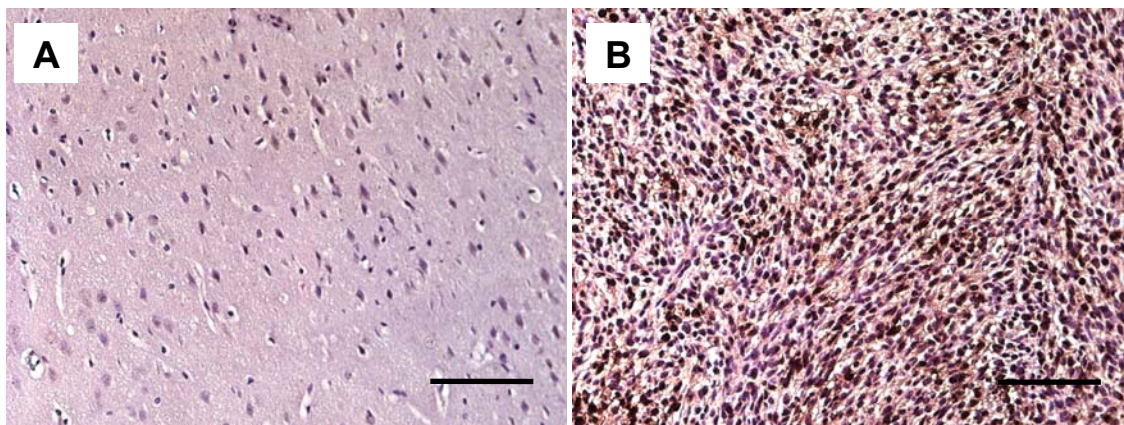


Figure 4.1. Aminopeptidase N is selectively over-expressed by 9L glioma tumors *in vivo*. Immunohistochemical analysis reveals expression of APN in tumor 12 days after inoculation. Brown horseradish peroxidase marks the location of APN in the fixed tissue. **(a)** Normal brain tissue serves as a negative control. **(b)** Tumor section obtained from Fisher 344 rat 12 days after intracranial 9L glioma tumor inoculation exhibiting elevated expression of APN. Scale bars represent 100 μm .

glioma. To evaluate *in vivo* expression, an intracranial tumor model was developed and APN expression was examined through immunohistochemistry on explanted brain tumors. The results confirmed that APN expression is elevated in intracranial 9L glioma compared to normal brain tissue (Figure 4.1). The established tumor, 12 days after implantation, demonstrated uniformly distributed APN expression while APN was not detected in normal brain tissue.

4.3.2. SURVIVAL STUDIES EVALUATING TREATMENT EFFICACY

Studies were performed to evaluate the therapeutic efficacy of non-targeted liposomal DXR compared to liposomal DXR targeted to APN or TfR. Using non-targeted and APN-targeted liposomes, the effect of treatment administration time point was examined. APN-targeted liposomes were equivalent to non-targeted liposomes with approximately 500 NGR peptides incorporated for targeting to APN. Animals received liposomal DXR either 4 or 12 days after tumor inoculation to determine the impact on treatment efficacy. The results of these studies are displayed in Figure 4.2. When

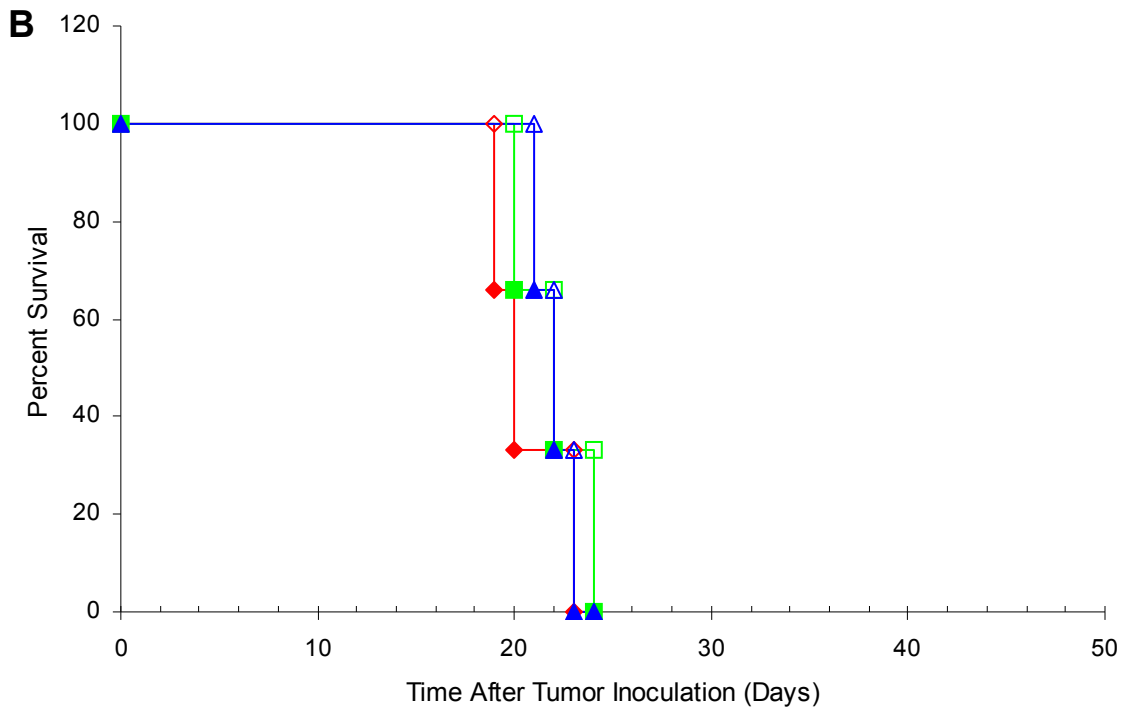
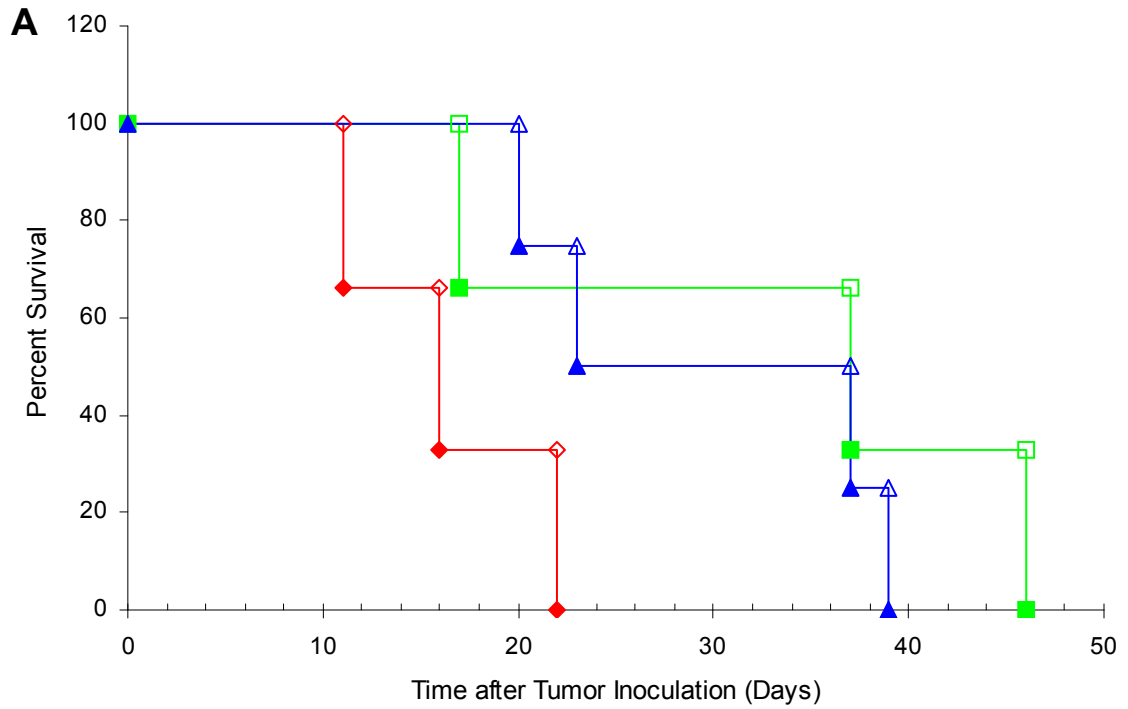


Figure 4.2. Use of NGR peptide to target liposomal DXR to APN does not prolong survival of tumor-bearing rats. Animals received saline sham (◆), non-targeted (■), or APN-targeted liposomal DXR (▲) i.v. 4 days (a) or 12 days (b) after tumor inoculation. There was no difference in survival of animals receiving non-targeted or targeted liposomal DXR at either time-point. Both liposomal treatments were able to prolong survival of tumor-bearing rats compared to saline-treated controls when administered 4 days after tumor inoculation, however, when treatment was delayed to 12 days after tumor inoculation, no difference in survival times was observed. Data represents mean ± SEM.

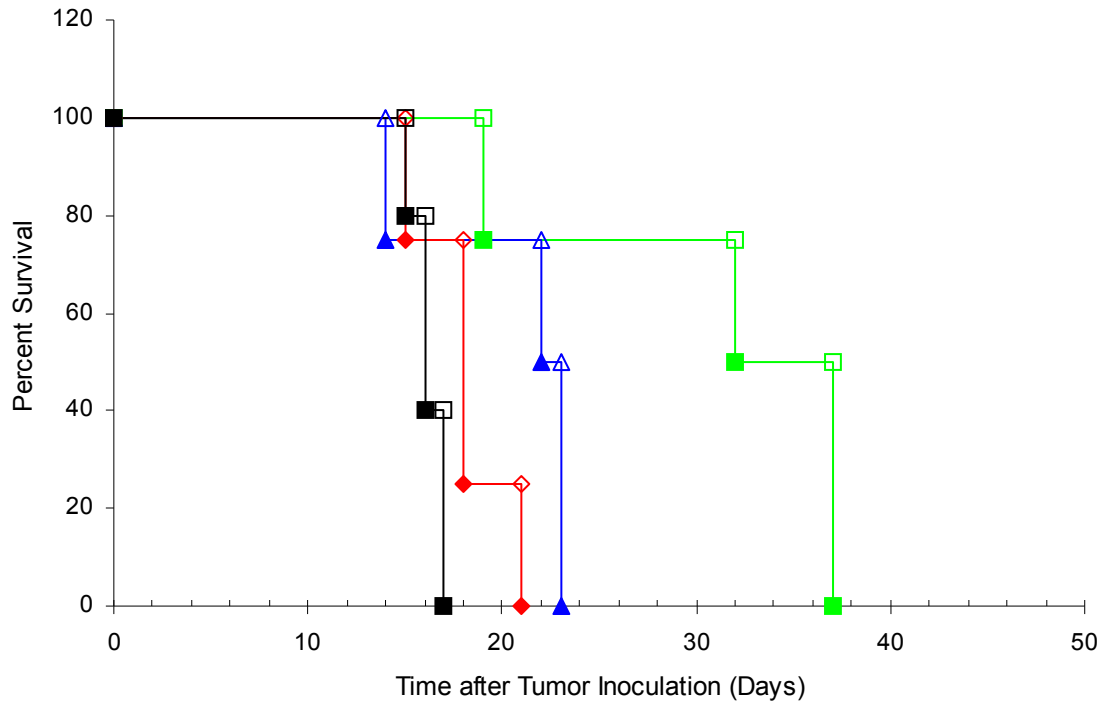


Figure 4.3. Use of OX26 antibody to target liposomal DXR to TfR does not prolong survival of tumor-bearing rats. Animals received a single dose of non-targeted (■) or TfR-targeted liposomal DXR (▲) i.v. 4 days after tumor inoculation. A subset of animals received an additional dose of non-targeted (◆) or TfR-targeted (■) liposomal DXR 11 days after tumor inoculation. There was no difference in survival of animals receiving non-targeted or targeted liposomal DXR under either treatment regimen. The addition of a second treatment administration doubled the cumulative dose of DXR and had a detrimental effect on survival times. Data represents mean \pm SEM.

animals received treatments 4 days after tumor inoculation, survival times of liposomal DXR treated animals were improved compared to saline-treated controls, however, there was no significant difference in survival between the groups receiving either non-targeted or APN-targeted liposomal DXR (Figure 4.2(a)). When treatments were delayed and administered 12 days after tumor inoculation, survival times of treated animals did not demonstrate any improvement over saline-treated controls (Figure 4.2(b)). In addition, as seen with animals receiving treatments 4 days after tumor inoculation, there was no significant difference in survival times between animals receiving non-targeted or APN-targeted liposomal DXR 12 days after tumor implantation.

To investigate the impact of the use of larger targeting agents on therapeutic efficacy and to explore the effect of multiple treatment administration, additional survival studies were conducted on tumor bearing rats receiving either non-targeted or TfR-targeted liposomal DXR. Animals received treatments 4 days after tumor inoculation, and a subset of animals received an additional treatment 11 days after tumor inoculation. Survival was monitored, and the results of this study are exhibited in Figure 4.3. No improvement in survival resulted upon the inclusion of OX26 for TfR targeting of liposomal DXR as demonstrated by the absence of a change in survival times between animals receiving non-targeted liposomal DXR compared to those receiving TfR-targeted liposomal DXR. In addition, increasing the number of treatments administered to tumor-bearing rats actually had a detrimental impact on survival times.

4.3.3. *IN VIVO* CIRCULATION STUDIES

In vivo circulation studies were performed on rats receiving non-targeted, APN-targeted, or TfR-targeted liposomal DXR to further explore the impact of targeting agent size and possibly elucidate the reason why an improvement in treatment efficacy was not observed in survival studies for animals receiving actively-targeted treatments. Figure 4.4 displays the results from the circulation study on rats receiving either non-targeted or APN-targeted liposomal DXR. Circulation data were fitted to bi-exponential curves. Areas under the curves (AUCs) and plasma half-lives were determined for each formulation and are reported in the table inset of Figure 4.4. Overall, the incorporation of APN-targeting NGR peptide into sterically stabilized liposomal DXR formulations had little effect on circulation times. The AUCs were not significantly different between the 3 formulations tested, and there was no difference between the plasma half-life of non-

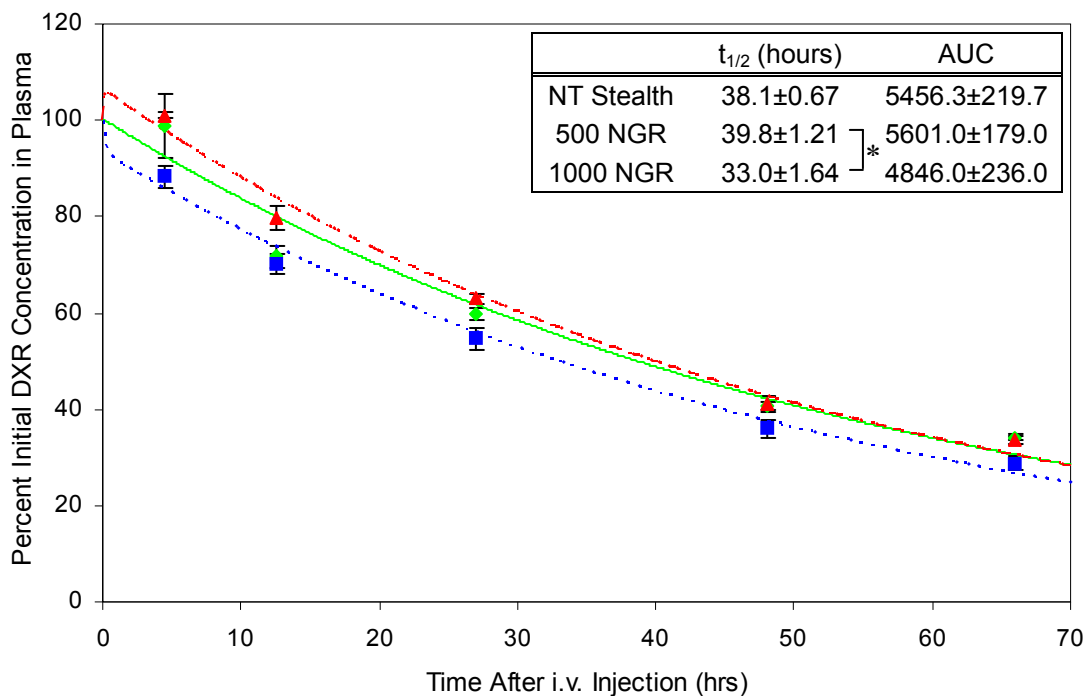


Figure 4.4. APN-targeted liposomes retain the ability to evade the RES. Circulating levels of DXR in the bloodstream, expressed as a percentage of initial DXR concentration, over time in animals receiving an i.v. injection of Stealth NT (◆) (n=3) or APN-targeted liposomal DXR containing 500 (▲) (n=3) or 1000 (■) (n=3) NGR peptides. Data were fit to exponential curves to determine half-lives and AUC's. Inclusion of targeting agents did not have a significant effect on calculated AUC. A significant decrease in half-life was observed when the number of NGR peptides inserted was increased from 500 to 1000 (*p=0.0192, ANOVA), although there was no significant difference in half-life between liposomes targeted with 1000 NGR peptides and Stealth NT liposomes. Data represent mean ± SEM.

targeted liposomes compared to either APN-targeted formulation. There was a significant decrease in half-life when the number of NGR peptides was increased from 500 to 1000; however, the latter formulation displayed a half-life that was comparable to that obtained with non-targeted liposomes demonstrating that this formulation retained the ability to evade the RES.

A dramatic difference in the circulation study results was observed when a larger targeting agent, OX26, was employed in liposomal formulations targeted to TfR (Figure 4.5). After fitting circulation data to bi-exponential curves, plasma half-lives and AUCs were compared and are displayed in the inset table in Figure 4.5. Every targeted

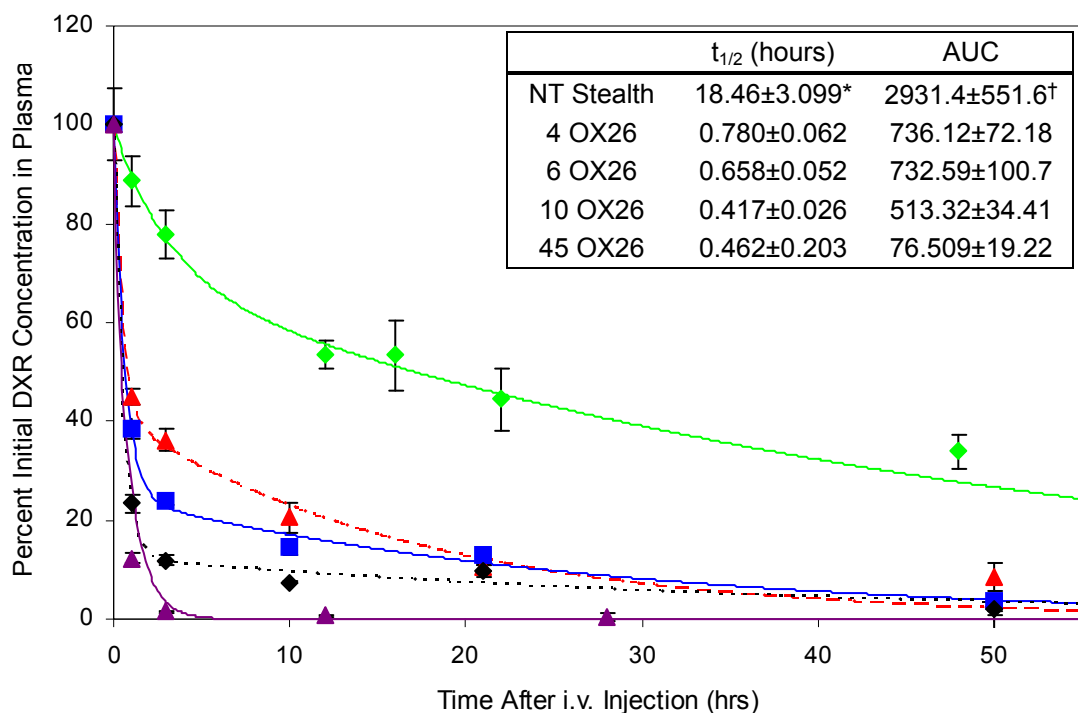


Figure 4.5. Inclusion of OX26 antibody to facilitate active targeting of sterically stabilized liposomes to TfR significantly decreases circulation times. Circulating levels of DXR in the bloodstream, expressed as a percentage of initial DXR concentration, over time in animals receiving an i.v. injection of Stealth NT (◆) (n=3) or TfR-targeted liposomal DXR containing 4 (▲) (n=3), 6 (■) (n=3), 10 (◆) (n=3), or 45 (▲) (n=3) OX26 antibodies. Data were fit to exponential curves to determine half-lives and AUC's. Inclusion of targeting agents had a significant and detrimental impact on calculated AUCs and plasma half-lives (* $p < 0.0003$, † $p < 0.007$, ANOVA). Data represent mean \pm SEM.

formulation tested exhibited a significant decrease in both plasma half-life and AUC compared to non-targeted liposome treated controls. The addition of as few as 4 OX26 antibodies decreased circulation half-life from 18.5 hours to a mere 47 minutes, and the AUC was reduced by a factor of 4. Liposomes formulated with higher levels of OX26 demonstrated even further reductions in half-lives and AUCs.

4.3.4. BIODISTRIBUTION IN TUMOR INOCULATED ANIMALS

Additional studies were performed to determine biodistribution of DXR in tumor-bearing animals after receiving either non-targeted or TfR-targeted liposomal DXR. Initially, studies were conducted on rats without tumors to determine ability to achieve

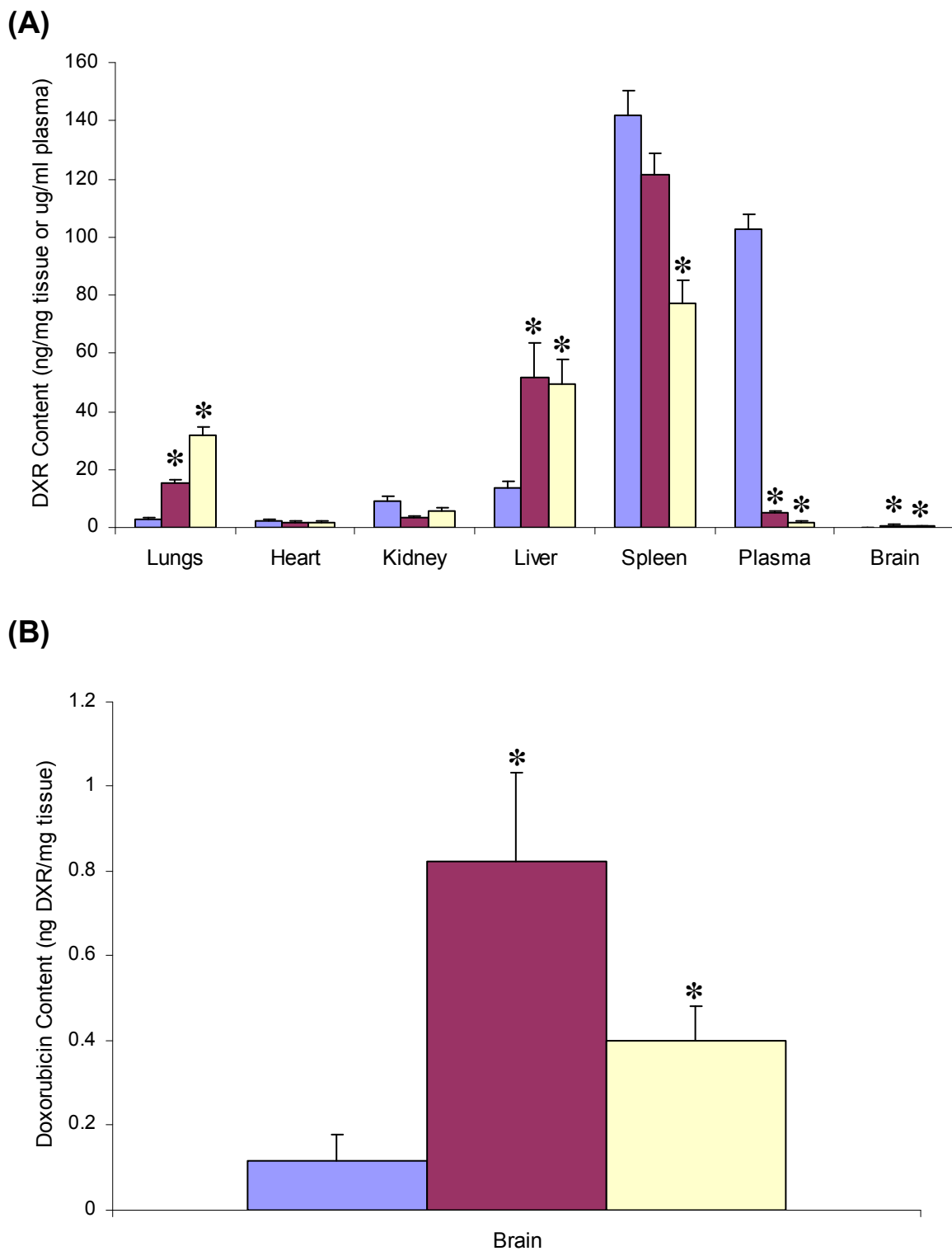


Figure 4.6. Targeting to TfR with OX26 alters the biodistribution of liposomal DXR 20 hours after treatment administration. Overall organ distribution (A) and brain uptake (B) of non-targeted liposomal DXR (■) or TfR-targeted liposomal DXR containing 45 (■) or 60 (■) OX26 is shown. *Statistically significant differences to non-targeted liposomes (Student's t-test), $p < 0.05$. Values represent mean \pm SEM.

delivery of drug to the brain through transcytosis across the BBB using 0, 45, or 60 OX26 antibodies to target TfR (Figure 4.6). Biodistribution was examined 20 hours after treatment administration. As predicted by the circulation study, plasma DXR levels were significantly reduced in animals receiving TfR-targeted liposomes compared to those treated with non-targeted liposomes. This reduction in plasma levels was reflected by a significant increase in lung, liver, and brain levels of drug uptake. The formulation containing 60 OX26 antibodies demonstrated a significant reduction in uptake by the spleen compared to the 2 other formulations. Levels of uptake by the heart were comparable for all 3 formulations. Delivery to the brain was significantly increased in animals receiving TfR-targeted liposomes compared to those treated with non-targeted liposomes (Figure 4.6(b)).

Additional biodistribution studies were performed on tumor-bearing animals 50 hours after the administration of either non-targeted liposomal DXR or TfR-targeted (45 OX26) liposomal DXR (Figure 4.7). At this time point, in contrast to the 20-hour study, levels of TfR-targeted drug detected in the spleen were significantly increased compared to non-targeted controls. Once again, there was a significant increase in uptake of targeted formulations by the brain compared to non-targeted liposomes. For both non-targeted and targeted liposomes, uptake at the tumor site was significantly increased compared to brain uptake, however, there was no significant difference in tumor uptake between the 2 formulations (Figure 4.7(b)).

Finally, delivery of liposomes to the brain 50 hours after treatment administration was investigated using lower amounts of OX26 (4, 6, and 10 OX26 per liposome) for TfR-targeted liposomes to determine whether an improvement in delivery to the brain

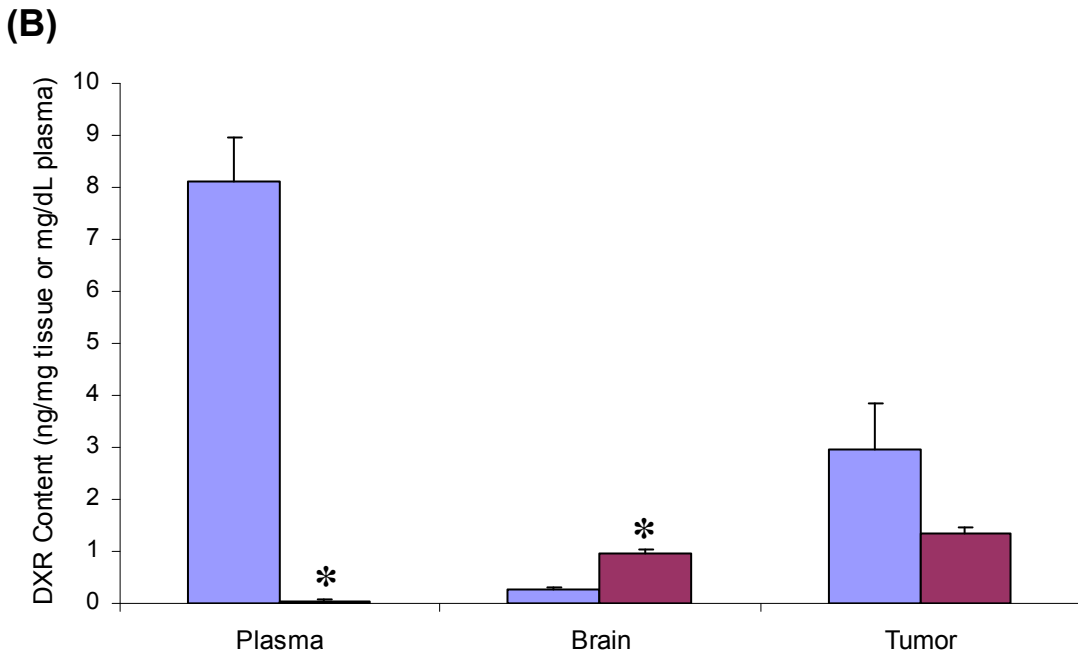
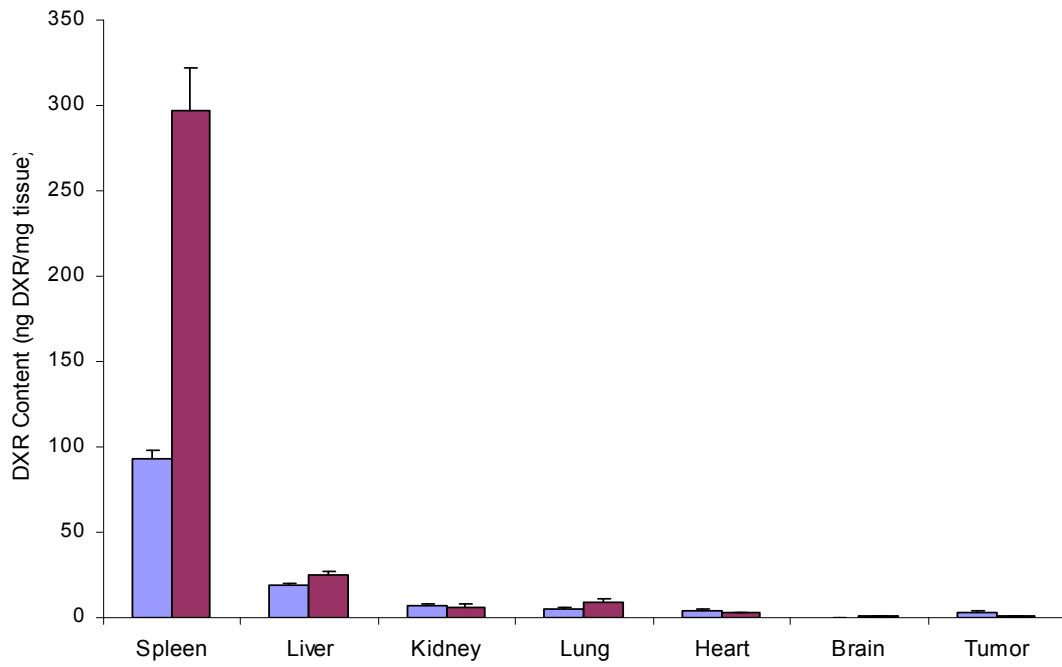


Figure 4.7. Targeting to TfR with OX26 alters the biodistribution of liposomal DXR 50 hours after treatment administration. Overall organ distribution (A) and plasma, brain, and tumor uptake (B) of non-targeted liposomal DXR (□) or TfR-targeted liposomal DXR containing 45 OX26 (■) is shown. *Statistically significant differences to non-targeted liposomes (Student's t-test), $p < 0.05$. Values represent mean \pm SEM.

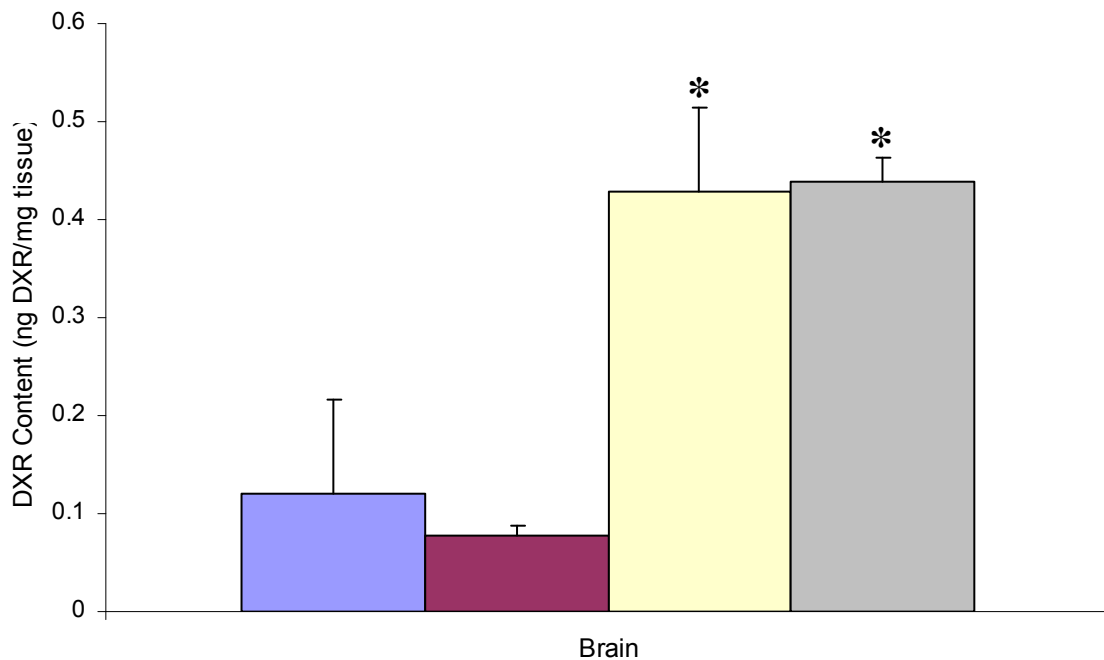


Figure 4.8. Targeting to TfR with lower levels of OX26 exposes the minimum number of antibodies necessary to achieve selective delivery to the brain 50 hours after treatment administration. Brain uptake of non-targeted liposomal DXR (■) or TfR-targeted liposomal DXR containing 4 (■), 6 (■), or 10 (■) OX26 per liposome is shown. *Statistically significant differences to non-targeted liposomes (Student's t-test), $p < 0.05$. Values represent mean \pm SEM.

could be achieved (Figure 4.8). There was no significant difference in brain delivery of liposomes targeted with 4 OX26 compared to non-targeted controls, however uptake was significantly increased when liposomes containing either 6 or 10 OX26 antibodies per liposomes were administered. It should be noted that brain uptake of these 2 formulations was about half that observed at the same time point for targeted formulations composed with 45 OX26 per liposome (Figure 4.7(b)).

4.4. DISCUSSION

The overall goal of these studies was to evaluate alterations in treatment performance in response to the incorporation of different targeting agents in liposomal

DXR formulations. Two different targeting agents were investigated; the first, a small peptide, was presented as an alternative solution to the issue of targeting agent recognition and accelerated clearance by the RES reported for actively targeted liposomes. This peptide containing the APN-targeting motif, NGR, has been reported to exhibit minimal immunogenicity *in vivo* and therefore, served as an ideal candidate in these attempts to maintain prolonged circulation of actively targeted liposomal nanocarriers. In addition, immunohistochemistry verified that APN is upregulated within 9L glioma tumors after implantation. The presence of APN within tumor 12 days after tumor inoculation in our model verifies that this target is available for tumor cell targeting in addition to vascular targeting of liposomal formulations. Survival studies utilizing APN-targeted liposomal DXR emphasized the importance of liposomal treatment administration time point in tumor-inoculated animals. Delaying treatment by 8 days in this tumor model, completely eradicated the benefits of treatment. In addition, it was shown that the inclusion of NGR peptide intended to facilitate targeting to APN on both the tumor vasculature and the tumor cell membranes did not have a significant impact on survival times of glioma tumor-bearing animals receiving a single dose of liposomal DXR.

An antibody to TfR, OX26, was the other targeting agent selected for these studies. Unfortunately, the inclusion of OX26 targeting agents in liposomal DXR formulations was also unable to improve the survival of tumor-bearing animals receiving a single dose of liposomal DXR. In an effort to enhance treatment efficacy, a multiple treatment regimen was adopted, however, increasing the treatment administration frequency from a single to a double dose was actually detrimental to animal survival.

This may have been due to the treatment dose (10 mg/kg DXR) chosen for these experiments. Instead of maintaining a constant cumulative dose of 10 mg/kg, animals receiving two doses of DXR actually received a cumulative dose of 20 mg/kg. Even though DXR was encapsulated within liposomes to decrease toxicity of the drug, this dosage may have been above the tolerable level for these animals. To address this issue, a longer period between treatment administrations should be utilized to ensure that the original dose is entirely cleared and recovery from non-target damage is complete or the individual doses should be reduced to maintain an equivalent cumulative treatment dose.

In an effort to determine why a positive impact on treatment efficacy was not achieved through the incorporation of APN-targeting peptides or TfR-targeting antibodies, *in vivo* circulation studies were performed to ensure that adequate circulating levels of drug were maintained in the bloodstream preserving the ability to passively target tumors. It was shown that NGR peptides did not impact circulation times of liposomal nanocarriers. This result was surprising given the inability of APN-targeted liposomal DXR to extend the survival of tumor-bearing rats. Additional studies must be performed to determine the reason why survival was not prolonged. First and foremost, *in vitro* uptake studies must be performed to verify that nuclear delivery may be achieved with APN-targeted liposomes. Biodistribution studies would serve to ensure that delivery across the BBB is possible using NGR peptides. Finally, alternative treatment regimens may be explored determine whether an improvement in treatment efficacy may be achieved with APN-targeted liposomal DXR.

While the inclusion of NGR peptides had little effect on the circulation of liposomes, OX26 antibodies had a severe detrimental impact on circulating levels of drug

in the bloodstream. As few as 4 OX26 antibodies per liposome were shown to cause a significant reduction in both AUC and half-lives of TfR-targeted liposomes compared to non-targeted control liposomes. Of these 2 targeting agents, the most obvious difference is size. In fact, there is a 75-fold difference in molecular weight between the NGR peptide and the OX26 antibody. Presumably, however, it is not size alone which determines the ability to evade the RES particularly since other targeting agents smaller than the peptide reported here have been shown to accelerate clearance of liposomal formulations from the bloodstream upon incorporation [21, 22]. Other factors such as polarity, hydrophobicity, overall surface charge, and targeting agent configuration among other characteristics must also play a role in the ability of the RES to recognize these molecules on the surface of liposomal formulations and accelerate clearance from the bloodstream. The NGR motif has been shown in these studies and by others to be minimally immunogenic. The primary reason suggested for the low immunogenicity of NGR has been its ability to mimic natural proteins in the bloodstream. The NGR motif is present in natural proteins such as fibronectin which contains 4 NGR sequences [23]. Structural similarities between the NGR motif and naturally present proteins may explain its ability to evade the RES [24]. Conversely, OX26 is much larger in size, presumably extending beyond the hydrophilic PEG barrier at the liposome surface, but more importantly, the antibody is of murine origin which most likely contributes to the triggered acceleration in RES clearance of TfR-targeted liposomes. Many investigators have utilized antibody fragments in lieu of entire antibodies to avoid Fc receptor-mediated clearance [3, 4] and the results presented here emphasize this need, however, opting for antibody fragments may result in a reduction in antigen binding affinity which

should also be taken into consideration. The entire OX26 antibody was utilized for these particular studies to ensure a vast difference in targeting agent size enabling comparison between 2 extremes.

TfR-targeted formulations were further investigated in biodistribution studies to investigate the true impact of drastically reduced circulating levels of drug on the ability to achieve delivery to target sites. Twenty hour biodistribution studies performed in the absence of tumor demonstrated a significant reduction in circulating levels of drug in the bloodstream when 45 or 60 OX26 antibodies were utilized for TfR targeting. The primary clearance route accounting for these reductions appeared to be through the liver, which demonstrated a significant increase in uptake of targeted formulations. An increase in delivery to the lungs was observed and may be attributed to binding to lung TfR since uptake was incrementally increased as the number of OX26 antibodies was increased. Uptake by the spleen was significantly reduced for liposomes targeted with 60 OX26 compared to non-targeted formulations and TfR-targeted formulations containing 45 OX26 antibodies. This may be due to RES recognition of maleimide at the terminal ends of unconjugated PEG chains and clearance via the spleen. This difference in uptake by the spleen was reversed 30 hours later when TfR-targeted liposomes surpassed spleen uptake of non-targeted liposomes. This was accompanied by a reduction in liver levels of targeted liposomes and may be due to either coagulation of TfR-targeted liposomes over time in the bloodstream which would favor RES clearance via the spleen or may be due to saturation of factors responsible for clearance via the liver forcing an increase in clearance through the spleen.

The major finding of the biodistribution studies was that brain levels of drug were elevated (approximately 4-8 fold) for targeted formulations (6, 10, 45, and 60 OX26) compared to non-targeted controls at both 20 hours and 50 hours, although brain uptake was relatively low in comparison to delivery to all of the other organs studied. The fact that delivery across the BBB to the brain was significantly increased despite the dramatic reduction in circulating levels of drug suggests that the presence of OX26 must significantly facilitate transcytosis across the BBB. If plasma clearance issues could be resolved, then delivery may be further improved. Unfortunately, we showed that decreasing the number of OX26 antibodies to as low as 4 per liposome does not significantly improve circulation times and the biodistribution study performed after reducing the number of targeting antibodies from 45 to 4, 6, or 10 OX26, therefore, did not demonstrate any further improvement in delivery to the brain. Formulations with 6 and 10 OX26 per liposome, however, did exhibit a significant increase in brain delivery compared to non-targeted controls and, as with liposomes containing 45 OX26, may have potential for targeting of liposomal nanocarriers to the brain if RES evasion can be restored for these formulations. Liposomes formulated with 4 OX26 performed the worst *in vivo* since they still exhibited accelerated clearance by the RES and failed to achieve a significant increase in delivery to the brain.

Unfortunately, uptake by the tumor was not enhanced by the inclusion of 45 OX26 even though the maximum brain delivery was attained with this formulation and a significant increase in brain delivery was achieved compared to non-targeted controls. The inability of TfR-targeted liposomes to surpass tumor uptake of non-targeted liposomes despite significant increases in delivery to the brain is most likely because the

transport mechanism is different between these 2 sites. In healthy brain where the BBB is intact, delivery occurs through transcytosis via TfR; however, delivery to glioma, where the BBB is discontinuous, results primarily from the passive process of extravasation through the leaky vasculature at the tumor site. This process is critically dependent on circulating levels of drug, and therefore, the impact of accelerated clearance was more apparent in the case of delivery to the tumor.

4.5. CONCLUSIONS

These studies have emphasized the importance of careful consideration of targeting agent selection upon formulation of actively targeted liposomal nanocarriers. The small peptide investigated for APN targeting had no impact on liposome circulation times in the bloodstream, whereas the inclusion of as few as 4 OX26 antibodies had a severe detrimental effect on liposome performance *in vivo*. Unfortunately, neither the inclusion of NGR peptide or OX26 targeting agents in liposomal DXR formulations was able to improve the survival of tumor-bearing animals receiving a single dose of liposomal DXR. This result is explained by reduced circulating levels of drug in the case of TfR-targeted liposomes; however, additional studies with APN-targeted liposomes must be performed to determine why this formulation was unable to extend survival of tumor-bearing animals despite maintenance of prolonged circulation times. We have successfully achieved an enhancement in drug delivery to the brain using TfR-targeted liposomes, which is significant considering the drastic reductions in circulation time upon inclusion of OX26 antibody as a targeting agent. These results further stress the need to address reductions in circulation times of actively targeted liposomal formulations and demonstrate that the use of smaller targeting agents or those able to mimic naturally

occurring substances in the body may provide an option to allow both RES evasion and active targeting *in vivo*.

4.6. REFERENCES

- [1] Pastorino, F., Brignole, C., Di Paolo, D., et al., Targeting liposomal chemotherapy via both tumor cell-specific and tumor vasculature-specific ligands potentiates therapeutic efficacy. *Cancer Res* **66**, 10073-10082 (2006).
- [2] Agarwal, A., Jaye, D. L., Giegerman, C. M. and Bellamkonda, R. V., Rational identification of a novel peptide for targeting nanocarriers to 9l glioma. *J Biomed Mater Res A* (2008).
- [3] Beduneau, A., Hindre, F., Clavreul, A., et al., Brain targeting using novel lipid nanovectors. *J Control Release* **126**, 44-49 (2008).
- [4] Maruyama, K., Takahashi, N., Tagawa, T., et al., Immunoliposomes bearing polyethyleneglycol-coupled fab' fragment show prolonged circulation time and high extravasation into targeted solid tumors in vivo. *FEBS Lett* **413**, 177-180 (1997).
- [5] Saiki, I., Fujii, H., Yoneda, J., et al., Role of aminopeptidase n (cd13) in tumor-cell invasion and extracellular matrix degradation. *Int J Cancer* **54**, 137-143 (1993).
- [6] Bhagwat, S. V., Lahdenranta, J., Giordano, R., et al., Cd13/apn is activated by angiogenic signals and is essential for capillary tube formation. *Blood* **97**, 652-659 (2001).
- [7] Pasqualini, R., Koivunen, E., Kain, R., et al., Aminopeptidase n is a receptor for tumor-homing peptides and a target for inhibiting angiogenesis. *Cancer Res* **60**, 722-727 (2000).
- [8] Curnis, F., Arrigoni, G., Sacchi, A., et al., Differential binding of drugs containing the ngr motif to cd13 isoforms in tumor vessels, epithelia, and myeloid cells. *Cancer Res* **62**, 867-874 (2002).
- [9] Pastorino, F., Brignole, C., Marimpietri, D., et al., Vascular damage and anti-angiogenic effects of tumor vessel-targeted liposomal chemotherapy. *Cancer Res* **63**, 7400-7409 (2003).
- [10] Wong, E. T. and Brem, S., Antiangiogenesis treatment for glioblastoma multiforme: Challenges and opportunities. *J Natl Compr Canc Netw* **6**, 515-522 (2008).

- [11] Jefferies, W. A., Brandon, M. R., Hunt, S. V., et al., Transferrin receptor on endothelium of brain capillaries. *Nature* **312**, 162-163 (1984).
- [12] Bickel, U., Kang, Y. S., Yoshikawa, T. and Pardridge, W. M., In vivo demonstration of subcellular localization of anti-transferrin receptor monoclonal antibody-colloidal gold conjugate in brain capillary endothelium. *J Histochem Cytochem* **42**, 1493-1497 (1994).
- [13] Huwyler, J. and Pardridge, W. M., Examination of blood-brain barrier transferrin receptor by confocal fluorescent microscopy of unfixed isolated rat brain capillaries. *J Neurochem* **70**, 883-886 (1998).
- [14] Moos, T. and Morgan, E. H., Transferrin and transferrin receptor function in brain barrier systems. *Cell Mol Neurobiol* **20**, 77-95 (2000).
- [15] O'Donnell, J. L., Joyce, M. R., Shannon, A. M., et al., Oncological implications of hypoxia inducible factor-1alpha (hif-1alpha) expression. *Cancer Treat Rev* **32**, 407-416 (2006).
- [16] Qing, Y., Shuo, W., Zhihua, W., et al., The in vitro antitumor effect and in vivo tumor-specificity distribution of human-mouse chimeric antibody against transferrin receptor. *Cancer Immunol Immunother* **55**, 1111-1121 (2006).
- [17] Cerletti, A., Drewe, J., Fricker, G., et al., Endocytosis and transcytosis of an immunoliposome-based brain drug delivery system. *J Drug Target* **8**, 435-446 (2000).
- [18] Lopes de Menezes, D. E., Kirchmeier, M. J., Gange, J.-F., et al., Cellular trafficking and cytotoxicity of anti-cd19-targeted liposomal doxorubicin in b lymphoma cells. *Journal of Liposome Research* **9**, 199-228 (1999).
- [19] Bolotin, E. M., Cohen, R., Bar, L. K., et al., Ammonium sulfate gradients for efficient and stable remote loading of amphipathic weak bases into liposomes and ligandoliposomes. *Journal of Liposome Research* **4**, 455-479 (1994).
- [20] Charrois, G. J. and Allen, T. M., Drug release rate influences the pharmacokinetics, biodistribution, therapeutic activity, and toxicity of pegylated liposomal doxorubicin formulations in murine breast cancer. *Biochim Biophys Acta* **1663**, 167-177 (2004).

- [21] McNeeley, K., Annapragada, A. and Bellamkonda, R., Decreased circulation time offsets increased efficacy of pegylated nanocarriers targeting folate receptors of glioma. *Nanotechnology* **18**, 1-11 (2007).
- [22] Gabizon, A., Horowitz, A. T., Goren, D., et al., In vivo fate of folate-targeted polyethylene-glycol liposomes in tumor-bearing mice. *Clinical Cancer Research* **9**, 6551-6559 (2003).
- [23] Kornblihtt, A. R., Vibe-Pedersen, K. and Baralle, F. E., Isolation and characterization of cDNA clones for human and bovine fibronectins. *Proc Natl Acad Sci U S A* **80**, 3218-3222 (1983).
- [24] Di Matteo, P., Curnis, F., Longhi, R., et al., Immunogenic and structural properties of the asn-gly-arg (ngr) tumor neovasculature-homing motif. *Mol Immunol* **43**, 1509-1518 (2006).

CHAPTER 5. DECREASED CIRCULATION TIME OFFSETS INCREASED EFFICACY OF PEGYLATED NANOCARRIERS TARGETING FOLATE RECEPTORS OF GLIOMA

As published with A.V. Annapragada and R.V. Bellamkonda, *Nanotechnology*, **18**, (2007) 385101.

5.1. ABSTRACT

Liposomal and other nanocarrier based drug delivery vehicles can localize to tumors through passive and/or active targeting. Passively targeted liposomal nanocarriers accumulate in tumors via ‘leaky’ vasculature through the enhanced permeability and retention (EPR) effect. Passive accumulation depends upon the circulation time and the degree of tumor vessel “leakiness”. After extravasation, actively targeted liposomal nanocarriers efficiently deliver their payload by receptor-mediated uptake. However, incorporation of targeting moieties can compromise circulation time in the blood due to recognition and clearance by the reticuloendothelial system, decreasing passive accumulation. Here, we compare efficacy of passively targeted doxorubicin-loaded PEGylated liposomal nanocarriers to actively targeted liposomal nanocarriers in a rat 9L brain tumor model. Although folate receptor (FR)-targeted liposomal nanocarriers had significantly reduced blood circulation time compared to PEGylated liposomal nanocarriers; intratumoral drug concentrations both at 20 and 50 h after administration were equal for both treatments. Both treatments significantly increased tumor-inoculated animal survival by 60-80% compared to non-treated controls, but no difference in survival was observed between FR-targeted and passively-targeted nanocarriers.

Therefore, alternate approaches allowing for active targeting without compromising circulation time may be important to fully realize the benefits of receptor-mediated active targeting of gliomas.

5.2. INTRODUCTION

In the past few decades, liposomal nanocarriers have been extensively investigated as drug carriers for cancer therapy and have been found to offer many benefits when utilized for drug delivery. One of the major benefits of PEGylated liposomal nanocarriers is their ability to evade the reticuloendothelial system (RES) and extend the circulation time of encapsulated drugs in the bloodstream. PEG chains on the outer leaflet of the liposomal bilayer are thought to provide a steric barrier to opsonin binding resulting in RES evasion [1-8]. Prolonged circulation in the bloodstream results in enhanced extravasation at sites exhibiting increased vasculature permeability [9-12]. For this reason, liposomal nanocarriers have shown increasing promise as drug delivery vehicles with the characteristic ability to passively accumulate in tumors and areas of injury.

Circulation time is an important factor for nanocarrier therapy of tumors and consequently much effort has gone into designing and optimizing liposomal nanocarriers to exhibit prolonged circulation times. Numerous studies have examined the effects of liposome size [13-15], charge [16], pH dependence [17], lipid composition [15, 18], cholesterol percentage [19], polymer incorporation [11], and degree of phospholipid saturation [20]. The results of these studies have confirmed that prolonged circulation is vital for passive targeting of liposomal nanocarriers at sites with “leaky” vasculature. Passive targeting is achieved when liposomal nanocarriers are formulated to evade the

RES and subsequently accumulate in areas with characteristic “leaky vasculature”, such as tumor sites or sites of injury. Drainage in tumors is typically limited, and the liposomal nanocarriers are retained at the site. This well-documented phenomenon has been designated the enhanced permeability and retention (EPR) effect and results in passive accumulation of liposomal nanocarriers at sites with compromised vasculature [9-12].

To further increase the efficacy of liposomal nanocarriers that reach the sites of interest, active targeting of drugs through the incorporation of targeting moieties on the exterior of nanocarriers has been explored. Active targeting offers many benefits including decreased side effects due to reduced accumulation in non-target organs [21-23]. When targeting moieties are included in the liposomal formulation, these carriers can be made to bind specifically to target cells and/or accumulate in areas of interest [24-28]. Several studies have examined the use of ligands [29-33], small peptides [34, 35], or antibodies [26, 36-38] to target over-expressed agents present on or around target cells.

Although active targeting of liposomal nanocarriers to tumors through the incorporation of targeting moieties has shown great promise *in vitro*, numerous *in vivo* studies utilizing targeting ligands designed to direct formulations to extravascular sites have not been as successful. FR-targeted studies, in particular, have shown very little success on solid tumors *in vivo* [39, 40]. Limited success has been achieved with FR-targeting in ascitic tumor models, but the increase in efficacy has been attributed to the fact that the tumors are disperse and do not limit drug diffusion or receptor binding [39, 41-44]. It has been suggested that solid tumors are more difficult to treat because drug delivery is impeded by the local tumor environment. High interstitial pressures

characteristic of tumors are known to prohibit transport of liposomal drugs beyond the perivascular space [45]. We suggest, and this study confirms, that while limited transport is a viable culprit, decreased circulating levels of drug also plays a substantial role in diminishing the success of these formulations. In fact, when circulation is not compromised, for example in immune-deficient animals, FR-targeted liposomal treatments have demonstrated greater success on solid tumors [46]. In addition, a study utilizing an *in vivo* adoptive tumor growth assay, which is unaffected by pharmacokinetic parameters, exhibited a distinct advantage of FR-targeted formulations over non-targeted in inhibiting tumor growth [47].

Therefore, long circulation times and receptor-targeted uptake comprise the 2 major facets of liposomal drug delivery, passive targeting and active targeting. Numerous studies have successfully documented the ability of targeted liposomal nanocarriers to bind specifically to target cells *in vitro* [29-31, 33, 47]; however, others have shown that the addition of targeting moieties often has a detrimental impact on RES evasion *in vivo* even when passive targeting methods, such as the inclusion of PEG, are used in combination [34, 39, 46, 48-50]. The liposomal drug delivery strategy to achieve the highest drug accumulation at the target site with limited uptake by non-target organs would ideally incorporate both active and passive methods of targeting where each method of delivery retains optimal performance.

In the present study, we attempted to specifically target a chemotherapeutic drug, doxorubicin, to a folate receptor (FR) over-expressing intracranial tumor in immunocompetent rats using a liposomal delivery vehicle. We chose a brain tumor model to perform these studies as it represents an invasive, non-localized tumor that is

difficult to treat by conventional methods such as surgical resection and/or radiation therapy. These tumors typically exhibit projections into the brain demonstrating the diffuse and invasive nature of the disease. The standard chemotherapeutic agents for brain tumors, nitrosoureas, have not been very effective as single agents and have failed to significantly improve survival times of patients compared with radiotherapy alone [51-54]. For this reason, targeted chemotherapeutics are desirable. We have chosen to target a chemotherapeutic, doxorubicin, to glioma using liposomal nanocarriers. Doxorubicin was selected for encapsulation since it is fluorescent, allowing for ease of detection, and it can be actively and stably loaded into liposomal nanocarriers, allowing for large drug payloads. In addition, doxorubicin has been shown to be more potent than nitrosoureas against glioma cells *in vitro* [55]. Liposomal doxorubicin has been investigated by several groups in the treatment of gliomas with promising results [56-58]. FR-targeted formulations have been studied extensively and represent an ideal targeting system [31, 39-44, 46, 49, 59-61]. Numerous tumors have been identified that over-express FR, and FR-targeted liposomal nanocarriers have been shown to actively bind these malignant cells and subsequently undergo endocytosis. Cellular uptake of FR-targeted liposomal nanocarriers has been shown to be dependent on the presence of adjacent PEG chains. Gabizon, *et al.* demonstrated that cell association of FR-targeted liposomal nanocarriers due to FR binding was completely inhibited when adjacent PEG chains were the same length as the folate-bearing PEG chains. Lengthening the folate-bearing PEG chains allowed for a dramatic increase in binding of FR-targeted liposomal nanocarriers to target cells [62]. In previous studies, we have investigated the liposomal delivery of doxorubicin to glioma cells *in vitro* utilizing FR as a target. We have previously

demonstrated that preferential uptake of doxorubicin by glioma cells can be achieved using FR-targeted liposomal nanocarriers containing an optimal number of targeting ligands [29]. For this study, folate-PEG conjugates were inserted into the bilayer of liposomal nanocarriers carrying doxorubicin to facilitate targeting to FR. We investigated whether this technique increases the doxorubicin dosage received by tumor cells while reducing non-specific delivery to tissues, which do not over-express FR receptor. In addition to dosage obtained at the tumor site, we evaluated delivery to non-target organs, clearance times, and overall increase in survival of tumor inoculated rodents relative to non-targeted or untreated control rodents. Ultimately, we examined the effect of converting a passively targeted formulation to actively targeted to determine whether the accompanying negative impact on passive accumulation offsets the benefit of active targeting. The resultant data emphasize the need to consider the effects, both beneficial and detrimental, of active targeting when formulating targeted liposomal nanocarriers to tumors.

5.3. MATERIALS AND METHODS

5.3.1. MATERIALS

A 9L glioma cell line was received as a generous donation from the Neurosurgery Tissue Bank at UCSF. Minimal essential medium containing Earle's balanced salt solution (MEM/EBSS) was purchased from Hyclone (Logan, UT). Gentamicin (50 mg/ml), fetal bovine serum (FBS), and Leibovitz's L-15 medium were obtained from Gibco (Carlsbad, CA). Trypsin-EDTA (0.05% trypsin, 0.53 mM EDTA) in Hanks' balanced salt solution was purchased from Mediatech (Herndon, VA). Heparin (1000 USP units/ml), isoflurane, and doxorubicin were obtained from Baxter Healthcare

(Deerfield, IL). Ketamine (100 mg/ml) was purchased from Fort Dodge Laboratories (Madison, NJ). Marcaine (0.5%) was obtained from Abbott Laboratories (Abbott Park, IL). Flunixin meglumine was purchased from Phoenix Scientific (San Marcos, CA). Xylazine (100 mg/ml) was purchased from The Butler Company (Dublin, OH). Acetylpromazine (10 mg/ml) was obtained from Boehringer Ingelheim (Ingelheim, Germany). Trifluoroacetic acid (TFA) and triethylamine (TEA) were obtained from Fisher Scientific (Pittsburgh, PA). Cholesterol, paraformaldehyde, and Triton X-100 were purchased from Sigma (St. Louis, MO). 1,2-Distearoyl-*sn*-glycerophospho-choline (DSPC), 1,2-Distearoyl-*sn*-glycero-3-phosphoethanolamine (DSPE), and 1,2-distearoyl-*sn*-glycerophosphoethanolamine poly(ethylene glycol)₂₀₀₀ (DSPE-PEG₂₀₀₀) were obtained from Avanti Polar Lipids (Birmingham, AL). t-Boc-HN-PEG₃₃₅₀-succinimidyl propionate (t-Boc-HN-PEG₃₃₅₀-SPA) was obtained from Shearwater Polymers (San Carlos, CA). A monoclonal antibody to nestin (mAb 353, IgG1) was purchased from Chemicon (Temecula, CA). Dialysis tubing (10,000 and 100,000 molecular weight cut-off) was purchased from Spectra/Por (Dominguez, CA). All animals were purchased from Harlan (Indianapolis, IN) and maintained on a folic acid deficient diet (<0.05 ppm) containing 1% succinylsulfathiozole obtained from Purina TestDiet (Richmond, IN). A stereotaxic frame was purchased from Kopf Instruments (Tujunga, CA) and utilized for tumor inoculation surgeries.

5.3.2. LIPOSOME FORMULATION

Liposomal nanocarriers were formulated using methods similar to those described elsewhere [63, 64]. In brief, a 62:35:3 molar ratio of DSPC:cholesterol:DSPE-PEG₂₀₀₀ was dissolved in ethanol (60°C) and then hydrated with 400 mM ammonium sulfate

buffer. The addition of 3% DSPE-PEG₂₀₀₀ was to enable RES evasion. The solution was extruded 5 times through a 0.2 µm filter and then 10 times through a 0.1 µm filter using a 10 ml Lipex Thermoline extruder (Northern Lipids, Vancouver, British Columbia, Canada) at 60°C. Liposomal nanocarriers were then dialyzed against decreasing concentrations of sodium chloride buffer to remove ethanol and establish an ammonium sulfate gradient used to facilitate doxorubicin loading. The average diameter of extruded liposomal nanocarriers was verified by dynamic light scattering (Brookhaven Instruments Corporation, Holtsville, NY) and determined to be approximately 110-115nm.

5.3.3. DSPE-PEG₃₃₅₀-FOLATE CONJUGATE SYNTHESIS

Since folate was to be utilized as a targeting ligand, it was necessary to formulate a DSPE-PEG₃₃₅₀-folate conjugate to allow insertion into the liposomal bilayer. A longer PEG chain (PEG₃₃₅₀) than those used to confer steric stabilization (PEG₂₀₀₀) was utilized to avoid the documented interference with FR binding when shorter PEG chains are used [62]. First, a DSPE-PEG₃₃₅₀-amine was synthesized according to methods described elsewhere [65]. Briefly, t-Boc-HN-PEG₃₃₅₀-SPA was dissolved in chloroform and mixed with DSPE followed by TEA (~1:1:3 molar ratio). The solution was heated to 60°C for 5 minutes and then mixed overnight at room temperature. The chloroform was rotary evaporated, and the residue was taken up with acetonitrile. The unreacted DSPE was precipitated by storing the mixture at 4°C for 6 hours. The solution was then centrifuged to remove the unreacted DSPE, evaporated, and dried over P₂O₅ under vacuum. A 10% solution of TFA in methylene chloride was added to the DSPE-PEG₃₃₅₀-t-Boc product and mixed at 0°C for 2 hours. The mixture was then washed 4 times with chloroform to remove the TFA and rehydrated with water. The solution was dialyzed (100,000

MWCO) against water to remove unreacted Boc-PEG₃₃₅₀-amine and then lyophilized to yield the DSPE-PEG₃₃₅₀-amine product.

Next, the DSPE-PEG₃₃₅₀-Folate conjugate was formed by previously described methods [29, 62]. Briefly, 36.8 mg of folate was dissolved in 1.415 ml of dry DMSO before adding 190 mg of DSPE-PEG₃₃₅₀-amine, 600 μ l of pyridine, and 46 mg of dicyclohexyl carbodiimide (DCC). The mixture was allowed to react for 4 hours at room temperature. The solution was rotary evaporated to remove pyridine and rehydrated with 17.5 ml water. Insoluble by-products were removed by centrifugation at 10,000g. The supernatant was dialyzed (100,000 MWCO) twice against 2 L 50 mM NaCl and three times against 2 L water. The retentate was then lyophilized to yield the final product, which was analyzed by thin-layer chromatography, ¹H NMR, and mass spectroscopy. $R_f=0.49$ in 1.48 N ammonium hydroxide. ¹H NMR (CDCl₃ solvent): DPPE [0.84 ppm (t), 1.2, 1.5(d), 2.25(d), 2.9(t), 3.1(t), 5.04(m)], PEG [3.3 ppm], and folic acid [1.91, 2.03, 2.3(t), 4.33(m), 4.48(d), 6.5(d), 6.93(t), 7.64(d), 8.12(d), 8.6(s)]. MW=3144Da.

5.3.4. DSPE-PEG₃₃₅₀-FOLATE INSERTION INTO PREFORMED LIPOSOMAL NANOCARRIERS

Folate-conjugates were inserted into preformed liposomal nanocarriers to create FR-targeted liposomal formulations. Non-targeted liposomal nanocarriers did not receive conjugates for insertion. Conjugate insertion was performed according to methods previously described [29, 66]. Briefly, DSPE-PEG₃₃₅₀-folate conjugates were micellized by dissolving in DMSO (60°C) to a concentration of 28 mM and then diluting 1:10 with water for a final concentration of 2.8 mM conjugate in 10% DMSO. Micelles were dialyzed (10,000 MWCO) twice against 1 L water to remove DMSO. Folate content of

the retentate was determined by measuring UV absorbance at 285 nm wavelength of micelles lysed in 10% SDS using a UV-visible spectrophotometer (Shimadzu Scientific Instruments Model 1601, Columbia, MD). Folate-conjugate micelles were then mixed with liposomal nanocarriers to achieve a concentration of 0.15% of the total lipid formulation. Our previous *in vitro* studies have demonstrated that maximum differentiation in drug uptake between malignant and cortical cells was achieved with 0.2% folate-conjugate insertion in the absence of adjacent DSPE-PEG₂₀₀₀ chains [29]. 0.15% folate-conjugate was inserted to generate the FR-targeted formulations for these *in vivo* studies since the insertion of higher numbers was partially hindered by adjacent DSPE-PEG₂₀₀₀ chains and this number allowed for consistent insertion efficiencies. Previous *in vitro* studies from our lab have also demonstrated that FR-targeted formulations containing as little as 0.05% folate-conjugate bind efficiently to malignant cells, consequently this reduction in targeting ligand insertion would still promote targeting to tumor cells [29]. The micelle/liposome mixture was then heated to 60°C for 1 hour to allow insertion. Afterwards, the liposomal nanocarriers were cooled on ice and then dialyzed (100,000 MWCO) to remove any ammonium sulfate or unincorporated folate-conjugates from the external phase of the liposomal nanocarriers. To verify adequate insertion, the folate content in the liposomal formulation was then analyzed by measuring the UV absorbance at 285 nm after lysing the liposomal nanocarriers with 10% SDS.

5.3.5. REMOTE LOADING OF DOXORUBICIN

Doxorubicin was loaded into the liposomal nanocarriers using an ammonium sulfate gradient as previously described [64]. In brief, liposomal nanocarriers were

mixed with doxorubicin reconstituted in PBS (15 mg/ml) at a ratio of 0.16 mg doxorubicin to 1 mg of lipid and heated to 60°C for 1 hour. The liposomal nanocarriers were then immediately cooled on ice and subsequently dialyzed to remove any remaining doxorubicin. The formulations were sterilized by passing through a 0.2 µm filter. Final doxorubicin content was assessed by lysing the liposomal nanocarriers with 5% Triton X-100 at 60°C and measuring the UV absorbance at 480 nm.

5.3.6. PLASMA CLEARANCE

In an effort to separate the effects of RES clearance and extravasation into tumor, these studies were performed in animals without tumors. Animals were given an intravenous (IV) injection of either non-targeted (n=5) or FR-targeted liposomal doxorubicin (n=5) via tail vein (10 mg/kg doxorubicin; ~60 mg/kg lipid). Blood was collected from the orbital sinus immediately before injection and at 1, 3, 12, 16, 22, 48, and 92 hours after injection. Plasma was isolated by centrifugation (2,200g, 15 min). Liposomal nanocarriers were lysed by treating with 5% Triton X-100 and heating to 60°C for 20 minutes. To accurately detect low levels of doxorubicin, fluorescent readings were obtained. Total doxorubicin content of each sample was analyzed ($\lambda_{\text{ex}}=485$, $\lambda_{\text{em}}=590$) using a fluorescence spectrometer (BIO-TEK, Synergy HT, Winooski, VT). Plasma samples obtained immediately prior to injection were used to correct for background fluorescence.

5.3.7. 9L GLIOMA CELL CULTURE

A 9L glioma cell line was maintained in MEM/EBSS medium supplemented with 10% fetal bovine serum and 0.05 mg/ml gentamicin. Cells were passaged by

trypsinization and washed with growth medium. Prior to implantation, cells were resuspended in serum-free Leibovitz's L-15 medium to a concentration of 2×10^8 cells/ml.

5.3.8. TUMOR INOCULATION

A rat glioma model was established by surgically implanting 2×10^6 9L glioma cells into the frontal lobe of 11-12 week old male Fisher 344 rats. All procedures were conducted under a protocol approved by the Institutional Animal Care and Use Committee (IACUC) at Georgia Institute of Technology. Animals were fed a folate-free diet containing 1% succinylsulfathiazole for approximately 18 days prior to surgery. Folate was eliminated from the diet in an attempt to prevent competitive binding of dietary folate to the folate receptors on tumor cells and to avoid possible down regulation of tumor FR after implantation. Although other studies have shown exclusion of dietary folate to have no effect on tumor uptake of exogenous folate, a succinylsulfathiazole supplement was not utilized to eliminate production of folate by the enteric microflora [39]. In addition, a study utilizing J6456 lymphoma *in vivo* demonstrated a quick down regulation of tumor FR expression when animals were kept on a normal folate-enriched diet [46]. Therefore, in our study, animals were maintained on the folate deficient diet for a minimum of 3 weeks prior to treatment as this has been proven adequate to sufficiently lower folate concentrations to a level comparable to that of humans [46]. During surgery, anesthesia was maintained through the administration of 2-3% inhalant isoflurane. The incision site was shaved and the animal mounted in a stereotaxic frame. The scalp was opened to expose the skull, and a burr hole was drilled 2 mm anterior and 2 mm lateral to the bregma. 2×10^6 9L glioma cells in $10 \mu\text{l}$ of Leibovitz's L-15 medium were slowly injected into the frontal lobe through a 21-gauge needle at a depth of 3 mm

below the brain surface. The burr hole was then sealed with bone wax, and the scalp was sutured closed. Animals received 5 ml Lactated Ringer's solution through intraperitoneal (IP) injection and a subcutaneous injection of 0.5% marcaine at the wound site. Flunixin meglumine (2.5 mg/kg) was administered through an intramuscular injection to alleviate pain as needed.

5.3.9. IMMUNOHISTOCHEMISTRY FOR CHARACTERIZATION OF ANGIOGENESIS

To ensure that the injection of liposomal nanocarriers would occur after the onset of angiogenesis, explanted brains were examined for new blood vessel formation. Four days after tumor inoculation, rats were anesthetized by an IP injection of 50, 10 and 1.67 mg/kg respectively of ketamine/xylazine/acetylpromazine and perfused with phosphate-buffered saline (PBS) containing heparin (1000 units/L) followed by 4% paraformaldehyde in PBS. Brains were explanted and stored in 4% paraformaldehyde for approximately 24 hours prior to being embedded in paraffin. Paraffin embedded tissues were sliced into 5 μ m sections using a rotary microtome. Representative sections containing tumor were immunostained for nestin, a marker of angiogenesis. In brief, sections were deparaffinized and rehydrated using xylene and a graded series of alcohols and then washed in PBS. Endogenous peroxidase was blocked by treating with 1% H₂O₂ in PBS, and the sections were treated with proteinase K (1 μ g/ml) for antigen retrieval. After washing with PBS and permeabilizing with 0.5% saponin in PBS, sections were exposed to a mouse monoclonal antibody to nestin (1 μ g/ml) in PBS containing 1% horse serum for 1 hour. Sections were then washed twice with PBS before applying the biotinylated secondary antibody in 0.5% saponin in 1% normal horse serum in PBS for 1 hour at room temperature. Slides were washed with PBS and incubated for 45 minutes

with Vectastain Elite ABC Reagent. Afterwards, sections were washed with PBS and then sterile deionized water and exposed to the Vector DAB substrate (0.067% in tris buffered saline with 0.024% H₂O₂). The reaction was terminated by washing with PBS, and the sections were then counterstained with Harris' hematoxylin.

5.3.10. BIODISTRIBUTION IN TUMOUR INOCULATED ANIMALS

Thirteen days after glioma inoculation, when tumor was deemed large enough for explantation, an orbital blood sample was collected from each animal prior to treating with either a saline sham, non-targeted 'Stealth' (20 hrs: n=8; 50 hrs: n=8), or FR-targeted (20 hrs: n=7; 50 hrs: n=10) liposomal doxorubicin IV injection (10 mg/kg doxorubicin; ~60 mg/kg lipid) via tail vein. At each of two designated time points following injection (20 or 50 hours), doxorubicin biodistribution was assessed.

Numerous investigators have reported liposomal accumulation in tumor to peak around 48 hours [39, 67, 68], which lead to the selection of the 50 hour time point for this study. The earlier time point (20 hours) was selected since it has been reported that FR-targeted liposomal nanocarriers may have an increased accumulation in tumor compared to non-targeted liposomal nanocarriers at earlier time points [39]. At each time point after doxorubicin administration, animals were anesthetized with an IP injection of 50, 10 and 1.67 mg/kg respectively of ketamine/xylazine/acetylpromazine, and a cardiac blood sample was obtained. Animals were then perfused with heparinized PBS (1000 units/L) to remove the blood. The spleen, brain, heart, lungs, liver, and kidneys were explanted, washed with PBS, and blotted dry. Tumor, identified by discoloration and variation in tissue texture, was dissected from the brain using a dissecting microscope at 7x magnification. Organs were weighed and frozen at -20°C until ready to be processed.

Plasma was isolated from each cardiac blood sample obtained prior to perfusion by centrifuging at 2,200g for 15 minutes. Plasma samples were stored at -20°C until ready to be analyzed. Doxorubicin was extracted from plasma and tissue samples in a manner similar to that described elsewhere [69]. Plasma was diluted 1:4 with water. Organs were homogenized in distilled, deionized water (20% wt/vol) using a Polytron Homogenizer (Brinkmann Instruments, Westbury, NY). Homogenates and 25% plasma samples (200µl) were mixed with 100µl of 10% Triton X-100, 200µl of water, and 1500µl of acidified isopropanol (0.75N HCl). Mixtures were stored overnight at -20°C to extract the drug and then warmed to room temperature and vortexed for 5 minutes. The samples were then centrifuged at 15,000g for 20 minutes. Fluorescence of supernatants was analyzed to determine doxorubicin content ($\lambda_{\text{ex}}=485$, $\lambda_{\text{em}}=590$). Organ samples from an animal treated with a saline sham IV injection and plasma samples obtained prior to doxorubicin injection were used to correct for background fluorescence.

5.3.11. SURVIVAL STUDIES

Four days after tumor inoculation, animals were treated with either a saline sham (n=5), non-targeted ‘Stealth’ (n=6), or FR-targeted (n=6) liposomal doxorubicin IV injection (10 mg/kg doxorubicin; ~60 mg/kg lipid) via tail vein. Equivalent volumes of 0.9% sterile saline solution were administered to animals receiving sham injections. Tumor growth was allowed to progress until the animal showed signs of morbidity, at which point, interventional euthanasia was administered. Time of death was determined to be the following day.

5.4. RESULTS

5.4.1. PLASMA CLEARANCE STUDIES

Analysis of doxorubicin in plasma samples obtained from treated rats revealed that the insertion of 0.15% folate-conjugates into liposomal nanocarriers resulted in accelerated clearance from blood plasma (Figure 5.1). ANOVA revealed that the plasma clearance was significantly different between the two formulations ($p < 0.001$). Within the first hour, the rapid reduction in circulating FR-targeted liposomal doxorubicin resulted in a 20% difference in plasma levels of FR-Targeted doxorubicin compared to non-targeted. Circulation data were fitted to bi-exponential curves. Areas under the curves

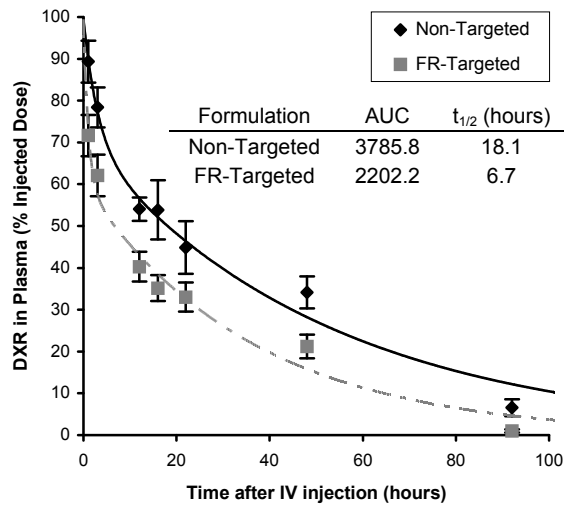


Figure 5.1. Plasma clearance of liposomal doxorubicin formulations. Accelerated clearance of FR-targeted liposomal formulations was exhibited by the rapid decrease of doxorubicin in the blood following an IV injection of 10 mg/kg liposomal doxorubicin. Plasma clearance of FR-targeted formulations was significantly higher than clearance of non-targeted liposomal nanocarriers as determined by ANOVA ($p < 0.001$). Both formulations included 3% DSPE-PEG₂₀₀₀ to promote RES evasion. Blood samples were collected from the orbital sinus at various time-points, and drug concentration was determined by fluorometry. Error bars represent standard error of means. Areas under the curves and plasma half-lives were calculated for each formulation and are reported in the inset table.

and plasma half-lives were determined for each formulation and are reported in Figure 4.1. The incorporation of 0.15% folate-conjugates resulted in a 41.8% reduction in AUC. Formulations containing 0.2% folate-conjugates were also investigated and found to exhibit a further decrease in circulation times demonstrated by a 61.9% reduction in AUC compared to non-targeted liposomal doxorubicin (data not shown).

5.4.2. TUMOR GROWTH CURVE

A growth curve was established to record tumor progression over time in untreated rats (Figure 5.2). The growth curve data was used to determine inter-animal variability in tumor growth and to verify our ability to consistently inoculate tumor. Tumor volume was shown to increase exponentially with a doubling time of 1.7 days for the intracranial 9L tumor model. Tumors were reliably produced in every animal

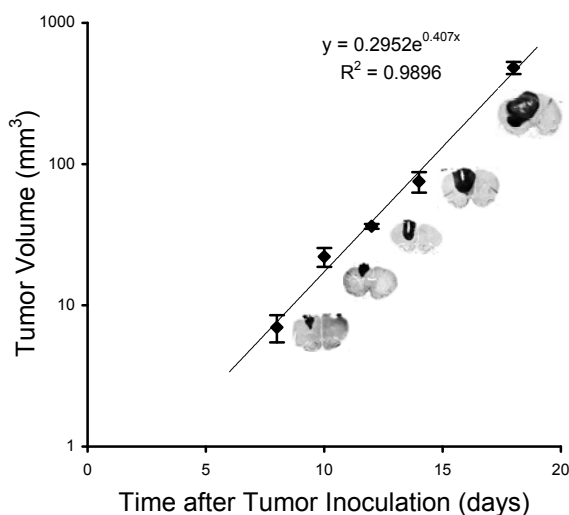


Figure 5.2. 9L glioma growth curve in Fisher 344 rats. Tumor volumes were determined through histological analysis. Representative slices stained with cresyl violet from brains explanted at each time point show tumor cross-sections (dark areas). Data is fitted to an exponential curve. Error bars represent standard error of means.

following stereotaxic implantation. Histological examination revealed that the tumors were infiltrative into normal brain tissue (data not shown).

5.4.3. NESTIN EXPRESSION

Angiogenesis is necessary for effective IV delivery of drug to tumors. For brain tumors, in particular, the formation of new blood vessels is critical because it disrupts the blood-brain barrier. Therefore, we performed immunohistochemistry to determine the onset of angiogenesis in our intracranial tumor model. Immunohistochemistry results confirmed that angiogenesis initiates as early as 4 days following tumor inoculation (Figure 5.3). Nestin, an intermediate filament protein expressed by neuroepithelial stem cells, was present in the tumor at this time point indicating the formation of new microvessels (Figure 5.3(b),(c),(d)). This protein was not detected in normal brain tissue (Figure 5.3(a)). The presence of new vessels 4 days after tumor inoculation in our model makes liposomal drug delivery to tumor feasible at this time point. Since treatments are typically most effective at an early time point, day 4 was chosen to be the treatment day for survival studies.

5.4.4. ORGAN DISTRIBUTION STUDIES

Organ analysis for doxorubicin content showed that the majority of drug was cleared by the liver and spleen for both formulations (Figure 5.4). RES saturation is unlikely since the lipid levels did not exceed those reported to cause saturation [70]. In addition, we did not observe an acceleration of clearance as the plasma levels dropped, which would have been indicative of RES saturation. Doxorubicin levels in the kidneys were comparable between the two different formulations. Plasma doxorubicin levels,

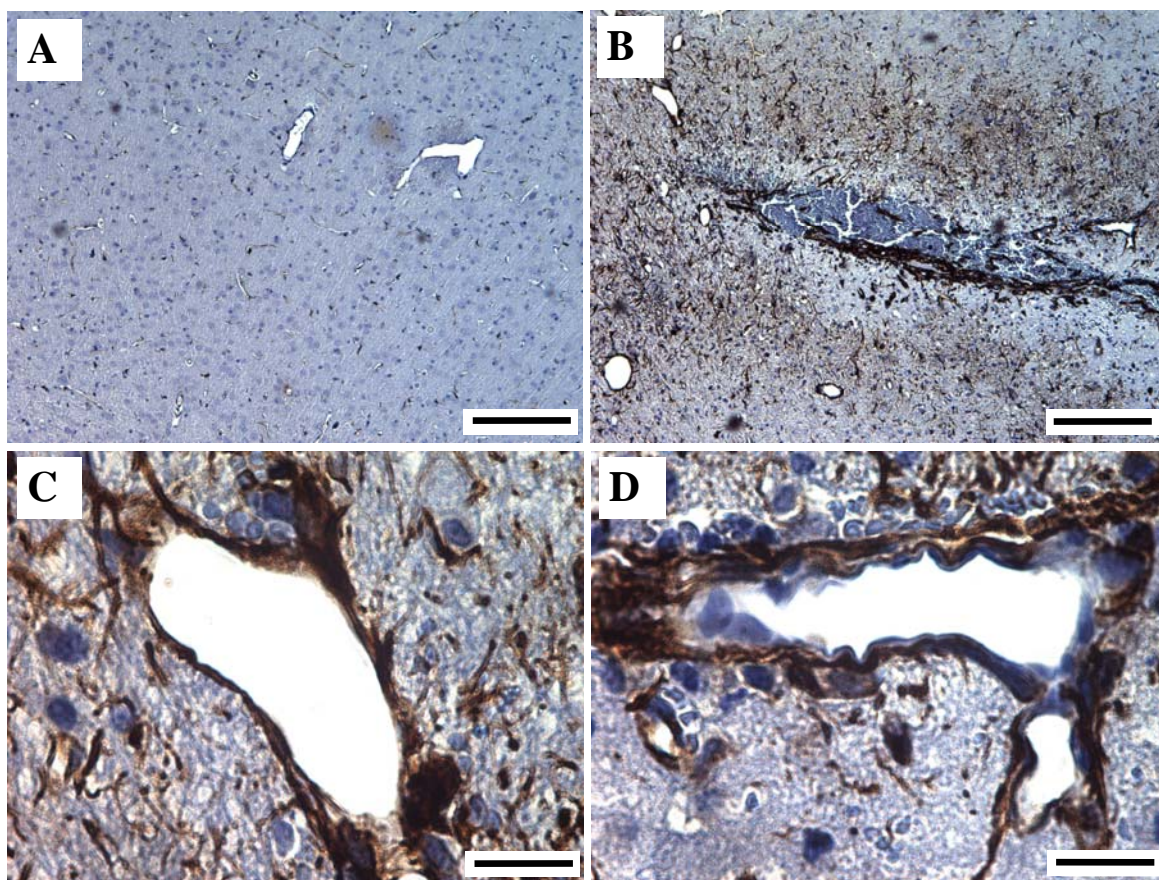


Figure 5.3. Nestin expression in normal brain and 9L glioma tumor. Immunohistochemical analysis reveals expression of nestin, a marker for angiogenesis, in tumor 4 days after inoculation. Brown horseradish peroxidase marks the location of nestin in the fixed tissue. **(a)** Normal brain tissue serves as a negative control. **(b)** Tumor section obtained from Fisher 344 rat 4 days after intracranial 9L glioma tumor inoculation exhibiting elevated expression of nestin. Scale bars represent 200 μm . **(c,d)** Magnifications of tumor image **(b)** displaying nestin staining along microvessel walls. Scale bars represent 20 μm .

however, were significantly different between the two formulations at each time point.

FR-targeted formulations showed lower plasma levels compared to non-targeted formulations at both 20 and 50 hours confirming the data obtained from our plasma clearance study. Plasma doxorubicin levels decreased significantly over time for both formulations. Spleen doxorubicin levels also decreased over time, however, the reduction was only statistically significant for FR-targeted formulations as determined by Student's t-test.

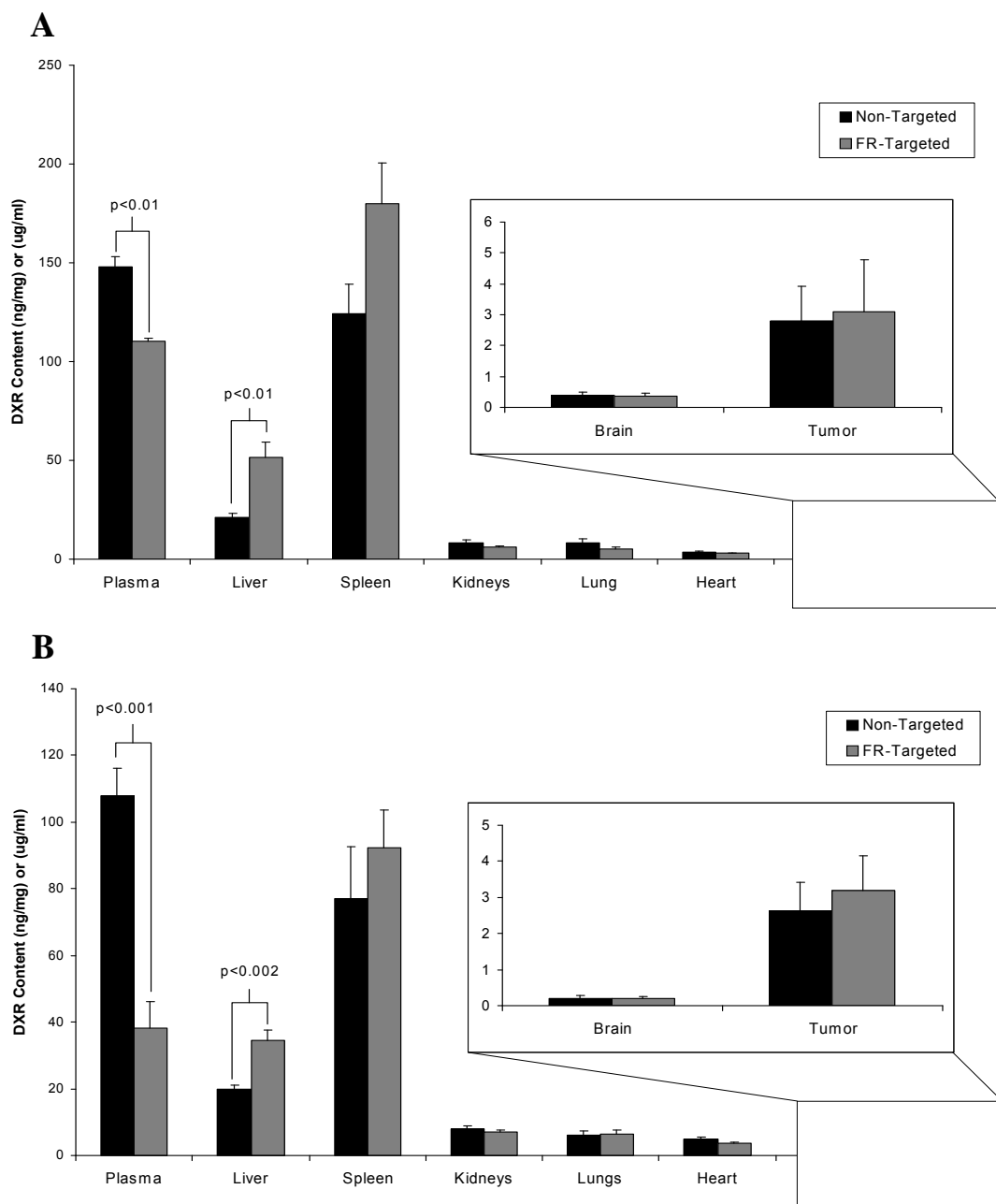


Figure 5.4. Biodistribution of liposomal doxorubicin formulations in Fisher 344 rats with 9L glioma tumor. Animals received 10 mg/kg doxorubicin IV in either non-targeted or FR-targeted liposomal nanocarriers. Fisher 344 rats were euthanized (a) 20 hours or (b) 50 hours after doxorubicin administration. Doxorubicin content in each organ (ng/mg) and within the plasma ($\mu\text{g/ml}$) was determined through fluorometric analysis. At both time points, plasma doxorubicin concentrations in animals treated with FR-targeted doxorubicin were significantly lower ($p < 0.01$, $p < 0.001$) and liver concentrations were significantly higher ($p < 0.01$, $p < 0.002$) than animals receiving non-targeted formulations (Student's t-test). Inset graphs illustrate tumor and brain doxorubicin levels. At 50 hours, both groups exhibited significantly higher doxorubicin levels in tumor compared to brain ($p < 0.01$). Error bars represent standard error of means.

Tumor doxorubicin levels were not significantly different between the two formulations at each time point despite the significantly lower amount of FR-targeted doxorubicin in the plasma. Doxorubicin tumor levels for non-targeted formulations decreased 6.5% from 20 to 50 hours, which was accompanied by a 27% reduction in plasma levels. In contrast, a 3% increase in tumor levels was observed over the same time period for FR-targeted formulations despite the corresponding 65% reduction in plasma doxorubicin levels. Both formulations exhibited higher doxorubicin content in the tumor compared to normal brain tissue at 20 and 50 hours, however, elevated doxorubicin levels in tumors were only statistically significant at the 50 hour time point.

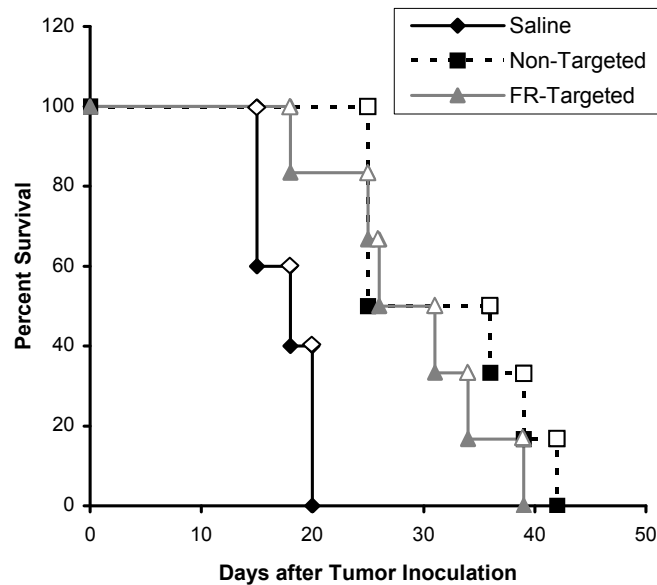


Figure 5.5. Survival of Fisher 344 rats with 9L glioma tumor in response to treatment. Intracranial tumor implantation occurred on day 0, and treatments were administered 4 days later. Liposomal doxorubicin was administered IV at a dose of 10 mg/kg. Animals in the saline sham group received equivalent volumes of 0.9% saline IV. Survival was monitored daily as described in Materials and Methods. Survival of animals receiving liposomal doxorubicin was significantly increased over saline treated animals ($p < 0.02$), however there was no significant difference in survival between animals receiving either non-targeted or FR-targeted liposomal doxorubicin (Student's t-test).

5.4.5. SURVIVAL STUDIES

The therapeutic effect of the non-targeted and FR-targeted treatments was determined by comparing the respective survival times in response to treatment type (Figure 5.5). Treatments were administered IV at a doxorubicin dosage of 10 mg/kg four days after tumor inoculation when new blood vessels have begun to emerge. Equivalent volumes of saline were administered for untreated animals. The data show a statistically significant increase in survival time for both non-targeted ($p=0.004$) and FR-targeted ($p=0.01$) treatments when compared to a saline sham injection as determined by Student's t-test. However, there was not a significant difference in survival between the non-targeted and FR-targeted liposomal treatments.

5.5. DISCUSSION

The present study was designed to explore the relative benefits of actively targeted FR compared to passively targeted 'Stealth' liposomal nanocarriers. Numerous *in vitro* studies have reported gains in targeting efficiency of liposomal nanocarriers to tumor cells through the inclusion of folate [29, 31, 41-44, 46, 49, 71]. While in this study tumor accumulation and survival were no different when compared to passively targeted Stealth liposomal nanocarriers, the fact that this occurred in spite of significantly compromised circulation time points to the advantages of active targeting on tumor states. We hypothesize that the increase in clearance exhibited by FR-targeted liposomal nanocarriers was due to recognition of folate by the RES. Exposure of folate on the liposomal surface is believed to elicit an interaction between liposomal nanocarriers and factors responsible for RES clearance. This interaction occurs even though PEG is included in the liposomal formulation. Increasing the numbers of PEG chains beyond 3%

in the liposomal formulation was not attempted because we have previously determined that increasing the number of PEG molecules tends to hinder insertion of folate-PEG₃₃₅₀-DSPE conjugates into the liposome bilayer and might compromise the access of folate to its receptor on tumor cells. The observed marked reduction in circulation times of FR-targeted formulations, while significant, was not as dramatic as that reported for formulations utilizing antibodies as targeting moieties [37, 50], but was slightly higher than that reported in a similar study utilizing a higher lipid dose in mice [39].

Survival studies verified that the inclusion of folate in the liposomal formulations did not extend survival beyond that achieved by passively targeted 'Stealth' liposomal nanocarriers. While this is consistent with the equivalent accumulation of doxorubicin in tumors in both cases, it is also possible that survival as the ultimate endpoint of this study is not sufficiently sensitive to assess differences in behavior of single doses. It is possible that because this tumor model exhibits exponential growth, a single injection may not be capable of halting growth enough to cause a substantial increase in survival. Tumor growth probably recovers rapidly following a single injection of chemotherapeutic making it impossible to see an effect weeks later. Even if tumor size was reduced to a larger degree by the targeted formulations, the aggressiveness of the tumor to recur and the ease to expand within an empty void may have made it impossible to ultimately resolve a difference in survival times. Numerous studies, in fact, have demonstrated greater success in extending survival times of animals and tumor accumulation of drug when multiple treatments are administered [67, 72]. The administration of multiple treatments may have revealed a difference in efficacy between the targeted and non-targeted liposomal treatments in the current study; however, this was not attempted

because our ultimate goal was to compare passively targeted and actively targeted formulations using a single treatment regimen to examine the effects of active targeting more closely.

To determine why survival times remained unaffected despite the inclusion of folate, biodistribution studies were performed to evaluate drug content in the vital organs. A significantly higher liver accumulation of FR-targeted over non-targeted liposomal nanocarriers (20 hours: $p < 0.01$, 50 hours: $p < 0.001$) obtained from this study suggests that the liver is primarily responsible for the accelerated plasma clearance observed for FR-targeted formulations. This is either due to specific targeting to the folate receptors on hepatic cells or a result of opsonization of FR-targeted formulations resulting in clearance through the liver. Since kidney levels were comparable for both formulations, we are confident that both formulations are equally stable and do not 'leak' doxorubicin. Therefore, significant reduction in plasma levels of FR-targeted drug compared to non-targeted observed at each time point was due to accelerated RES clearance.

Comparable amounts of drug were attained in the tumor for both formulations despite significantly lower plasma levels of FR-targeted drug at each time point. Passive accumulation of liposomal nanocarriers at pathological sites has been shown to be a function of circulation kinetics [73]. This is true up to a certain lipid dose, at which saturation of tumor with liposomal nanocarriers would occur. The fact that FR-targeted liposomal nanocarriers demonstrated decreased plasma levels suggests that tumor accumulation of doxorubicin should have been proportionately lower compared to non-targeted, however, this was not the case. Saturation of tumor with doxorubicin is an unlikely cause of this result since tumor levels continued to increase over time, and even

at the maximum accumulation levels, it is estimated that only 18% of the tumor interstitial volume would have been occupied by liposomal nanocarriers. Total percent of interstitial volume occupied by liposomal nanocarriers was calculated assuming a tumor density close to 1 g/cm³ and an interstitial volume fraction of 0.4 as determined by previous investigators [74].

Since it is assumed that the tumor input of doxorubicin is decreased for FR-targeted formulations due to lower circulating levels, the fact that comparable drug levels were discovered in the tumors suggests that FR-targeted formulations may have been retained to a better degree within the tumor due to the presence of the folate ligand. While we acknowledge the fact that direct evidence for active targeting and enhanced retention is not reported in this study, others have demonstrated that active targeting to cells obtained from solid mass tumors with FR-targeted liposomal formulations is achievable *in vivo* [44]. In addition, the relationship between circulation time and passive targeting of liposomes to tumor sites is well established [70, 73, 75]. Decreased circulating levels of liposomes have been proven to lead to decreased tumor uptake; however, this was not the case in our studies presumably due to active targeting and improved retention of targeted formulations at the tumor site. Altering the dosage of lipids (number of nanocarriers) administered was not attempted because higher dosages would have led to RES saturation and lower dosages would have resulted in a further reduction in passive targeting to tumor. We did attempt to increase the amount of targeting ligand present on the liposomes in an effort to enhance the ability to actively target tumor and overcome the loss in circulation time, however, this simply resulted in even lower circulating levels of liposomes in the bloodstream further strengthening our

thesis that the presence of folate causes the accelerated clearance. Decreasing the amount of folate present on the liposomes was not attempted because our previous *in vitro* studies have indicated that this would lead to a reduction in tumor targeting [29]. These studies reinforce the central finding of this report: while active targeting and retention at the tumor site confers a major advantage of FR-targeted over non-targeted formulations, decreases in nanocarrier circulating time effectively offset the gain in drug retention resulting in comparable survival times with both treatments.

The results obtained from these experiments stress the importance of carefully considering all of the effects related to active targeting. There exists a definite need to properly balance the effects of passive and active targeting when preparing liposomal formulations. Potential therapeutic formulations must be tailored so that the benefits of active targeting are not offset by a potential decrease in circulating levels of drug. To address this need, special considerations must be made upon the inclusion of targeting moieties to not only allow for adequate drug targeting, but also ensure that time spent in circulation is not compromised.

5.6. CONCLUSIONS

To date, the majority of studies utilizing FR-targeted formulations have shown very modest, if any, improvements in treatment efficacy. Lack of success achieved with FR-targeted formulations has been attributed to the limitations on the transport of liposomal nanocarriers within solid tumors. We believe, however, that the inability to improve treatment efficacy with targeted liposomal nanocarriers *in vivo* may also be due, in part, to the losses in passive accumulation in tumors due to compromised circulation times associated with actively targeted formulations. This information contributes to the

current understanding of how potential therapeutic formulations may be tailored to address the combined effects of drug retention in tumor and time spent in circulation. If plasma clearance issues can be resolved, the ability to specifically target chemotherapeutics to malignant brain tumors would alleviate some of the issues associated with current therapies and possibly allow for improved prognoses.

5.7. ACKNOWLEDGEMENTS

This work was funded by the National Science Foundation (NSF), Bioengineering and Environmental Systems (0401627 to RVB) and the Georgia Cancer Coalition. We express gratitude to GTEC (EEC-9731643), a NSF Engineering Research Center based at Georgia Tech/Emory, for use of its core facilities and to GAANN (P200A030077) fellowships in drug and gene therapy development at Georgia Tech for additional support. The authors would like to acknowledge Justin Saul, Chen-Yu Kao, Abhiruchi Agarwal, and Efstathios Karathanasis for useful discussions. We also thank Sehar Mehmood, Nikhil Joshi, and Swati Vishnubhakat for help preparing biodistribution tissue samples for analysis.

5.8. REFERENCES

- [1] Blume, G. and Cevc, G., Liposomes for the sustained drug release *in vivo*. *Biochim Biophys Acta* **1029**, 91-97. (1990).
- [2] Klibanov, A. L., Maruyama, K., Torchilin, V. P. and Huang, L., Amphipathic polyethyleneglycols effectively prolong the circulation time of liposomes. *FEBS Lett* **268**, 235-237. (1990).
- [3] Maruyama, K., Yuda, T., Okamoto, A., et al., Effect of molecular weight in amphipathic polyethyleneglycol on prolonging the circulation time of large unilamellar liposomes. *Chem Pharm Bull (Tokyo)* **39**, 1620-1622. (1991).
- [4] Allen, T. M., Hansen, C., Martin, F., et al., Liposomes containing synthetic lipid derivatives of poly(ethylene glycol) show prolonged circulation half-lives *in vivo*. *Biochim Biophys Acta* **1066**, 29-36. (1991).
- [5] Harris, J. M., Martin, N. E. and Modi, M., Pegylation: a novel process for modifying pharmacokinetics. *Clin Pharmacokinet* **40**, 539-551 (2001).
- [6] Allen, C., Dos Santos, N., Gallagher, R., et al., Controlling the physical behavior and biological performance of liposome formulations through use of surface grafted poly(ethylene glycol). *Bioscience Reports* **22**, 225-250 (2002).
- [7] Moghimi, S. and Szebeni, J., Stealth liposomes and long circulating nanoparticles: critical issues in pharmacokinetics, opsonization and protein-binding properties. *Progress in Lipid Research* **42**, 463-478 (2003).
- [8] Hong, R. L., Huang, C. J., Tseng, Y. L., et al., Direct Comparison of Liposomal Doxorubicin with or without Polyethylene Glycol Coating in C-26 Tumor-bearing Mice: Is Surface Coating with Polyethylene Glycol Beneficial? *Clin Cancer Res* **5**, 3645-3652 (1999).
- [9] Duncan, R., Polymer conjugates for tumour targeting and intracytoplasmic delivery. The EPR effect as a common gateway? *Pharm Sci Technolo Today* **11**, 441-449 (1999).

- [10] Maeda, H., Wu, J., Sawa, T., et al., Tumor vascular permeability and the EPR effect in macromolecular therapeutics: a review. *J Control Release* **65**, 271-284 (2000).
- [11] Takeuchi, H., Kojima, H., Yamamoto, H. and Kawashima, Y., Passive targeting of doxorubicin with polymer coated liposomes in tumor bearing rats. *Biol Pharm Bull* **24**, 795-799 (2001).
- [12] Maeda, H., The enhanced permeability and retention (EPR) effect in tumor vasculature: the key role of tumor-selective macromolecular drug targeting. *Adv Enzyme Regul* **41**, 189-207 (2001).
- [13] Ishida, O., Maruyama, K., Sasaki, K. and Iwatsuru, M., Size-dependent extravasation and interstitial localization of polyethyleneglycol liposomes in solid tumor-bearing mice. *Int J Pharm* **190**, 49-56. (1999).
- [14] Litzinger, D. C., Buiting, A. M., van Rooijen, N. and Huang, L., Effect of liposome size on the circulation time and intraorgan distribution of amphipathic poly(ethylene glycol)-containing liposomes. *Biochim Biophys Acta* **1190**, 99-107. (1994).
- [15] Mayer, L. D., Tai, L. C., Ko, D. S., et al., Influence of vesicle size, lipid composition, and drug-to-lipid ratio on the biological activity of liposomal doxorubicin in mice. *Cancer Res* **49**, 5922-5930. (1989).
- [16] Campbell, R. B., Fukumura, D., Brown, E. B., et al., Cationic charge determines the distribution of liposomes between the vascular and extravascular compartments of tumors. *Cancer Res* **62**, 6831-6836 (2002).
- [17] Simoes, S., Moreira, J., Fonseca, C., et al., On the formulation of pH-sensitive liposomes with long circulation times. *Adv Drug Deliv Rev* **56**, 947-965 (2004).
- [18] Maruyama, K., Kennel, S. and Huang, L., Lipid composition is important for highly efficient target binding and retention of immunoliposomes. *Proc Natl Acad Sci U S A* **87**, 5744-5748 (1990).
- [19] Patel, H., Tuzel, N. and Ryman, B., Inhibitory effect of cholesterol on the uptake of liposomes by liver and spleen. *Biochim Biophys Acta* **761**, 142-151 (1983).
- [20] Woodle, M. C. and Lasic, D. D., Sterically stabilized liposomes. *Biochim Biophys Acta* **1113**, 171-199 (1992).

- [21] Minko, T., Pakunlu, R., Wang, Y., et al., New generation of liposomal drugs for cancer. *Anticancer Agents Med Chem* **6**, 537-552 (2006).
- [22] Gutman, R. L., Peacock, G. and Lu, D. R., Targeted drug delivery for brain cancer treatment. *J Control Release* **65**, 31-41. (2000).
- [23] Torchilin, V. P., Drug targeting. *Eur J Pharm Sci* **11 Suppl 2**, S81-91. (2000).
- [24] Lestini, B. J., Sagnella, S. M., Xu, Z., et al., Surface modification of liposomes for selective cell targeting in cardiovascular drug delivery. *J Control Release* **78**, 235-247. (2002).
- [25] Klibanov, A. L., in *Long circulating liposomes: old drugs, new therapeutics*, edited by M. Woodle and G. Storm (Springer-Verlag and Landes Biosciences, 1998), pp. 269-286.
- [26] Maruyama, K., Ishida, O., Takizawa, T. and Moribe, K., Possibility of active targeting to tumor tissues with liposomes. *Adv Drug Deliv Rev* **40**, 89-102. (1999).
- [27] Blume, G., Cevc, G., Crommelin, M. D., et al., Specific targeting with poly(ethylene glycol)-modified liposomes: coupling of homing devices to the ends of the polymeric chains combines effective target binding with long circulation times. *Biochim Biophys Acta* **1149**, 180-184 (1993).
- [28] Allen, T. M., Brandeis, E., Hansen, C. B., et al., A new strategy for attachment of antibodies to sterically stabilized liposomes resulting in efficient targeting to cancer cells [published erratum appears in *Biochim Biophys Acta* 1995 Dec 13;1240(2):285]. *Biochim Biophys Acta* **1237**, 99-108 (1995).
- [29] Saul, J. M., Annapragada, A., Natarajan, J. V. and Bellamkonda, R. V., Controlled targeting of liposomal doxorubicin via the folate receptor *in vitro*. *J Control Release* **92**, 49-67 (2003).
- [30] Saul, J. M., Annapragada, A. V. and Bellamkonda, R. V., A dual-ligand approach for enhancing targeting selectivity of therapeutic nanocarriers. *J Control Release* **114**, 277-287 (2006).
- [31] Lee, R. J. and Low, P. S., Folate-mediated tumor cell targeting of liposome-entrapped doxorubicin *in vitro*. *Biochim Biophys Acta* **1233**, 134-144 (1995).

- [32] Ishida, O., Maruyama, K., Tanahashi, H., et al., Liposomes bearing polyethyleneglycol-coupled transferrin with intracellular targeting property to the solid tumors *in vivo*. *Pharm Res* **18**, 1042-1048. (2001).
- [33] Eavarone, D. A., Yu, X. and Bellamkonda, R. V., Targeted drug delivery to C6 glioma by transferrin-coupled liposomes. *J Biomed Mater Res* **51**, 10-14. (2000).
- [34] Pastorino, F., Brignole, C., Marimpietri, D., et al., Vascular damage and anti-angiogenic effects of tumor vessel-targeted liposomal chemotherapy. *Cancer Res.* **63**, 7400-7409 (2003).
- [35] Moreira, J. N., Ishida, T., Gaspar, R. and Allen, T. M., Use of the post-insertion technique to insert peptide ligands into pre- formed stealth liposomes with retention of binding activity and cytotoxicity. *Pharm Res* **19**, 265-269. (2002).
- [36] Park, J. W., Hong, K., Kirpotin, D. B., et al., Anti-HER2 immunoliposomes for targeted therapy of human tumors. *Cancer Lett* **118**, 153-160 (1997).
- [37] Park, J. W., Hong, K., Kirpotin, D. B., et al., Anti-HER2 immunoliposomes: enhanced efficacy attributable to targeted delivery. *Clin Cancer Res* **8**, 1172-1181 (2002).
- [38] Maruyama, K., Takizawa, T., Yuda, T., et al., Targetability of novel immunoliposomes modified with amphipathic poly(ethylene glycol)s conjugated at their distal terminals to monoclonal antibodies. *Biochim Biophys Acta* **1234**, 74-80. (1995).
- [39] Gabizon, A., Horowitz, A. T., Goren, D., et al., *In vivo* fate of folate-targeted polyethylene-glycol liposomes in tumor-bearing mice. *Clinical Cancer Research* **9**, 6551-6559 (2003).
- [40] Leamon, C. P., Cooper, S. R. and Hardee, G. E., Folate-liposome-mediated antisense oligodeoxynucleotide targeting to cancer cells: evaluation *in vitro* and *in vivo*. *Bioconjug Chem* **14**, 738-747 (2003).
- [41] Shmeeda, H., Mak, L., Tzemach, D., et al., Intracellular uptake and intracavitary targeting of folate-conjugated liposomes in a mouse lymphoma model with up-regulated folate receptors. *Mol Cancer Ther* **5**, 818-824 (2006).

- [42] Reddy, J. A., Abburi, C., Hofland, H., et al., Folate-targeted, cationic liposome-mediated gene transfer into disseminated peritoneal tumors. *Gene Ther* **9**, 1542-1550 (2002).
- [43] Pan, X. Q. and Lee, R. J., *In vivo* antitumor activity of folate receptor-targeted liposomal daunorubicin in a murine leukemia model. *Anticancer Res* **25**, 343-346 (2005).
- [44] Turk, M. J., Waters, D. J. and Low, P. S., Folate-conjugated liposomes preferentially target macrophages associated with ovarian carcinoma. *Cancer Lett* **213**, 165-172 (2004).
- [45] Yuan, F., Leunig, M., Huang, S. K., et al., Microvascular permeability and interstitial penetration of sterically stabilized (stealth) liposomes in a human tumor xenograft. *Cancer Res* **54**, 3352-3356. (1994).
- [46] Pan, X. Q., Hang, H. and Lee, R. J., Antitumor activity of folate receptor-targeted liposomal doxorubicin in a KB oral carcinoma murine xenograft model. *Pharmaceutical research* **20**, 417-422 (2003).
- [47] Goren, D., Horowitz, A. T., Tzemach, D., et al., Nuclear delivery of doxorubicin via folate-targeted liposomes with bypass of multidrug-resistance efflux pump. *Clin Cancer Res* **6**, 1949-1957 (2000).
- [48] Gabizon, A., Shmeeda, H., Horowitz, A. T. and Zalipsky, S., Tumor cell targeting of liposome-entrapped drugs with phospholipid-anchored folic acid-PEG conjugates. *Adv Drug Deliv Rev* **56**, 1177-1192 (2004).
- [49] Wu, J., Liu, Q. and Lee, R. J., A folate receptor-targeted liposomal formulation for paclitaxel. *Int J Pharm* **316**, 148-153 (2006).
- [50] Huwyler, J., Wu, D. and Pardridge, W. M., Brain drug delivery of small molecules using immunoliposomes. *Proc Natl Acad Sci U S A* **93**, 14164-14169 (1996).
- [51] Walker, M. D., Green, S. B., Byar, D. P., et al., Randomized comparisons of radiotherapy and nitrosoureas for the treatment of malignant glioma after surgery. *N Engl J Med* **303**, 1323-1329 (1980).

- [52] Walker, M. D., Alexander, E., Jr., Hunt, W. E., et al., Evaluation of BCNU and/or radiotherapy in the treatment of anaplastic gliomas. A cooperative clinical trial. *J Neurosurg* **49**, 333-343 (1978).
- [53] Hatlevoll, R., Lindegaard, K. F., Hagen, S., et al., Combined modality treatment of operated astrocytomas grade 3 and 4. A prospective and randomized study of misonidazole and radiotherapy with two different radiation schedules and subsequent CCNU chemotherapy. Stage II of a prospective multicenter trial of the Scandinavian Glioblastoma Study Group. *Cancer* **56**, 41-47 (1985).
- [54] Trojanowski, T., Peszynski, J., Turowski, K., et al., Postoperative radiotherapy and radiotherapy combined with CCNU chemotherapy for treatment of brain gliomas. *J Neurooncol* **6**, 285-291 (1988).
- [55] Wolff, J. E., Trilling, T., Molenkamp, G., et al., Chemosensitivity of glioma cells *in vitro*: a meta analysis. *J Cancer Res Clin Oncol* **125**, 481-486. (1999).
- [56] Chua, S. L., Rosenthal, M. A., Wong, S. S., et al., Phase 2 study of temozolomide and Caelyx in patients with recurrent glioblastoma multiforme. *Neuro-oncol* **6**, 38-43 (2004).
- [57] Hau, P., Fabel, K., Baumgart, U., et al., Pegylated liposomal doxorubicin-efficacy in patients with recurrent high-grade glioma. *Cancer* **100**, 1199-1207 (2004).
- [58] Steiniger, S., Kreuter, J., Khalansky, A., et al., Chemotherapy of glioblastoma in rats using doxorubicin-loaded nanoparticles. *International Journal of Cancer* **109**, 759-767 (2004).
- [59] Ghaghada, K. B., Saul, J., Natarajan, J. V., et al., Folate targeting of drug carriers: A mathematical model. *J Control Release* **104**, 113-128 (2005).
- [60] Sudimack, J. and Lee, R. J., Targeted drug delivery via the folate receptor. *Adv Drug Deliv Rev* **41**, 147-162 (2000).
- [61] Sudimack, J. J., Adams, D., Rotaru, J., et al., Folate receptor-mediated liposomal delivery of a lipophilic boron agent to tumor cells *in vitro* for neutron capture therapy. *Pharm Res* **19**, 1502-1508 (2002).

- [62] Gabizon, A., Horowitz, A. T., Goren, D., et al., Targeting folate receptor with folate linked to extremities of poly(ethylene glycol)-grafted liposomes: *in vitro* studies. *Bioconjug Chem* **10**, 289-298 (1999).
- [63] Lasic, D., in *Liposomes: from physics to applications*, edited by D. Lasic (Elsevier, New York, 1993), pp. 63-107.
- [64] Bolotin, E. M., Cohen, R., Bar, L. K., et al., Ammonium sulfate gradients for efficient and stable remote loading of amphipathic weak bases into liposomes and ligandoliposomes. *Journal of Liposome Research* **4**, 455-479 (1994).
- [65] Zalipsky, S., Brandeis, E., Newman, M. S. and Woodle, M. C., Long circulating, cationic liposomes containing amino-PEG- phosphatidylethanolamine. *FEBS Lett* **353**, 71-74 (1994).
- [66] Ishida, T., Iden, D. L. and Allen, T. M., A combinatorial approach to producing sterically stabilized (Stealth) immunoliposomal drugs. *FEBS Lett* **460**, 129-133. (1999).
- [67] Siegal, T., Horowitz, A. and Gabizon, A., Doxorubicin encapsulated in sterically stabilized liposomes for the treatment of a brain tumor model: biodistribution and therapeutic efficacy. *J Neurosurg* **83**, 1029-1037 (1995).
- [68] Kirpotin, D. B., Drummond, D. C., Shao, Y., et al., Antibody targeting of long-circulating lipidic nanoparticles does not increase tumor localization but does increase internalization in animal models. *Cancer Res* **66**, 6732-6740 (2006).
- [69] Charrois, G. J. and Allen, T. M., Drug release rate influences the pharmacokinetics, biodistribution, therapeutic activity, and toxicity of pegylated liposomal doxorubicin formulations in murine breast cancer. *Biochim Biophys Acta* **1663**, 167-177 (2004).
- [70] Gabizon, A., Tzemach, D., Mak, L., et al., Dose dependency of pharmacokinetics and therapeutic efficacy of pegylated liposomal doxorubicin (DOXIL) in murine models. *J Drug Target* **10**, 539-548 (2002).
- [71] Lee, R. J. and Low, P. S., Delivery of liposomes into cultured KB cells via folate receptor- mediated endocytosis. *J Biol Chem* **269**, 3198-3204 (1994).

- [72] Arnold, R. D., Mager, D. E., Slack, J. E. and Straubinger, R. M., Effect of repetitive administration of Doxorubicin-containing liposomes on plasma pharmacokinetics and drug biodistribution in a rat brain tumor model. *Clin Cancer Res* **11**, 8856-8865 (2005).
- [73] Schiffelers, R. M., Bakker-Woudenberg, I. A. and Storm, G., Localization of sterically stabilized liposomes in experimental rat *Klebsiella pneumoniae* pneumonia: dependence on circulation kinetics and presence of poly(ethylene)glycol coating. *Biochim Biophys Acta* **1468**, 253-261 (2000).
- [74] Weissleder, R., Cheng, H. C., Marecos, E., et al., Non-invasive *in vivo* mapping of tumour vascular and interstitial volume fractions. *Eur J Cancer* **34**, 1448-1454 (1998).
- [75] Gabizon, A. and Papahadjopoulos, D., Liposome formulations with prolonged circulation time in blood and enhanced uptake by tumors. *Proc Natl Acad Sci USA* **85**, 6949-6953 (1988).

CHAPTER 6. MASKING AND TRIGGERED UNMASKING OF TARGETING LIGANDS ON NANOCARRIERS IMPROVES DRUG DELIVERY TO BRAIN TUMORS

As prepared for submission to Nature Materials with E. Karathanasis, A.V. Annapragada and R.V. Bellamkonda.

6.1. ABSTRACT

Long-circulating nanocarriers have been extensively studied to deliver chemotherapeutics, however, inclusion of targeting agents compromises circulation times and passive accumulation at tumors thereby offsetting the benefits of active targeting. Here, we utilize cysteine cleavable phospholipid-polyethylene glycol (PEG) to ‘mask’ targeting ligands on nanocarriers, prolong circulation times, enhance passive tumor targeting, and, after cysteine infusion to detach PEG and expose folate, promote active targeting to tumor cells. *In vivo* blood circulation studies verified the ‘masking’ ability of cleavable phospholipid-PEG, and modulation of uptake and cytotoxicity of nanocarriers using cleavable phospholipid-PEG was demonstrated through *in vitro* studies. Finally, studies analyzing uptake by tumor cells *in vivo* confirmed enhanced delivery when tumor-inoculated animals received targeted liposomes containing cleavable PEG followed by a cysteine infusion to expose folate. These results indicate that cleavable phospholipid-PEG can be used in nanocarrier formulations for controlled masking and unmasking of targeting ligands to enhance efficacy of targeted chemotherapeutics.

6.2. INTRODUCTION

The ability to specifically target systemically delivered chemotherapeutics to tumors offers potential advantages over conventional non-targeted chemotherapy, most notably a reduction in toxic drug side effects due to decreased delivery to non-target organs [1-3]. Receptor-targeted nanocarriers can be used to package drugs and facilitate delivery of high drug payloads to tumors while shielding healthy organs and limiting degradation of drug [4, 5]. Long circulating nanocarriers, in particular, have been studied extensively as delivery vehicles for chemotherapeutics due to the inherent ability to preferentially accumulate in solid tumors by passive convective transport through leaky endothelium (a process termed extravasation) [6-9]. The long blood residence time and repeated passage through the microvascular bed results in high intratumoral concentrations. The efficacy of these passively targeted nanocarriers is dependent on the extent of their extravasation to tumors. The degree of passive accumulation in turn is dependent on the nanocarrier circulation time [10]. While passive targeting of nanocarriers results in accumulation of drug at the target site, *in vitro* studies have shown that uptake by cells is limited unless a targeting agent is utilized to promote active targeting to cells [11-15]. Unfortunately, we have recently demonstrated that there is an inherent optimization problem as the properties that confer prolonged nanocarrier circulation times, such as the sphere of hydration made possible by incorporation of polyethylene glycol (PEG), are compromised by the presence of receptor targeting ligands on nanocarrier surface [16]. As a result of the incorporation of targeting moieties into nanocarriers, reduced circulation times substantially decrease passive dosing of tumors [16-22]. This consequence partially accounts for the limited success of receptor-

targeted nanocarriers *in vivo* despite the promising results of *in vitro* experiments [18, 23]. In this study, we demonstrate an elegant solution that masks the targeting ligands while in circulation, and unmasks the ligands after extravasation to the tumors solving the optimization conundrum (Figure 6.1).

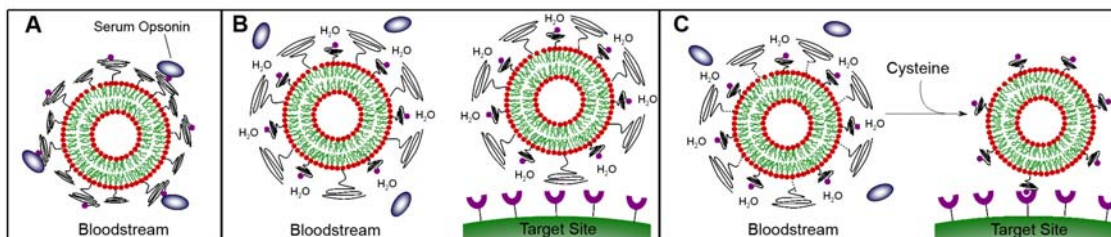


Figure 6.1. Schematic depicting FR-targeted nanocarrier options. A) When attached to PEG chains longer than those incorporated for RES evasion, folate targeting ligands are readily recognized by the RES resulting in accelerated clearance. These liposomes are often removed from circulation before extravasation to the target site is achieved. B) Longer PEG chains conceal folate from the RES but hinder receptor-mediated uptake by target cells over-expressing the folate receptor. C) Long cysteine-cleavable PEG-phospholipid conjugates mask folate during circulation to enable passive targeting to tumor but may be removed through the administration of cysteine at a later time after a majority of the nanocarriers have extravasated to the target site. Resultant exposure of folate enables targeting to cells over-expressing the folate receptor.

Here, we report a novel multifunctional nanocarrier system using a cleavable PEG-lipid conjugate to allow for precise control over ligand access beyond the stealth PEG layer on the nanocarrier surface. PEG chains are capable of creating a hydrophilic barrier around liposomes preventing binding of opsonins by steric hindrance and thereby preventing recognition by the reticuloendothelial system (RES) which consists of phagocytic cells responsible for clearance of nanoparticles from circulation [24-28]. Therefore, protein deposition and the binding of opsonins responsible for RES clearance should be prevented and the targeting ligands ‘masked’ when they are presented on PEG

chains shorter than adjacent PEG chains conferring the hydrophilic, stealth coating on the nanocarriers.

The cleavable conjugate reported consists of a phospholipid bound to PEG₅₀₀₀ via a disulfide bridge and is incorporated into the bilayer of receptor-targeted liposomes. While present, the cleavable PEG₅₀₀₀ conjugates conceal the targeting ligands (folate), which are conjugated to PEG₂₀₀₀, from the immune system allowing for prolonged circulation times and passive targeting to tumor. Once the desired amount of drug is passively delivered to the tumor, active targeting is initiated through cleavage of the disulfide bridge and removal of PEG₅₀₀₀ from the liposomes. Targeting ligands are then exposed to promote active targeting and uptake by tumor cells. This distinct ability to control the method of targeting using a cleavable PEG conjugate allows for maximization of both passive and active targeting while reducing the detrimental effects of targeting ligand incorporation.

Many strategies have been employed to develop conjugates for triggered drug delivery systems cleavable by mild acidic pH [29-31], thiols [29-36] or matrix metalloproteinase [37, 38]. Thiol reducible cross-linkers offer the advantage of precise control over cleavage since they require an externally delivered reducing agent such as cysteine, which is only present in the unbound, reduced form at low concentrations in the body (~10 μ M in blood), to sever the linkage. In addition, cysteine is innocuous to the body at the doses administered for cleavage (~1 mmol/kg). For these reasons, a cysteine-cleavable phospholipid PEG conjugate was selected as the ideal candidate for this 'triggerable' receptor-targeting liposomal system. As a test system, we chose folate as the targeting ligand, targeting folate receptors on a rat glioblastoma model. Folate is a

versatile tumor targeting ligand, and the folate receptor has been shown to be over-expressed in tumors of the ovary, lung, colon, endometrium, brain, breast, and kidney [39].

The following data demonstrate our ability to design these multifunctional nanocarriers with the ability to 1) conceal targeting ligands, 2) expose targeting ligands on demand, 3) enable receptor mediated targeting, and 4) deliver large payloads of drug into the nucleus of target cells.

6.3. RESULTS AND DISCUSSION

To test this liposomal system, we first synthesized a cysteine-cleavable conjugate by linking a lipid, distearoyl-phosphatidyl ethanolamine (DSPE), to a PEG₅₀₀₀ via a disulfide bridge using methods similar to those described elsewhere [34, 36, 40, 41]. NMR and mass spectroscopy verified the structure of the final conjugate, DSPE-S-S-PEG₅₀₀₀, which had a purity of 85% with the remaining being inert compounds (see methods for details on characterization).

The thiolytic cleavability of the conjugate was confirmed by treating micellar conjugate with cysteine. Upon exposure to cysteine, the parent spot on thin layer chromatography ($R_f=0.25$) disappeared while the native lipid ($R_f=0.05$) and PEG ($R_f=0.5$) appeared. The degree of cleavage was quantified via normal-phase HPLC analysis which confirmed that treatment with a 10-fold excess of cysteine resulted in fragmentation of 86% of the conjugate (data not shown).

In vivo plasma clearance studies were performed to determine the minimal percentage of DSPE-S-S-PEG₅₀₀₀ required to adequately mask DSPE-PEG₂₀₀₀-folate on

Table 6.1. Phospholipid-PEG components (mol %) for each nanocarrier formulation.

Formulation	% DSPE-PEG ₂₀₀₀	% DSPE-PEG ₅₀₀₀	% DSPE-S-S-PEG ₅₀₀₀	% DSPE-PEG ₂₀₀₀ -folate	%DSPE-PEG ₃₃₅₀ -folate
Conventional NT	0	0	0	0	0
Conventional FRT	0	0	0	0.15	0
Noncleavable NT	0	8	0	0	0
Noncleavable FRT	0	8	0	0.15	0
Cleavable NT	0	0	8	0	0
Cleavable FRT	0	0	8	0.15	0
Stealth NT	3	0	0	0	0
Traditional FRT	3	0	0	0	0.15

the surface of the liposomes and achieve circulation times comparable to those obtained with non-targeted ‘Stealth’ formulations. All procedures were conducted under a protocol approved by the Institutional Animal Care and Use Committee (IACUC). Male Fisher rats received different types of liposomal nanocarriers encapsulating a chemotherapeutic, doxorubicin (DXR), intravenously (i.v.) and orbital blood samples were obtained at various time points and analyzed for doxorubicin content. Table 6.1 contains details regarding formulation components for all treatments used in these studies. The cleavable FRT formulation containing 8 mol% DSPE-S-S-PEG₅₀₀₀ demonstrated optimal *in vivo* circulation performance compared to other percentages of DSPE-S-S-PEG tested and is included in Figure 6.2 which displays the percentage of initial DXR in plasma over time for animals receiving either non-targeted liposomes (Stealth NT), masked folate-targeted liposomes (Cleavable FRT), or traditional folate-targeted liposomes (Traditional FRT). This plot clearly shows that cleavable FRT formulations circulate better than traditional FRT liposomes having a significantly longer plasma half-life ($p < 0.0001$) and greater $AUC_{0..25}$ ($p < 0.0001$) and $AUC_{0..∞}$ ($p = 0.0001$) as determined by ANOVA. These results indicate that this level of cleavable conjugate is capable of concealing DSPE-PEG₂₀₀₀-folate from the RES. In fact, the circulation profile

of this ‘masked’ FRT formulation is comparable to that of Stealth NT liposomes actually outperforming the Stealth NT nanocarriers for the first 25 hours after injection. The slow acceleration in plasma clearance over time exhibited by the cleavable FRT formulation is presumably due to the low levels (~10 μ M) of reduced thiols naturally present in the bloodstream slowly cleaving some the PEG chains from the liposomes and gradually exposing folate which accelerates RES clearance. The AUC and half-life of cleavable FRT formulations, however, are still dramatically increased compared to traditional FRT

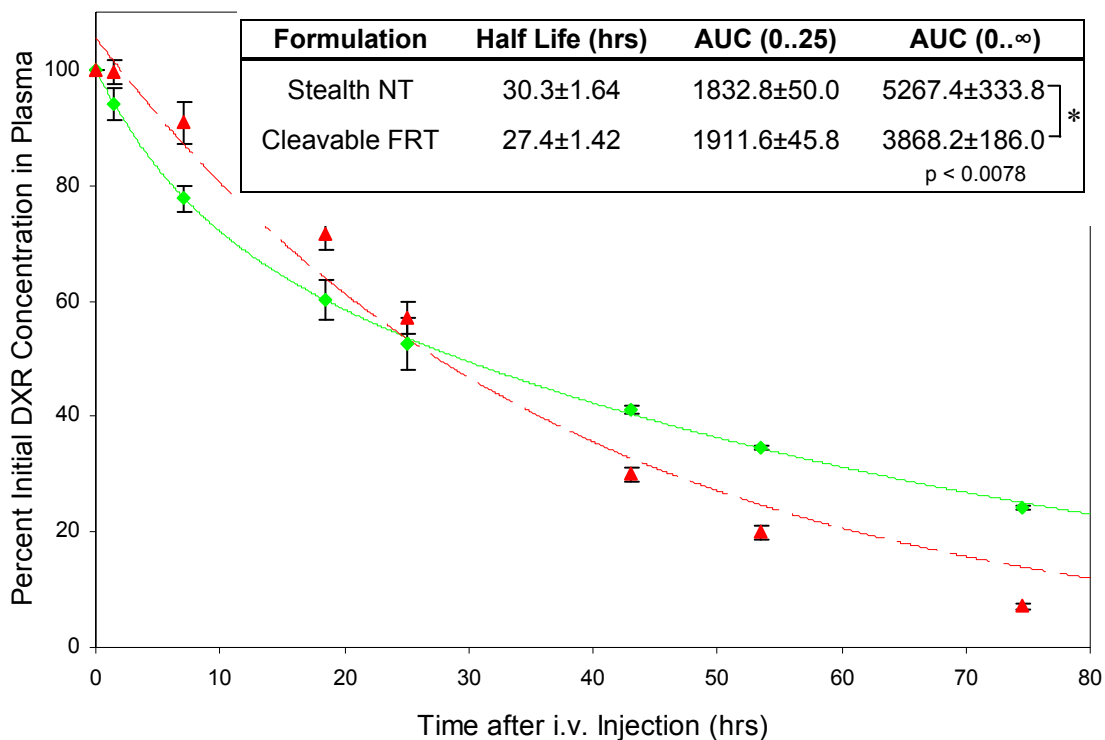


Figure 6.2. Inclusion of 8% DSPE-S-S-PEG₅₀₀₀ prolongs circulation of FR-targeted nanocarriers. Circulating levels of DXR in the bloodstream, expressed as a percentage of initial DXR concentration, over time in animals receiving an i.v. injection of Stealth NT (◆) (n=3) or cleavable FRT (▲) (n=3) liposomal DXR. Data were fit to exponential curves to determine half-lives and AUC’s. The cleavable FRT formulation shown contained 8% DSPE-S-S-PEG₅₀₀₀ and demonstrated improved circulation time compared to the traditional FRT formulation reported in Chapter 5 exhibiting a significant increase in both AUC and half life (ANOVA). The half-lives and AUC’s from t=0 to 25 hours of Stealth NT and cleavable FRT nanocarriers were similar demonstrating the ability of DSPE-S-S-PEG₅₀₀₀ to adequately mask folate from the RES during this timeframe, however, the AUC calculated from t=0 to infinity for Stealth NT liposomes was significantly greater than the AUC of cleavable FRT liposomes (ANOVA). Data represent mean ± SEM.

liposomes despite this gradual cleavage of PEG. These data prove that DSPE-PEG₂₀₀₀-folate can be concealed by DSPE-S-S-PEG₅₀₀₀ *in vivo* enabling RES evasion and prolonged circulation times.

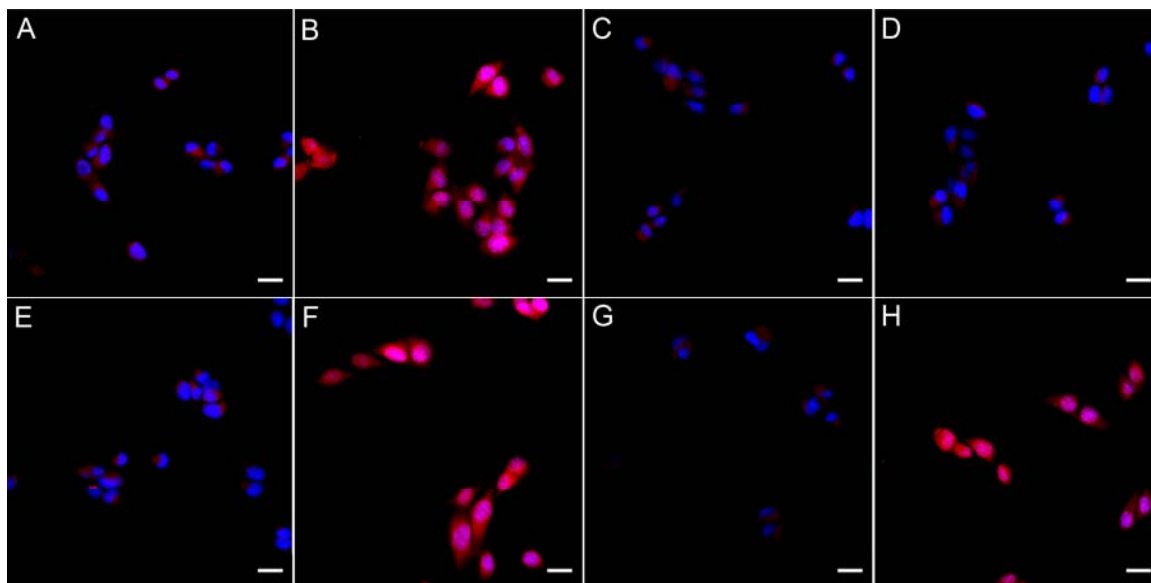


Figure 6.3. DSPE-S-S-PEG₅₀₀₀ enables triggered uptake of DXR encapsulated within liposomal nanocarriers by glioma cells. Confocal images demonstrate DXR uptake (red) by cells and delivery to DAPI-stained cell nuclei (blue). Cells received either unaltered formulations (A-D) or those pre-treated with cysteine (E-H). Treatment with Stealth NT formulations (A and E) resulted in negligible DXR uptake, whereas cells treated with conventional FRT (B and F) demonstrated bright red staining indicative of DXR uptake. The addition of non-cleavable FRT liposomes did not result in DXR uptake by cells (panels C and G). Cleavable FRT liposomes were not taken up by cells (D) unless pre-treated with cysteine to remove PEG chains and expose folate (H). Cells receiving cysteine-treated cleavable FRT liposomes demonstrated bright red staining which was co-localized with DAPI (blue) indicating nuclear localization similar to that exhibited by cells treated with conventional FRT nanocarriers (B and F). Scale bars represent 20 μm .

In vitro studies were performed to evaluate our ability to precisely control ligand presentation and cellular uptake and cytotoxicity using 8% cysteine-cleavable DSPE-S-S-PEG₅₀₀₀. 9L glioma cells were exposed to DXR encapsulated in Stealth NT liposomes, conventional FRT liposomes, non-cleavable FRT liposomes, or cleavable FRT liposomes (see Table 6.1 for formulation details). Treatments were either applied directly to cells or

after pre-treatment with cysteine. In addition, excess folate was added to a subset of treatments before being applied to cells. Images of cells were obtained through confocal microscopy after 1 hour treatment exposure (Figure 6.3). Cells treated with Stealth NT formulations demonstrated negligible uptake with or without cysteine pre-treatment, while those treated with conventional FRT liposomes exhibited substantial uptake and nuclear localization of DXR under both conditions. These data demonstrate the need for active targeting to facilitate uptake and nuclear localization of liposomal therapeutics. When applied without cysteine pre-treatment, “masked” FRT formulations containing either non-cleavable or cleavable DSPE-PEG₅₀₀₀ were not internalized by cells. Pre-treatment with cysteine, however, considerably enhanced cellular uptake of cleavable FRT liposomes. When treatments were applied in the presence of excess folate, uptake of conventional FRT and cysteine-treated cleavable FRT liposomes was considerably reduced (data not shown). The outcome of these studies indicates that removal of PEG₅₀₀₀ chains is necessary to expose folate and promote cellular uptake of FRT formulations. In addition, these data prove that cleavage of PEG₅₀₀₀ and controlled exposure of folate is achievable with cysteine and subsequently results in uptake of liposomes by glioma cells.

Cytotoxicity of each formulation was determined by evaluating cell viability after treatment exposure to ensure that not only targeted uptake was achieved but that the extent of DXR uptake was cytotoxic (Figure 6.4). Cells exposed to Stealth NT liposomal DXR remained largely unaffected by treatment application and exhibited approximately 100% viability under all four conditions. Conventional FRT liposomal DXR demonstrated a significant ($p < 0.0001$) increase in cytotoxicity exhibited by a dramatic

reduction in cell viability. The addition of excess folate significantly ($p < 0.0001$) reduced the cytotoxicity verifying that uptake occurred via the folate receptor. Cysteine had no effect on cytotoxicity, and the results obtained from cells receiving cysteine treated conventional FRT liposomes in the presence of excess folate were comparable to those resulting from treatment application (without cysteine pre-treatment) in the presence of excess folate. “Masked” formulations (both cleavable and non-cleavable FRT) did not demonstrate any cytotoxic effects with or without excess folate, and cysteine had no effect on the cytotoxicity of non-cleavable FRT liposomes. Pre-treatment with cysteine, however, did significantly ($p < 0.0001$) decrease viability of cells treated with cleavable

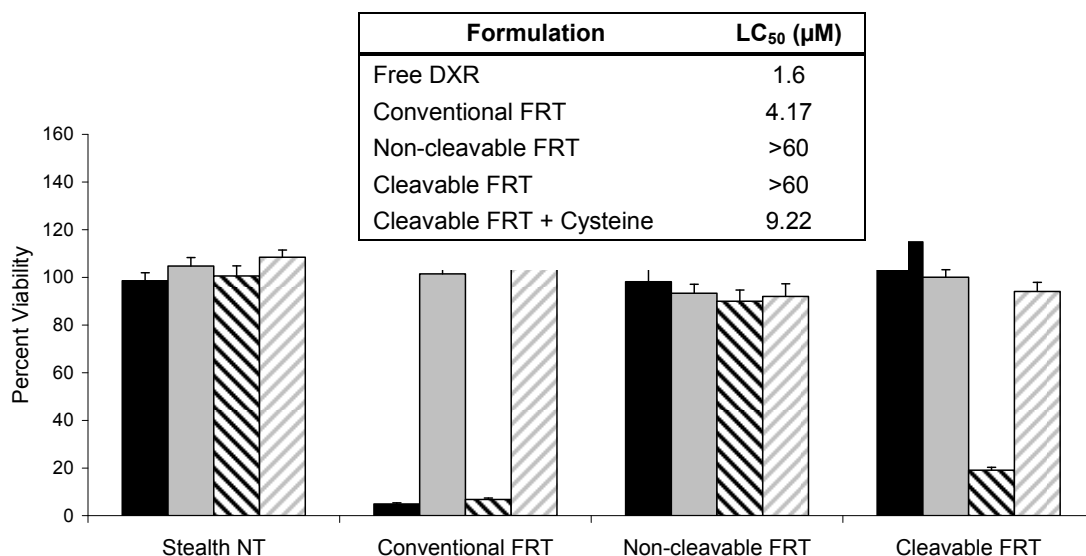


Figure 6.4. Cytotoxicity of liposomal DXR is controllably altered through the inclusion of DSPE-S-S-PEG₅₀₀₀. Percent viability of cells after treatment with liposomal DXR formulations is shown. Treatments were applied alone (■), with excess folate (■), cysteine-treated (▨), or with excess folate and cysteine pre-treatment (▩). Stealth NT nanocarrier DXR did not demonstrate any cytotoxic effect on 9L glioma cells under any of these conditions. Conventional FRT DXR was considerably cytotoxic except in the presence of excess folate verifying that uptake occurred via the folate receptor. Cells treated with non-cleavable FRT liposomal DXR did not exhibit any decrease in viability. Treatment with cleavable FRT nanocarrier DXR did not alter cell viability unless the formulations were pre-treated with cysteine. The addition of excess folate to cells receiving cysteine-cleaved FRT liposomes resulted in a significant increase in cell viability indicating that folate sufficiently blocked uptake via folate receptors. Data represent mean ± SEM.

FRT liposomes verifying that the application of cysteine allows for controlled release of PEG₅₀₀₀ and exposure of folate to facilitate cellular uptake of drug. When excess folate was applied to cells exposed to cysteine treated cleavable FRT liposomal DXR, cytotoxicity was significantly ($p < 0.0001$) decreased due to competitive inhibition confirming that uptake of ‘unmasked’ FRT formulations occurred via the folate receptor. Cleavable NT formulations were also investigated and did not demonstrate any effect on cellular viability with or without cysteine pre-treatment (see supplementary data). These results support the data obtained from *in vitro* uptake studies and clearly demonstrate that cytotoxic effect of targeted liposomal DXR can be manipulated through the inclusion of cleavable PEG conjugates that conceal targeting ligands.

Results from studies conducted to determine the lethal concentration that kills 50% of the cells (LC_{50}) of select formulations corroborate the outcome of the cytotoxicity studies (Figure 6.4 inset). The LC_{50} of free DXR on 9L glioma cells was very low (1.6 μM) as was the LC_{50} of conventional FRT liposomal DXR (4.2 μM). Masked formulations, however, were not cytotoxic at any of the concentrations tested (0-60 μM). Upon the addition of cysteine, cleavable FRT liposomal DXR exhibited a substantial reduction in LC_{50} (9.2 μM) verifying successful removal of PEG₅₀₀₀ and exposure of folate due to cysteine cleavage of the conjugate disulfide bridges. These studies demonstrate that cleavable phospholipid-PEG conjugates can be inserted into targeted nanocarriers to enable precise control over cytotoxic effects.

To determine intracellular uptake of systemically delivered nanocarriers by tumor cells *in vivo* and the ability to control uptake using cleavable PEG, we performed studies on brain tumor-bearing rats (9L/LacZ glioma model) receiving either Stealth NT

liposomes or cleavable FRT liposomes encapsulating a fluorochrome (ADS645WS) and a subsequent infusion of either saline or cysteine. Animals were euthanized, tumors were dissociated and stained for β -gal production, and cells were analyzed through flow cytometry. Cultured 9L/LacZ cells and nontransfected 9L glioma cells were stained and served as positive and negative controls, respectively, for β -gal production. Cytometric detection of β -gal in the 9L/LacZ glioma tumors delineated two populations of cells, β -gal(+) tumor cells and β -gal(-) nontumor cells. The β -gal(-) populations exhibited similar, minimal ADS645WS staining intensity per cell regardless of treatment type (NT +/- cysteine, FRT +/- cysteine) indicating that the uptake of liposomes by nontumor cells was nominal (Figure 6.5). The β -gal(+) population of cells obtained from animals receiving cleavable FRT liposomes followed up by a cysteine infusion, however, demonstrated a significant shift in liposome uptake indicated by an increase in ADS645WS signal detected in the APC channel (Figure 6.5d). β -gal(+) cells obtained

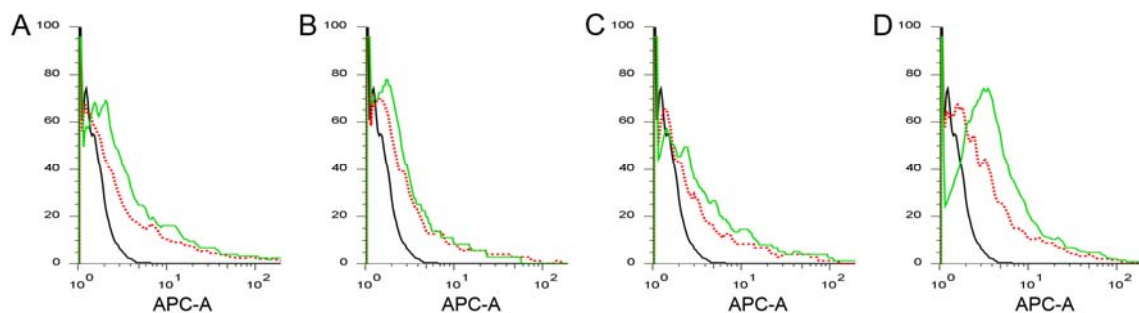


Figure 5.5. *In vivo* cellular uptake of liposomes is enhanced when folate on FR-targeted nanocarriers is masked during circulation and ultimately exposed after extravasation into tumor. Uptake of liposomes represented by APC staining intensity, is shown for A) Stealth NT/saline treated (n=8), B) Stealth NT/cysteine treated (n=6), C) cleavable FRT/saline (n=6), or D) cleavable FRT/cysteine treated (n=6) rats after gating the non-tumor (....) and tumor (—) populations. Saline treated animals (n=3) served as a negative control for APC staining (—). There was no significant difference in uptake between treatment groups by non-tumor cells. However, a significant shift in the APC peak was observed in tumor cells of animals treated with cleavable FRT liposomes and a subsequent cysteine infusion (see Table 6.2 for quantitative analysis).

from the other treatment groups showed comparably low uptake of liposomally encapsulated dye with only a minimal shift in uptake compared to β -gal(-) cells (Figure 6.5a-c). Frequency profiles of β -gal and liposome signal intensity on two-dimensional graphs also demonstrated a shift in the β -gal(+) cell population obtained from animals treated with cleavable FRT liposomes and cysteine into higher liposome signals (Figure 6.6). The percentage of tumor cells from these animals that demonstrated liposome uptake (APC+/FITC+) was significantly ($p < 0.0001$) greater than that of other treatment

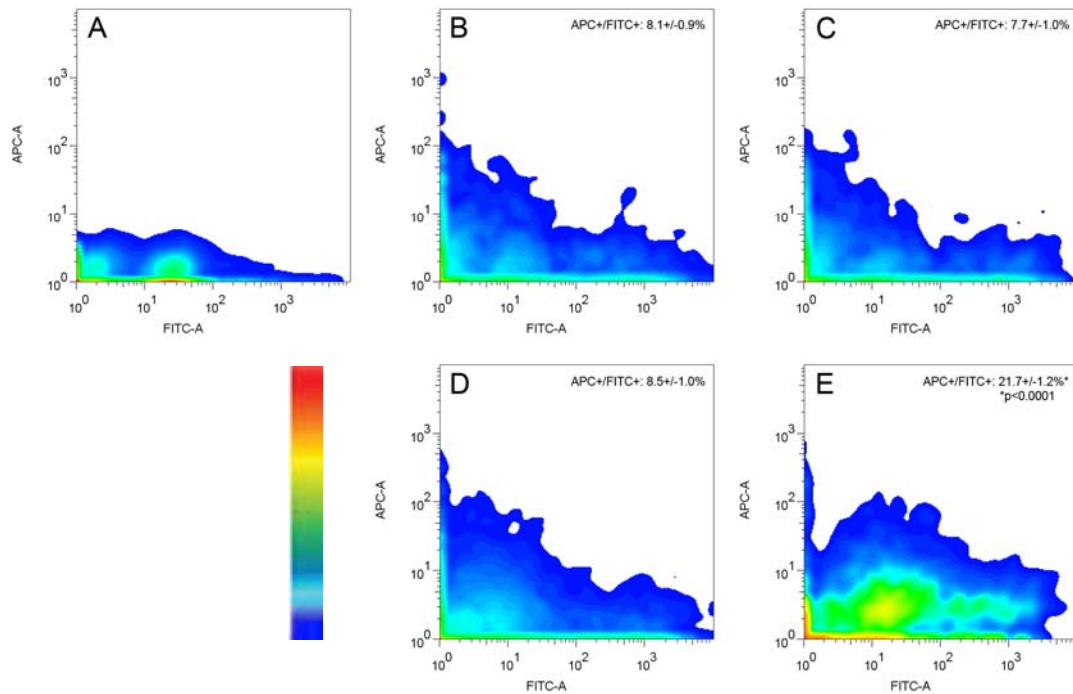


Figure 6.6. Cysteine cleavage of PEG and exposure of folate on FRT liposomal nanocarriers at the target site significantly increases frequency of drug uptake by tumor cells. Two dimensional event density profiles of disaggregated tumor cell suspensions obtained from animals receiving Stealth NT (B and C) or cleavable FRT (D and E) liposomal nanocarriers display β -gal (FITC channel) and ADS645WS staining intensity (APC channel). Animals received a saline (B and D) or cysteine (C and E) infusion following treatment administration. A mixture of untransfected 9L glioma cells and transfected 9L/LacZ glioma cells obtained from *in vitro* culture was stained for β -gal production to identify β -gal(-) and β -gal(+) populations (A). A shift in the β -gal(+) (tumor) population obtained from cleavable FRT/cysteine treated animals demonstrates a significant increase in the percentage of target cells positive for liposome uptake ($p < 0.0001$, ANOVA). Data represent mean \pm SEM.

groups, with the percentage of tumor cells demonstrating liposome uptake in cleavable FRT/cysteine treated animals being approximately 2.7 times that of Stealth NT/saline treated animals.

Increased uptake of cleavable FRT formulations by tumor cells obtained from animals receiving a cysteine infusion is indicative of PEG removal *in vivo*. Further verification of cleavage was obtained through analysis of blood samples obtained from animals immediately prior to euthanasia. Fluorometric detection of liposomal ADS645WS in blood samples demonstrated a 25-30% reduction in liposome blood levels of animals receiving FRT liposomes and a cysteine infusion compared to other treatment groups confirming that cleavage of PEG, leading to immune recognition of exposed folate, was achieved *in vivo*.

Cytometric data allowed for quantitative analysis of the results obtained from treated animals (Table 6.2). The shift in fluorescent intensity representing liposomal uptake per cell observed in the group receiving cleavable FRT nanocarriers and a cysteine infusion was significant compared to the remaining treatment groups. In addition, mean liposome associated fluorescence in tumor cells obtained from FRT liposome/cysteine treated animals was about 2.8 times greater than that of host cells

Table 6.2. Flow cytometric analysis of uptake of liposomal formulations by tumor cells recovered from 9L/LacZ tumors in rats.

Formulation	APC Median Signal Intensity \pm SEM	
	Tumor Cells	Tumor/Host Ratio
Stealth NT + Saline	1.371 \pm 0.099	1.355 \pm 0.099
Stealth NT + Cysteine	1.425 \pm 0.110	1.411 \pm 0.109
Cleavable FRT + Saline	1.398 \pm 0.102	1.384 \pm 0.101
Cleavable FRT + Cysteine	2.845 \pm 0.160*	2.715 \pm 0.180*
	*p<0.0001	*p<0.0001

verifying specificity for tumor cells. This tumor/host uptake ratio was significantly greater than that obtained from other treatment groups, which did not demonstrate selectivity for tumor cells. These results verify that cleavage of the PEG₅₀₀₀ chains on cleavable FRT nanocarriers is achievable at the tumor site *in vivo* using an i.v. cysteine infusion. This cleavage is sufficient to allow for increased binding and internalization of liposomes by tumor cells due to exposure of the targeting ligand, folate. Animals that received cleavable FRT liposomes that were ultimately ‘unmasked’ demonstrated a significantly higher uptake of liposomes per tumor cell as well as a significantly greater percentage of tumor cells internalizing liposomes. These data were obtained from animals that were euthanized only 1.5 hours after PEG₅₀₀₀ chains were detached. At later time points, when cells have had a longer exposure to the targeted liposomes, the difference may be even greater. Even considering the fact that circulating levels of cleavable FRT nanocarriers will decrease after cysteine infusion, longer exposure times at the tumor site should allow for a further increase in specific uptake (tumor/nontumor uptake ratio) compared to Stealth NT liposome treated rats.

We have previously demonstrated and discussed the importance of circulation time on efficacy of therapeutics encapsulated within actively targeted nanocarriers [16]. With the knowledge that passive accumulation is critically dependent on circulation times [10], it is imperative that prolonged circulation of nanocarriers is uncompromised upon inclusion of targeting moieties. Here, we have shown that cleavable phospholipid-PEG conjugates can be used to enable precise control over ligand exposure, effectively concealing ligands to prolong liposomal circulation times and exposing targeting moieties at the desired time point upon administration of an *in vivo* safe cleaving agent such as

cysteine. Appropriate PEG lengths and percentages included in each liposomal formulation need to be considered for various applications (i.e. utilizing an alternative targeting moiety) as these parameters greatly affect the ability to conceal targeting agents and prolong circulation times. Utilizing the system described here for FRT liposomal formulations, we are confident that we have succeeded in satisfying the criteria for maximizing passive targeting of liposomal formulations containing targeting ligands and preventing the offset of active targeting.

Through these studies, we have also demonstrated that cleavable phospholipid-PEG conjugates can be utilized to promote active targeting in a controlled manner through the ability to regulate uptake and cytotoxicity of targeted nanocarriers. *In vitro*, cleavage of the PEG conjugates on FRT formulations was achieved with cysteine and resulted in nuclear localization of drug payloads, a mandate for DXR efficacy. In addition, treatment with cleaved FRT formulations resulted in a significant enhancement of uptake and cytotoxicity, which approached values attained with conventional FRT liposomes. Conventional FRT liposomes have been shown to outperform FRT liposomes with adjacent DSPE-PEG chains *in vitro* [42], however, until now, DSPE-PEG has been present on FRT liposomes at the tumor site *in vivo* because it is mandatory to prolong circulation time. Removal of adjacent PEG chains *in vivo*, a feat made possible with this multifunctional liposomal system, should promote uptake of these formulations beyond that previously achieved, thereby maximizing active targeting of liposomal formulations. *In vivo*, we demonstrated a significant increase in uptake compared to Stealth NT liposomes both in the number of tumor cells positive for liposomes and the number of liposomes per cell when animals received FRT liposomes followed by a cysteine

infusion. This data confirms that cysteine is capable of cleaving phospholipid-PEG conjugates, exposing targeting ligands, and promoting uptake *in vivo*. In addition, these studies demonstrate that utilization of these cleavable conjugates in targeted nanocarrier formulations reduces the detrimental effects of targeting ligand incorporation and enables true optimization of both passive and active targeting to tumors. These findings should allow for a significant enhancement in treatment efficacy of targeted nanocarrier chemotherapeutics *in vivo*.

6.4. METHODS

6.4.1. SYNTHESIS OF DSPE-S-S-PEG₅₀₀₀

A cysteine-cleavable PEG conjugate was synthesized using *N*-Succinimidyl 3-[2-pyridyldithio]-propionamido (SPDP) as a crosslinker between 1,2-distearoyl-*sn*-glycero-3-phosphoethanolamine (DSPE) and PEG₅₀₀₀-SH. In brief, DSPE (790 mg, 1.05 mmol) was dissolved in chloroform (22 mL) with triethylamine (900 μ L) at 55 °C. SPDP (263 mg, 0.844 mmol) was dissolved in 3 mL of chloroform and then added to the DSPE solution. The reaction mixture was stirred for 5 hours at room temperature. The reaction progress was monitored by thin-layer chromatography (TLC) which demonstrated the conversion of DSPE to a faster running product. PEG₅₀₀₀-SH (1.75 g, 0.351 mmol) was then dissolved in 9 mL of chloroform before being added to the solution of PDP-DSPE. The mixture was allowed to react overnight at room temperature. The reaction progress was monitored by the UV absorbance at 343 nm of the pyridyl-2-thione byproduct released from the DSPE-PDP intermediate once the disulfide bridge between the lipid and the PEG was formed. TLC was also utilized to monitor the reaction progress. Following evaporation of the organic solvents, excess DSPE was then removed by

precipitation in acetonitrile and centrifugation. The supernatant was recovered, and acetonitrile was then removed by rotary evaporation. The residue was dissolved in dichloromethane and applied to a silica gel column. The column was washed with 200 mL of each of the following concentrations of methanol in dichloromethane: 4%, 6%, 9%, 12%, and 15%. During chromatography, 4 mL fractions were collected, and those determined by TLC to contain product were pooled and lyophilized. The product (DSPE-S-S-PEG₅₀₀₀) was characterized by matrix assisted laser desorption ionization time-of-flight mass spectroscopy (MALDI-TOFMS), high performance liquid chromatography (HPLC), and thin layer chromatography (TLC). TLC confirmed the presence of the final product (R_f=0.25 in CHCl₃:MeOH=85:15). MALDI-TOFMS resulted in a bell-shaped spectra verifying the expected molecular weight of ~6,210 Da with lines spaced at 44 Da. ¹HNMR (DMSO-d₆, solvent): δ 0.83 (t, CH₃, 6H), 1.2 (s, CH₂, 56H), 1.6 (br, CH₂ CH₂C=O, 56H), 2.24 (2xt, CH₂C=O, 4H), 2.5 (2xt, S=CH₂ CH₂CON, 4H), 2.85 (t, CH₂CONHDSPE, 4H), 3.22 (s, CH₃O, 3H), 3.5 (s, PEG, ~456H), 3.7 (t, NCH₂CH₂OP, 2H), 5.0 (m, OCH₂CHCH₂O, 1H).

6.4.2. THIOLYTIC CLEAVABILITY OF DSPE-S-S-PEG

The thiolytic cleavability of the conjugate was confirmed by treating 1 mM micellar conjugate with cysteine of 10 mM concentration in PBS for 30 min at 37°C. The degree of cleavage was monitored by TLC and quantified via normal-phase HPLC analysis.

6.4.3. *IN VIVO* CIRCULATION STUDIES

To form the folate conjugate, a DSPE-PEG₂₀₀₀-amine was mixed with folate dissolved in DMSO. This mixture was reacted with pyridine and dicyclohexyl

carbodiimide, rotary evaporated, and rehydrated with water to form micelles. DSPE-PEG₃₃₅₀-folate conjugates were synthesized in a similar manner [16]. Non-targeted liposomes were composed from a 62:35:3 molar ratio of DPPC:cholesterol:DSPE-mPEG₂₀₀₀, and liposomes with detachable PEG were prepared using DPPC:cholesterol:DSPE-S-S-PEG₅₀₀₀ where the percentage of DSPE-S-S-PEG₅₀₀₀ was varied (2%, 6%, 8%) with a corresponding decrease in DPPC content (63%, 59%, 57%). 100 nm liposomes were formulated following previously described methods [11, 16, 43]. Targeted formulations received 0.15 mol% of either DSPE-PEG₃₃₅₀-folate or DSPE-PEG₂₀₀₀-folate for insertion following established procedures [11, 16]. DXR (120 mg DXR/mmol lipid) was then remotely loaded into liposomes according the previously described methods [16, 44]. Prior to administration, treatments were sterilized by passing through a 0.2µm filter. Final doxorubicin content was assessed by lysing the liposomal nanocarriers with 5% Triton X-100 at 60°C and measuring the UV absorbance at 480 nm.

Plasma clearance studies were conducted under a protocol approved by the Institutional Animal Care and Use Committee (IACUC) at Georgia Institute of Technology. Adult, male Fisher 344 rats were given an i.v. injection of liposomal DXR (10 mg/kg DXR; ~60 mg/kg lipid). Each group received one of the following formulations: non-targeted with DSPE-PEG₂₀₀₀ (n=3), FR-targeted with DSPE-PEG₃₃₅₀-folate and DSPE-PEG₂₀₀₀ (n=5), or FR-targeted with DSPE-PEG₂₀₀₀-folate and DSPE-S-S-PEG₅₀₀₀ (n=3 for each level of cleavable PEG incorporation). Blood was collected from the orbital sinus immediately before injection and at 1.5, 7, 18.5, 25, 43, 53.5, and 74.5 hours after injection. Plasma was isolated by centrifugation. Liposomes were lysed by diluting plasma 1:10 with 5% Triton X-100 and heating to 60°C. Total DXR content

of each sample was analyzed ($\lambda_{\text{ex}}=485$, $\lambda_{\text{em}}=590$) using a fluorescence spectrometer. Plasma samples obtained immediately prior to injection were used to correct for background fluorescence.

6.4.4. *IN VITRO* STUDIES

A 9L glioma cell line received as a generous donation from the Neurosurgery Tissue Bank at UCSF was maintained in MEM/EBSS medium supplemented with 10% fetal bovine serum and 0.05 mg/mL gentamicin. Liposomal DXR was prepared as describe above using 0% DSPE-PEG (conventional), 3% DSPE-PEG₂₀₀₀ (Stealth), or 8% DSPE-S-S-PEG₅₀₀₀ (cleavable). FR-targeted formulations received 0.15% DSPE-PEG₂₀₀₀-folate for insertion. Prior to applying to cells, formulations were split in half and mixed with either cysteine (10:1 molar ratio of cysteine:lipid) or an equivalent volume of saline for 30 minutes at 37°C and then dialyzed. 9L glioma cells were washed with folate-free RPMI medium, and then treatments were applied (10 μM DXR) in RPMI medium containing either 0 or 2 mM folate for 2 hours at 37°C. Cells treated on chamber slides for uptake imaging were then washed three times with ice cold PBS containing calcium and magnesium before fixing with 4% paraformaldehyde/1.5% methanol in PBS for 20 minutes. Cells were then washed with PBS and stained with DAPI for 10 minutes before a final PBS wash. Images of the treated cells were obtained on a Zeiss confocal microscope (LSM 510).

Cells treated for cytotoxicity analysis were washed three times with folate-free RPMI after treatment application and then incubated at 37°C for 5 days in folate-free RPMI medium. Viability was then determined using a formazan based cell counting kit (CCK-8). Untreated cells served as live controls for normalization of the data. LC₅₀

values were determined in a similar manner with cells exposed to increasing concentrations of liposomal doxorubicin (1.56, 3.13, 6.25, 12.5, 25, 50 μ M). The best fit line of at least 3 points in the linear range of cell viability was then used to determine LC₅₀.

Flow cytometry experiments were performed to determine the amount of intracellular drug and to distinguish uptake between tumor and non-tumor cells. For these studies, liposomes were fabricated as described above and loaded with a water soluble fluorophore, ADS645WS (American Dye Source). Encapsulation was carried out by mixing the lipids with 10 mg/mL ADS645WS in 0.9% NaCl after dissolving in ethanol. Formulations were extruded to 100 nm and then loaded onto a Sepharose CL-4B chromatography column to remove unencapsulated dye. Insertion of targeting ligands was conducted as described above.

6.4.5. TUMOR INOCULATION

A 9L glioma cell line transfected with the bacterial β -galactosidase encoding gene, LacZ, was maintained in MEM/EBSS medium supplemented with 10% fetal bovine serum and 0.05 mg/mL gentamicin. A rat glioma model was established by orthotopic inoculation of 2×10^6 9L/LacZ glioma cells following established methods [16]. Animals were fed a folate-free diet containing 1% succinylsulfathiazole for approximately 18 days prior to surgery to eliminate competitive inhibition of FR-targeted liposome uptake and prevent down-regulation of folate receptors *in vivo*.

6.4.6. FLOW CYTOMETRIC STUDIES

Animals were allowed to recover from surgery, and 21 days later, saline sham, Stealth NT (3% DSPE-PEG₂₀₀₀), or cleavable FRT (8% cleavable DSPE-PEG₅₀₀₀)

liposomal ADS645WS (1.77 mg/kg ADS645WS; ~70 mg/kg lipid) treatments were administered i.v. After 28.5 hours, either 0.9% NaCl or a solution of 60 mg/ml cysteine in 0.9% NaCl was infused over 15 minutes at a dose of 2 ml/kg. Animals were anesthetized with 5% isoflurane 1.5 hours later and decapitated immediately after obtaining a cardiac blood sample. Tumors were dissected from explanted brains, mechanically fragmented, and treated for 60 minutes at 37°C with a solution of collagenase (0.1 U/ml PBS) and dispase (0.8 U/ml PBS) to dissociate cells. The cell solution was resuspended in 4% fetal bovine serum in PBS and treated with a *FluoReporter*[®] lacZ flow cytometry kit. Tumor cells expressing the lacZ reporter gene product, beta-galactosidase, hydrolyzed the fluorogenic beta-galactosidase substrate allowing fluorescent detection of expression to distinguish tumor cells from non-tumor cells. A LIVE/DEAD[®] fixable red dead cell stain kit was also used separately to identify dead cell populations during flow cytometric analysis. Flow cytometry was conducted using a Becton-Dickinson DLSR digital flow cytometer equipped with a 488 nm excitation laser using the APC channel for detection of liposomal ADS645WS, the FITC channel for tumor cell (lacZ) detection, and the Texas Red channel to identify dead cell populations. Liposome uptake by lacZ⁺ (tumor) cells and lacZ⁻ (non-tumor) cells was then quantified. Tumor cells obtained from saline treated animals served as a negative control for ADS645WS while untransfected 9L glioma cells stained with the *FluoReporter*[®] lacZ flow cytometry kit were utilized as a negative control for lacZ staining. Blood samples were analyzed for liposome content after centrifugation to isolate plasma and treatment with 10% SDS to lyse liposomes. Fluorescent signal of samples was then quantified to determine liposome concentration.

6.4.7. STATISTICAL ANALYSIS

Means were determined for each variable in this study and the resulting values from each experiment were subjected to an analysis of variance (ANOVA) with Tukey post-hoc pairwise comparisons. Significance was determined using a 95% confidence level. Normality of each data set was confirmed using the Ryan-Joiner test.

6.5. COMPETING FINANCIAL INTERESTS

The authors declare no competing financial interests.

6.6. ACKNOWLEDGEMENTS

This work was funded by the National Science Foundation (NSF), Bioengineering and Environmental Systems (0401627 to RVB), the Nora L. Redman Fund, and the Georgia Cancer Coalition. We express gratitude to GTEC (EEC-9731643), a NSF Engineering Research Center based at Georgia Tech/Emory, for use of its core facilities and to GAANN (P200A030077) fellowships in drug and gene therapy development at Georgia Tech for additional support. The authors would also like to acknowledge Abhiruchi Agarwal for useful discussions, Les Gelbaum for NMR analysis, and Emmanuel Chen and Asha Nadipuram for help with conjugate purification and *in vitro* cleavage studies.

6.7. SUPPLEMENTARY INFORMATION

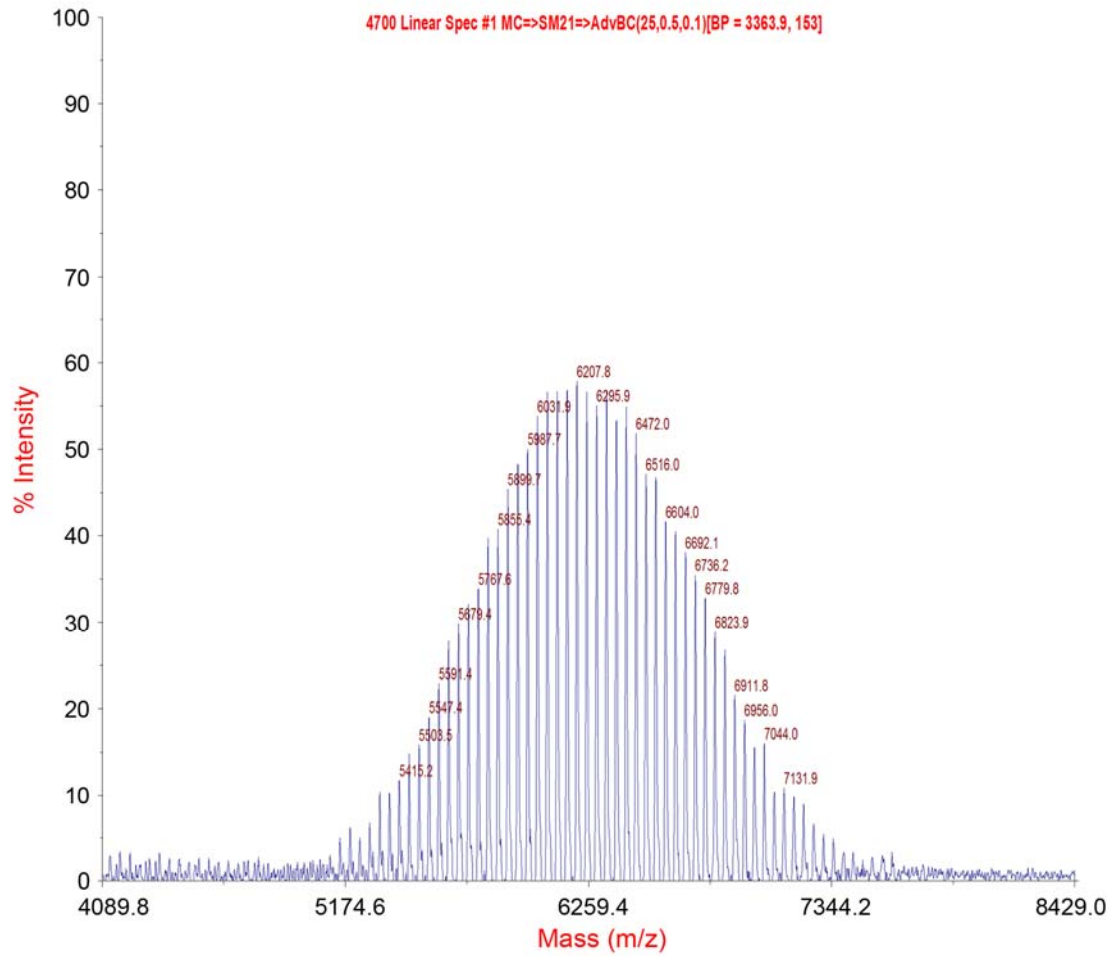


Figure 6.7. Matrix assisted laser desorption ionization time-of-flight mass spectrum (MALDI-TOFMS) of DSPE-S-S-PEG₅₀₀₀. A bell-shaped spectrum is shown verifying the expected molecular weight of ~6,210 Da. Lines are spaced at 44 Da, the molecular weight of PEG monomer, due to the polydispersity of PEG.

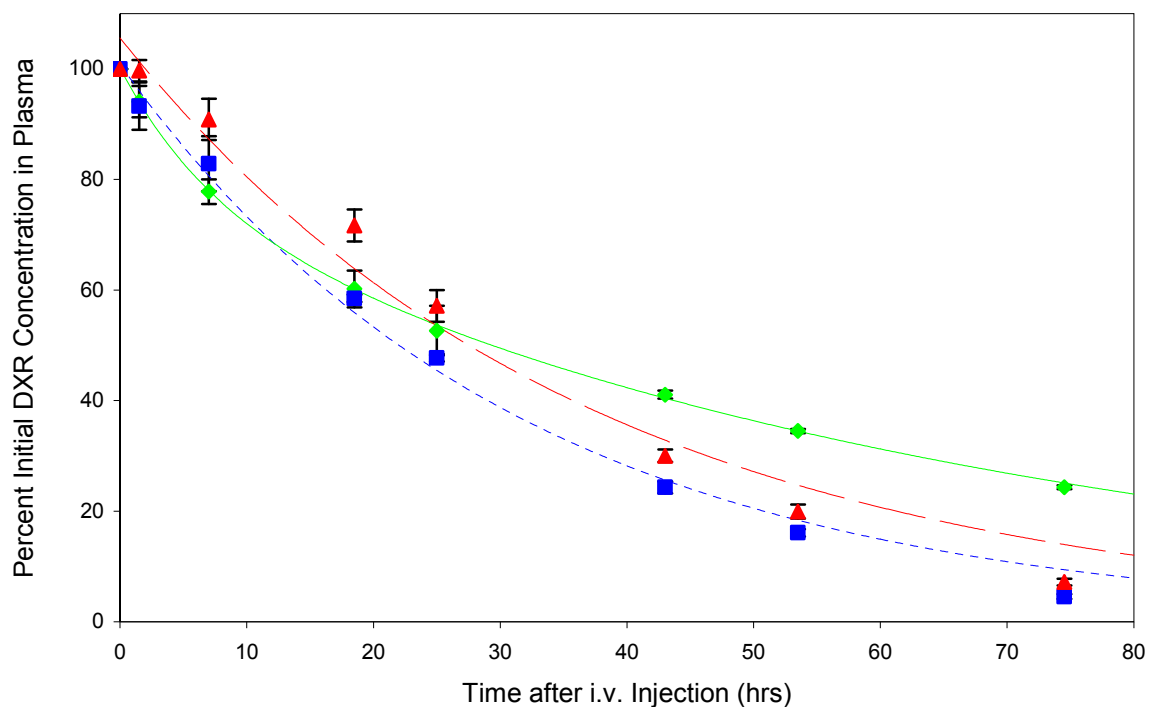


Figure 6.8. Supplement to Figure 6.2: Inclusion of 8% DSPE-S-S-PEG₅₀₀₀ prolongs circulation of FR-targeted nanocarriers. Circulating levels of DXR in the bloodstream, expressed as a percentage of initial DXR concentration, over time in animals receiving an i.v. injection of Stealth NT (◆) (n=3) or cleavable FRT containing 8% DSPE-S-S-PEG₅₀₀₀ (▲) (n=3) liposomal DXR. This plot also displays data obtained from the treatment group receiving cleavable FRT containing 6% DSPE-S-S-PEG₅₀₀₀ (■) (n=3) liposomal DXR, which was omitted from Figure 6.2. An increase in circulating levels of drug was observed when the DSPE-S-S-PEG₅₀₀₀ percentage was increased from 6% to 8% indicating an improvement in the ability to mask folate from the RES. Data represent mean ± SEM.

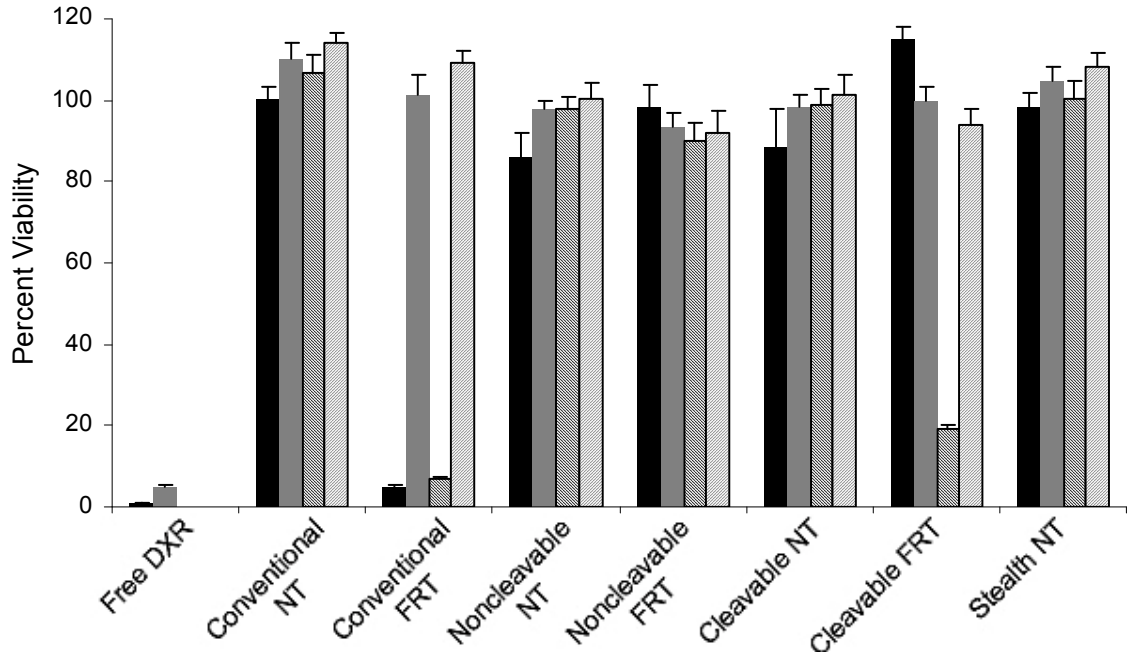


Figure 6.9. Supplement to Figure 6.4: Cytotoxicity of liposomal DXR is controllably altered through the inclusion of DSPE-S-S-PEG₅₀₀₀. Percent viability of cells after treatment with liposomal DXR formulations is shown. Plot displays additional control treatment groups (free DXR, conventional NT, noncleavable NT, cleavable NT) omitted from Figure 6.4. Treatments were applied alone (■), with excess folate (■), cysteine-treated (▨), or with excess folate and cysteine pre-treatment (▩). Free DXR demonstrated significant cytotoxicity to cells, while the 3 additional NT control treatment groups (conventional NT, noncleavable NT, cleavable NT) did not demonstrate a substantial cytotoxic effect under any of the 4 conditions. Data represent mean ± SEM.

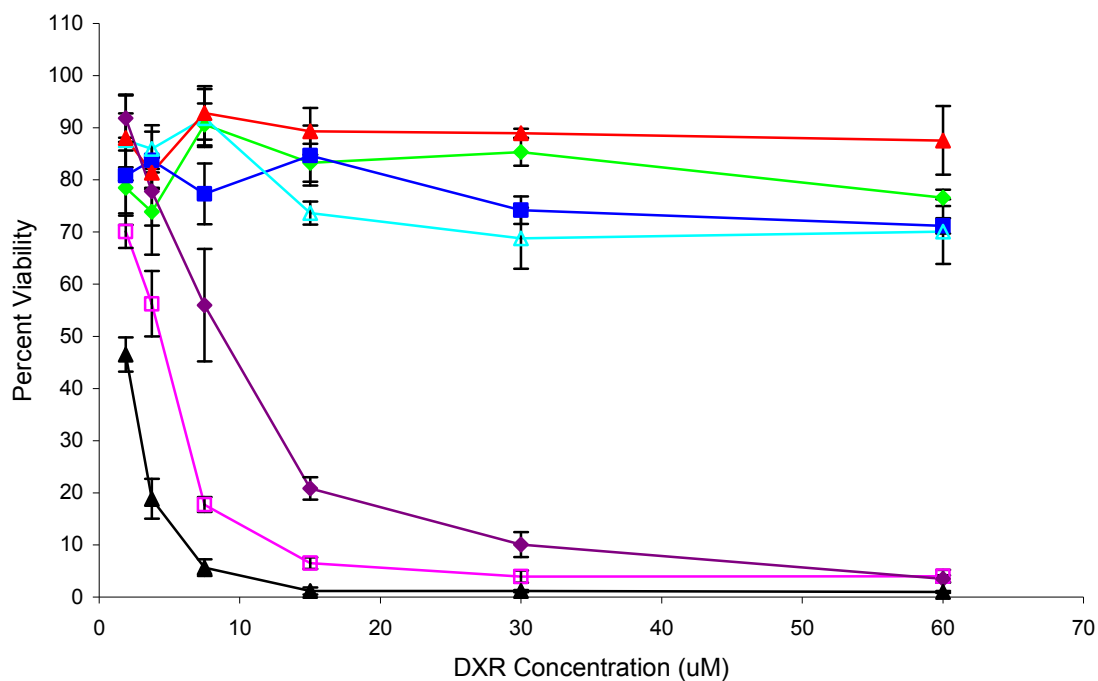


Figure 6.10. Cytotoxicity of liposomal DXR as a function of applied DXR concentration. 9L glioma cells were exposed to increasing numbers of DXR-loaded liposomes for 2 hours, washed, and then incubated for 5 days before assessing viability to determine the LC_{50} of each liposomal formulation. The best fit line of at least 3 points in the linear range of cell viability was used to calculate LC_{50} . Conventional NT (◆), noncleavable NT (■), noncleavable FRT (△), and cleavable FRT (▲) did not demonstrate any cytotoxic effect over the range of DXR concentrations tested (up to 60 μ M). After pre-treatment with cysteine, however, the cleavable FRT formulation (◆) exhibited a dramatic effect on cell viability, reducing the LC_{50} to 9.22 μ M. Conventional FRT liposomal DXR (◻) and free DXR (▲) also exhibited cytotoxic effects on 9L glioma cells with LC_{50} s of 4.17 μ M and 1.6 μ M, respectively. Data represents mean \pm SEM.

6.8. REFERENCES

- [1] Minko, T., Pakunlu, R., Wang, Y., et al., New generation of liposomal drugs for cancer. *Anticancer Agents Med Chem* 6, 537-552 (2006).
- [2] Gutman, R. L., Peacock, G. and Lu, D. R., Targeted drug delivery for brain cancer treatment. *J Control Release* 65, 31-41. (2000).
- [3] Torchilin, V. P., Drug targeting. *Eur J Pharm Sci* 11 Suppl 2, S81-91. (2000).
- [4] Gabizon, A., Dagan, A., Goren, D., et al., Liposomes as in vivo carriers of adriamycin: reduced cardiac uptake and preserved antitumor activity in mice. *Cancer Res* 42, 4734-4739 (1982).
- [5] Daoud, S. S. and Juliano, R. L., Reduced toxicity and enhanced antitumor effects in mice of the ionophoric drug valinomycin when incorporated in liposomes. *Cancer Res* 46, 5518-5523 (1986).
- [6] Duncan, R., Polymer conjugates for tumour targeting and intracytoplasmic delivery. The EPR effect as a common gateway? *Pharm Sci Technolo Today* 11, 441-449 (1999).
- [7] Maeda, H., Wu, J., Sawa, T., et al., Tumor vascular permeability and the EPR effect in macromolecular therapeutics: a review. *J Control Release* 65, 271-284 (2000).
- [8] Takeuchi, H., Kojima, H., Yamamoto, H. and Kawashima, Y., Passive targeting of doxorubicin with polymer coated liposomes in tumor bearing rats. *Biol Pharm Bull* 24, 795-799 (2001).
- [9] Maeda, H., The enhanced permeability and retention (EPR) effect in tumor vasculature: the key role of tumor-selective macromolecular drug targeting. *Adv Enzyme Regul* 41, 189-207 (2001).
- [10] Schiffelers, R. M., Bakker-Woudenberg, I. A. and Storm, G., Localization of sterically stabilized liposomes in experimental rat *Klebsiella pneumoniae* pneumonia: dependence on circulation kinetics and presence of poly(ethylene)glycol coating. *Biochim Biophys Acta* 1468, 253-261 (2000).

- [11] Saul, J. M., Annapragada, A., Natarajan, J. V. and Bellamkonda, R. V., Controlled targeting of liposomal doxorubicin via the folate receptor in vitro. *J Control Release* 92, 49-67 (2003).
- [12] Saul, J. M., Annapragada, A. V. and Bellamkonda, R. V., A dual-ligand approach for enhancing targeting selectivity of therapeutic nanocarriers. *J Control Release* 114, 277-287 (2006).
- [13] Lee, R. J. and Low, P. S., Folate-mediated tumor cell targeting of liposome-entrapped doxorubicin in vitro. *Biochim Biophys Acta* 1233, 134-144 (1995).
- [14] Eavarone, D. A., Yu, X. and Bellamkonda, R. V., Targeted drug delivery to C6 glioma by transferrin-coupled liposomes. *J Biomed Mater Res* 51, 10-14. (2000).
- [15] Goren, D., Horowitz, A. T., Tzemach, D., et al., Nuclear delivery of doxorubicin via folate-targeted liposomes with bypass of multidrug-resistance efflux pump. *Clin Cancer Res* 6, 1949-1957 (2000).
- [16] McNeeley, K., Annapragada, A. and Bellamkonda, R., Decreased circulation time offsets increased efficacy of PEGylated nanocarriers targeting folate receptors of glioma. *Nanotechnology* 18, 1-11 (2007).
- [17] Pastorino, F., Brignole, C., Marimpietri, D., et al., Vascular damage and anti-angiogenic effects of tumor vessel-targeted liposomal chemotherapy. *Cancer Res.* 63, 7400-7409 (2003).
- [18] Gabizon, A., Horowitz, A. T., Goren, D., et al., In vivo fate of folate-targeted polyethylene-glycol liposomes in tumor-bearing mice. *Clinical Cancer Research* 9, 6551-6559 (2003).
- [19] Pan, X. Q., Hang, H. and Lee, R. J., Antitumor activity of folate receptor-targeted liposomal doxorubicin in a KB oral carcinoma murine xenograft model. *Pharmaceutical research* 20, 417-422 (2003).
- [20] Gabizon, A., Shmeeda, H., Horowitz, A. T. and Zalipsky, S., Tumor cell targeting of liposome-entrapped drugs with phospholipid-anchored folic acid-PEG conjugates. *Adv Drug Deliv Rev* 56, 1177-1192 (2004).

- [21] Wu, J., Liu, Q. and Lee, R. J., A folate receptor-targeted liposomal formulation for paclitaxel. *Int J Pharm* 316, 148-153 (2006).
- [22] Huwylar, J., Wu, D. and Pardridge, W. M., Brain drug delivery of small molecules using immunoliposomes. *Proc Natl Acad Sci U S A* 93, 14164-14169 (1996).
- [23] Leamon, C. P., Cooper, S. R. and Hardee, G. E., Folate-liposome-mediated antisense oligodeoxynucleotide targeting to cancer cells: evaluation in vitro and in vivo. *Bioconjug Chem* 14, 738-747 (2003).
- [24] Klibanov, A. L., Maruyama, K., Torchilin, V. P. and Huang, L., Amphipathic polyethyleneglycols effectively prolong the circulation time of liposomes. *FEBS Lett* 268, 235-237. (1990).
- [25] Maruyama, K., Yuda, T., Okamoto, A., et al., Effect of molecular weight in amphipathic polyethyleneglycol on prolonging the circulation time of large unilamellar liposomes. *Chem Pharm Bull (Tokyo)* 39, 1620-1622. (1991).
- [26] Allen, T. M., Hansen, C., Martin, F., et al., Liposomes containing synthetic lipid derivatives of poly(ethylene glycol) show prolonged circulation half-lives in vivo. *Biochim Biophys Acta* 1066, 29-36. (1991).
- [27] Harris, J. M., Martin, N. E. and Modi, M., Pegylation: a novel process for modifying pharmacokinetics. *Clin Pharmacokinet* 40, 539-551 (2001).
- [28] Allen, C., Dos Santos, N., Gallagher, R., et al., Controlling the physical behavior and biological performance of liposome formulations through use of surface grafted poly(ethylene glycol). *Bioscience Reports* 22, 225-250 (2002).
- [29] Kirpotin, D., Hong, K., Mullah, N., et al., Liposomes with detachable polymer coating: destabilization and fusion of dioleoylphosphatidylethanolamine vesicles triggered by cleavage of surface-grafted poly(ethylene glycol). *FEBS Lett* 388, 115-118 (1996).
- [30] Ishida, T., Kirchmeier, M. J., Moase, E. H., et al., Targeted delivery and triggered release of liposomal doxorubicin enhances cytotoxicity against human B lymphoma cells. *Biochim Biophys Acta* 1515, 144-158 (2001).

- [31] Zhang, J. X., Zalipsky, S., Mullah, N., et al., Pharmaco attributes of dioleoylphosphatidylethanolamine/cholesterylhemisuccinate liposomes containing different types of cleavable lipopolymers. *Pharmacol Res* 49, 185-198 (2004).
- [32] Karathanasis, E., Ayyagari, A. L., Bhavane, R., et al., Preparation of in vivo cleavable agglomerated liposomes suitable for modulated pulmonary drug delivery. *J Control Release* 103, 159-175 (2005).
- [33] Karathanasis, E., Bhavane, R. and Annapragada, A. V., Triggered release of inhaled insulin from the agglomerated vesicles: pharmacodynamic studies in rats. *J Control Release* 113, 117-127 (2006).
- [34] Maeda, T. and Fujimoto, K., A reduction-triggered delivery by a liposomal carrier possessing membrane-permeable ligands and a detachable coating. *Colloids Surf B Biointerfaces* 49, 15-21 (2006).
- [35] Zalipsky, S., Qazen, M., Walker, J. A., 2nd, et al., New detachable poly(ethylene glycol) conjugates: cysteine-cleavable lipopolymers regenerating natural phospholipid, diacyl phosphatidylethanolamine. *Bioconjug Chem* 10, 703-707 (1999).
- [36] Mercadal, M., Domingo, J. C., Petriz, J., et al., Preparation of immunoliposomes bearing poly(ethylene glycol)-coupled monoclonal antibody linked via a cleavable disulfide bond for ex vivo applications. *Biochim Biophys Acta* 1509, 299-310 (2000).
- [37] Terada, T., Iwai, M., Kawakami, S., et al., Novel PEG-matrix metalloproteinase-2 cleavable peptide-lipid containing galactosylated liposomes for hepatocellular carcinoma-selective targeting. *J Control Release* 111, 333-342 (2006).
- [38] Hatakeyama, H., Akita, H., Kogure, K., et al., Development of a novel systemic gene delivery system for cancer therapy with a tumor-specific cleavable PEG-lipid. *Gene Ther* 14, 68-77 (2007).
- [39] Low, P. S. and Antony, A. C., Folate receptor-targeted drugs for cancer and inflammatory diseases. *Adv Drug Deliv Rev* 56, 1055-1058 (2004).
- [40] Allen, T. M., Brandeis, E., Hansen, C. B., et al., A new strategy for attachment of antibodies to sterically stabilized liposomes resulting in efficient targeting to cancer

cells [published erratum appears in *Biochim Biophys Acta* 1995 Dec 13;1240(2):285]. *Biochim Biophys Acta* 1237, 99-108 (1995).

- [41] Mercadal, M., Domingo, J. C., Petriz, J., et al., A novel strategy affords high-yield coupling of antibody to extremities of liposomal surface-grafted PEG chains. *Biochim Biophys Acta* 1418, 232-238 (1999).
- [42] Gabizon, A., Horowitz, A. T., Goren, D., et al., Targeting folate receptor with folate linked to extremities of poly(ethylene glycol)-grafted liposomes: in vitro studies. *Bioconjug Chem* 10, 289-298 (1999).
- [43] Lasic, D., *Liposomes: From Physics to Applications*. (Elsevier, Amsterdam, 1993).
- [44] Bolotin, E. M., Cohen, R., Bar, L. K., et al., Ammonium sulfate gradients for efficient and stable remote loading of amphipathic weak bases into liposomes and ligandoliposomes. *Journal of Liposome Research* 4, 455-479 (1994).

CHAPTER 7. SUMMARY OF FINDINGS

7.1. INTRODUCTION

Liposomes have been studied extensively since their initial discovery in the 1960's. By the 1970's, realization of their potential use as therapeutic nanocarriers spurred thorough investigation toward drug delivery applications. Soon afterward, sterically stabilized liposomes were introduced with the potential to passively target tumors due to the combination of 1) prolonged circulation in the bloodstream resulting from RES evasion and 2) the enhanced permeability and retention effect attributed to the intrinsic properties of the tumor vasculature and compromised lymphatics. Today, despite the fact that several "Stealth" liposomal formulations have been clinically approved, little progress has been made toward the clinical approval of an actively targeted liposomal chemotherapeutic.

The inclusion of targeting agents into liposomal nanocarriers to promote active targeting to tumors has been studied extensively. *In vitro* studies with a wide variety of targeting agents have demonstrated considerable success in facilitating specific binding and uptake by tumor cells [1-9]. *In vivo*, however, actively targeted liposomal nanocarriers have failed to meet the expectations established by the promising outcomes of *in vitro* studies. Disappointing *in vivo* results have been attributed to the fact that the delivery of liposomes to solid tumors is limited by elevated interstitial pressures and inability to diffuse beyond the perivascular space [10]. This certainly is a valid explanation, however diffusion limitations only partially account for *in vivo* failure of actively targeted liposomal nanocarriers.

It has been shown that the inclusion of targeting agents in liposomal formulations results in reductions in circulation time within the bloodstream due to RES recognition and clearance. Since passive accumulation to tumor is directly related to circulating levels in the bloodstream, accelerated clearance of actively targeted liposomal formulations reduces passive targeting to tumor. This decrease in passive targeting effectively offsets the benefits of active targeting to tumor.

The global objective of the body of work described here was to further investigate the impact of targeting ligand incorporation into sterically stabilized liposomes and to explore a possible solution to the negative effects of ligand insertion using cleavable phospholipid-PEG conjugates. To accomplish this objective, this study was divided into two parts. Preliminary experiments were conducted to gain a more thorough understanding of the *in vivo* effects of folate insertion in liposomes, and subsequent studies explored the ability to modulate folate exposure *in vitro* and *in vivo* using detachable PEG chains.

7.2. EVALUATION OF ALTERNATIVE TARGETING AGENTS TO IMPROVE TREATMENT EFFICACY

Through *in vivo* studies utilizing both a small peptide targeted to APN and a large antibody targeted to TfR in liposomal DXR formulations, the impact of targeting agent selection was investigated. Survival studies performed on tumor-bearing animals demonstrated the importance of administration time point selection. When treatment was administered at an earlier time point, a more favorable response in treatment efficacy was achieved. Delaying the treatment administration by 8 days resulted in the complete inability to prolong survival beyond that achieved with saline sham treated animals. At

this time point, the tumor size had progressed to a point where a response to any treatment was unattainable. Additional survival studies were performed to investigate alternative treatment regimens. The results of these studies showed that a single treatment with liposomal DXR at a dose of 10 mg/kg was superior to the administration of 2 weekly treatments adding to a cumulative dose of 20 mg/kg. Unfortunately, utilizing a single treatment regimen, neither the inclusion of NGR peptide or OX26 targeting agents in liposomal DXR formulations was able to improve the survival of tumor-bearing animals over the survival of animals receiving non-targeted liposomal DXR.

Circulation studies emphasized the importance of careful consideration of targeting agent selection upon formulation of actively targeted liposomal nanocarriers. The small peptide investigated for APN targeting had no impact on liposome circulation times in the bloodstream, whereas the inclusion of as few as 4 OX26 antibodies had a severe detrimental effect on liposome performance *in vivo*. The drastic dissimilarity in circulation of these targeted liposomal nanocarriers may be attributed to the 75-fold difference in targeting agent size; however, it is not size alone which determines the ability to evade the RES. Other factors such as polarity, hydrophobicity, overall surface charge, and 3-dimensional configuration among other characteristics must also play a role in the ability of the RES to recognize these molecules on the surface of liposomal formulations and accelerate clearance from the bloodstream. The primary reason suggested for the low immunogenicity of NGR has been its ability to mimic natural proteins in the bloodstream [11]. These studies have provided insight into additional factors which may be considered during targeting agent selection to ensure prolonged circulation in the bloodstream.

Through biodistribution studies, we determined that an enhancement in drug delivery to the brain may be achieved using TfR-targeted liposomes, which is significant considering the drastic reductions in circulation time upon inclusion of OX26 antibody as a targeting agent. These results further stressed the need to address reductions in circulation times of actively targeted liposomal formulations. If, as shown here, enhanced drug delivery to the brain may be achieved with such low circulating levels of drug, improvements in circulation times should significantly increase delivery to the brain. Therefore, it is imperative that circulation times of actively targeted liposomal nanocarriers are improved, and the use of smaller targeting agents or those able to mimic naturally occurring substances in the body may provide an option to do so *in vivo*.

7.3. DECREASED CIRCULATION TIME OFFSETS INCREASED EFFICACY OF PEGYLATED NANOCARRIERS TARGETING FOLATE RECEPTORS OF GLIOMA

Experiments conducted to investigate the impact of targeting ligand insertion into passively targeted liposomes included the development and characterization of an orthotopic glioma model, *in vivo* blood circulation studies, biodistribution studies, and survival studies. Previous reports have indicated a negative impact on targeting ligand inclusion through demonstrated reductions in circulating levels of actively targeted formulations in the bloodstream; however, the full consequences had not been directly addressed or investigated in detail [8, 10, 12-15]. The current studies reported here also revealed a dramatic and significant reduction in circulating levels of FR-targeted liposomes compared to passively-targeted Stealth liposomes.

Intravascular administration of liposomal DXR demonstrated that the insertion of DSPE-PEG₃₃₅₀-folate into Stealth liposomes caused a 42% reduction in AUC and a 63%

reduction in plasma half-life. These results were attributed to recognition of folate, present on PEG chains (PEG₃₃₅₀) longer than those incorporated for steric stabilization (PEG₂₀₀₀), by the RES and subsequent acceleration of clearance from the bloodstream. Having successfully replicated results from previous work, we then conducted additional experiments to explore the effects of accelerated clearance from the bloodstream on the biodistribution and ultimate therapeutic efficacy of DXR encapsulated within FR-targeted liposomal nanocarriers.

For these studies, an orthotopic glioma tumor model was developed in rats to assess FR-targeted liposomal DXR performance *in vivo*. The majority of studies on FR-targeted liposomes to date have utilized either subcutaneous [10, 13, 16, 17] or intraperitoneal [10, 18-21] tumor models for *in vivo* analysis. These studies typically utilize cell lines, such as the human oral carcinoma KB cell line, which vastly overexpress the folate receptor compared to normal tissue [6]. We were interested in evaluating the ability to target and treat tumors which exhibit relatively moderate overexpression of the folate receptor compared to KB cells since this provides a better representation of the difficult to treat tumors presented in the clinic. Therefore, a glioma cell line was selected for intracranial tumor inoculation. An intracranial model was chosen for these experiments to more accurately represent the environment in which gliomas naturally occur. The presence of the BBB is a major component of this environment and orthotopic inoculation of tumor ensured that the BBB remained a factor in our experimental studies.

The 9L glioma tumor model was characterized by evaluating growth and angiogenesis. Inoculated tumors proved to be aggressive demonstrating exponential

growth with a doubling time of only 1.7 days. Interventional euthanasia was required for all untreated animals on or before 22 days due to the onset of severe debilitating symptoms resulting from tumor growth and increased intracranial pressure. There were no signs of metastasis in any of the euthanized animals confirming that symptoms resulted solely from rapid progression of the primary tumor. Tumors were infiltrative and reproducible, therefore, this model was deemed appropriate for further studies. Angiogenesis of the tumor model was evaluated through histological examination. The onset of angiogenesis was detected as early as 4 days following tumor inoculation. These results helped to determine the proper time of treatment for survival studies evaluating therapeutic efficacy since established vasculature is mandatory for tumor delivery of treatments administered i.v.

Studies were conducted on tumor-bearing animals to evaluate biodistribution of Stealth and FR-targeted liposomal DXR 20 and 50 hours after treatment administration. At both time points, the majority of DXR was located within the spleen and liver, the organs responsible for RES clearance. There was no significant difference between the biodistribution of the two liposomal formulations with the exception of amount of drug detected within the liver. Liver accumulation of FR-targeted liposomes was significantly greater than that of Stealth liposomes, accounting for the dramatic difference in circulating levels of DXR in the bloodstream between the formulations at each time point. Tumor drug levels were not significantly different despite the vast disparity in bloodstream concentration of drug between the Stealth and FR-targeted nanocarriers, which may indicate that FR-targeted liposomes are retained within the tumor to a greater extent due to receptor binding and uptake.

Survival studies investigating the therapeutic efficacy of each formulation were conducted on tumor-bearing animals receiving a single i.v. injection of liposomal DXR. Survival was prolonged for all animals receiving treatments compared to saline treated controls; however, there was no significant difference between the survival of animals treated with either Stealth or FR-targeted liposomal DXR. This may simply be due to the aggressive nature of the tumor, where a single treatment is incapable of elucidating a detectable response in survival, however, the biodistribution results which demonstrated no difference in uptake by tumor between the 2 formulations, suggest that there are additional barriers *in vivo* preventing an increase in therapeutic efficacy of targeted formulations. While diffusion limitations within solid tumors are certainly considered to be partially responsible, reductions in circulating levels of drug decreasing passive targeting to tumor may also play a role in the inability to realize a survival advantage using actively targeted formulations. In fact, the only studies that have demonstrated prolonged survival using FR-targeted liposomes have involved i.p. administration of treatments to i.p. tumors thus bypassing the bloodstream and RES elimination [18, 22] or i.p. injection of treatments to athymic animals bearing s.c. tumors where the compromised immune system failed to accelerate clearance of targeted formulations [13]. Another study demonstrated tumor growth reduction in tumors treated with FR-targeted liposomal DXR, however this study involved the administration of treatment ex vivo and subsequent implantation of treated cells thereby avoiding treatment exposure to the RES [3]. In addition, enhancement in tumor uptake of FR-targeted liposomes has only been demonstrated in i.p. tumor-bearing animals receiving the treatments i.p. [19-21]. As reported here, others have also shown that i.v. injection of FR-targeted treatments fails to

result in an increase in tumor uptake [16, 17], however discussion regarding reductions in circulating drug and the impact this may have on delivery to tumor have been absent from the literature.

The conclusions of this study have served to verify that the negative impact in targeting ligand insertion into Stealth liposomes, namely the recognition of nanocarriers by the RES and subsequent acceleration in plasma clearance, has a detrimental effect on tumor targeting. Lower circulating levels of drug effectively reduce passive targeting to tumor thereby offsetting the benefits of active targeting. This information should aid investigators in the design of future formulations where careful consideration regarding the effects of targeting agent insertion on circulation times should be made. A compromise in passive targeting to tumor will likely be required unless an alternative solution such as transient masking of targeting agents from the RES is utilized.

7.4. MASKING AND TRIGGERED UNMASKING OF TARGETING LIGANDS ON NANOCARRIERS IMPROVES DRUG DELIVERY TO BRAIN TUMORS

In an attempt to address the issue of accelerated clearance and reduction in passive tumor accumulation of targeted liposomes, we developed a controllable liposomal system by which exposure of folate may be modulated using detachable PEG chains. Cysteine cleavable phospholipid-PEG₅₀₀₀ conjugates were formulated and characterized, the ability to mask folate with these conjugates was tested through *in vivo* circulation studies, controllable modulation of folate exposure on liposomes was tested and verified *in vitro*, and *in vivo* intracellular uptake of liposomal formulations was examined through flow cytometric analysis of explanted tumors.

Following established methods, a cysteine cleavable DSPE-PEG₅₀₀₀ conjugate was formulated using SPDP, containing a reducible disulfide bridge, to crosslink DSPE and PEG₅₀₀₀-SH. Mass spectroscopy, TLC, and ¹H-NMR verified successful formation of the conjugate, and *in vitro* cleavage studies confirmed the ability to efficiently cleave the conjugate with as little as a 10-fold molar excess of cysteine.

Blood circulation studies were performed on rats receiving FR-targeted liposomes with increasing concentrations of DSPE-S-S-PEG₅₀₀₀ to determine the minimum amount of cleavable conjugate necessary to adequately mask folate from the RES and enable prolonged circulation comparable to that achieved with Stealth liposomal nanocarriers. From this study, it was concluded that 8% DSPE-S-S-PEG₅₀₀₀ was sufficient to mask DSPE-PEG₂₀₀₀-folate from the RES while in circulation. This formulation exhibited a 3.8-fold increase in plasma half-life and a 65.5% increase in AUC compared to traditional FR-targeted liposomes containing 0.15% DSPE-PEG₃₃₅₀-folate and 3% DSPE-PEG₂₀₀₀. The inclusion of detachable PEG₅₀₀₀ increased the half-life of FR-targeted liposomes to 27.4 hours which was comparable to the half-life of non-targeted Stealth liposomes, 30.3 hours. For the first 25 hours in circulation, concentrations of cleavable FR-targeted liposomes in the bloodstream actually surpassed the circulating levels of Stealth liposomes, however, the clearance of cleavable FR-targeted liposomes slowly increased over time presumably due to gradual cleavage and removal of PEG₅₀₀₀ by endogenous cysteine. Subsequent exposure of folate would likely trigger opsonization and clearance of the liposomes by the RES accounting for this reduction in circulating levels. Fortunately, the AUC calculated between 0 and 25 hours was comparable between the cleavable FRT and Stealth liposomes indicating that passive accumulation to

tumor should remain unaffected until much later when circulating cleavable FRT liposomes begin to clear at a faster rate, however, by that time the benefits of active targeting from triggered PEG removal and exposure of folate should surpass any gains from elevated circulating levels of drug.

In vitro studies on cultured 9L glioma cells were conducted to verify the ability to modulate folate exposure using detachable PEG chains enabling control over uptake and cytotoxicity of FR-targeted liposomal DXR. Confocal uptake images verified substantial uptake of conventional FR-targeted liposomes (0% DSPE-PEG) irrespective of cysteine pre-treatment. Cells did not take up non-targeted Stealth liposomes or FR-targeted liposomes masked with non-cleavable DSPE-PEG₅₀₀₀ under either condition. Cleavable FR-targeted formulations, however, demonstrated a distinct dependence on cysteine pre-treatment. In the absence of cysteine treatment, uptake of the liposomes was negligible, whereas after the application of cysteine, uptake by cells was substantially increased and resulted in nuclear localization of drug payloads.

Cytotoxicity studies confirmed the *in vitro* uptake results. DXR encapsulated within non-targeted liposomes and FR-targeted liposomes masked with non-cleavable DSPE-PEG₅₀₀₀ did not exhibit any cytotoxic potential. Cytotoxicity of conventional FR-targeted liposomal DXR was significantly increased. Treatment with cysteine had no effect on the cytotoxicity, however, cell viability was significantly greater when excess folate was introduced indicating that uptake of the liposomal DXR was dependent on the availability of folate receptors. Cytotoxicity of FR-targeted liposomal DXR formulated with detachable PEG chains demonstrated a significant dependence on cysteine pre-treatment. Only those formulations pre-treated with cysteine to remove PEG and expose

folate demonstrated cytotoxicity to FR-expressing 9L glioma cells. In the absence of cysteine pre-treatment, the LC_{50} of cleavable PEG FR-targeted liposomal DXR could not be determined since cytotoxicity was not observed at any of the tested concentrations up to 60 μ M DXR. Cysteine pre-treatment, however, lowered the LC_{50} to 9.22 μ M which approached the LC_{50} value of 4.17 μ M obtained with conventional FR-targeted liposomal DXR. The addition of excess folate significantly decreased the cytotoxic potential of cysteine treated FR-targeted liposomal DXR with cleavable PEG indicating that uptake occurred via the folate receptor. These *in vitro* experiments verified the ability to modulate uptake and cytotoxicity of FR-targeted liposomal DXR using detachable PEG chains. Cleaved formulations successfully regained the ability to bind and enter target cells with cytotoxicity approaching values attained with conventional FR-targeted liposomes, and uptake was shown to remain dependent on the folate receptor.

To assess intracellular delivery *in vivo*, liposomal formulations were administered i.v. to tumor-bearing animals. Treated animals then received either a saline or cysteine i.v. infusion. Explanted tumors were dissociated and analyzed for liposomal content. This procedure enabled specific analysis of intracellular uptake in contrast to the previous study which simply measured bulk tumor uptake of liposomes. Flow cytometry was utilized to distinguish between disaggregated tumor cells and host cells. Animals treated with cleavable PEG FR-targeted liposomes followed by a cysteine infusion demonstrated a significant increase in uptake of liposomes by tumor cells and a significantly greater ratio of uptake between tumor and host cells compared to those animals treated with either Stealth liposomes or cleavable PEG FR-targeted liposomes followed by a saline infusion or Stealth liposomes followed by a cysteine infusion. In addition, the percentage

of tumor cells positive for liposome uptake was significantly greater in tumors explanted from animals treated with cleavable PEG FR-targeted liposomes and a cysteine infusion compared to the other treatment groups. These results indicate that the removal of PEG and subsequent exposure of folate through an i.v. infusion of cysteine was sufficient to promote specific binding and internalization of liposomes by target cells within an intracranial tumor site. This increase in uptake was dependent on cysteine removal of PEG chains since uptake was not increased in animals treated with cleavable PEG FR-targeted formulations and a saline infusion. Selectivity of cysteine-cleaved FR-targeted formulations was proven through the significant increase in uptake by tumor cells compared to host cells.

These studies verified the ability to ‘unmask’ folate on FR-targeted liposomes in a controlled manner *in vivo* to promote specific uptake by FR-expressing tumor cells. This experiment was able to distinguish intracellular and extracellular liposomes and also differentiate uptake by tumor and host cells. In this manner, it was determined that cysteine cleavage of PEG on FR-targeted formulations relays a distinct advantage for specific targeting to tumor cells since FR-targeted liposome treated animals receiving a cysteine infusion demonstrated a significantly higher uptake of liposomes per tumor cell as well as a significantly greater percentage of tumor cells internalizing liposomes. In addition, uptake was proven to be controllable since it was dependent on exogenous administration of cysteine.

Another potential benefit of PEG detachment from the liposomal surface is further diffusion of liposomes into the tumor and away from the perivascular space. Studies have shown that the presence of PEG inhibits diffusion within tumor [23, 24],

and neutrally charged liposomes lacking a PEG coating have been shown to diffuse more deeply into spheroid structures [25]. Since surface modification is a requirement for prolonged circulation *in vivo*, PEG is invariably present upon long-circulating liposomes even after extravasation to tumor. The cleavable PEG nanocarrier system presented here allows for controlled removal of PEG after extravasation to promote further diffusion within tumor and increased uptake by tumor cells.

These studies have proven that the use of cleavable PEG on actively targeted liposomal nanocarriers is a viable solution to the negative impact of targeting agent insertion into liposomes. With the knowledge that passive accumulation is critically dependent on circulation times [26], it is imperative that prolonged circulation of nanocarriers is uncompromised upon inclusion of targeting moieties. Here, we have shown that cleavable phospholipid-PEG conjugates can be used to enable precise control over ligand exposure, effectively concealing ligands to prolong liposomal circulation times and exposing targeting moieties at the desired time point after extravasation to tumor to promote specific uptake by tumor cells.

7.5. CONCLUSIONS

The studies presented here have provided further insight into the effects of targeting agent inclusion within passively targeted liposomal nanocarriers and demonstrated a potential solution to address the associated negative impact on circulation time in the bloodstream. Inability to achieve enhanced delivery to tumor and prolonged survival times *in vivo* using actively targeted liposomal chemotherapeutics was shown to be due, in part, to the reductions in circulation time resulting from the use of targeting agents in liposomal formulations. To address this issue, we successfully formulated a

nanocarrier system which allows for precisely controlled exposure of targeting agents on the liposomal surface. This liposomal system utilizing cysteine-cleavable phospholipid-PEG conjugates was shown to restore prolonged circulation of FR-targeted liposomes by masking folate targeting ligands from the RES. Modulation of uptake and cytotoxicity of these formulations through controlled removal of PEG was demonstrated and verified that liposomally encapsulated DXR reaches the cell nuclei in a functional active form. In addition, enhancement of specific targeting to tumor cells was demonstrated *in vivo*. These findings should allow for increased efficacy of actively targeted nanocarrier chemotherapeutics *in vivo*.

7.6. REFERENCES

- [1] Eavarone, D. A., Yu, X. and Bellamkonda, R. V., Targeted drug delivery to c6 glioma by transferrin-coupled liposomes. *J Biomed Mater Res* **51**, 10-14. (2000).
- [2] Gabizon, A., Horowitz, A. T., Goren, D., et al., Targeting folate receptor with folate linked to extremities of poly(ethylene glycol)-grafted liposomes: In vitro studies. *Bioconjug Chem* **10**, 289-298 (1999).
- [3] Goren, D., Horowitz, A. T., Tzemach, D., et al., Nuclear delivery of doxorubicin via folate-targeted liposomes with bypass of multidrug-resistance efflux pump. *Clin Cancer Res* **6**, 1949-1957 (2000).
- [4] Joo, S. Y. and Kim, J. S., Enhancement of gene transfer to cervical cancer cells using transferrin-conjugated liposome. *Drug Dev Ind Pharm* **28**, 1023-1031 (2002).
- [5] Mamot, C., Drummond, D. C., Greiser, U., et al., Epidermal growth factor receptor (egfr)-targeted immunoliposomes mediate specific and efficient drug delivery to egfr- and egfrviii-overexpressing tumor cells. *Cancer Res* **63**, 3154-3161 (2003).
- [6] Saul, J. M., Annapragada, A., Natarajan, J. V. and Bellamkonda, R. V., Controlled targeting of liposomal doxorubicin via the folate receptor in vitro. *J Control Release* **92**, 49-67 (2003).
- [7] Saul, J. M., Annapragada, A. V. and Bellamkonda, R. V., A dual-ligand approach for enhancing targeting selectivity of therapeutic nanocarriers. *J Control Release* **114**, 277-287 (2006).
- [8] Wu, J., Liu, Q. and Lee, R. J., A folate receptor-targeted liposomal formulation for paclitaxel. *Int J Pharm* **316**, 148-153 (2006).
- [9] Zhang, Y., Guo, L., Roeske, R. W., et al., Pteroyl-gamma-glutamate-cysteine synthesis and its application in folate receptor-mediated cancer cell targeting using folate-tethered liposomes. *Anal Biochem* **332**, 168-177 (2004).
- [10] Gabizon, A., Horowitz, A. T., Goren, D., et al., In vivo fate of folate-targeted polyethylene-glycol liposomes in tumor-bearing mice. *Clinical Cancer Research* **9**, 6551-6559 (2003).

- [11] Di Matteo, P., Curnis, F., Longhi, R., et al., Immunogenic and structural properties of the asn-gly-arg (ngr) tumor neovasculature-homing motif. *Mol Immunol* **43**, 1509-1518 (2006).
- [12] Pastorino, F., Brignole, C., Marimpietri, D., et al., Vascular damage and anti-angiogenic effects of tumor vessel-targeted liposomal chemotherapy. *Cancer Res.* **63**, 7400-7409 (2003).
- [13] Pan, X. Q., Hang, H. and Lee, R. J., Antitumor activity of folate receptor-targeted liposomal doxorubicin in a kb oral carcinoma murine xenograft model. *Pharmaceutical research* **20**, 417-422 (2003).
- [14] Gabizon, A., Shmeeda, H., Horowitz, A. T. and Zalipsky, S., Tumor cell targeting of liposome-entrapped drugs with phospholipid-anchored folic acid-peg conjugates. *Adv Drug Deliv Rev* **56**, 1177-1192 (2004).
- [15] Huwyler, J., Wu, D. and Pardridge, W. M., Brain drug delivery of small molecules using immunoliposomes. *Proc Natl Acad Sci U S A* **93**, 14164-14169 (1996).
- [16] Leamon, C. P., Cooper, S. R. and Hardee, G. E., Folate-liposome-mediated antisense oligodeoxynucleotide targeting to cancer cells: Evaluation in vitro and in vivo. *Bioconjug Chem* **14**, 738-747 (2003).
- [17] Stephenson, S., Yang, W., Stevens, P., et al., Folate receptor-targeted liposomes as possible delivery vehicles for boron neutron capture therapy. *Anticancer Res* **23**, 3341-3346 (2003).
- [18] Pan, X. Q. and Lee, R. J., In vivo antitumor activity of folate receptor-targeted liposomal daunorubicin in a murine leukemia model. *Anticancer Res* **25**, 343-346 (2005).
- [19] Turk, M. J., Waters, D. J. and Low, P. S., Folate-conjugated liposomes preferentially target macrophages associated with ovarian carcinoma. *Cancer Lett* **213**, 165-172 (2004).
- [20] Shmeeda, H., Mak, L., Tzemach, D., et al., Intracellular uptake and intracavitary targeting of folate-conjugated liposomes in a mouse lymphoma model with up-regulated folate receptors. *Mol Cancer Ther* **5**, 818-824 (2006).

- [21] Reddy, J. A., Abburi, C., Hofland, H., et al., Folate-targeted, cationic liposome-mediated gene transfer into disseminated peritoneal tumors. *Gene Ther* **9**, 1542-1550 (2002).
- [22] Pan, X. Q., Zheng, X., Shi, G., et al., Strategy for the treatment of acute myelogenous leukemia based on folate receptor beta-targeted liposomal doxorubicin combined with receptor induction using all-trans retinoic acid. *Blood* **100**, 594-602. (2002).
- [23] Yuan, F., Leunig, M., Huang, S. K., et al., Microvascular permeability and interstitial penetration of sterically stabilized (stealth) liposomes in a human tumor xenograft. *Cancer Res* **54**, 3352-3356. (1994).
- [24] Wu, N., Da, D., Rudoll, T., et al., Increased microvascular permeability contributes to preferential accumulation of stealth liposomes in tumor tissue. *Cancer Res* **53**, 3765-3770 (1993).
- [25] Kostarelos, K., Emfietzoglou, D., Papakostas, A., et al., Binding and interstitial penetration of liposomes within avascular tumor spheroids. *Int J Cancer* **112**, 713-721 (2004).
- [26] Schiffelers, R. M., Bakker-Woudenberg, I. A. and Storm, G., Localization of sterically stabilized liposomes in experimental rat klebsiella pneumoniae pneumonia: Dependence on circulation kinetics and presence of poly(ethylene)glycol coating. *Biochim Biophys Acta* **1468**, 253-261 (2000).

CHAPTER 8. FUTURE PERSPECTIVES

An actively targeted liposomal chemotherapeutic has yet to make it into the clinic despite promising *in vitro* results demonstrating the potential for increased cytotoxicity due to specific uptake by tumor cells. *In vivo* studies have typically failed to exhibit enhanced efficacy with actively targeted liposomal chemotherapeutics because the inclusion of targeting agents results in accelerated clearance from the bloodstream and reductions in passive targeting to tumor. The work reported in this dissertation has focused on the use of targeted nanocarriers engineered to allow controlled presentation of targeting agents. Cleavable phospholipid-PEG conjugates were utilized to mask targeting ligands on nanocarriers and maintain RES evasion in an attempt to reestablish enhanced passive accumulation within tumors. Unmasking of targeting agents was triggered by exogenous cysteine administration to promote specific uptake by tumor cells after the nanocarriers had passively extravasated to the target site. This chapter is devoted to the discussion of additional aspects which may be investigated to further optimize this multifunctional liposomal system.

8.1. BIODISTRIBUTION STUDIES

While the studies presented here included the examination and differentiation of uptake by tumor cells and host cells at the tumor site, additional studies need to be performed to evaluate whole organ distribution of drug. These studies would determine whether the inclusion and subsequent removal of cleavable PEG chains in FR-targeted liposomes alters the biodistribution of drug. It would be interesting to follow the progression of liver and spleen uptake to verify that it accounts for the slow acceleration in clearance of masked formulations over time. In addition, levels of uptake by the liver

of targeted liposomes formulated with detachable PEG at early time points (<25 hours) may be compared to the liver uptake of Stealth liposomal DXR to determine whether the inclusion of cleavable PEG chains reduces the significant difference in liver uptake previously observed between Stealth and traditional FR-targeted liposomes. Bulk tumor uptake measurements would determine total intracellular and extracellular liposomal DXR delivered to the tumor.

8.2. SPATIAL DISTRIBUTION WITHIN TUMOR

Histological examination of tumors explanted from animals treated with liposomal formulations could be performed to reveal the spatial distribution of drug within the tumor. Vascular staining would serve to identify the perivascular regions to determine whether the treatments colocalize within this space. Fluorescent microscopy following the administration of an encapsulated or membrane-inserted fluorophore may be utilized to determine spatial distribution of liposomes. Alternatively, microdistribution within tumor tissue could be visualized using light microscopic examination of tissue sections obtained from animals treated with gold-loaded liposomes to compare tumor penetration and cellular localization.

Ideally, uniform distribution of drug would ensure treatment delivery to the entire tumor; however, this is unlikely to occur for a number of reasons. First, modifications introduced to achieve long-circulation, such as PEGylation, have been shown to inhibit diffusion within tumors and tumor spheroids [1-3]. Therefore, the diffusion of treatments within tumor prior to the removal of PEG from FR-targeted formulations may be limited; however, subsequent PEG detachment should facilitate transport within tumor. Another reason to expect heterogeneous distribution of liposomes within tumor is due to the

“binding site barrier”. This refers to the condition where targeted agents bind to the first line of target cells after extravasation, are sequestered to the perivascular space, and consequently obstruct the extravasation of additional drug [4]. This phenomenon has been observed with antibodies targeted for cancer therapy where it was shown that the larger the antibody and higher its binding affinity, the lower its therapeutic efficacy [5]. Fortunately, prior to cysteine administration, concealed folate should not participate in a binding site barrier; therefore, these formulations may diffuse further than other actively targeted liposomes. Successive ‘unmasking’ of folate upon detachment of PEG, however, may serve to inhibit further transport within tumor. This effect may counteract the enhanced diffusion benefit of PEG removal; however studies investigating spatial distribution within tumor are warranted to determine the overall effects of PEG removal at the tumor site. Another major obstacle to uniform drug distribution of targeted agents within tumor is the fact that the interstitial fluid pressure is higher in the tumor center compared to the periphery and surrounding tissue [6-8]. This pressure differential along with heterogeneity in blood supply leads to lower fluid extravasation in the tumor core reducing drug delivery to this region. In addition, this condition makes it difficult for macromolecules delivered to the periphery to diffuse into tumor since they have to overcome the outward convection of fluid from regions of high to low pressure [9]. Spatial distribution studies would help to identify diffusion limitations within tumor. Possible methods to overcome transport barriers, should they have a major impact on spatial distribution and treatment efficacy, are presented in a later section of this chapter.

8.3. *IN VIVO* CYTOTOXICITY

Having investigated uptake by both tumor and host cells at the tumor site, additional studies should be performed to evaluate treatment cytotoxicity *in vivo*. Ideally, cell populations would be differentiated either through histological staining or flow cytometry to distinguish cytotoxic effects among the different populations of cells at the tumor site. It would be interesting to compare the cytotoxic effects after varying the time point of cysteine administration. In this manner, the optimal time point for cysteine infusion following treatment administration could be determined.

8.4. TUMOR MODEL SELECTION

The studies presented here investigated drug delivery to an intracranial glioma model. It would be useful to determine the effectiveness of delivery utilizing this system with different tumor types and sites of implantation.

8.4.1. TUMOR TYPE

With the ultimate goal of clinical application of this liposomal system, studies investigating its potential use to treat alternate tumor types would be beneficial. The choice of targeting agent must be considered for different tumor types since expression profiles may differ between tumors. This success of this system will be dependent on the type of tumor to be treated. For example, treatment of tumors known to exhibit highly permeable vasculature should demonstrate greater success over tumors with vessels that are less “leaky” because it is the vascular permeability, in large part, which determines the extent of extravasation. In addition, tumors expressing targets which facilitate transport of intact drug into the cell would be ideal for this delivery system. Tumor types should be selected which display expression levels of target that are much higher than

that of surrounding non-target cells. Additional studies with this liposomal delivery system will warrant the use of human cell lines inoculated into nude animals to verify its clinical applicability for the future treatment of human tumors. The studies reported here did not investigate delivery to human tumor xenografts because RES clearance of administered treatments was a major component of this experiment, and the lack of a competent immune system in the nude animals required for human tumor models would have compromised the experimental findings.

8.4.2. SITE OF IMPLANTATION

The site of implantation, particularly for glioma models, should be carefully considered. A human glioma, for example, has been shown to display high vascular permeability when grown subcutaneously in immuno-deficient mice, however, when grown in a cranial window, the same tumor demonstrated BBB characteristics [9]. Therefore, orthotopic implantation provides the closest representation of the tumor microenvironment for glioma models. Subcutaneous implantation may be appropriate for other tumor types, such as breast tumors. Subcutaneous tumors are advantageous since they offer ease of measurement with a caliper and allow monitoring of growth progression in a live animal. Alternatively, an intraperitoneal tumor model may be utilized to eliminate negative effects on delivery due to diffusional limitations. An i.p. tumor model is not the best representation for brain tumors, especially due to the lack of the BBB; however, it could be utilized for the sole purpose of removing the reductions in tumor delivery due to diffusional limitations to gain a better understanding of this cleavable PEG liposomal system under optimal conditions.

8.5. *IN VIVO* THERAPEUTIC EFFICACY

To analyze *in vivo* therapeutic efficacy, the ability to prolong survival or reduce tumor growth through the use of ‘masked’ FR-targeted liposomal DXR should be tested *in vivo*. In these studies, treatments would be administered to tumor-bearing animals, and after sufficient drug is expected to accumulate at the tumor site, cysteine would be injected to cleave PEG chains from FR-targeted, cysteine-cleavable PEG nanocarriers and promote uptake by tumor cells.

8.5.1. TREATMENT REGIMEN

Most studies investigating targeted chemotherapeutics have not demonstrated a positive impact on therapeutic efficacy unless an aggressive treatment regimen involving multiple administrations of treatment is followed. For studies utilizing targeted liposomes with cleavable PEG, a single i.v. injection of treatment may be attempted initially to determine whether the advantages of this system are enough to convey a distinct improvement in efficacy resulting in either prolonged survival times or reductions in tumor growth. If necessary, multiple treatments may be administered in an attempt to further distinguish survival advantages.

The administration of cysteine should be performed via i.v. infusion. While the length of infusion and amount of cysteine to be delivered for the studies presented here were determined through *in vitro* cleavage experiments, alternate durations of infusion and/or amounts of cysteine may be investigated for *in vivo* use since the cleavage experiments simply provide an approximation of the optimal cysteine dosage. In addition, the time point of cysteine administration needs to be further investigated. This may be done through *in vivo* cytotoxicity studies, biodistribution studies, or directly

through survival studies. *In vivo* cytotoxicity studies would identify the optimal time point for cysteine administration by determining the time point which results in the highest cytotoxicity toward tumor cells. The optimal time point for cysteine infusion, presumably, would be at the time when passive delivery of liposomes to tumor occurs. Passive tumor accumulation may be measured through biodistribution studies at various time points. The time at which maximum passive delivery to tumor occurs could then be determined and used as the time point for the administration of cysteine.

It is acknowledged that the injection of cysteine will result in a reduction in circulating levels of targeted liposomes compared to non-targeted due to the exposure of the targeting agent and RES clearance. To diminish the effects of this consequence, a booster dose of Stealth liposomal DXR equivalent to the amount of drug lost due to rapid cysteine triggered PEG detachment could be administered after cysteine administration in animals receiving FR-targeted liposomes.

8.5.2. OUTCOME MEASURES

Therapeutic efficacy could be analyzed through evaluation of survival time following treatment administration or through determination of tumor size at a predetermined time point following treatment administration. Evaluation of tumor size using an intracranial tumor model is not a straight-forward process; therefore, survival times are typically utilized for determination of therapeutic efficacy. The drawback to this method is that reductions in tumor volume due to treatment may not be realized if the tumor is aggressive and growth recovers rapidly resulting in no significant change in survival times. Using survival as the sole measure of treatment efficacy, therefore, may not be the best method to evaluate treatment efficacy.

Tumor size may be estimated through histological means, medical imaging, changes in body weight, or caliper measurements. With the exception of histological analysis, all of these approaches allow for tumor progression to be monitored over time after treatment administration. The site of tumor implantation limits the choice of size estimation method since some of these techniques are unsuitable for certain tumors.

8.6. ADDRESSING EXTRAVASATION AND DIFFUSION LIMITATIONS

Since it is acknowledged that extravasation and diffusion limitations also play a part in the *in vivo* failure of actively targeted formulations, the ideal targeted drug delivery system would include the multifunctional liposomal system presented here to prolong circulation times combined with methods to address extravasation and/or diffusion limitations. As discussed in an earlier section, “leaky” tumors may be ideal candidates for this drug delivery system due to reductions in extravasation limitations. Alternative approaches to increase delivery to tumors which may not possess highly permeable blood vessels are presented here in addition to strategies to increase diffusion of treatments within tumor.

8.6.1. METHODS TO INCREASE EXTRAVASATION TO TUMOR

Numerous techniques have been studied in an attempt to increase extravasation of nanocarriers into tumors. The use of localized hypothermia, either by direct heating [10] or by the application of radio-frequency [11], has been shown to enhance extravasation and localization of liposomes to tumors. Others have demonstrated that targeting to vascular receptors which undergo transcytosis, such as the transferrin receptor, increases delivery to tumors [12, 13]. Altering the vascular endothelial pore sizes through the use of agents such as mannitol [14], vascular endothelial growth factor [15], or tumor

necrosis factor α [16] has been shown to promote extravasation to tumor. Unfortunately, some of these agents may also affect the permeability of blood vessels within non-target tissue. Another approach to improve delivery to tumors involves “normalization” of the tumor vasculature with antiangiogenic agents prior to treatment administration. Tumor blood vessels are structurally abnormal with a haphazard pattern of connections and tortuous paths often terminating in ‘dead-ends’. The basement membrane lining these vessels may be either unusually thick or entirely absent [17, 18]. Hyperpermeability leads to lack of pressure gradients and impairs the flow of fluids leading to the heterogeneous delivery of drug to tumors. Normalizing the vasculature by pruning excess endothelial cells with judicious administration of antiangiogenic agents would alleviate some of these issues leading to more efficient delivery of drugs to tumor cells [19, 20]. Finally, extravasation to tumor has been shown to be size dependent [21, 22], therefore, future studies may investigate alterations in liposome size for this cleavable PEG system to optimize extravasation to tumor.

8.6.2. INCREASING DIFFUSION OF TARGETED AGENTS AFTER EXTRAVASATION

Since diffusional barriers within tumors prohibit uniform drug delivery, numerous methods have been studied to overcome these limitations. If the binding site barrier proves to be a major obstacle to diffusion beyond the perivascular space after PEG removal, studies may be conducted to establish the minimum number of targeting ligands required to enable specific binding and uptake by tumor cells. Liposomal formulations utilizing this number of targeting ligands may then be investigated to reduce the binding site barrier effects. Another means of promoting further diffusion within tumor is to utilize liposomes which may be destabilized. Temperature-triggered destabilization has

been shown to lead to rapid release of free drug from within nanocarriers [23, 24]. Free drug should not suffer from diffusion limitations due to its small size and will be able to penetrate more deeply into the tumor resulting in a more uniform intratumoral distribution.

8.7. ALTERNATIVE TARGETING AGENTS

As discussed in Chapter 3, many different tumor targeting agents have been reported in the literature. It would be worthwhile to investigate the use of alternative targeting ligands with this liposomal system. In addition, this system may allow for or be modified to allow for the use of antibodies which tend to demonstrate higher binding affinities for tumor targets. Antibodies presented on nanocarriers usually elicit immune responses resulting in accelerated clearance making them impractical for *in vivo* applications, however, masking with cleavable PEG may finally allow for their use in targeted formulations. Due to the large size of antibodies compared to the folate targeting ligand utilized here, longer PEG chains may be necessary to adequately mask the antibodies from the RES. To determine the optimal length, additional studies would need to be performed examining variation in PEG chain length and the resultant effects on circulation times. Selection of specific agents for future studies would ultimately be dependent on the type of tumor to be treated.

8.8. CONTRAST AGENT DELIVERY

The nanoscale delivery system presented here was designed for the delivery of chemotherapeutic agents. Another promising application of this system would involve the encapsulation and delivery of contrast agents for medical imaging of tumors. By targeting contrast agents to tumors, improvements in imaging would be achieved

allowing for earlier detection of tumors. In addition, images obtained before and after triggered removal of PEG could be compared to gain information on tumor vasculature, which tends to be difficult to resolve using traditional imaging techniques. Images obtained prior to PEG cleavage would display contrast from both the tumor and the tumor vasculature while images subsequent to cysteine administration would simply display contrast at the tumor site since the unmasking of targeting agents results in clearance of liposomes from the bloodstream. Image subtraction may then be performed to yield a clear picture of the tumor vasculature.

8.9. CONCLUSIONS

While much progress has been made using the cleavable phospholipid-PEG conjugates presented here to successfully mask and unmask targeting agents on nanocarriers, additional studies must be performed before the multifunctional system is truly optimized for *in vivo* therapeutic use. This chapter has presented some of the experiments which should yield a more thorough understanding of this system as well as some additional applications which may prove to be useful in the future.

8.10. REFERENCES

- [1] Yuan, F., Leunig, M., Huang, S. K., et al., Microvascular permeability and interstitial penetration of sterically stabilized (stealth) liposomes in a human tumor xenograft. *Cancer Res* **54**, 3352-3356. (1994).
- [2] Wu, N., Da, D., Rudoll, T., et al., Increased microvascular permeability contributes to preferential accumulation of Stealth liposomes in tumor tissue. *Cancer Res* **53**, 3765-3770 (1993).
- [3] Kostarelos, K., Emfietzoglou, D., Papakostas, A., et al., Binding and interstitial penetration of liposomes within avascular tumor spheroids. *Int J Cancer* **112**, 713-721 (2004).
- [4] Emanuel, N., Kedar, E., Bolotin, E. M., et al., Targeted delivery of doxorubicin via sterically stabilized immunoliposomes: pharmacokinetics and biodistribution in tumor-bearing mice. *Pharm Res* **13**, 861-868 (1996).
- [5] van Osdol, W., Fujimori, K. and Weinstein, J. N., An analysis of monoclonal antibody distribution in microscopic tumor nodules: consequences of a "binding site barrier". *Cancer Res* **51**, 4776-4784 (1991).
- [6] Jain, R. K. and Baxter, L. T., Mechanisms of heterogeneous distribution of monoclonal antibodies and other macromolecules in tumors: significance of elevated interstitial pressure. *Cancer Res* **48**, 7022-7032 (1988).
- [7] Baxter, L. T. and Jain, R. K., Transport of fluid and macromolecules in tumors. I. Role of interstitial pressure and convection. *Microvasc Res* **37**, 77-104 (1989).
- [8] Boucher, Y., Baxter, L. T. and Jain, R. K., Interstitial pressure gradients in tissue-isolated and subcutaneous tumors: implications for therapy. *Cancer Res* **50**, 4478-4484 (1990).
- [9] Jain, R. K., Delivery of molecular and cellular medicine to solid tumors. *Adv Drug Deliv Rev* **46**, 149-168 (2001).
- [10] Kong, G., Braun, R. D. and Dewhirst, M. W., Characterization of the effect of hyperthermia on nanoparticle extravasation from tumor vasculature. *Cancer Res* **61**, 3027-3032 (2001).

- [11] Monsky, W. L., Kruskal, J. B., Lukyanov, A. N., et al., Radio-frequency ablation increases intratumoral liposomal doxorubicin accumulation in a rat breast tumor model. *Radiology* **224**, 823-829 (2002).
- [12] Huwyler, J., Wu, D. and Pardridge, W. M., Brain drug delivery of small molecules using immunoliposomes. *Proc Natl Acad Sci U S A* **93**, 14164-14169 (1996).
- [13] Huwyler, J., Yang, J. and Pardridge, W. M., Receptor mediated delivery of daunomycin using immunoliposomes: pharmacokinetics and tissue distribution in the rat. *J Pharmacol Exp Ther* **282**, 1541-1546 (1997).
- [14] Rapoport, S. I., Osmotic opening of the blood-brain barrier: principles, mechanism, and therapeutic applications. *Cell Mol Neurobiol* **20**, 217-230 (2000).
- [15] Monsky, W. L., Fukumura, D., Gohongi, T., et al., Augmentation of transvascular transport of macromolecules and nanoparticles in tumors using vascular endothelial growth factor. *Cancer Res* **59**, 4129-4135 (1999).
- [16] Seynhaeve, A. L., Hoving, S., Schipper, D., et al., Tumor necrosis factor alpha mediates homogeneous distribution of liposomes in murine melanoma that contributes to a better tumor response. *Cancer Res* **67**, 9455-9462 (2007).
- [17] Warren, B. A., in *Tumor blood circulation*, edited by H. I. Peterson (CRC Press, Boca Raton, Fl, 1979), pp. 1-47.
- [18] Jain, R. K., Determinants of tumor blood flow: a review. *Cancer Res* **48**, 2641-2658 (1988).
- [19] Jain, R. K., Normalizing tumor vasculature with anti-angiogenic therapy: a new paradigm for combination therapy. *Nat Med* **7**, 987-989 (2001).
- [20] Jain, R. K., Normalization of tumor vasculature: an emerging concept in antiangiogenic therapy. *Science* **307**, 58-62 (2005).
- [21] Ishida, O., Maruyama, K., Sasaki, K. and Iwatsuru, M., Size-dependent extravasation and interstitial localization of polyethyleneglycol liposomes in solid tumor-bearing mice. *Int J Pharm* **190**, 49-56. (1999).

- [22] Mayer, L. D., Tai, L. C., Ko, D. S., et al., Influence of vesicle size, lipid composition, and drug-to-lipid ratio on the biological activity of liposomal doxorubicin in mice. *Cancer Res* **49**, 5922-5930. (1989).
- [23] Kono, K., Thermosensitive polymer-modified liposomes. *Adv Drug Deliv Rev* **53**, 307-319 (2001).
- [24] Yatvin, M. B., Weinstein, J. N., Dennis, W. H. and Blumenthal, R., Design of liposomes for enhanced local release of drugs by hyperthermia. *Science* **202**, 1290-1293 (1978).

APPENDIX A. IMAGING NANOPROBE FOR PREDICTION OF NANOPARTICLE CHEMOTHERAPY USING MAMMOGRAPHY

As published with E. Karathanasis, S. Suryanarayanan, S.R. Balusu, I. Sechopoulos, A. Karellas, A.V. Annapragada, and R.V. Bellamkonda, *Radiology*, (2008), accepted.

The following text, figures, and tables comprise a manuscript submitted to *Radiology* related to the passive targeting of contrast agents to tumors using liposomes where the degree of extravasation is shown to be an accurate predictor of chemotherapeutic efficacy. The manuscript is included for reference purposes in regards to the dissertational work provided in the main text.

Advances in Knowledge:

1. Imaging studies of a rat breast tumor model using a clinical digital mammography system identified a dose of a long-circulating 100nm-scale liposomal probe containing a high concentration of iodinated contrast agent (155 mg/mL) that produced undetectable signal from the blood while the accumulation of the agent in the tumor produced adequate signal for detection.

2. Imaging of the extravascular, intratumoral accumulation of the nanoprobe allowed detection and quantification of the tumor vascular permeability which varied between animals.

3. The imaging measurements of the tumor vascular permeability to the nanoprobe allowed prediction of the effect of a subsequent treatment with liposomal doxorubicin of similar composition and particle size as the nanoprobe.

Implications for Patient Care:

An a priori determination of the extent of tumor vascular permeability to nanoparticle-based therapy can facilitate personalized therapy, and spare potential non-responders from the rigors of a chemotherapy regimen.

A.1. ABSTRACT

Purpose: To prospectively predict the efficacy of a clinically used nanochemotherapeutic by detecting and measuring the intratumoral uptake of an X-ray contrast nanoprobe using digital mammography.

Materials and Methods: All animal procedures were approved by the Institutional Animal Care and Use Committee. A long-circulating 100nm-scale injectable liposomal probe was developed encapsulating 155 mg/mL iodine. Preliminary studies were performed to identify the agent dose that would result in adequate tumor enhancement without enhancement of the normal vasculature in rats. This dose was used to image a rat breast tumor (n=14) over a period of three days using a digital mammography system, and subsequently the animals were treated with liposomal doxorubicin. The predictive capability of the probe was characterized by creating ‘good’ and ‘bad’ prognosis subgroups, based on the tumor enhancement found during imaging and analyzing the tumor growth after treatment of the animals in these two subgroups.

Results: A dose of 455 mg I/kg body weight was found to produce an undetectable signal from the blood while achieving enough intratumoral accumulation of

the probe so as to produce adequate signal for detection. The ‘good prognosis’ and ‘bad prognosis’ subgroups demonstrated differential tumor growth rates ($p < 0.003$). An inverse linear relationship between the contrast enhancement rate constant during imaging and the tumor growth rate constant during treatment was found (slope = -0.576, $R^2 = 0.838$).

Conclusions: In this animal model, quantitative measure of vascular permeability enabled prediction of therapeutic responsiveness of tumors to liposomal doxorubicin treatment.

A.2. INTRODUCTION

Nanoscale therapeutic interventions are increasingly important elements of cancer therapy [1, 2]. Nanoparticles [3, 4] can be effective delivery vehicles for toxic chemotherapeutic drugs, increasing delivery efficiency to the targeted tumor while reducing off-target delivery [5]. Liposomal anthracyclines were the first nanotherapeutics to be approved for clinical use as the first line for treatment of AIDS-related Kaposi’s Sarcoma and relapsed ovarian cancer [6] and are under numerous clinical trials (128 active studies) for treatment of many types of cancer, especially breast cancer which accounts for 41 active clinical trials [7].

In addition to the cytotoxic effect of the drug at the molecular level, the success of systemically delivered nanotherapeutics for solid tumors is critically dependent on the access that these agents have to tumors via the so-called leaky vasculature of the tumor microvasculature network. This network consists of an immature blood microvessel system with hypervascularization, abnormal vascular architecture, increased leakage through the vessel wall and lack of lymphatic drainage [8, 9]. Nanoparticles preferentially accumulate in solid tumors by passive convective transport through leaky endothelium

(extravasation) that is due to pores varying from ~100 to 800 nm in size [10-12]. The phenomenon is termed the Enhanced Permeation and Retention (EPR) effect. To date however, to our knowledge, there exist no clinical tools to determine whether tumor blood vessels are permeable to nanoparticles in this fashion. For instance, the current clinical protocols for liposomal doxorubicin consist of a standard dose every 3-4 weeks [13]. No prior knowledge of tumor vessel status, especially leakiness, is taken into account for the dose scheduling. However, it is well-known that the degree of tumor vasculature leakiness differs not only among same type tumors but even spatially within the same tumor [14-16].

Our purpose was to prospectively predict the efficacy of a clinically used nanochemotherapeutic by detecting and measuring the intratumoral uptake of an X-ray contrast nanoprobe using digital mammography.

A.3. MATERIALS AND METHODS

A.3.1. FABRICATION OF THE NANOSCALE X-RAY PROBE

A highly concentrated iodine solution (650 mg I/mL) was prepared by dissolving iodixanol powder (lyophilized from Visipaque 320; GE Healthcare, Milwaukee, WI) in ultrapure water under stirring and heating at 70°C. The rest of the procedures were similar to those described previously [17] (E.K., with 7 years of experience in nanoparticle fabrication). The liposomal probe contained 72 mg/ml lipids and 155 mg/mL iodine and 100% of the iodine was encapsulated within the liposomes. The average diameter of the liposomes was 96 nm (SD=8), a size known to prevent renal clearance. An in vitro leakage experiment against isotonic phosphate buffered saline exhibited very

low leakage of the encapsulated iodine (less than 5% of the initial payload) over a period of 3 days.

A.3.2. ANIMAL MODEL

All animal procedures were approved by the Institutional Animal Care and Use Committee. Our study took place from February 15, 2007 to December 10, 2007. A 0.2 mL aliquot containing 10^6 cancer cells (13762 MAT B III cell line (American Type Culture Collection, Manassas, VA), a mammary adenocarcinoma) was subcutaneously injected into the right flank of 53 8-9 weeks old female Fisher rats (Harlan, Indianapolis, IN). Caliper measurements were used to estimate tumor size and the tumor volume was calculated as: $V_{\text{tumor}}=(d_1^2 \times d_2)/2$, where d_1 and d_2 are the minimum and maximum diameters (E.K., with 6 years of experience in animal handling and procedures).

A.3.3. X-RAY IMAGING

Imaging was performed using a clinical digital mammography system (Senographe 2000D, GE Healthcare, Milwaukee, WI) (S.S. and I.S., with 10 and 6 years experience in medical physics, respectively). To maximize the number of photons with energies above the K-edge of iodine (~ 33.2 keV) [18], imaging was performed at 49 kVp and 63 mAs, using a rhodium target and the available 25 μm thick rhodium filter with an added 0.254 mm thick copper filter [19]. The resultant x-ray spectrum was estimated using the XSPECT simulation program (Henry Ford Health Systems, Detroit, MI), which uses semi-empirical models [20].

To estimate the radiation dose to the animals during imaging, a previously validated Monte Carlo simulation for dosimetry studies [21] was modified to include a simplified version of the animal geometry (I.S.). In the simulation, the animals were

represented as a 10 cm long cylinder of water with a 4 cm diameter. To estimate the dose to the cylinder from the x-ray spectrum used in the imaging studies, the Monte Carlo simulation was performed repeatedly with monochromatic x-rays with energies from 20 keV to 49 keV in 0.5 keV steps. To achieve the necessary statistical accuracy, one million photons per energy level were simulated. The monochromatic results were combined with the x-ray spectrum obtained with the XSPECT simulation program using the method described by Boone [22].

A.3.4. PRELIMINARY DOSE STUDY

Initially, pilot imaging sessions were performed to determine the appropriate dose of the probe that would result in appropriate tumor enhancement with no detectable enhancement of the vasculature. For this task, 16 animals were injected with the probe at doses resulting in iodine concentrations in the blood ranging from 6 to 20 mg/mL with 2 mg/mL intermediate steps (2 animals per dose) and were subsequently imaged at $t=0.5, 1, 5, 10$ min and 24, 72, 120 h. From the acquired images the dose threshold above which the vasculature was not highlighted was identified by visual inspection by two reviewers in consensus (E.K., S.S.).

A.3.5. EFFICACY PREDICTION STUDY

At day 6 after tumor inoculation (tumor volume $\sim 300 \text{ mm}^3$), 14 animals were imaged before ($t=0$) and at defined time points ($t=2$ and 30 min, 24 and 72 h) after intravascular (IV) injection of the probe at the dose identified in the preliminary dose study. As a control for the imaging portion of the study, 6 animals that were also inoculated with the tumor but only injected with 0.5 mL of saline were imaged at the same time points. Immediately after the last imaging session (at day 9 after tumor

inoculation), the animals were IV injected with liposomal doxorubicin at a dose of 10 mg/kg doxorubicin. As a control for the treatment portion of the study, 15 animals that underwent the same tumor inoculation and probe injection at the same time points as the study group was not injected with liposomal doxorubicin. Liposomal doxorubicin was prepared following established methods [23]. The tumor growth of each animal was monitored every day using caliper measurements. The maximum tumor size that was allowed was 3 cm. When the tumor reached this size or the animals showed signs of pain, prostration, labored breathing, sunken eyes, any skin ulcers, emaciation or anorexia, the animals were euthanized using a CO₂ chamber. Otherwise the animals were euthanized 21 days after tumor inoculation.

A.3.6. IMAGE ANALYSIS

The sequential image acquisitions provided the dynamics of the probe's intratumoral accumulation over time. The grey levels were measured in raw data (DICOM format) using ImageJ software (NIH, Bethesda, MD). An ellipsoid region of interest (ROI) was used for the measurements surrounding the entire tumor lesion (E.K.) and the average value of the grey levels in the ROI was used as the tumor enhancement. Since mammography is not a tomographic modality, the observed tumor enhancement represents the summation of the absolute enhancement due to the contrast agent and the enhancement of overlying tissue structures. To normalize with respect to the overlying tissues, a relative enhancement was computed by subtracting the pre-contrast enhancement value ($t=0$) from the post-contrast enhancement value ($t>0$). Tumors that presented a relative enhancement lower than 50 digital units in the 24 h post-injection

image were assigned to a ‘bad prognosis’ subgroup, while tumors with a relative enhancement of 50 digital units or above were assigned to a ‘good prognosis’ subgroup.

As a control, the relative enhancement of a normal section of tissue was also measured in each image by selecting a ROI that included only soft tissue and completely excluded the tumor (E.K.). The relative enhancement of this ROI was computed using the same methodology as that described for the tumor’s relative enhancement.

For enhanced visibility of the images for publication, the images in Figures A.2, A.3, and A.4 , were histogram matched and sharpened using unsharp masking. Both processes were performed using ImageJ. This processing was performed for display of the images only; the quantitative analysis was performed with the original, unprocessed images.

A.3.7. IMMUNOHISTOCHEMISTRY AND HISTOLOGICAL EVALUATION OF EXPLANTED TUMORS

For histological examination, animals (n=2) were injected at day 6 with the probe (455 mg I/kg) tagged with rhodamine. At 48-h post-injection, the animals were euthanized and the tumors were explanted. To visualize the tumor microvasculature, the tissue slices were immunohistochemically stained for the specific endothelial antigen CD31 (BD Biosciences Pharmingen, San Diego, CA). The tissues were also stained with the nuclear stain DAPI. The staining procedures followed established methods [24]. The tumor sections were imaged at 10x on the Nikon Eclipse 80i upright microscope using a Microfire CCD camera (Optronics, Golate, CA) that interfaced with the NeuroLucida software (MicroBrightField Bioscience, Williston, VT) to obtain a montage of each section. The histological analysis was performed to verify the presence of extravascular

intratumoral accumulation of the probe and its location with respect to the tumor vasculature (E.K.).

A.3.8. DATA AND STATISTICAL ANALYSIS

To determine the significance of the grey levels variation and tumor volumes among the various animal groups at different time points, one-way ANOVA with post-hoc Bonferroni test was performed (SPSS 15, Chicago, IL). A p-value less than 0.05 was used to confirm significant differences at the 95% confidence level. The Anderson-Darling test was performed to verify that the data follow a normal distribution. The tumor enhancement profiles and tumor growth curves were fitted into an exponential function [25] using nonlinear regression (Levenberg-Marquardt algorithm) to compute the enhancement rate constant ($K^{\text{enhancement}}$) and the tumor growth rate constant ($K^{\text{tumor growth}}$), respectively (Polymath 5.0, Willimantic, CT). The area under the curve of the signal enhancement profiles was estimated using the Gauss-Legendre orthogonal polynomial approximation. The correlation between the signal enhancement and the tumor growth rate was determined using linear regression. Besides the Pearson's correlation, the correctness of the model was evaluated by examining the residuals plots and other statistical tests (SPSS 15, Chicago, IL).

A.4. RESULTS

A.4.1. IMAGING USING A CLINICAL MAMMOGRAPHY SYSTEM

Figure A.1 shows the modeled x-ray spectrum resulting from the tube voltage and filter settings and the addition of the copper filter. Under these operating conditions, the animal received an estimated radiation dose of 0.39 mGy per imaging session. In the pilot

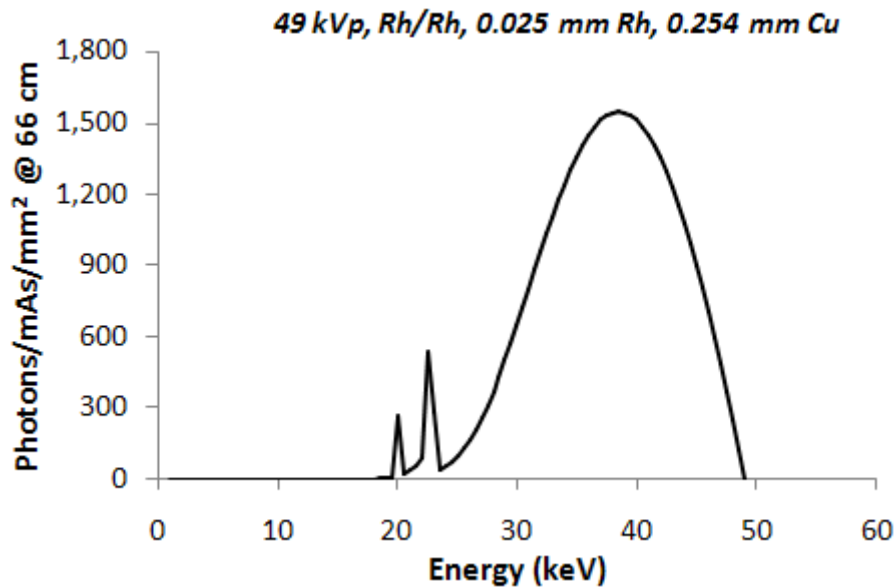


Figure A.1. Estimation of the 49 kVp rhodium/rhodium x-ray spectrum with the added 0.254 mm copper filter, according to the XSPECT simulation program.

imaging sessions where animals were injected with different doses of the probe, the threshold for visualization of blood vessels was ~ 12 mg I/mL in the blood (or a dose of 800 mg I/kg b.w.). For instance, while no vessels were visible pre-injection, they became clearly visible in normal tissue and at the tumor one minute after injection of the probe at a dose of 1344 mg I/kg body weight (bw) producing a concentration of ~ 20 mg I/mL in blood (Figure A.2). To eliminate signal from the blood vessels and probe the extravasation into the tumor, the dose selected for contrast-enhanced imaging was 455 mg I/kg bw, producing a concentration of ~ 7 mg I/mL in blood; a concentration below the threshold for detection of iodine in the blood. This allowed detection of the extravasated nanoprobe as early as 24 h post-injection, with no interference from the vascular signal (Figure A.3). In the post-injection images no blood vessels were visible in the normal tissue while enhancement of the spleen, liver and the tumor can be clearly seen. Spleen and liver enhancement is consistent with clearance of liposomes via the

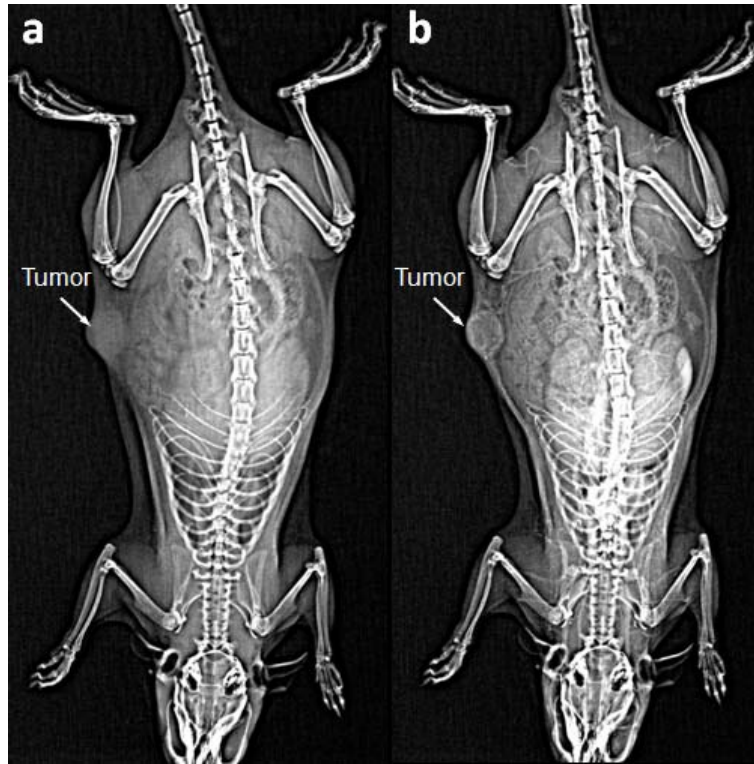


Figure A.2. Whole body images of a rat with a breast tumor in its right flank obtained using a clinical digital mammography system (a) before and (b) 1 minute after administration of a high dose (1344 mg I/kg) of the probe resulting in vasculature visualization of the tumor site and the normal tissues.

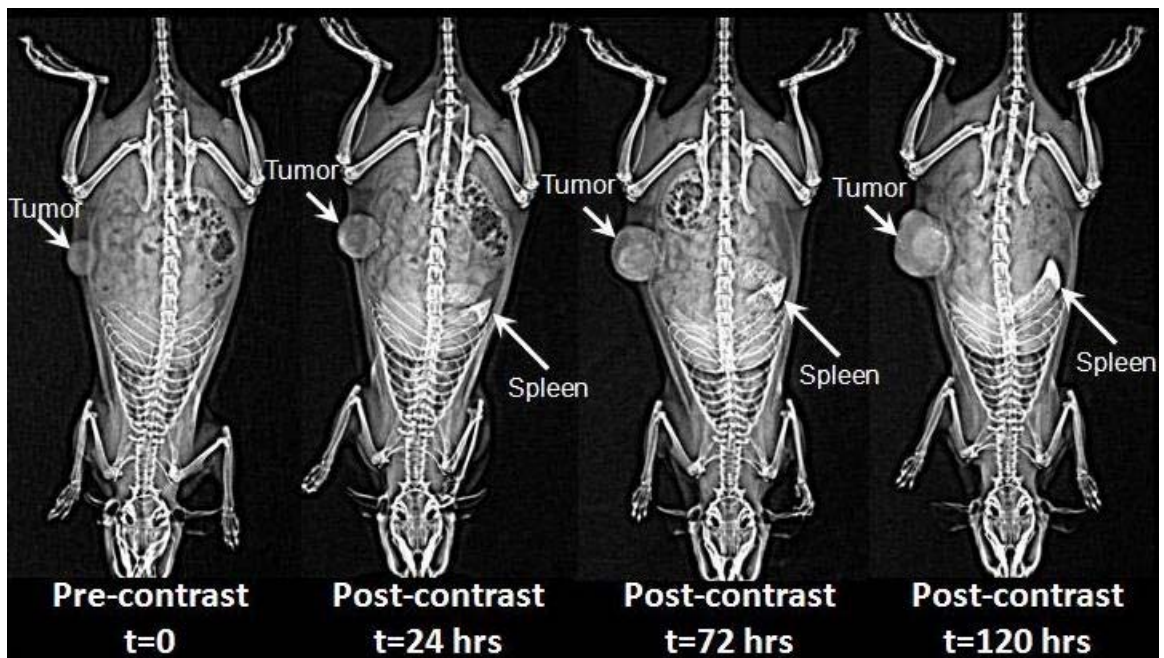


Figure A.3. X-ray images display the 5-day intratumoral fate of the probe in a rat breast tumor model before and 24, 72, and 120 h after administration of the probe at a dose of 455 mg I/kg bw. In the post-injection images no blood vessels were visible in the normal tissue while the spleen, liver and the tumor were clearly seen.

reticulo endothelial system (RES). Figure A.4 shows two examples of how tumors were enhanced by the extravasated probe. The spatial and temporal variability of this enhancement, suggesting that each tumor had different tumor vasculature leakiness, can be clearly seen.

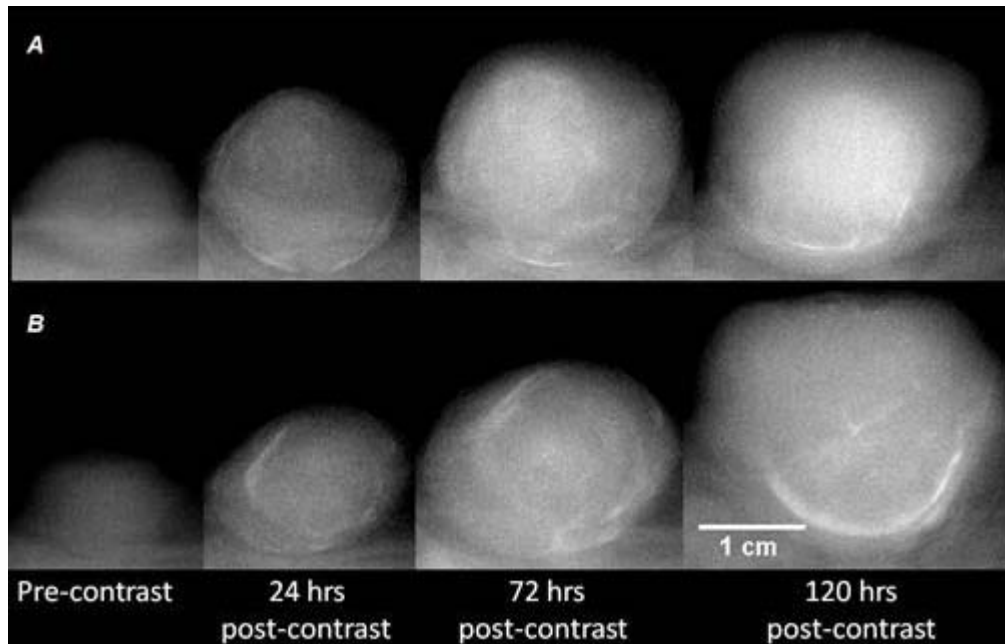


Figure A.4. X-ray images of two tumors before and after injection of the probe at a dose of 455 mg I/kg with signal enhancement in terms of grey levels of tumor A is higher than tumor B by 40 and 70 digital units at $t=72$ and 120 h post-injection respectively, a difference that is clearly visible in the images.

A.4.2. HISTOLOGICAL EVALUATION OF EXTRAVASATED PROBE TUMOR DISTRIBUTION

The tumor was characterized by a highly vascularized peripheral rim and an internal core with low vascularization. The extravasated liposomes were localized in the well-vascularized periphery of the tumor in a patchy distribution (Figure A.5).

A.4.3. TUMOR IMAGING

During the 3-day time course of imaging, some tumors exhibited a rapid and substantial increase of the enhancement whereas other tumors showed a slow and low

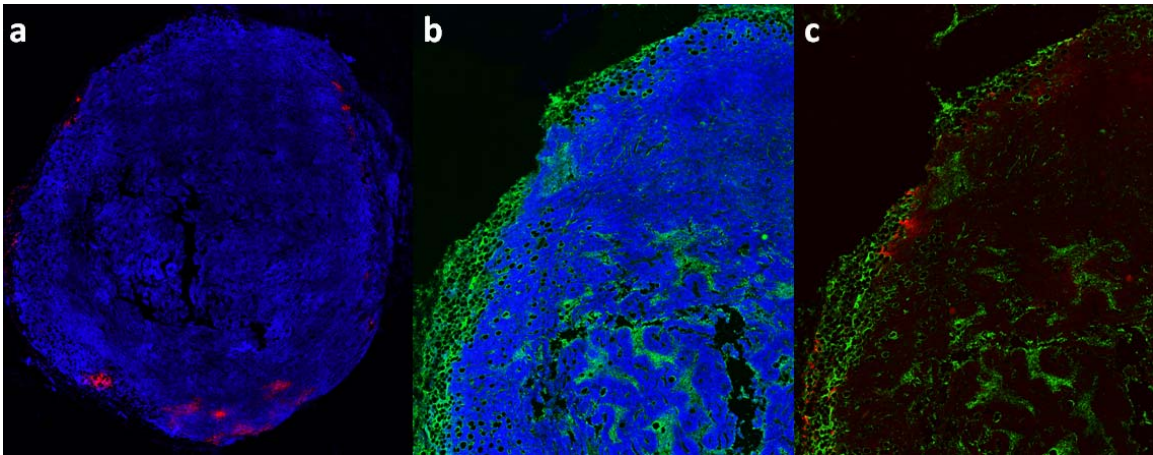


Figure A.5. Microdistribution of the probe in a breast tumor lesion 48 h after IV injection of rhodamine-tagged iodinated liposomes (appeared as red dots on fluorescent microscopy); **(a)** The liposomes localized in the periphery of the tumor showing a patchy distribution (DAPI was used as a nuclear stain; appeared as blue; 10x magnification); **(b)** Immunohistochemical microvascular staining was achieved by staining for the specific endothelial antigen CD31 (appeared as green) revealing a highly vascularized peripheral rim and a less vascularized inner core (top left quadrant of the lesion is shown; 10x magnification); **(c)** In the same histological slice, the probe was localized within the well-vascularized rim.

increase (Figure A.6). Overall, the tumor enhancement displayed a variation among the animals with the standard deviation of 55 digital units representing 50% of the mean value of 110 digital units 3 days post-injection (Figure A.6.b). While the tumor displays substantial enhancement, no enhancement was observed in normal tissues confirming that the nanoprobe levels in the blood were below the detectable threshold by mammography. In contrast, tumors within the control group of rats not given a contrast agent remained unenhanced implying that no endogenous changes of the tumor tissue contributed to the enhancement.

A.4.4. QUANTIFYING TREATMENT EFFICACY AS A FUNCTION OF PROBE

EXTRAVASATION

Liposomal doxorubicin slowed the progress of the tumor displaying statistically significant effectiveness 3 days after initiation of treatment comparing the control to treated groups (Figure A.6.c, d). The tumor response exhibited a variation reflected by

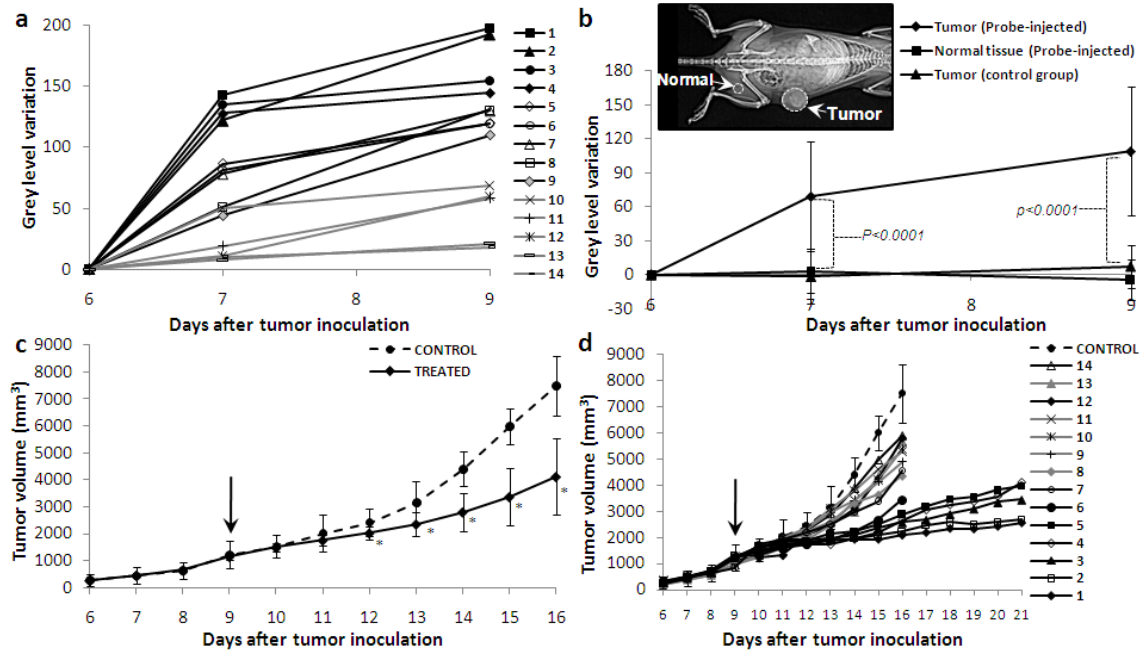


Figure A.6. (a) The 3-day pattern of the enhancement following injection of the probe (455 mg I/kg) to a group of rats (n=14) indicates a high variability of the tumors leakiness; (b) The tumor enhancement due to the probe was significantly higher than that of normal tissue (the region used for the measurement of normal tissue is indicated in the inset) which showed no substantial enhancement. Without administration of the probe, the tumor lesion of a control group of animals (n=6) showed no substantial enhancement (data presented as mean \pm standard deviation); (c) Comparison of the tumor growth rate of an untreated group (n=15) and a group treated with liposomal doxorubicin (n=14) at day 9 (arrow) showed significance difference after day 12 (* indicates $p < 0.005$; data presented as mean \pm standard deviation); (d) The tumor of each animal of the treated group responded differently to the nanotherapeutic as indicated by the variable tumor growth curves.

the tumor growth curve having standard deviations ranging from 10-35% of the mean value. Higher uptake of the probe by the tumor indicating leakier vasculature was associated with a slower tumor growth rate suggesting a better therapeutic outcome of liposomal doxorubicin. While the tumors of five animals grew marginally, the rest of the animals had to be euthanized since their tumors reached notably large sizes affecting the animals' quality of life.

We found a strong correlation between $K^{\text{tumor growth}}$ and $K^{\text{enhancement}}$ with the less leaky tumors (low $K^{\text{enhancement}}$) having faster tumor progress (high $K^{\text{tumor growth}}$) and vice

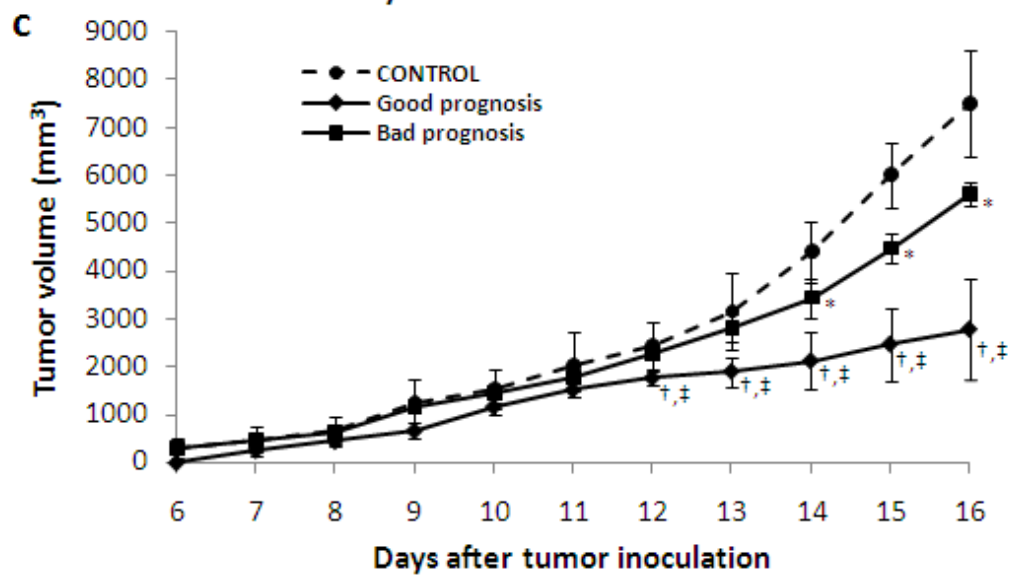
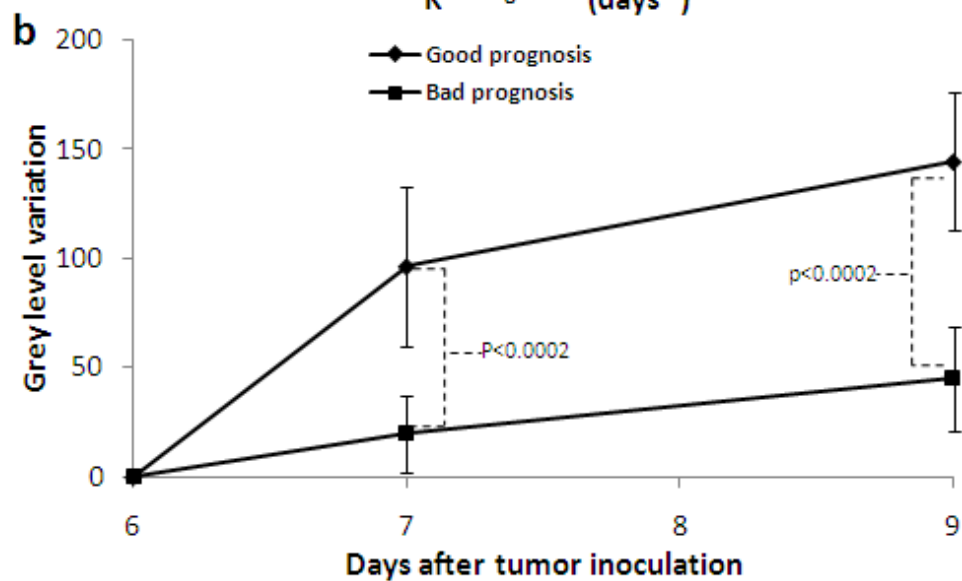
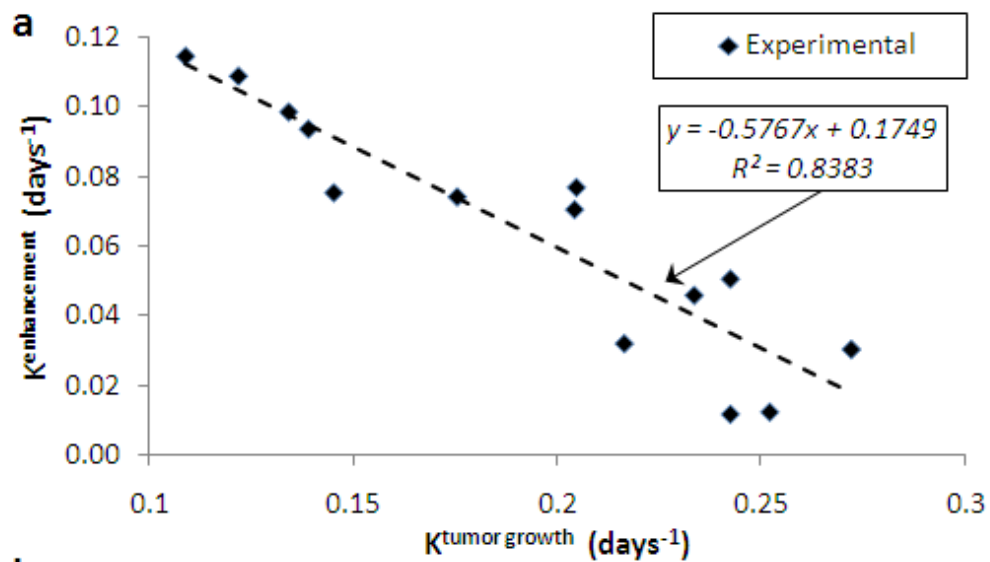


Figure A.7. (a) The correlation of the tumor growth ($K^{\text{tumor growth}}$) and the prognostic assessment ($K^{\text{enhancement}}$) was statistically significant ($R^2=0.838$; $p<0.001$). Based on the imaging-based prediction, the group of treated animals was divided into two subgroups: ‘good prognosis’ (n=9) and ‘bad prognosis’ (n=5). (b) The tumor enhancement of the two subgroups was significantly different; (c) The response of the ‘good prognosis’ subgroup to the chemotherapy was significantly better († and ‡ indicate statistical significance of $p<0.0005$ and $p<0.002$ compared to the control group and the ‘bad prognosis’ subgroup, respectively). The ‘bad prognosis’ subgroup showed decreased tumor growth when compared to the control group (* indicates $p<0.005$).

versa (Fig 7). Besides the enhancement rate constant, the predictive power of other descriptive parameters (such as the area under the enhancement curve) were examined displaying similarly good correlations ($R^2=0.856$). A better therapeutic outcome was observed in the ‘good prognosis’ subgroup from day 12 when compared to the untreated and the ‘bad prognosis’ subgroup. The ‘bad prognosis’ subgroup still benefited from the liposomal therapy; showing decreased tumor growth after day 14 when compared to the untreated control group.

A.5. DISCUSSION

The variability in tumor enhancement found in our study is consistent with a published study where the standard deviation of the accumulation of liposomal doxorubicin in a rat brain tumor was 150% of the mean value [23]. Numerous studies with liposomal doxorubicin conducted in invasive and well-vascularized xenograft mouse models have shown substantial variation in intratumoral accumulation and antitumor effects [26-29]. Besides animal studies, the biodistribution of radiolabeled liposomes was studied in cancer patients showing a considerable heterogeneity of the liposomal intratumoral deposition between different cancer types and between patients with the same tumor type [30]. However, no attempt was made in that study to correlate the efficiency of a subsequent liposomal doxorubicin treatment.

The variability of the intratumoral contrast agent uptake captured during the 3-day imaging sessions provided an accurate prognosis of the effect of liposomal doxorubicin on tumor growth rate. Since the timescale of extravasation of nanocarriers such as liposomal doxorubicin to tumors is in the order of few days, the 3-day imaging derived enhancement rate constant correlated well with the tumor growth. The variable tumor response to the treatment observed in our study is consistent with human breast tumor xenografts in nude mice treated with liposomal doxorubicin where the tumor growth curve had standard deviations of about 30% of the mean value [26]. The variability of tumor response to treatment depends on the type and the status of the tumor when treatment is initiated. Even in the aggressive model [31] used in our study where imaging probed the vascular permeability of a tumor growing at a fast rate, the prognosis and antitumor effect of liposomal doxorubicin were significantly correlated.

Consistent with earlier reports [12, 27, 32], the liposomes showed a patchy distribution concentrated on the periphery of the tumor, where there is high vascularization, associated with high levels of angiogenic and permeability factors [33, 34].

It is important to note that the goal of our study was not to induce regression, but to be able to non-invasively probe EPR status of a given tumor in a given animal and correlate this to the extent of change in tumor growth rate with administration of systemic nanotherapeutic. In this aggressive tumor model, the protocol to induce regression of tumor would require multiple injections of systemic nanotherapeutic but this would obfuscate the goals of the study which were to facilitate non-invasive probing of EPR

status of tumors so as to predict the degree of extravasation of systemically administered nanotherapeutics.

A limitation of our study is that the feasibility of the predictive capability of the nanoprobe was demonstrated on a single tumor model although human cancer as a disease is much more heterogeneous than one experimental tumor model in terms of both tumors and hosts. Further testing in more tumor models is required to fully assess the value of this approach in clinical practice.

In summary, the nanoprobe's extravasation was probed in a rat breast tumor using a clinical mammography unit, and the animals were subsequently treated with liposomal doxorubicin of similar composition and particle size as the probe (and as the clinically used liposomal chemotherapy), to evaluate the probe's predictive efficacy. Imaging allowed the identification of two subgroups prior to treatment: a 'good prognosis' and a 'bad prognosis' subgroup and indeed these demonstrated differential tumor growth rates following administration of therapeutic. **Our study demonstrates a contrast agent with the potential of predicting the therapeutic outcome of a clinically used nanoparticle-based chemotherapy.** Taking under consideration that mammography prevails as the only method of low cost mass screening of the general population for non-palpable breast cancer, the visualization of the extravascular accumulation of the probe and at the same time invisibility of the vasculature makes mammography an attractive non-invasive method for prediction of cancer therapy. Finally, though planar x-ray imaging enabled prognosis in our study by employing a clinically relevant, breast cancer imaging modality, mammography, we hypothesize such strategy would also be possible with tomographic methods (e.g. CT) yielding further insights.

A.6. PRACTICAL APPLICATIONS

Prediction of systemic liposomal chemotherapy efficacy with iodinated liposomal probes and clinical digital mammography would facilitate personalized treatment of breast cancer.

A.7. REFERENCES

- [1] Ferrari, M., Cancer nanotechnology: Opportunities and challenges. *Nat Rev Cancer* **5**, 161-171 (2005).
- [2] Service, R. F., Materials and biology. Nanotechnology takes aim at cancer. *Science* **310**, 1132-1134 (2005).
- [3] Gradishar, W. J., Tjulandin, S., Davidson, N., et al., Phase iii trial of nanoparticle albumin-bound paclitaxel compared with polyethylated castor oil-based paclitaxel in women with breast cancer. *J Clin Oncol* **23**, 7794-7803 (2005).
- [4] Lasic, D. D., Doxorubicin in sterically stabilized liposomes. *Nature* **380**, 561-562 (1996).
- [5] Yezhelyev, M. V., Gao, X., Xing, Y., et al., Emerging use of nanoparticles in diagnosis and treatment of breast cancer. *Lancet Oncol* **7**, 657-667 (2006).
- [6] Lasic, D. D. and Papahadjopoulos, D., Liposomes revisited. *Science* **267**, 1275-1276 (1995).
- [7] Yang, W., Barth, R. F., Leveille, R., et al., Evaluation of systemically administered radiolabeled epidermal growth factor as a brain tumor targeting agent. *J Neurooncol* **55**, 19-28 (2001).
- [8] Folkman, J., Angiogenesis in cancer, vascular, rheumatoid and other disease. *Nat Med* **1**, 27-31 (1995).
- [9] Carmeliet, P. and Jain, R. K., Angiogenesis in cancer and other diseases. *Nature* **407**, 249-257 (2000).
- [10] Maeda, H., Smancs and polymer-conjugated macromolecular drugs: Advantages in cancer chemotherapy. *Adv Drug Deliv Rev* **46**, 169-185 (2001).
- [11] Maeda, H., Wu, J., Sawa, T., et al., Tumor vascular permeability and the epr effect in macromolecular therapeutics: A review. *J Control Release* **65**, 271-284 (2000).

- [12] Yuan, F., Leunig, M., Huang, S. K., et al., Microvascular permeability and interstitial penetration of sterically stabilized (stealth) liposomes in a human tumor xenograft. *Cancer Res* **54**, 3352-3356. (1994).
- [13] Wolff, A. C., Liposomal anthracyclines and new treatment approaches for breast cancer. *Oncologist* **8 Suppl 2**, 25-30 (2003).
- [14] Fukumura, D. and Jain, R. K., Tumor microenvironment abnormalities: Causes, consequences, and strategies to normalize. *J Cell Biochem* **101**, 937-949 (2007).
- [15] Hobbs, S. K., Monsky, W. L., Yuan, F., et al., Regulation of transport pathways in tumor vessels: Role of tumor type and microenvironment. *Proc Natl Acad Sci U S A* **95**, 4607-4612 (1998).
- [16] Yuan, F., Chen, Y., Dellian, M., et al., Time-dependent vascular regression and permeability changes in established human tumor xenografts induced by an anti-vascular endothelial growth factor/vascular permeability factor antibody. *Proc Natl Acad Sci U S A* **93**, 14765-14770 (1996).
- [17] Mukundan, S., Ghaghada, K. B., Badea, C. T., et al., A liposomal nanoscale contrast agent for preclinical ct in mice. *AJR Am J Roentgenol* **186**, 300-307 (2006).
- [18] <http://physics.nist.gov/PhysRefData/XrayMassCoef/cover.html>, Tables of x-ray mass attenuation coefficients and mass energy-absorption coefficients 1996. Accessed December 05, 2007.
- [19] Ullman, G., Sandborg, M., Dance, D. R., et al., A search for optimal x-ray spectra in iodine contrast media mammography. *Phys Med Biol* **50**, 3143-3152 (2005).
- [20] Flynn, M. J. and Samei, E., Experimental comparison of noise and resolution for 2k and 4k storage phosphor radiography systems. *Med Phys* **26**, 1612-1623 (1999).
- [21] Sechopoulos, I., Suryanarayanan, S., Vedantham, S., et al., Computation of the glandular radiation dose in digital tomosynthesis of the breast. *Medical Physics* **34**, 221-232 (2007).
- [22] Boone, J. M., Normalized glandular dose (dgn) coefficients for arbitrary x-ray spectra in mammography: Computer-fit values of monte carlo derived data. *Medical Physics* **29**, 869-875 (2002).

- [23] McNeeley, K. M., Annapragada, A. and Bellamkonda, R. V., Decreased circulation time offsets increased efficacy of pegylated nanocarriers targeting folate receptors of glioma. *Nanotechnology* **18** 385101 (2007).
- [24] Jain, A., Kim, Y. T., McKeon, R. J. and Bellamkonda, R. V., In situ gelling hydrogels for conformal repair of spinal cord defects, and local delivery of bdnf after spinal cord injury. *Biomaterials* **27**, 497-504 (2006).
- [25] Brown, B. W., Atkinson, E. N., Bartoszynski, R., et al., Estimation of human tumor growth rate from distribution of tumor size at detection. *J Natl Cancer Inst* **72**, 31-38 (1984).
- [26] Park, J. W., Hong, K., Kirpotin, D. B., et al., Anti-her2 immunoliposomes: Enhanced efficacy attributable to targeted delivery. *Clin Cancer Res* **8**, 1172-1181 (2002).
- [27] Kirpotin, D. B., Drummond, D. C., Shao, Y., et al., Antibody targeting of long-circulating lipidic nanoparticles does not increase tumor localization but does increase internalization in animal models. *Cancer Res* **66**, 6732-6740 (2006).
- [28] Saucier, J. M., Yu, J., Gaikwad, A., et al., Determination of the optimal combination chemotherapy regimen for treatment of platinum-resistant ovarian cancer in nude mouse model. *J Oncol Pharm Pract* **13**, 39-45 (2007).
- [29] Drummond, D. C., Meyer, O., Hong, K., et al., Optimizing liposomes for delivery of chemotherapeutic agents to solid tumors. *Pharmacol Rev* **51**, 691-743 (1999).
- [30] Harrington, K. J., Mohammadtaghi, S., Uster, P. S., et al., Effective targeting of solid tumors in patients with locally advanced cancers by radiolabeled pegylated liposomes. *Clin Cancer Res* **7**, 243-254. (2001).
- [31] Parish, C. R., Freeman, C., Brown, K. J., et al., Identification of sulfated oligosaccharide-based inhibitors of tumor growth and metastasis using novel in vitro assays for angiogenesis and heparanase activity. *Cancer Res* **59**, 3433-3441 (1999).
- [32] Huang, S. K., Lee, K. D., Hong, K., et al., Microscopic localization of sterically stabilized liposomes in colon carcinoma-bearing mice. *Cancer Res* **52**, 5135-5143 (1992).

- [33] Damert, A., Machein, M., Breier, G., et al., Up-regulation of vascular endothelial growth factor expression in a rat glioma is conferred by two distinct hypoxia-driven mechanisms. *Cancer Res* **57**, 3860-3864 (1997).
- [34] Takano, S., Yoshii, Y., Kondo, S., et al., Concentration of vascular endothelial growth factor in the serum and tumor tissue of brain tumor patients. *Cancer Res* **56**, 2185-2190 (1996).

BIBLIOGRAPHY

- Agarwal, A., Jaye, D. L., Giegerman, C. M. and Bellamkonda, R. V., Rational identification of a novel peptide for targeting nanocarriers to 9l glioma. *J Biomed Mater Res A* (2008).
- Akiyama, Y., Nagasaki, Y. and Kataoka, K., Synthesis of heterotelechelic poly(ethylene glycol) derivatives having alpha-benzaldehyde and omega-pyridyl disulfide groups by ring opening polymerization of ethylene oxide using 4-(diethoxymethyl)benzyl alkoxide as a novel initiator. *Bioconjug Chem* **15**, 424-427 (2004).
- Alakhov, V., Moskaleva, E., Batrakova, E. V. and Kabanov, A. V., Hypersensitization of multidrug resistant human ovarian carcinoma cells by pluronic p85 block copolymer. *Bioconjug Chem* **7**, 209-216 (1996).
- Alexandridis, P., Athanassiou, V., Fukuda, S. and Hatton, T. A., Surface activity of poly(ethylene oxide)-block-poly(propylene oxide)-block-poly(ethylene oxide) copolymers. *Langmuir* **10**, 2604-2612 (1994).
- Ali-Boucetta, H., Al-Jamal, K. T., McCarthy, D., et al., Multiwalled carbon nanotube-doxorubicin supramolecular complexes for cancer therapeutics. *Chem Commun (Camb)* 459-461 (2008).
- Allen, C., Dos Santos, N., Gallagher, R., et al., Controlling the physical behavior and biological performance of liposome formulations through use of surface grafted poly(ethylene glycol). *Bioscience Reports* **22**, 225-250 (2002).
- Allen, T. M., Hansen, C., Martin, F., et al., Liposomes containing synthetic lipid derivatives of poly(ethylene glycol) show prolonged circulation half-lives in vivo. *Biochim Biophys Acta* **1066**, 29-36. (1991).
- Allen, T. M., Brandeis, E., Hansen, C. B., et al., A new strategy for attachment of antibodies to sterically stabilized liposomes resulting in efficient targeting to cancer cells. *Biochim Biophys Acta* **1237**, 99-108 (1995).
- Arnold, R. D., Mager, D. E., Slack, J. E. and Straubinger, R. M., Effect of repetitive administration of doxorubicin-containing liposomes on plasma pharmacokinetics and drug biodistribution in a rat brain tumor model. *Clin Cancer Res* **11**, 8856-8865 (2005).

- Banerjee, R., Tyagi, P., Li, S. and Huang, L., Anisamide-targeted stealth liposomes: A potent carrier for targeting doxorubicin to human prostate cancer cells. *Int J Cancer* **112**, 693-700 (2004).
- Barker, F. G., 2nd, Chang, S. M., Gutin, P. H., et al., Survival and functional status after resection of recurrent glioblastoma multiforme. *Neurosurgery* **42**, 709-720; discussion 720-703 (1998).
- Batrakova, E., Lee, S., Li, S., et al., Fundamental relationships between the composition of pluronic block copolymers and their hypersensitization effect in mdr cancer cells. *Pharm Res* **16**, 1373-1379 (1999).
- Batrakova, E. V., Dorodnych, T. Y., Klinskii, E. Y., et al., Anthracycline antibiotics non-covalently incorporated into the block copolymer micelles: In vivo evaluation of anti-cancer activity. *Br J Cancer* **74**, 1545-1552 (1996).
- Batrakova, E. V., Li, S., Vinogradov, S. V., et al., Mechanism of pluronic effect on p-glycoprotein efflux system in blood-brain barrier: Contributions of energy depletion and membrane fluidization. *J Pharmacol Exp Ther* **299**, 483-493 (2001).
- Baxter, L. T. and Jain, R. K., Transport of fluid and macromolecules in tumors. I. Role of interstitial pressure and convection. *Microvasc Res* **37**, 77-104 (1989).
- Beduneau, A., Hindre, F., Clavreul, A., et al., Brain targeting using novel lipid nanovectors. *J Control Release* **126**, 44-49 (2008).
- Benahmed, A., Ranger, M. and Leroux, J. C., Novel polymeric micelles based on the amphiphilic diblock copolymer poly(n-vinyl-2-pyrrolidone)-block-poly(d,l-lactide). *Pharm Res* **18**, 323-328 (2001).
- Bhagwat, S. V., Lahdenranta, J., Giordano, R., et al., Cd13/apn is activated by angiogenic signals and is essential for capillary tube formation. *Blood* **97**, 652-659 (2001).
- Bickel, U., Kang, Y. S., Yoshikawa, T. and Pardridge, W. M., In vivo demonstration of subcellular localization of anti-transferrin receptor monoclonal antibody-colloidal gold conjugate in brain capillary endothelium. *J Histochem Cytochem* **42**, 1493-1497 (1994).

- Black, K. L. and Pikul, B. K., Gliomas--past, present, and future. *Clin Neurosurg* **45**, 160-163 (1999).
- Blume, G. and Cevc, G., Liposomes for the sustained drug release in vivo. *Biochim Biophys Acta* **1029**, 91-97. (1990).
- Blume, G., Cevc, G., Crommelin, M. D., et al., Specific targeting with poly(ethylene glycol)-modified liposomes: Coupling of homing devices to the ends of the polymeric chains combines effective target binding with long circulation times. *Biochim Biophys Acta* **1149**, 180-184 (1993).
- Bolotin, E. M., Cohen, R., Bar, L. K., et al., Ammonium sulfate gradients for efficient and stable remote loading of amphipathic weak bases into liposomes and ligandoliposomes. *Journal of Liposome Research* **4**, 455-479 (1994).
- Boone, J. M., Normalized glandular dose (dgn) coefficients for arbitrary x-ray spectra in mammography: Computer-fit values of monte carlo derived data. *Medical Physics* **29**, 869-875 (2002).
- Boucher, Y., Baxter, L. T. and Jain, R. K., Interstitial pressure gradients in tissue-isolated and subcutaneous tumors: Implications for therapy. *Cancer Res* **50**, 4478-4484 (1990).
- Brem, H., Piantadosi, S., Burger, P. C., et al., Placebo-controlled trial of safety and efficacy of intraoperative controlled delivery by biodegradable polymers of chemotherapy for recurrent gliomas. The polymer-brain tumor treatment group. *Lancet* **345**, 1008-1012 (1995).
- Brignole, C., Marimpietri, D., Pagnan, G., et al., Neuroblastoma targeting by c-myc-selective antisense oligonucleotides entrapped in anti-gd2 immunoliposome: Immune cell-mediated anti-tumor activities. *Cancer Lett* **228**, 181-186 (2005).
- Broniscer, A., Past, present, and future strategies in the treatment of high-grade glioma in children. *Cancer Invest* **24**, 77-81 (2006).
- Brown, B. W., Atkinson, E. N., Bartoszynski, R., et al., Estimation of human tumor growth rate from distribution of tumor size at detection. *J Natl Cancer Inst* **72**, 31-38 (1984).

- Burger, P. C., Vogel, F. S., Green, S. B. and Strike, T. A., Glioblastoma multiforme and anaplastic astrocytoma. Pathologic criteria and prognostic implications. *Cancer* **56**, 1106-1111 (1985).
- Campbell, R. B., Fukumura, D., Brown, E. B., et al., Cationic charge determines the distribution of liposomes between the vascular and extravascular compartments of tumors. *Cancer Res* **62**, 6831-6836 (2002).
- Carmeliet, P. and Jain, R. K., Angiogenesis in cancer and other diseases. *Nature* **407**, 249-257 (2000).
- Cerletti, A., Drewe, J., Fricker, G., et al., Endocytosis and transcytosis of an immunoliposome-based brain drug delivery system. *J Drug Target* **8**, 435-446 (2000).
- Chang, J. E., Khuntia, D., Robins, H. I. and Mehta, M. P., Radiotherapy and radiosensitizers in the treatment of glioblastoma multiforme. *Clin Adv Hematol Oncol* **5**, 894-902, 907-815 (2007).
- Charrois, G. J. and Allen, T. M., Drug release rate influences the pharmacokinetics, biodistribution, therapeutic activity, and toxicity of pegylated liposomal doxorubicin formulations in murine breast cancer. *Biochim Biophys Acta* **1663**, 167-177 (2004).
- Cheng, J., Teply, B. A., Sherifi, I., et al., Formulation of functionalized plga-peg nanoparticles for in vivo targeted drug delivery. *Biomaterials* **28**, 869-876 (2007).
- Cheng, Y., Wang, J., Rao, T., et al., Pharmaceutical applications of dendrimers: Promising nanocarriers for drug delivery. *Frontiers in Bioscience* **13**, 1447-1471 (2008).
- Choi, S. W. and Mason, J. B., Folate and carcinogenesis: An integrated scheme. *J Nutr* **130**, 129-132 (2000).
- Chua, S. L., Rosenthal, M. A., Wong, S. S., et al., Phase 2 study of temozolomide and caelyx in patients with recurrent glioblastoma multiforme. *Neuro-oncol* **6**, 38-43 (2004).

- Chung, J. E., Yokoyama, M. and Okano, T., Inner core segment design for drug delivery control of thermo-responsive polymeric micelles. *J Control Release* **65**, 93-103 (2000).
- Croy, S. R. and Kwon, G. S., The effects of pluronic block copolymers on the aggregation state of nystatin. *J Control Release* **95**, 161-171 (2004).
- Curnis, F., Arrigoni, G., Sacchi, A., et al., Differential binding of drugs containing the ngr motif to cd13 isoforms in tumor vessels, epithelia, and myeloid cells. *Cancer Res* **62**, 867-874 (2002).
- Damert, A., Machein, M., Breier, G., et al., Up-regulation of vascular endothelial growth factor expression in a rat glioma is conferred by two distinct hypoxia-driven mechanisms. *Cancer Res* **57**, 3860-3864 (1997).
- Danson, S., Ferry, D., Alakhov, V., et al., Phase i dose escalation and pharmacokinetic study of pluronic polymer-bound doxorubicin (sp1049c) in patients with advanced cancer. *Br J Cancer* **90**, 2085-2091 (2004).
- Daoud, S. S. and Juliano, R. L., Reduced toxicity and enhanced antitumor effects in mice of the ionophoric drug valinomycin when incorporated in liposomes. *Cancer Res* **46**, 5518-5523 (1986).
- Dass, C. R., Drug delivery in cancer using liposomes. *Methods Mol Biol* **437**, 177-182 (2008).
- DeFrees, S., Phillips, L., Guo, L. and Zalipsky, S., Sialyl lewis liposomes as a multivalent ligand and inhibitor of e-selectin mediated cellular adhesion. *J Am Chem Soc* **118**, 6101-6104 (1996).
- Devalapally, H., Duan, Z., Seiden, M. V. and Amiji, M. M., Paclitaxel and ceramide co-administration in biodegradable polymeric nanoparticulate delivery system to overcome drug resistance in ovarian cancer. *Int J Cancer* **121**, 1830-1838 (2007).
- Di Matteo, P., Curnis, F., Longhi, R., et al., Immunogenic and structural properties of the asn-gly-arg (ngr) tumor neovasculature-homing motif. *Mol Immunol* **43**, 1509-1518 (2006).

- Dreis, S., Rothweiler, F., Michaelis, M., et al., Preparation, characterisation and maintenance of drug efficacy of doxorubicin-loaded human serum albumin (hsa) nanoparticles. *Int J Pharm* **341**, 207-214 (2007).
- Drummond, D. C., Meyer, O., Hong, K., et al., Optimizing liposomes for delivery of chemotherapeutic agents to solid tumors. *Pharmacol Rev* **51**, 691-743 (1999).
- Dufes, C., Uchegbu, I. F. and Schatzlein, A. G., Dendrimers in gene delivery. *Adv Drug Deliv Rev* **57**, 2177-2202 (2005).
- Duncan, R., Polymer conjugates for tumour targeting and intracytoplasmic delivery. The epr effect as a common gateway? *Pharm Sci Technolo Today* **11**, 441-449 (1999).
- Eavarone, D. A., Yu, X. and Bellamkonda, R. V., Targeted drug delivery to c6 glioma by transferrin-coupled liposomes. *J Biomed Mater Res* **51**, 10-14. (2000).
- Ellens, H., Bentz, J. and Szoka, F. C., Ph-induced destabilization of phosphatidylethanolamine-containing liposomes: Role of bilayer contact. *Biochemistry* **23**, 1532-1538 (1984).
- Ellens, H., Bentz, J. and Szoka, F. C., Destabilization of phosphatidylethanolamine liposomes at the hexagonal phase transition temperature. *Biochemistry* **25**, 285-294 (1986).
- Emanuel, N., Kedar, E., Bolotin, E. M., et al., Targeted delivery of doxorubicin via sterically stabilized immunoliposomes: Pharmacokinetics and biodistribution in tumor-bearing mice. *Pharm Res* **13**, 861-868 (1996).
- Ewend, M. G., Elbabaa, S. and Carey, L. A., Current treatment paradigms for the management of patients with brain metastases. *Neurosurgery* **57**, S66-77; discussion S61-64 (2005).
- Ferrari, M., Cancer nanotechnology: Opportunities and challenges. *Nat Rev Cancer* **5**, 161-171 (2005).
- Fine, H. A., Dear, K. B., Loeffler, J. S., et al., Meta-analysis of radiation therapy with and without adjuvant chemotherapy for malignant gliomas in adults. *Cancer* **71**, 2585-2597 (1993).

- Flynn, M. J. and Samei, E., Experimental comparison of noise and resolution for 2k and 4k storage phosphor radiography systems. *Med Phys* **26**, 1612-1623 (1999).
- Folkman, J., Angiogenesis in cancer, vascular, rheumatoid and other disease. *Nat Med* **1**, 27-31 (1995).
- Fukumura, D. and Jain, R. K., Tumor microenvironment abnormalities: Causes, consequences, and strategies to normalize. *J Cell Biochem* **101**, 937-949 (2007).
- Gabizon, A., Dagan, A., Goren, D., et al., Liposomes as in vivo carriers of adriamycin: Reduced cardiac uptake and preserved antitumor activity in mice. *Cancer Res* **42**, 4734-4739 (1982).
- Gabizon, A. and Papahadjopoulos, D., Liposome formulations with prolonged circulation time in blood and enhanced uptake by tumors. *Proc Natl Acad Sci U S A* **85**, 6949-6953 (1988).
- Gabizon, A., Catane, R., Uziely, B., et al., Prolonged circulation time and enhanced accumulation in malignant exudates of doxorubicin encapsulated in polyethylene-glycol coated liposomes. *Cancer Res* **54**, 987-992 (1994).
- Gabizon, A., Horowitz, A. T., Goren, D., et al., Targeting folate receptor with folate linked to extremities of poly(ethylene glycol)-grafted liposomes: In vitro studies. *Bioconj Chem* **10**, 289-298 (1999).
- Gabizon, A., Tzemach, D., Mak, L., et al., Dose dependency of pharmacokinetics and therapeutic efficacy of pegylated liposomal doxorubicin (doxil) in murine models. *J Drug Target* **10**, 539-548 (2002).
- Gabizon, A., Horowitz, A. T., Goren, D., et al., In vivo fate of folate-targeted polyethylene-glycol liposomes in tumor-bearing mice. *Clinical Cancer Research* **9**, 6551-6559 (2003).
- Gabizon, A., Shmeeda, H. and Barenholz, Y., Pharmacokinetics of pegylated liposomal doxorubicin: Review of animal and human studies. *Clin Pharmacokinet* **42**, 419-436 (2003).

- Gabizon, A., Shmeeda, H., Horowitz, A. T. and Zalipsky, S., Tumor cell targeting of liposome-entrapped drugs with phospholipid-anchored folic acid-peg conjugates. *Adv Drug Deliv Rev* **56**, 1177-1192 (2004).
- Gannon, C. J., Cherukuri, P., Yakobson, B. I., et al., Carbon nanotube-enhanced thermal destruction of cancer cells in a noninvasive radiofrequency field. *Cancer* **110**, 2654-2665 (2007).
- Ghaghada, K. B., Saul, J., Natarajan, J. V., et al., Folate targeting of drug carriers: A mathematical model. *J Control Release* **104**, 113-128 (2005).
- Giese, A. and Westphal, M., Treatment of malignant glioma: A problem beyond the margins of resection. *J Cancer Res Clin Oncol* **127**, 217-225 (2001).
- Goren, D., Horowitz, A. T., Tzemach, D., et al., Nuclear delivery of doxorubicin via folate-targeted liposomes with bypass of multidrug-resistance efflux pump. *Clin Cancer Res* **6**, 1949-1957 (2000).
- Gosk, S., Vermehren, C., Storm, G. and Moos, T., Targeting anti-transferrin receptor antibody (ox26) and ox26-conjugated liposomes to brain capillary endothelial cells using in situ perfusion. *J Cereb Blood Flow Metab* **24**, 1193-1204 (2004).
- Gradishar, W. J., Tjulandin, S., Davidson, N., et al., Phase iii trial of nanoparticle albumin-bound paclitaxel compared with polyethylated castor oil-based paclitaxel in women with breast cancer. *J Clin Oncol* **23**, 7794-7803 (2005).
- Gupta, U., Agashe, H. B., Asthana, A. and Jain, N. K., Dendrimers: Novel polymeric nanoarchitectures for solubility enhancement. *Biomacromolecules* **7**, 649-658 (2006).
- Gutman, R. L., Peacock, G. and Lu, D. R., Targeted drug delivery for brain cancer treatment. *J Control Release* **65**, 31-41. (2000).
- Harrington, K. J., Mohammadtaghi, S., Uster, P. S., et al., Effective targeting of solid tumors in patients with locally advanced cancers by radiolabeled pegylated liposomes. *Clin Cancer Res* **7**, 243-254. (2001).
- Harris, J. M., Martin, N. E. and Modi, M., Pegylation: A novel process for modifying pharmacokinetics. *Clin Pharmacokinet* **40**, 539-551 (2001).

- Hatakeyama, H., Akita, H., Maruyama, K., et al., Factors governing the in vivo tissue uptake of transferrin-coupled polyethylene glycol liposomes in vivo. *Int J Pharm* **281**, 25-33 (2004).
- Hatakeyama, H., Akita, H., Kogure, K., et al., Development of a novel systemic gene delivery system for cancer therapy with a tumor-specific cleavable peg-lipid. *Gene Ther* **14**, 68-77 (2007).
- Hatlevoll, R., Lindegaard, K. F., Hagen, S., et al., Combined modality treatment of operated astrocytomas grade 3 and 4. A prospective and randomized study of misonidazole and radiotherapy with two different radiation schedules and subsequent ccnu chemotherapy. Stage ii of a prospective multicenter trial of the scandinavian glioblastoma study group. *Cancer* **56**, 41-47 (1985).
- Hau, P., Fabel, K., Baumgart, U., et al., Pegylated liposomal doxorubicin-efficacy in patients with recurrent high-grade glioma. *Cancer* **100**, 1199-1207 (2004).
- Hess, K. R., Extent of resection as a prognostic variable in the treatment of gliomas. *J Neurooncol* **42**, 227-231 (1999).
- Hess, K. R., Broglio, K. R. and Bondy, M. L., Adult glioma incidence trends in the united states, 1977-2000. *Cancer* **101**, 2293-2299 (2004).
- Hobbs, S. K., Monsky, W. L., Yuan, F., et al., Regulation of transport pathways in tumor vessels: Role of tumor type and microenvironment. *Proc Natl Acad Sci U S A* **95**, 4607-4612 (1998).
- Hong, R. L., Huang, C. J., Tseng, Y. L., et al., Direct comparison of liposomal doxorubicin with or without polyethylene glycol coating in c-26 tumor-bearing mice: Is surface coating with polyethylene glycol beneficial? *Clin Cancer Res* **5**, 3645-3652 (1999).
- Horowitz, A. T., Barenholz, Y. and Gabizon, A. A., In vitro cytotoxicity of liposome-encapsulated doxorubicin: Dependence on liposome composition and drug release. *Biochim Biophys Acta* **1109**, 203-209 (1992).
- Huang, S. K., Lee, K. D., Hong, K., et al., Microscopic localization of sterically stabilized liposomes in colon carcinoma-bearing mice. *Cancer Res* **52**, 5135-5143 (1992).

- <http://physics.nist.gov/PhysRefData/XrayMassCoef/cover.html>, Tables of x-ray mass attenuation coefficients and mass energy-absorption coefficients 1996. Accessed December 05, 2007.
- Huwyler, J., Wu, D. and Pardridge, W. M., Brain drug delivery of small molecules using immunoliposomes. *Proc Natl Acad Sci U S A* **93**, 14164-14169 (1996).
- Huwyler, J., Yang, J. and Pardridge, W. M., Receptor mediated delivery of daunomycin using immunoliposomes: Pharmacokinetics and tissue distribution in the rat. *J Pharmacol Exp Ther* **282**, 1541-1546 (1997).
- Huwyler, J. and Pardridge, W. M., Examination of blood-brain barrier transferrin receptor by confocal fluorescent microscopy of unfixed isolated rat brain capillaries. *J Neurochem* **70**, 883-886 (1998).
- Iijima, S., Helical microtubules of graphitic carbon. *Nature (London)* **354**, 56-58 (1991).
- Iijima, S. and Ichihashi, T., Single-shell carbon nanotubes of 1-nm diameter. *Nature (London)* **363**, 603-605 (1993).
- Ikegami, S., Tadakuma, T., Yamakami, K., et al., Selective gene therapy for prostate cancer cells using liposomes conjugated with igm type monoclonal antibody against prostate-specific membrane antigen. *Hum Cell* **18**, 17-23 (2005).
- Ikegami, S., Yamakami, K., Ono, T., et al., Targeting gene therapy for prostate cancer cells by liposomes complexed with anti-prostate-specific membrane antigen monoclonal antibody. *Hum Gene Ther* **17**, 997-1005 (2006).
- Ishida, O., Maruyama, K., Sasaki, K. and Iwatsuru, M., Size-dependent extravasation and interstitial localization of polyethyleneglycol liposomes in solid tumor-bearing mice. *Int J Pharm* **190**, 49-56. (1999).
- Ishida, O., Maruyama, K., Tanahashi, H., et al., Liposomes bearing polyethyleneglycol-coupled transferrin with intracellular targeting property to the solid tumors in vivo. *Pharm Res* **18**, 1042-1048. (2001).
- Ishida, T., Iden, D. L. and Allen, T. M., A combinatorial approach to producing sterically stabilized (stealth) immunoliposomal drugs. *FEBS Lett* **460**, 129-133. (1999).

- Ishida, T., Kirchmeier, M. J., Moase, E. H., et al., Targeted delivery and triggered release of liposomal doxorubicin enhances cytotoxicity against human b lymphoma cells. *Biochim Biophys Acta* **1515**, 144-158 (2001).
- Israelachvili, J., in *Intermolecular and surface forces, second edition* (Academic Press, San Diego, CA, 1992), pp. 366-394.
- Jain, A., Kim, Y. T., McKeon, R. J. and Bellamkonda, R. V., In situ gelling hydrogels for conformal repair of spinal cord defects, and local delivery of bdnf after spinal cord injury. *Biomaterials* **27**, 497-504 (2006).
- Jain, R. K., Determinants of tumor blood flow: A review. *Cancer Res* **48**, 2641-2658 (1988).
- Jain, R. K. and Baxter, L. T., Mechanisms of heterogeneous distribution of monoclonal antibodies and other macromolecules in tumors: Significance of elevated interstitial pressure. *Cancer Res* **48**, 7022-7032 (1988).
- Jain, R. K., Delivery of molecular and cellular medicine to solid tumors. *Adv Drug Deliv Rev* **46**, 149-168 (2001).
- Jain, R. K., Normalizing tumor vasculature with anti-angiogenic therapy: A new paradigm for combination therapy. *Nat Med* **7**, 987-989 (2001).
- Jain, R. K., Normalization of tumor vasculature: An emerging concept in antiangiogenic therapy. *Science* **307**, 58-62 (2005).
- Jefferies, W. A., Brandon, M. R., Hunt, S. V., et al., Transferrin receptor on endothelium of brain capillaries. *Nature* **312**, 162-163 (1984).
- Jiang, W., Kim, B., Rutka, J. and Chan, W., Advances and challenges of nanotechnology-based drug delivery systems. *Expert Opin. Drug Deliv.* **4**, 621-633 (2007).
- Joo, S. Y. and Kim, J. S., Enhancement of gene transfer to cervical cancer cells using transferrin-conjugated liposome. *Drug Dev Ind Pharm* **28**, 1023-1031 (2002).

- Kam, N. W., O'Connell, M., Wisdom, J. A. and Dai, H., Carbon nanotubes as multifunctional biological transporters and near-infrared agents for selective cancer cell destruction. *Proc Natl Acad Sci U S A* **102**, 11600-11605 (2005).
- Kanellos, J., Pietersz, G. A. and McKenzie, I. F., Studies of methotrexate-monoclonal antibody conjugates for immunotherapy. *J Natl Cancer Inst* **75**, 319-332 (1985).
- Karathanasis, E., Ayyagari, A. L., Bhavane, R., et al., Preparation of in vivo cleavable agglomerated liposomes suitable for modulated pulmonary drug delivery. *J Control Release* **103**, 159-175 (2005).
- Karathanasis, E., Bhavane, R. and Annapragada, A. V., Triggered release of inhaled insulin from the agglomerated vesicles: Pharmacodynamic studies in rats. *J Control Release* **113**, 117-127 (2006).
- Kelemen, L. E., The role of folate receptor alpha in cancer development, progression and treatment: Cause, consequence or innocent bystander? *Int J Cancer* **119**, 243-250 (2006).
- Keles, G. E., Anderson, B. and Berger, M. S., The effect of extent of resection on time to tumor progression and survival in patients with glioblastoma multiforme of the cerebral hemisphere. *Surg Neurol* **52**, 371-379 (1999).
- Khlobystov, A. N., Britz, D. A. and Briggs, G. A., Molecules in carbon nanotubes. *Acc Chem Res* **38**, 901-909 (2005).
- Kirpotin, D., Hong, K., Mullah, N., et al., Liposomes with detachable polymer coating: Destabilization and fusion of dioleoylphosphatidylethanolamine vesicles triggered by cleavage of surface-grafted poly(ethylene glycol). *FEBS Lett* **388**, 115-118 (1996).
- Kirpotin, D., Park, J. W., Hong, K., et al., Sterically stabilized anti-her2 immunoliposomes: Design and targeting to human breast cancer cells in vitro. *Biochemistry* **36**, 66-75 (1997).
- Kirpotin, D. B., Drummond, D. C., Shao, Y., et al., Antibody targeting of long-circulating lipidic nanoparticles does not increase tumor localization but does increase internalization in animal models. *Cancer Res* **66**, 6732-6740 (2006).

- Klibanov, A. L., Maruyama, K., Torchilin, V. P. and Huang, L., Amphipathic polyethyleneglycols effectively prolong the circulation time of liposomes. *FEBS Lett* **268**, 235-237. (1990).
- Klibanov, A. L., Maruyama, K., Beckerleg, A. M., et al., Activity of amphipathic poly(ethylene glycol) 5000 to prolong the circulation time of liposomes depends on the liposome size and is unfavorable for immunoliposome binding to target. *Biochim Biophys Acta* **1062**, 142-148 (1991).
- Klibanov, A. L., in *Long circulating liposomes: Old drugs, new therapeutics*, edited by M. Woodle and G. Storm (Springer-Verlag and Landes Biosciences, 1998), pp. 269-286.
- Kojima, C., Kono, K., Maruyama, K. and Takagishi, T., Synthesis of polyamidoamine dendrimers having poly(ethylene glycol) grafts and their ability to encapsulate anticancer drugs. *Bioconjug Chem* **11**, 910-917 (2000).
- Konda, S. D., Aref, M., Wang, S., et al., Specific targeting of folate-dendrimer mri contrast agents to the high affinity folate receptor expressed in ovarian tumor xenografts. *Magma* **12**, 104-113 (2001).
- Kong, G., Braun, R. D. and Dewhirst, M. W., Characterization of the effect of hyperthermia on nanoparticle extravasation from tumor vasculature. *Cancer Res* **61**, 3027-3032 (2001).
- Kono, K., Thermosensitive polymer-modified liposomes. *Adv Drug Deliv Rev* **53**, 307-319 (2001).
- Kornblihtt, A. R., Vibe-Pedersen, K. and Baralle, F. E., Isolation and characterization of cDNA clones for human and bovine fibronectins. *Proc Natl Acad Sci U S A* **80**, 3218-3222 (1983).
- Kornblith, P. L. and Walker, M. D., *In "Advances in neuro-oncology"*. (Future Publishing Co., Mount Kisco, NY, 1988).
- Kostarelos, K., Emfietzoglou, D., Papakostas, A., et al., Binding and interstitial penetration of liposomes within avascular tumor spheroids. *Int J Cancer* **112**, 713-721 (2004).

- Kostarelos, K., Lacerda, L., Pastorin, G., et al., Functionalized carbon nanotube cellular uptake and internalization mechanism is independent of functional group and cell type. *Nature Nanotechnology* **2**, 108-113 (2007).
- Koukourakis, M. I., Koukouraki, S., Fezoulidis, I., et al., High intratumoural accumulation of stealth liposomal doxorubicin (caelyx) in glioblastomas and in metastatic brain tumours. *Br J Cancer* **83**, 1281-1286. (2000).
- Krishna, R. and Mayer, L. D., Multidrug resistance (mdr) in cancer. Mechanisms, reversal using modulators of mdr and the role of mdr modulators in influencing the pharmacokinetics of anticancer drugs. *Eur J Pharm Sci* **11**, 265-283 (2000).
- Kwon, G. S., Polymeric micelles for delivery of poorly water-soluble compounds. *Crit Rev Ther Drug Carrier Syst* **20**, 357-403 (2003).
- Laperriere, N. J., Leung, P. M., McKenzie, S., et al., Randomized study of brachytherapy in the initial management of patients with malignant astrocytoma. *Int J Radiat Oncol Biol Phys* **41**, 1005-1011 (1998).
- Lasic, D., in *Liposomes: From physics to applications*, edited by D. Lasic (Elsevier, New York, 1993), pp. 63-107.
- Lasic, D., *Liposomes: From physics to applications*. (Elsevier, Amsterdam, 1993).
- Lasic, D. and Martin, F., *Stealth liposomes*, 1st ed. (CRC Press, Boca Raton, Fla., 1995).
- Lasic, D. D., Ceh, B., Stuart, M. C., et al., Transmembrane gradient driven phase transitions within vesicles: Lessons for drug delivery. *Biochim Biophys Acta* **1239**, 145-156 (1995).
- Lasic, D. D. and Papahadjopoulos, D., Liposomes revisited. *Science* **267**, 1275-1276 (1995).
- Lasic, D. D., Doxorubicin in sterically stabilized liposomes. *Nature* **380**, 561-562 (1996).
- Leamon, C. P. and Low, P. S., Delivery of macromolecules into living cells: A method that exploits folate receptor endocytosis. *Proc Natl Acad Sci U S A* **88**, 5572-5576. (1991).

- Leamon, C. P. and Low, P. S., Cytotoxicity of momordin-folate conjugates in cultured human cells. *J Biol Chem* **267**, 24966-24971 (1992).
- Leamon, C. P., Pastan, I. and Low, P. S., Cytotoxicity of folate-pseudomonas exotoxin conjugates toward tumor cells. Contribution of translocation domain. *J Biol Chem* **268**, 24847-24854 (1993).
- Leamon, C. P., Cooper, S. R. and Hardee, G. E., Folate-liposome-mediated antisense oligodeoxynucleotide targeting to cancer cells: Evaluation in vitro and in vivo. *Bioconjug Chem* **14**, 738-747 (2003).
- Lee, C. C., Gillies, E. R., Fox, M. E., et al., A single dose of doxorubicin-functionalized bow-tie dendrimer cures mice bearing c-26 colon carcinomas. *Proc Natl Acad Sci U S A* **103**, 16649-16654 (2006).
- Lee, R. J. and Low, P. S., Delivery of liposomes into cultured kb cells via folate receptor-mediated endocytosis. *J Biol Chem* **269**, 3198-3204 (1994).
- Lee, R. J. and Low, P. S., Folate-mediated tumor cell targeting of liposome-entrapped doxorubicin in vitro. *Biochim Biophys Acta* **1233**, 134-144 (1995).
- Lestini, B. J., Sagnella, S. M., Xu, Z., et al., Surface modification of liposomes for selective cell targeting in cardiovascular drug delivery. *J Control Release* **78**, 235-247. (2002).
- Lin, R., Shi Ng, L. and Wang, C. H., In vitro study of anticancer drug doxorubicin in plga-based microparticles. *Biomaterials* **26**, 4476-4485 (2005).
- Litzinger, D. C., Buiting, A. M., van Rooijen, N. and Huang, L., Effect of liposome size on the circulation time and intraorgan distribution of amphipathic poly(ethylene glycol)-containing liposomes. *Biochim Biophys Acta* **1190**, 99-107. (1994).
- Liu, Z., Sun, X., Nakayama-Ratchford, N. and Dai, H., Supramolecular chemistry on water-soluble carbon nanotubes for drug loading and delivery. *ACS Nano* **1**, 50-56 (2007).
- Lockman, P. R., Mumper, R. J., Khan, M. A. and Allen, D. D., Nanoparticle technology for drug delivery across the blood-brain barrier. *Drug Dev Ind Pharm* **28**, 1-13 (2002).

- Lopes de Menezes, D. E., Kirchmeier, M. J., Gange, J.-F., et al., Cellular trafficking and cytotoxicity of anti-cd19-targeted liposomal doxorubicin in b lymphoma cells. *Journal of Liposome Research* **9**, 199-228 (1999).
- Low, P. S. and Antony, A. C., Folate receptor-targeted drugs for cancer and inflammatory diseases. *Adv Drug Deliv Rev* **56**, 1055-1058 (2004).
- Luppi, B., Orienti, I., Bigucci, F., et al., Poly(vinylalcohol-co-vinylolate) for the preparation of micelles enhancing retinyl palmitate transcutaneous permeation. *Drug Deliv* **9**, 147-152 (2002).
- Maeda, H., Wu, J., Sawa, T., et al., Tumor vascular permeability and the epr effect in macromolecular therapeutics: A review. *J Control Release* **65**, 271-284 (2000).
- Maeda, H., Smancs and polymer-conjugated macromolecular drugs: Advantages in cancer chemotherapy. *Adv Drug Deliv Rev* **46**, 169-185 (2001).
- Maeda, H., The enhanced permeability and retention (epr) effect in tumor vasculature: The key role of tumor-selective macromolecular drug targeting. *Adv Enzyme Regul* **41**, 189-207 (2001).
- Maeda, T. and Fujimoto, K., A reduction-triggered delivery by a liposomal carrier possessing membrane-permeable ligands and a detachable coating. *Colloids Surf B Biointerfaces* **49**, 15-21 (2006).
- Mamot, C., Drummond, D. C., Greiser, U., et al., Epidermal growth factor receptor (egfr)-targeted immunoliposomes mediate specific and efficient drug delivery to egfr- and egfrviii-overexpressing tumor cells. *Cancer Res* **63**, 3154-3161 (2003).
- Maruyama, K., Kennel, S. and Huang, L., Lipid composition is important for highly efficient target binding and retention of immunoliposomes. *Proc Natl Acad Sci U S A* **87**, 5744-5748 (1990).
- Maruyama, K., Yuda, T., Okamoto, A., et al., Effect of molecular weight in amphipathic polyethyleneglycol on prolonging the circulation time of large unilamellar liposomes. *Chem Pharm Bull (Tokyo)* **39**, 1620-1622. (1991).

- Maruyama, K., Takizawa, T., Yuda, T., et al., Targetability of novel immunoliposomes modified with amphipathic poly(ethylene glycol)s conjugated at their distal terminals to monoclonal antibodies. *Biochim Biophys Acta* **1234**, 74-80. (1995).
- Maruyama, K., Takahashi, N., Tagawa, T., et al., Immunoliposomes bearing polyethyleneglycol-coupled fab' fragment show prolonged circulation time and high extravasation into targeted solid tumors in vivo. *FEBS Lett* **413**, 177-180 (1997).
- Maruyama, K., Ishida, O., Takizawa, T. and Moribe, K., Possibility of active targeting to tumor tissues with liposomes. *Adv Drug Deliv Rev* **40**, 89-102. (1999).
- Mayer, L. D., Tai, L. C., Ko, D. S., et al., Influence of vesicle size, lipid composition, and drug-to-lipid ratio on the biological activity of liposomal doxorubicin in mice. *Cancer Res* **49**, 5922-5930. (1989).
- McDermott, M. W. and Sneed, P. K., Radiosurgery in metastatic brain cancer. *Neurosurgery* **57**, S45-53; discussion S41-44 (2005).
- McNeeley, K., Annapragada, A. and Bellamkonda, R., Decreased circulation time offsets increased efficacy of pegylated nanocarriers targeting folate receptors of glioma. *Nanotechnology* **18**, 1-11 (2007).
- McNeeley, K. M., Annapragada, A. and Bellamkonda, R. V., Decreased circulation time offsets increased efficacy of pegylated nanocarriers targeting folate receptors of glioma. *Nanotechnology* **18** 385101 (2007).
- Medina, O. P., Kairemo, K., Valtanen, H., et al., Radionuclide imaging of tumor xenografts in mice using a gelatinase-targeting peptide. *Anticancer Res* **25**, 33-42 (2005).
- Mehta, M. P., The physical, biologic, and clinical basis of radiosurgery. *Curr Probl Cancer* **19**, 265-329 (1995).
- Mehta, M. P. and Khuntia, D., Current strategies in whole-brain radiation therapy for brain metastases. *Neurosurgery* **57**, S33-44; discussion S31-34 (2005).
- Mercadal, M., Domingo, J. C., Petriz, J., et al., A novel strategy affords high-yield coupling of antibody to extremities of liposomal surface-grafted peg chains. *Biochim Biophys Acta* **1418**, 232-238 (1999).

- Mercadal, M., Domingo, J. C., Petriz, J., et al., Preparation of immunoliposomes bearing poly(ethylene glycol)-coupled monoclonal antibody linked via a cleavable disulfide bond for ex vivo applications. *Biochim Biophys Acta* **1509**, 299-310 (2000).
- Minko, T., Pakunlu, R., Wang, Y., et al., New generation of liposomal drugs for cancer. *Anticancer Agents Med Chem* **6**, 537-552 (2006).
- Moghimi, S. and Szebeni, J., Stealth liposomes and long circulating nanoparticles: Critical issues in pharmacokinetics, opsonization and protein-binding properties. *Progress in Lipid Research* **42**, 463-478 (2003).
- Mohan, D. S., Suh, J. H., Phan, J. L., et al., Outcome in elderly patients undergoing definitive surgery and radiation therapy for supratentorial glioblastoma multiforme at a tertiary care institution. *Int J Radiat Oncol Biol Phys* **42**, 981-987 (1998).
- Monsky, W. L., Fukumura, D., Gohongi, T., et al., Augmentation of transvascular transport of macromolecules and nanoparticles in tumors using vascular endothelial growth factor. *Cancer Res* **59**, 4129-4135 (1999).
- Monsky, W. L., Kruskal, J. B., Lukyanov, A. N., et al., Radio-frequency ablation increases intratumoral liposomal doxorubicin accumulation in a rat breast tumor model. *Radiology* **224**, 823-829 (2002).
- Moos, T. and Morgan, E. H., Transferrin and transferrin receptor function in brain barrier systems. *Cell Mol Neurobiol* **20**, 77-95 (2000).
- Moreira, J. N., Ishida, T., Gaspar, R. and Allen, T. M., Use of the post-insertion technique to insert peptide ligands into pre- formed stealth liposomes with retention of binding activity and cytotoxicity. *Pharm Res* **19**, 265-269. (2002).
- Mori, A., Klivanov, A. L., Torchilin, V. P. and Huang, L., Influence of the steric barrier activity of amphipathic poly(ethyleneglycol) and ganglioside gm1 on the circulation time of liposomes and on the target binding of immunoliposomes in vivo. *FEBS Lett* **284**, 263-266. (1991).
- Mukundan, S., Ghaghada, K. B., Badea, C. T., et al., A liposomal nanoscale contrast agent for preclinical ct in mice. *AJR Am J Roentgenol* **186**, 300-307 (2006).

- Nakanishi, T., Fukushima, S., Okamoto, K., et al., Development of the polymer micelle carrier system for doxorubicin. *J Control Release* **74**, 295-302 (2001).
- New, R. R. C., *Liposomes: A practical approach*. (Oxford University Press, Oxford, UK, 1990).
- Ni, S., Stephenson, S. M. and Lee, R. J., Folate receptor targeted delivery of liposomal daunorubicin into tumor cells. *Anticancer Res* **22**, 2131-2135. (2002).
- Nwokedi, E. C., DiBiase, S. J., Jabbour, S., et al., Gamma knife stereotactic radiosurgery for patients with glioblastoma multiforme. *Neurosurgery* **50**, 41-46; discussion 46-47 (2002).
- O'Donnell, J. L., Joyce, M. R., Shannon, A. M., et al., Oncological implications of hypoxia inducible factor-1alpha (hif-1alpha) expression. *Cancer Treat Rev* **32**, 407-416 (2006).
- Order, S. E., Hellman, S., Von Essen, C. F. and Kligerman, M. M., Improvement in quality of survival following whole-brain irradiation for brain metastasis. *Radiology* **91**, 149-153 (1968).
- Pan, X. Q., Zheng, X., Shi, G., et al., Strategy for the treatment of acute myelogenous leukemia based on folate receptor beta-targeted liposomal doxorubicin combined with receptor induction using all-trans retinoic acid. *Blood* **100**, 594-602. (2002).
- Pan, X. Q., Hang, H. and Lee, R. J., Antitumor activity of folate receptor-targeted liposomal doxorubicin in a kb oral carcinoma murine xenograft model. *Pharmaceutical research* **20**, 417-422 (2003).
- Pan, X. Q. and Lee, R. J., In vivo antitumor activity of folate receptor-targeted liposomal daunorubicin in a murine leukemia model. *Anticancer Res* **25**, 343-346 (2005).
- Pantarotto, D., Singh, R., McCarthy, D., et al., Functionalized carbon nanotubes for plasmid DNA gene delivery. *Angew Chem Int Ed Engl* **43**, 5242-5246 (2004).
- Parish, C. R., Freeman, C., Brown, K. J., et al., Identification of sulfated oligosaccharide-based inhibitors of tumor growth and metastasis using novel in vitro assays for angiogenesis and heparanase activity. *Cancer Res* **59**, 3433-3441 (1999).

- Park, J. W., Hong, K., Carter, P., et al., Development of anti-p185her2 immunoliposomes for cancer therapy. *Proc Natl Acad Sci U S A* **92**, 1327-1331. (1995).
- Park, J. W., Hong, K., Kirpotin, D. B., et al., Anti-her2 immunoliposomes for targeted therapy of human tumors. *Cancer Lett* **118**, 153-160 (1997).
- Park, J. W., Hong, K., Kirpotin, D. B., et al., Anti-her2 immunoliposomes: Enhanced efficacy attributable to targeted delivery. *Clin Cancer Res* **8**, 1172-1181 (2002).
- Parveen, S. and Sahoo, S. K., Polymeric nanoparticles for cancer therapy. *J Drug Target* **16**, 108-123 (2008).
- Pasqualini, R., Koivunen, E., Kain, R., et al., Aminopeptidase n is a receptor for tumor-homing peptides and a target for inhibiting angiogenesis. *Cancer Res* **60**, 722-727 (2000).
- Pastorin, G., Wu, W., Wieckowski, S., et al., Double functionalization of carbon nanotubes for multimodal drug delivery. *Chem Commun (Camb)* 1182-1184 (2006).
- Pastorino, F., Brignole, C., Marimpietri, D., et al., Vascular damage and anti-angiogenic effects of tumor vessel-targeted liposomal chemotherapy. *Cancer Res.* **63**, 7400-7409 (2003).
- Pastorino, F., Brignole, C., Di Paolo, D., et al., Targeting liposomal chemotherapy via both tumor cell-specific and tumor vasculature-specific ligands potentiates therapeutic efficacy. *Cancer Res* **66**, 10073-10082 (2006).
- Patchell, R. A., Tibbs, P. A., Walsh, J. W., et al., A randomized trial of surgery in the treatment of single metastases to the brain. *N Engl J Med* **322**, 494-500 (1990).
- Patel, H., Tuzel, N. and Ryman, B., Inhibitory effect of cholesterol on the uptake of liposomes by liver and spleen. *Biochim Biophys Acta* **761**, 142-151 (1983).
- Peer, D. and Margalit, R., Tumor-targeted hyaluronan nanoliposomes increase the antitumor activity of liposomal doxorubicin in syngeneic and human xenograft mouse tumor models. *Neoplasia* **6**, 343-353 (2004).

- Prato, M., Kostarelos, K. and Bianco, A., Functionalized carbon nanotubes in drug design and discovery. *Acc Chem Res* **41**, 60-68 (2008).
- Pruitt, J. D. and Pitt, W. G., Sequestration and ultrasound-induced release of doxorubicin from stabilized pluronic p105 micelles. *Drug Deliv* **9**, 253-258 (2002).
- Qi, L., Xu, Z. and Chen, M., In vitro and in vivo suppression of hepatocellular carcinoma growth by chitosan nanoparticles. *Eur J Cancer* **43**, 184-193 (2007).
- Qing, Y., Shuo, W., Zhihua, W., et al., The in vitro antitumor effect and in vivo tumor-specificity distribution of human-mouse chimeric antibody against transferrin receptor. *Cancer Immunol Immunother* **55**, 1111-1121 (2006).
- Quintana, A., Raczka, E., Pehler, L., et al., Design and function of a dendrimer-based therapeutic nanodevice targeted to tumor cells through the folate receptor. *Pharm Res* **19**, 1310-1316 (2002).
- Rapoport, S. I., Osmotic opening of the blood-brain barrier: Principles, mechanism, and therapeutic applications. *Cell Mol Neurobiol* **20**, 217-230 (2000).
- Ratcheson, R. A. and Ommaya, A. K., Experience with the subcutaneous cerebrospinal-fluid reservoir. Preliminary report of 60 cases. *N Engl J Med* **279**, 1025-1031 (1968).
- Rautio, J. and Chikhale, P. J., Drug delivery systems for brain tumor therapy. *Current pharmaceutical design* **10**, 1341-1353 (2004).
- Reddy, J. A., Abburi, C., Hofland, H., et al., Folate-targeted, cationic liposome-mediated gene transfer into disseminated peritoneal tumors. *Gene Ther* **9**, 1542-1550 (2002).
- Ries, L., Melbert, D., Krapcho, M., et al. (eds.) *Seer cancer statistics review, 1975-2005*, National Cancer Institute. Bethesda, MD, http://seer.cancer.gov/csr/1975_2005/, based on November 2007 SEER data submission, posted to the SEER web site, 2008. Accessed June 1, 2008.
- Saiki, I., Fujii, H., Yoneda, J., et al., Role of aminopeptidase n (cd13) in tumor-cell invasion and extracellular matrix degradation. *Int J Cancer* **54**, 137-143 (1993).

- Saito, G., Swanson, J. A. and Lee, K. D., Drug delivery strategy utilizing conjugation via reversible disulfide linkages: Role and site of cellular reducing activities. *Adv Drug Deliv Rev* **55**, 199-215 (2003).
- Saito, R., Krauze, M. T., Noble, C. O., et al., Convection-enhanced delivery of ls-tpt enables an effective, continuous, low-dose chemotherapy against malignant glioma xenograft model. *Neuro Oncol* **8**, 205-214 (2006).
- Sapra, P. and Allen, T. M., Improved outcome when b-cell lymphoma is treated with combinations of immunoliposomal anticancer drugs targeted to both the cd19 and cd20 epitopes. *Clin Cancer Res* **10**, 2530-2537 (2004).
- Sapra, P., Tyagi, P. and Allen, T., Ligand-targeted liposomes for cancer treatment. *Current Drug Delivery* **2**, 369-381 (2005).
- Saucier, J. M., Yu, J., Gaikwad, A., et al., Determination of the optimal combination chemotherapy regimen for treatment of platinum-resistant ovarian cancer in nude mouse model. *J Oncol Pharm Pract* **13**, 39-45 (2007).
- Saul, J. M., Annapragada, A., Natarajan, J. V. and Bellamkonda, R. V., Controlled targeting of liposomal doxorubicin via the folate receptor in vitro. *J Control Release* **92**, 49-67 (2003).
- Saul, J. M., Annapragada, A. V. and Bellamkonda, R. V., A dual-ligand approach for enhancing targeting selectivity of therapeutic nanocarriers. *J Control Release* **114**, 277-287 (2006).
- Schiffelers, R. M., Bakker-Woudenberg, I. A. and Storm, G., Localization of sterically stabilized liposomes in experimental rat klebsiella pneumoniae pneumonia: Dependence on circulation kinetics and presence of poly(ethylene)glycol coating. *Biochim Biophys Acta* **1468**, 253-261 (2000).
- Schiffelers, R. M., Koning, G. A., ten Hagen, T. L., et al., Anti-tumor efficacy of tumor vasculature-targeted liposomal doxorubicin. *J Control Release* **91**, 115-122 (2003).
- Sechopoulos, I., Suryanarayanan, S., Vedantham, S., et al., Computation of the glandular radiation dose in digital tomosynthesis of the breast. *Medical Physics* **34**, 221-232 (2007).

- Selker, R. G., Shapiro, W. R., Burger, P., et al., The brain tumor cooperative group nih trial 87-01: A randomized comparison of surgery, external radiotherapy, and carmustine versus surgery, interstitial radiotherapy boost, external radiation therapy, and carmustine. *Neurosurgery* **51**, 343-355; discussion 355-347 (2002).
- Service, R. F., Materials and biology. Nanotechnology takes aim at cancer. *Science* **310**, 1132-1134 (2005).
- Seymour, L. W., Duncan, R., Strohalm, J. and Kopecek, J., Effect of molecular weight (mw) of n-(2-hydroxypropyl)methacrylamide copolymers on body distribution and rate of excretion after subcutaneous, intraperitoneal, and intravenous administration to rats. *J Biomed Mater Res* **21**, 1341-1358 (1987).
- Seynhaeve, A. L., Hoving, S., Schipper, D., et al., Tumor necrosis factor alpha mediates homogeneous distribution of liposomes in murine melanoma that contributes to a better tumor response. *Cancer Res* **67**, 9455-9462 (2007).
- Shao, N., Lu, S., Wickstrom, E. and Panchapakesan, B., Integrated molecular targeting of igf1r and her2 surface receptors and destruction of breast cancer cells using single wall carbon nanotubes. *Nanotechnology* **18**, 315101 (2007).
- Sharma, U. S., Sharma, A., Chau, R. I. and Straubinger, R. M., Liposome-mediated therapy of intracranial brain tumors in a rat model. *Pharm Res* **14**, 992-998. (1997).
- Shenoy, D. B. and Amiji, M. M., Poly(ethylene oxide)-modified poly(epsilon-caprolactone) nanoparticles for targeted delivery of tamoxifen in breast cancer. *Int J Pharm* **293**, 261-270 (2005).
- Shi, N. and Pardridge, W. M., Noninvasive gene targeting to the brain. *Proc Natl Acad Sci U S A* **97**, 7567-7572. (2000).
- Shmeeda, H., Mak, L., Tzemach, D., et al., Intracellular uptake and intracavitary targeting of folate-conjugated liposomes in a mouse lymphoma model with up-regulated folate receptors. *Mol Cancer Ther* **5**, 818-824 (2006).
- Siegel, T., Horowitz, A. and Gabizon, A., Doxorubicin encapsulated in sterically stabilized liposomes for the treatment of a brain tumor model: Biodistribution and therapeutic efficacy. *J Neurosurg* **83**, 1029-1037 (1995).

- Sills, A. K., Current treatment approaches to surgery for brain metastases. *Neurosurgery* **57**, S24-32; discussion S21-24 (2005).
- Simoes, S., Moreira, J., Fonseca, C., et al., On the formulation of pH-sensitive liposomes with long circulation times. *Adv Drug Deliv Rev* **56**, 947-965 (2004).
- Simon, S. A. and McIntosh, T. J., Depth of water penetration into lipid bilayers. *Methods Enzymol* **127**, 511-521 (1986).
- Siwak, D. R., Tari, A. M. and Lopez-Berestein, G., The potential of drug-carrying immunoliposomes as anticancer agents. Commentary re: J. W. Park et al., anti-her2 immunoliposomes: Enhanced efficacy due to targeted delivery. *Clin. Cancer res.*, 8: 1172-1181, 2002. *Clin Cancer Res* **8**, 955-956 (2002).
- Small, D. M., *Handbook of lipid research: The physical chemistry of lipids, from alkanes to phospholipids*, Vol. 4. (Plenum Press, New York, NY, 1986).
- Steiniger, S., Kreuter, J., Khalansky, A., et al., Chemotherapy of glioblastoma in rats using doxorubicin-loaded nanoparticles. *International Journal of Cancer* **109**, 759-767 (2004).
- Stephenson, S., Yang, W., Stevens, P., et al., Folate receptor-targeted liposomes as possible delivery vehicles for boron neutron capture therapy. *Anticancer Res* **23**, 3341-3346 (2003).
- Stubbs, J. B., Frankel, R. H., Schultz, K., et al., Preclinical evaluation of a novel device for delivering brachytherapy to the margins of resected brain tumor cavities. *J Neurosurg* **96**, 335-343 (2002).
- Sudimack, J. and Lee, R. J., Targeted drug delivery via the folate receptor. *Adv Drug Deliv Rev* **41**, 147-162 (2000).
- Sudimack, J. J., Adams, D., Rotaru, J., et al., Folate receptor-mediated liposomal delivery of a lipophilic boron agent to tumor cells in vitro for neutron capture therapy. *Pharm Res* **19**, 1502-1508 (2002).
- Sutton, D., Nasongkla, N., Blanco, E. and Gao, J., Functionalized micellar systems for cancer targeted drug delivery. *Pharm Res* **24**, 1029-1046 (2007).

- Takano, S., Yoshii, Y., Kondo, S., et al., Concentration of vascular endothelial growth factor in the serum and tumor tissue of brain tumor patients. *Cancer Res* **56**, 2185-2190 (1996).
- Takeuchi, H., Kojima, H., Yamamoto, H. and Kawashima, Y., Passive targeting of doxorubicin with polymer coated liposomes in tumor bearing rats. *Biol Pharm Bull* **24**, 795-799 (2001).
- Tasis, D., Tagmatarchis, N., Bianco, A. and Prato, M., Chemistry of carbon nanotubes. *Chem Rev* **106**, 1105-1136 (2006).
- Tatter, S. B., Shaw, E. G., Rosenblum, M. L., et al., An inflatable balloon catheter and liquid ¹²⁵I radiation source (gliasite radiation therapy system) for treatment of recurrent malignant glioma: Multicenter safety and feasibility trial. *J Neurosurg* **99**, 297-303 (2003).
- Teng, Y., Morrison, M. E., Munk, P., et al., Release kinetics studies of aromatic molecules into water from block polymer micelles *Macromolecules* **31**, 3578-3587 (1998).
- Terada, T., Iwai, M., Kawakami, S., et al., Novel peg-matrix metalloproteinase-2 cleavable peptide-lipid containing galactosylated liposomes for hepatocellular carcinoma-selective targeting. *J Control Release* **111**, 333-342 (2006).
- Torchilin, V. P., *Self-assembling complexes for gene delivery: From laboratory to clinical trial*. (Wiley, New York, 1998).
- Torchilin, V. P., Drug targeting. *Eur J Pharm Sci* **11 Suppl 2**, S81-91. (2000).
- Torchilin, V. P. and Weissig, V., *Liposomes*. (Oxford University Press, New York, 2003).
- Torchilin, V. P., Micellar nanocarriers: Pharmaceutical perspectives. *Pharm Res* **24**, 1-16 (2007).
- Trojanowski, T., Peszynski, J., Turowski, K., et al., Postoperative radiotherapy and radiotherapy combined with ccnu chemotherapy for treatment of brain gliomas. *J Neurooncol* **6**, 285-291 (1988).

- Turk, M. J., Waters, D. J. and Low, P. S., Folate-conjugated liposomes preferentially target macrophages associated with ovarian carcinoma. *Cancer Lett* **213**, 165-172 (2004).
- Ulbrich, K., Etrych, T., Chytil, P., et al., Antibody-targeted polymer-doxorubicin conjugates with ph-controlled activation. *J Drug Target* **12**, 477-489 (2004).
- Ullman, G., Sandborg, M., Dance, D. R., et al., A search for optimal x-ray spectra in iodine contrast media mammography. *Phys Med Biol* **50**, 3143-3152 (2005).
- Valtonen, S., Timonen, U., Toivanen, P., et al., Interstitial chemotherapy with carmustine-loaded polymers for high-grade gliomas: A randomized double-blind study. *Neurosurgery* **41**, 44-48; discussion 48-49 (1997).
- van Osdol, W., Fujimori, K. and Weinstein, J. N., An analysis of monoclonal antibody distribution in microscopic tumor nodules: Consequences of a "Binding site barrier". *Cancer Res* **51**, 4776-4784 (1991).
- Vecht, C. J., Haaxma-Reiche, H., Noordijk, E. M., et al., Treatment of single brain metastasis: Radiotherapy alone or combined with neurosurgery? *Ann Neurol* **33**, 583-590 (1993).
- Walker, M. D., Alexander, E., Jr., Hunt, W. E., et al., Evaluation of bcnu and/or radiotherapy in the treatment of anaplastic gliomas. A cooperative clinical trial. *J Neurosurg* **49**, 333-343 (1978).
- Walker, M. D., Green, S. B., Byar, D. P., et al., Randomized comparisons of radiotherapy and nitrosoureas for the treatment of malignant glioma after surgery. *N Engl J Med* **303**, 1323-1329 (1980).
- Wang, P. P., Frazier, J. and Brem, H., Local drug delivery to the brain. *Adv Drug Deliv Rev* **54**, 987-1013 (2002).
- Warren, B. A., in *Tumor blood circulation*, edited by H. I. Peterson (CRC Press, Boca Raton, FL, 1979), pp. 1-47.
- Weissig, V., Whiteman, K. R. and Torchilin, V. P., Accumulation of protein-loaded long-circulating micelles and liposomes in subcutaneous lewis lung carcinoma in mice. *Pharm Res* **15**, 1552-1556 (1998).

- Weissleder, R., Cheng, H. C., Marecos, E., et al., Non-invasive in vivo mapping of tumour vascular and interstitial volume fractions. *Eur J Cancer* **34**, 1448-1454 (1998).
- Weitman, S. D., Lark, R. H., Coney, L. R., et al., Distribution of the folate receptor gp38 in normal and malignant cell lines and tissues. *Cancer Res* **52**, 3396-3401 (1992).
- West, K. R. and Otto, S., Reversible covalent chemistry in drug delivery. *Curr Drug Discov Technol* **2**, 123-160 (2005).
- Wolff, A. C., Liposomal anthracyclines and new treatment approaches for breast cancer. *Oncologist* **8 Suppl 2**, 25-30 (2003).
- Wolff, J. E., Trilling, T., Molenkamp, G., et al., Chemosensitivity of glioma cells in vitro: A meta analysis. *J Cancer Res Clin Oncol* **125**, 481-486. (1999).
- Wong, E. T. and Brem, S., Antiangiogenesis treatment for glioblastoma multiforme: Challenges and opportunities. *J Natl Compr Canc Netw* **6**, 515-522 (2008).
- Woodle, M. C. and Lasic, D. D., Sterically stabilized liposomes. *Biochim Biophys Acta* **1113**, 171-199 (1992).
- Wu, J., Liu, Q. and Lee, R. J., A folate receptor-targeted liposomal formulation for paclitaxel. *Int J Pharm* **316**, 148-153 (2006).
- Wu, N., Da, D., Rudoll, T., et al., Increased microvascular permeability contributes to preferential accumulation of stealth liposomes in tumor tissue. *Cancer Res* **53**, 3765-3770 (1993).
- Xu, Y. and Du, Y., Effect of molecular structure of chitosan on protein delivery properties of chitosan nanoparticles. *Int J Pharm* **250**, 215-226 (2003).
- Yamamoto, Y., Nagasaki, Y., Kato, Y., et al., Long-circulating poly(ethylene glycol)-poly(D,L-lactide) block copolymer micelles with modulated surface charge. *J Control Release* **77**, 27-38 (2001).

- Yang, W., Barth, R. F., Leveille, R., et al., Evaluation of systemically administered radiolabeled epidermal growth factor as a brain tumor targeting agent. *J Neurooncol* **55**, 19-28 (2001).
- Yatvin, M. B., Weinstein, J. N., Dennis, W. H. and Blumenthal, R., Design of liposomes for enhanced local release of drugs by hyperthermia. *Science* **202**, 1290-1293 (1978).
- Yemisci, M., Bozdog, S., Cetin, M., et al., Treatment of malignant gliomas with mitoxantrone-loaded poly (lactide-co-glycolide) microspheres. *Neurosurgery* **59**, 1296-1302; discussion 1302-1293 (2006).
- Yezhelyev, M. V., Gao, X., Xing, Y., et al., Emerging use of nanoparticles in diagnosis and treatment of breast cancer. *Lancet Oncol* **7**, 657-667 (2006).
- Yoo, H. S., Lee, E. A. and Park, T. G., Doxorubicin-conjugated biodegradable polymeric micelles having acid-cleavable linkages. *J Control Release* **82**, 17-27 (2002).
- Yuan, F., Leunig, M., Huang, S. K., et al., Microvascular permeability and interstitial penetration of sterically stabilized (stealth) liposomes in a human tumor xenograft. *Cancer Res* **54**, 3352-3356. (1994).
- Yuan, F., Chen, Y., Dellian, M., et al., Time-dependent vascular regression and permeability changes in established human tumor xenografts induced by an anti-vascular endothelial growth factor/vascular permeability factor antibody. *Proc Natl Acad Sci U S A* **93**, 14765-14770 (1996).
- Zalipsky, S., Brandeis, E., Newman, M. S. and Woodle, M. C., Long circulating, cationic liposomes containing amino-peg- phosphatidylethanolamine. *FEBS Lett* **353**, 71-74 (1994).
- Zalipsky, S., Puntambekar, B., Boulikas, P., et al., Peptide attachment to extremities of liposomal surface grafted peg chains: Preparation of the long-circulating form of laminin pentapeptide, yigr. *Bioconjug Chem* **6**, 705-708 (1995).
- Zalipsky, S., Mullah, N., Harding, J. A., et al., Poly(ethylene glycol)-grafted liposomes with oligopeptide or oligosaccharide ligands appended to the termini of the polymer chains. *Bioconjug Chem* **8**, 111-118 (1997).

- Zalipsky, S., Qazen, M., Walker, J. A., 2nd, et al., New detachable poly(ethylene glycol) conjugates: Cysteine-cleavable lipopolymers regenerating natural phospholipid, diacyl phosphatidylethanolamine. *Bioconjug Chem* **10**, 703-707 (1999).
- Zalipsky, S., Mullah, N. and Qazen, M., Preparation of poly(ethylene glycol)-grafted liposomes with ligands at the extremities of polymer chains. *Methods Enzymol* **387**, 50-69 (2004).
- Zhang, J. X., Zalipsky, S., Mullah, N., et al., Pharmacological attributes of dioleoylphosphatidylethanolamine/cholesterylhemisuccinate liposomes containing different types of cleavable lipopolymers. *Pharmacol Res* **49**, 185-198 (2004).
- Zhang, L., Yu, K. and Eisenberg, A., Ion-induced morphological changes in "Crew-cut" Aggregates of amphiphilic block copolymers. *Science* **272**, 1777-1779 (1996).
- Zhang, Y., Guo, L., Roeske, R. W., et al., Pteroyl-gamma-glutamate-cysteine synthesis and its application in folate receptor-mediated cancer cell targeting using folate-tethered liposomes. *Anal Biochem* **332**, 168-177 (2004).
- Zhang, Z. and Feng, S. S., The drug encapsulation efficiency, in vitro drug release, cellular uptake and cytotoxicity of paclitaxel-loaded poly(lactide)-tocopheryl polyethylene glycol succinate nanoparticles. *Biomaterials* **27**, 4025-4033 (2006).
- Gliadel wafer [package insert]. Bloomington, MN: MGI PHARMA, INC.; 2006.
- Doxil: Prescribing information. Raritan, NJ: Ortho Biotech Products, LP; 2008.
- National Comprehensive Cancer Network: Central nervous system cancers version 1.2008. Available at: http://www.nccn.org/professionals/physician_gls/pdf/cns.pdf. Accessed June 19, 2008.
- www.cancer.gov/clinicaltrials, Vol. 2008: National Cancer Institute, 2008. Accessed June 1, 2008.